Dosimetric studies in Image Guided Adaptive Brachytherapy in Gynaecological Cancers

By

S. V . Jamema

HLTH 09 2011 04003

Tata Memorial Centre, Mumbai

A thesis submitted to the

Board of Studies in Health Sciences

In partial fulfillment of requirements

for the Degree of

DOCTOR OF PHILOSOPHY

of

HOMI BHABHA NATIONAL INSTITUTE

November, 2014

Homi Bhabha National Institute

Recommendations of the Viva Voce Committee

As members of the Viva Voce Committee, we certify that we have read the dissertation prepared by S.V Jamema entitled "Dosimetric Studies in Image Guided Adaptive Brachytherapy in Gynaecological Cancers" and recommend that it may be accepted as fulfilling the thesis requirement for the award of Degree of Doctor of Philosophy.

Chairman	Prof. S. K Shrivastava	**Date:**
Guide / Convener	Prof. D D Deshpande	**Date:**
Examiner	Prof M Ravi Kumar	**Date:**
Member 1	Prof Rajiv Sarin	**Date:**
Member 2	Prof. J P Agarwal	**Date:**
Member 2	Dr S D Sharma	**Date:**

I hereby certify that I have read this thesis prepared under my direction and recommend that it may be accepted as fulfilling the thesis requirement.

Date:
Place: Mumbai, India

Guide

STATEMENT BY AUTHOR

This dissertation has been submitted in partial fulfillment of requirements for an advanced degree at Homi Bhabha National Institute (HBNI) and is deposited in the Library to be made available to borrowers under rules of the HBNI.

Brief quotations from this dissertation are allowable without special permission, provided that accurate acknowledgement of source is made. Requests for permission for extended quotation from or reproduction of this manuscript in whole or in part may be granted by the Competent Authority of HBNI when in his or her judgment the proposed use of the material is in the interests of scholarship. In all other instances, however, permission must be obtained from the author.

S V Jamema

DECLARATION

I, hereby declare that the investigation presented in the thesis has been carried out by me. The work is original and has not been submitted earlier as a whole or in part for a degree / diploma at this or any other Institution / University.

S V Jamema

List of Publications arising from the thesis

Journals

1. **Jamema SV**, Mahantshetty U, Tanderup K, Malvankar D, Sharma S, Engineer R, Chopra S, Shrivastava SK, Deshpande DD. Inter-application variation of dose and spatial location of D_{2cm^3} volumes of OARs during MR image based cervix brachytherapy. Radiother Oncol. 2013; 107:58-62.
2. **Jamema SV,** Sharma S, Mahantshetty U, Engineer R, Shrivastava SK, Deshpande DD. Comparison of IPSA with dose-point optimization and manual optimization for interstitial template brachytherapy for gynecologic cancers. Brachytherapy. 2011;10:306-12.
3. **Jamema SV**,Mahantshetty U, Deshpande D, Sharma S, Shrivastava S, Does help structures play a role in reducing the variation of dwell time in IPSA planning for gynecological brachytherapy application? J Contemp Brachytherapy. 2011;3 :142-9.
4. **Jamema SV**, Kirisits C, Mahantshetty U, Trnkova P, Deshpande DD, Shrivastava SK, Pötter R. Comparison of DVH parameters and loading patterns of standard loading, manual and inverse Optimization for intracavitary brachytherapy on a subset of tandem/ovoid cases. RadiotherOncol. 2010; 97:501-6.

Chapters in books

1. Umesh Mahantshetty, **Jamema Swamidas**, S. K Shrivastava, Institutional experiences, Practical Approaches to Image Guided Brachytherapy. India: Tata Memorial Hospital Mumbai, Gynaecologic Radiation Therapy, Novel Approaches to Image Guidance and management, Editors: A N Viswanathan, C Kirisits, B Erickson, R. Potter. ISBN: 978-3-540-68954-6.

Manuscripts communicated:

1. **S V Jamema**, Umesh Mahantshetty, E Anderson, K Noe, T Sangild, JF Kallehauge SK Shrivastava, DD Deshpande, K Tanderup. Uncertainties of deformable image registration for dose accumulation of brachytherapy high dose regions in bladder and rectum. Brachytherapy – Under Review
2. **S V Jamema,** Umesh Mahantshetty, M Pathan, A Shrivastava, S K Shrivastava, DD Deshpande. Evaluation of inter-application variation of dose and spatial location of organs at risk in 2D orthogonal image based intracavitary brachytherapy. Journal of Medical Physics.

Conference proceedings:

1. **Jamema SV,** Umesh Mahantshetty, M Pathan, A Shrivastava, S K Shrivastava, DD Deshpande. Evaluation of inter-application variation of dose and spatial location of organs at risk in 2D orthogonal image based intracavitary Brachytherapy. Indian Brachytherapy Society Annual meeting, March 2014- Oral Presentation.
2. **Jamema SV**, U. Mahantshetty, V. Jagtap, et al 160, Oral, Inter fraction variation of high dose regions in OAR in MR Image based cervix brachytherapy using rigid registration.Radiotherapy and Oncology, Volume 99, Supplement 1, May 2011, Pages S61-S62. ESTRO Annual meeting, Barcelona, Spain.
3. **Jamema SV**, Christian Kirisits, Umesh Mahantshetty, et al. Loading pattern calculated by inverse optimization vs traditional dosimetry systems of intracavitary brachytherapy of cervical cancer – A dosimetric study**.** Brachytherapy, Volume 8, Issue 2, April–June 2009, pages 127-128. ABS annual meeting, Atlanta, USA.
4. Pragya Shukla, Supriya Chopra, Reena Engineer, Umesh Mahantshetty, **Jamema SV**, Shyam Kishore Shrivastava. Quality assurance of multi-fractionated pelvic interstitial brachytherapy for gynecologic cancers**.** Brachytherapy, volume 10, supplement 1, May–June 2011, pages S60-S61.

5. V. Jagtap, A. Mawlong, U. Mahantshetty, **S. Jamema**, et al. 634 Poster CT image based dosimetric evaluation of Gyn Gec-ESTRO DVH parameters for HDR brachytherapy in cervical cancers. Radiotherapy and Oncology, volume 99, Supplement 1, May 2011, Page S258.
6. S. Kumar, U. Mahantshetty, S. Roy, **S. Jamema,**791 Poster Dosimetric evaluation of impact of bladder filling status on three dimensional dosimetry (3D – DVH) in High-Dose-Rate intracavitary brachtherapy with tandem-ring application for cervical cancers**.** Radiotherapy and Oncology, Volume 99, Supplement 1, May 2011, Page S310.
7. Manpreet Singh Tiwana, Umesh M. Mahantshetty, **Jamema V. Swamidas** et al., Spatial distribution and DVH parameters correlation of additional rectal/sigmoid mucosal points, in high-dose-rate intracavitary brachytherapy for carcinoma of the cervix – A dosimetric study**.** Brachytherapy, volume 8, Issue 2, April–June 2009, Page 128.
8. Umesh M. Mahantshetty**, Jamema V. Swamidas**, Nehal R. Khanna, et al. MRI guided high-dose-rate intracavitary brachytherapy in cervical cancers at Tata Memorial Hospital: The initial clinical outcome . Brachytherapy, volume 8, Issue 2, April–June 2009, Page 112.
9. Pramod K. Sharma, **S.V. Jamema** et al.3D Image-based dosimetric evaluation of gynecologic high-dose-rate interstitial brachytherapy**.** Brachytherapy, volume 7, Issue 2, April–June 2008, Page 135.
10. Smriti Sharma, Deepak Deshpande**, Swamidas V. Jamema**, et al. Inverse Planning Simulated Annealing planning for 3D image-based HDR brachytherapy in cervical cancers: A dosimetric comparision. Brachytherapy, volume 9, supplement 1, April–June 2010, Page S26.
11. Umesh M. Mahantshetty, Nehal R. Khanna, Reena Z. Engineer, Shyam K. Shrivastava, Kailash Narayan, **Jamema Swamidas**, Deepak D. Deshpande, Ketayun A. Dinsahw. Abdominal ultrasonography for conformal High-Dose-Rate intracavitary brachytherapy in carcinoma of the cervix**.** Brachytherapy, volume 7, Issue 2, April–June 2008, Pages 149-150.
12. Nikhilesh G. Patil, Sherly Saju, **S.V. Jamema**, et al. Comparative analysis of CT-based 3D volumetric dosimetry and radiography-based

2D dosimetry for High-Dose-Rate intracavitary applications**.** Brachytherapy, Volume 5, Issue 2, April–June 2006, Page 99.

Other Publications of the student in Refereed Journals related to the current work

1. Sharma PK, Sharma PK, **Swamidas VJamema** et al. Dose optimization in gynaecological 3D image based brachytherapy using Martinez Universal Perineal Interstitial Template (MUPIT)- an institutional experience. J Med Phys, 2014;39:197-202.
2. Mahantshetty U, Kalyani N, Engineer R, Chopra S, **JamemaS** et al. Reirradiation using high-dose-rate brachytherapy in recurrent carcinoma of uterine cervix. Brachytherapy. 2014; S1538-4721 (14)00569-8.
3. Sapru S, Mohamed S, Fokdal L, Nkiwane K, **Jamema SV**, Mahantshetty U, Kirisits C, Pötter R, Christian Lindegaard J, Tanderup K,Dose to the non-involved uterine corpus with MRI guided brachytherapy in locally advanced cervical cancer. Radiother Oncol. 2013 ;107:93-8.
4. Nesvacil N, Tanderup K, Hellebust TP, De Leeuw A, Lang S, Mohamed S, **Jamema SV,** Anderson C, Pötter R, Kirisits C. A multicentre comparison of the dosimetric impact of inter- and intra-fractional anatomical variations in fractionated cervix cancer brachytherapy. Radiother Oncol. 2013;107:20-5.
5. ChopraS, Shukla P, Paul SN, Engineer R, Phurailatpam R, **Swamidas Jamema**, et al. Evaluation of quality indices during multifractionated pelvic interstitial brachytherapy for cervical cancer. Brachytherapy. 2013 ;12:156-61.
6. Mahantshetty U, Khanna N, **Swamidas Jamema**, Engineer R, Thakur MH, Merchant NH, Deshpande DD, Shrivastava S. Trans-abdominal ultrasound (US) and magnetic resonance imaging (MRI) correlation for conformal intracavitary brachytherapy in carcinoma of the uterine cervix.Radiother Oncol. 2012 ;102(1):130-4.
7. Mahantshetty U, **Jamema SV**, Khanna N, Engineer R, Merchant NH, Deshpande DD, Shrivastava S. Reporting and validation of

gynaecological Groupe European de Curietherapie European Society for Therapeutic Radiology and Oncology (ESTRO) brachytherapy recommendations for MR image-based dose volume parameters and clinical outcome with high dose-rate brachytherapy in cervical cancers: asingle-institution initial experience. Int J Gynecol Cancer. 2011;21:1110-6.

8. Mahantshetty U, **Jamema SV**, Khanna N, Engineer R, Merchant NH, Shrivastava S. Magnetic resonance image-based dose volume parameters and clinical outcome with high dose rate brachytherapy in cervical cancers--a validation of GYN GEC-ESTRO brachytherapy recommendations. Clin Oncol (R Coll Radiol). 2011;23:376-7.
9. Mahantshetty U, Tiwana MS, **Jamema SV**, et al. Additional rectal and sigmoid mucosal points and doses in high dose rate intracavitary brachytherapy for carcinoma cervix: a dosimetric study. J Cancer Res Ther. 2011;7:298-303
10. **Jamema SV,** Saju S, Mahantshetty U, Pallad S, Deshpande DD, Shrivastava SK, Dinshaw KA. Dosimetric evaluation of rectum and bladder using image-based CT planning and orthogonal radiographswith ICRU 38 recommendations in intracavitary brachytherapy. J Med Phys. 2008;33:3-8.
11. **Jamema SV**, Saju S, Shetty UM, Pallad S, Deshpande DD, Shrivastava SK Dosimetric comparison of inverse optimization with geometric optimization in combination with graphical optimization for HDR prostate implants.J Med Phys. 2006;31:89-94.

S.V.Jamema.

Acknowledgements

I would like to express my special appreciation and thanks to my guide Prof.D D Deshpande, who has been a great mentor for me, and for having encouraged my research and for allowing me to grow.

I would also like to thank my doctoral committee members, Prof S K Shrivastava, Prof Rajiv Sarin, Prof J P Agarwal and Dr S D Sharma for their brilliant comments and suggestions during the progress of the work.

Most of the results described in this thesis would not have been obtained without a close collaboration with few laboratories. I owe a great deal of appreciation and gratitude to Prof. Christian Kirisits, Medical University of Vienna and Prof. Kari Tanderup, Aarhus University, Denmark. I would especially like to thank Prof. S K Shrivastava and Dr Umesh Mahantshetty of Gynaecology DMG, forthey were the force behind these collaborative projects between Tata Memorial Hospital and GEC ESTRO.

A very special thanks goes to all my colleagues and friends at Department of Medical Physics, Tata Memorial Hospital for all their support, especially Siji,who supported me in writing the thesis.

Words cannot express how grateful I am to my family, for all of the sacrifices that they have made on my behalf. Their prayer for me was what sustained me thus far.

. S V Jamema

CONTENTS

Abstract:

Image Guided Adaptive Brachytherapy (IGABT) has evolved into a high-technology modality of radiotherapy incorporating modern imaging and advanced computational algorithms as standards of care. This has raised many questions concerning both the benefit and the reliability of the procedure, since brachytherapy is subject to uncertainties from imaging, treatment planning, dose delivery, and anatomical variations. The overall aim of this thesis was to address specific issues and practical solutions concerning technical and physical aspects of IGABT with specific focus to treatment planning, new algorithms such as inverse planning and dose accumulation uncertainties in gynaecological brachytherapy.

The use of inverse planning algorithms in external beam therapy is an established procedure and widely accepted in the clinics, while in brachytherapy, it is still in the investigational stage, not well accepted, and practiced as yet. Although successful in prostate brachytherapy, its use in gynaecological brachytherapy is not common. There are certain issues with currently available inverse planning algorithms, which need to be understood for various clinical situations before clinical implementation. The first part of this thesis addresses issues related to inverse planning for various clinical scenarios using two commercially available inverse planning algorithms. The major findings of this part of the thesis is that the current inverse planning algorithms deviate from the standard loading pattern for intracavitary brachytherapy, and hence need to used with caution, however for interstitial application (MUPIT), they produce reproducible and conformal plans with significant sparing of OARs.

The second part of this thesis addresses the uncertainties in IGABT, which have not been adequately addressed so far. It is essential to identify these uncertainties, their magnitude, and their impact on the overall uncertainty of dose delivery to the patient. Having this knowledge may provide correct dose assessment in IGABT, and subsequently improved clinical outcome when using better planning aims with constraints. Hence, to address this uncertainty component, a systematic investigation was carried out for various clinical scenarios using rigid and deformable image registration algorithms. In this part of the thesis, it was found that the inter application variation was most stable for rectum and to a large extent for bladder which implies that ‘DVH addition’ could be applicable. The results of dose accumulation using deformable image registration indicate that the direct addition provide a reasonable estimate to the dose to the OARs, as the current DIR algorithms are not robust enough to handle large deformations especially in high dose gradient region associated with brachytherapy dose distribution.

Synopsis:

IGABT has evolved into a high-technology modality of radiotherapy incorporating modern imaging and advanced computational algorithms as standards of care. This has raised many questions concerning both the benefit and the reliability of the procedure, since brachytherapy is subject to uncertainties from imaging, treatment planning, dose delivery, and anatomical variations. The overall aim of this thesis was to address specific issues and practical solutions concerning technical and physical aspects of IGABT procedure with specific focus to treatment planning, new algorithms such as inverse planning and dose accumulation uncertainties in gynaecological Brachytherapy

The use of inverse planning algorithms in external beam therapy is an established procedure and widely accepted in the clinics, while in brachytherapy, it is still in the investigational stage, not well accepted, and practiced as yet. Although successful in prostate brachytherapy, its use in gynaecological brachytherapy is not common. There are certain issues with currently available inverse planning algorithms, especially for intracavitary brachytherapy, which need to be clearly understood for various clinical situations before clinical implementation. The first part of this thesis addresses issues related to inverse planning for various clinical scenarios in IGABT using two commercially available inverse planning algorithms, inverse planning simulated annealing (IPSA) and hybrid inverse planning optimization (HIPO).

The second part of this thesis addresses the uncertainties in IGABT, which have not been adequately addressed so far. It is essential to identify these uncertainties, their magnitude, and their impact on the overall uncertainty of dose delivery to the patient. Having this knowledge may provide correct dose assessment in IGABT, dose effect modeling, and subsequently improved clinical outcome when using better planning aims with dose and volume constraints. It was reported that inter and intra-fraction organ movements are the most significant uncertainty component with a dose variations of 20% standard deviation [252]. Hence, to address this uncertainty component, a systematic investigation was carried out for various clinical scenarios such as multi-fractional 2D orthogonal radiograph based dosimetry and 3D image based brachytherapy using rigid and deformable image registration algorithms.

Objectives of the work undertaken for the thesis:

1. To analyze the dosimetric difference between the standard loading, manually optimized and inverse optimized dosimetric plans using IPSA and HIPO for various applications in IGABT in gynecological cancers such as:
    a. Intracavitary brachytherapy – Tandem & Ovoid and Tandem & Ring applicators.
    b. Combined intracavitary and interstitial (IC+IS) Vienna applicator.
    c. Interstitial template for gynecological applications – Martinez Universal Perennial Interstitial Template (MUPIT).
2. To analyze the inter application variation for
    a. 2D orthogonal radiograph image based brachytherapy.
    b. MR image based IGABT using rigid registration.
    c. MR image based IGABT using deformable image registration.

This thesis has been divided into five chapters; the first chapter describes the introductory details about brachytherapy including history, technological developments and implantation techniques. The second chapter describes the conventional method of treatment planning, its limitation and the newer developments such as MR IGABT, the processes involved in the transition and its rationale. Third chapter describes the application of inverse planning for various gynaecological applications. Fourth chapter addresses the uncertainties in IGABT, especially, organ motion related to inter application variation in multi fractional brachytherapy in both 2D and 3D IGABT. The evaluation also used the new deformable registration algorithm. Finally fifth chapter summarizes the important findings of this thesis and also discusses the future direction of research.

Chapter 1:Introduction

Brachytherapy is the delivery of radiation dose using radioactive sources positioned in close proximity to the tumour for treatment of cancer. One of the advantages of brachytherapy as compared to external beam radiotherapy is that the dose is highly localized to the tumour with a sharp fall off of dose to neighboring OARs, which constitutes the very challenge due to high dose gradients that may result in geometric errors and thus deviation between the calculated and the delivered doses. Thus, to achieve maximum therapeutic ratio of the treatment, precise localization and treatment planning of tumours is paramount.

The history of brachytherapy dates back to 1898, when Marie and Pierre Curie discovered radium. Radium was used in pre-loaded needles for implantation, which exposed the personnel to high radiation levels. Later, manual after loaders came into existence with new sources such as Cobalt-60, Caesium-137, and Iridium-192, which improved the implantation technique and reduced the radiation exposure. The manual after-loaders were replaced by remote after-loaders, which completely eliminated the radiation exposure to the personnel and introduced optimization which has improved the treatment planning capabilities to a large extent. Image guidance in brachytherapy was first introduced using ultrasound images for prostate cancer in 1981, and was later used for cervical cancer using CT and MR images in late 1980s. However it was being practiced only in few centers in Europe. In early 2000, the 3D image guidance technology was rapidly used in the external beam, however the use of 3D image guidance in brachytherapy has been sparse.

Cancer of the uterine cervix is the leading cancer among the female population in India [20]. External beam radiotherapy and brachytherapy forms the mainstay of the treatment, especially brachytherapy plays a pivotal role for clinical outcome. High cure rates have been reported even in patients with locally advanced disease [60]. Brachytherapy for cervical cancer is generally done using two techniques, intracavitary and interstitial. In intracavitary brachytherapy, the radioactive sources are inserted into the natural body cavities, eg. uterus, vagina. Interstitial brachytherapy refers to the implantation of radioactive sources directly into the affected tissue. Under some special circumstances, where tumour is large extending upto the parametrium, intracavitary is not possible, then, interstitial implantation is the standard of care in the treatment of cancer of uterine cerivx.

Conventionally, brachytherapy planning was carried out by means of a pair of orthogonal radiographs. The major limitation of the conventional imaging modalities is the lack of information on the tumour volumes and OARs. With the new imaging modalities, various other technological and process advancements have been introduced such as new CT/MR compatible applicators, intracavitary and interstitial (IC+IS) Vienna applicators to cover large volume tumours [2], new concepts for tumour volume definition [83,124], new inverse planning algorithms, new model based dose calculation algorithms which include tissue heterogeneities, uncertainty budget analysis among others [233]. Among these new developments, there were largely two big areas which were unexplored, the application of inverse planning algorithms and the inter application variation as part of uncertainty analysis. In Multi fractionated Brachytherapy, a new dimension, time is added in to the process, as imaging and treatment planning is carried out for

each fraction, and the inter application/fraction variation has been a major concern during dose accumulation. Since time is being introduced into the process, interms of imaging, adaptation to tumour volume, a new terminology "IGABT" has been coined and has been used worldwide. The organ deformation by means of bladder/rectum filling, tumour shrinkage, and movement of sigmoid colon has resulted in large uncertainties in the dose accumulation process, which has also been the subject of investigation in this thesis.

Chapter 2: Transition from 2D orthogonal radiograph based planning to 3D MRI Image Guided Adaptive Brachytherapy:

In past 10-15 years, IGABT approach has been standardized with many mono-institutional series of clinical outcome being reported [128].Potter et al have published their single institution experience with MRI based IGABT, where they reported three year pelvic control rate of 96% for tumours 2-5cm in diameter, and 90% for tumours >5cm in diameter with a three year actuarial rate of grade 3-4 bowel and urinary toxicity of 2% as compared to the historical series. All the available evidence gives favourable results interms excellent local control and reduced toxicities as compared to historical series. The landmark French STIC trial that compared 2D vs 3D brachytherapy also concludes that 3DBT results in improved local control with reduced toxicity observed with 2D dosimetry. They conclude that for patients with advanced tumours, it is necessary to improve coverage of target volumes without increasing the toxicity [129].

The above clinical results strongly justifies the transition from 2D dosimetry to 3D IGABT, especially for patients presented with advanced tumours, which is a typical situation in India and other developing countries. However, the implementation of IGABT in India and other developing countries is a big challenge due to the resources, expertise and financial constraints. It is necessary to focus research on cost effective methods of IGABT practice, some of which has been underway in Tata Memorial Hospital (TMH), Mumbai, India. It should also be recognized that as any other advanced techniques, IGABT too requires systematic clinical implementation that includes familiarization of the processes. In-appropriate implementation of IGABT and change of clinical practice based on this could be detrimental to the patients. Unlike treatment delivery errors, which are usually random in nature, the errors from the TPS and applicator commissioning are more often systematic and can be avoided. During this thesis period, clinical implementation of IGABT for cervical cancer was implemented in TMH. The successful implementation of IGABT in to clinical routine, which is of international standard, is the basis of this thesis. We are also a part of an ongoing multicentric collaborative trial

Int**E**rnational study on **M**RI-guided **BR**achytherapy in locally **A**dvanced **CE**rvical cancer (EMBRACE) which will reveal more information on the dose effect relationship on local control/morbidity of the tumour and toxicities of organs at risks (OAR). There are various steps in the process of IGABT such as applicator selection, contouring, imaging, treatment planning and optimization that may quite differ from the conventional brachytherapy planning. In the year 2004, GYN GEC ESTRO working group first published its recommendations, which describes the concepts and terms used in IGABT, and later published guidelines related to contouring, imaging, applicator reconstruction, dose volume reporting and uncertainty analysis [83,124,233,135,145]. The transition to IGABT at TMH was based on these recommendations. Some of the salient features of this transition in TMH is described briefly in this chapter.

Although, imaging is an important component of the IGABT process, clinical examination plays a crucial role in the evaluation of disease extent / residual tumour during IGABT. In India, 2D radiographic localization is widely available for BT, however in the recent past, with the increasing number of CT scanners available in new radiotherapy centers, CT imaging is being widely used for both external RT and BT planning. However, access to MRI for BT planning is limited to a few centers including TMH [60]. Studies were undertaken to compare the contouring in CT and MR which showed that the tumour volume can be significantly over estimated in CT images as compared to MR. No systematic differences in the volume or in the dose to OARs were found, although MRI has in general better visualization of OARs [100]. A systematic multi centric study of comparison of CT and MRI for target volume delineation, which will bring new guidelines for CT based IGABT is under way in TMH.

IGABT mandates the use of CT/MR compatible applicators that do not throw artifacts and interfere with the CT or MRI signal such that tumour visualization is possible. Applicator reconstruction with CT images is more straightforward as compared to MRI. Visualization of applicators in MR images is quite challenging and hence the reconstruction. During the implementation of this transition in our hospital, as a part of quality assurance programme for applicator reconstruction, an in-house phantom with the fiducials/markers with the known geometry was fabricated which can house the applicator in fixed geometry. Various sequences of MR imaging which will aid in target volume definition and applicator reconstruction have been acquired. The MR images of this phantom have been compared with the corresponding CT images by means of image registration to quantify the artifacts and spatial distortion.

Although in MR images, where we can visualize the tumour and the OARs clearly, the optimization procedure is still conservative, where, the starting point is to follow a standard loading pattern, followed by normalization to point A, minimal optimization such that there is no large deviation in the loading pattern while, reducing the dose to OARs without compromising the target coverage. In IGABT, the dose prescription and reporting is on HR-CTV, however, it is recommended to report the dose to point A. Newer inverse planning algorithms have not been used clinically at this moment, which have been tested in great detail in this thesis and presented in the later chapters.

In multi-fractional brachytherapy, inter-application/fraction variations occur between different treatments/applicator insertions, both in terms of geometric and dosimetric parameters [155]. In a multi centric study, a maximum dose variation of 20% for OARs and 10% for HR-CTV was reported [252]. The current practice of determining the D_{2cm3} cumulative dose to OARs during brachytherapy is based on what has previously been called ‘‘the worst-case scenario’’, which is the assumption that the D_{2cm3} regions are located in the same anatomical part of the organ in each fraction [155]. These issues are still a matter of research and emerging clinical data with long-term outcome may provide a better platform for IGABT practice. Inter fraction variation due to organ movements and the resultant uncertainty in dose accumulation has been studied in detail in this thesis.

IGABT process mandates a team approach. Every process in the IGABT process is vital and requires a strict quality assurance and standardization. With increasing conformity of dose it becomes important that the delivery of dose is in accordance with what is planned on the TPS. Optimal source geometry, timing and stability are prerequisites for safe delivery of optimized dose. Both patient related factors and technical issues associated with the brachytherapy equipment can give rise to uncertainties in the delivered dose. It is well recognized that equipment related quality assurance has to be conducted periodically to prevent the dose delivery errors. Patient related factors are being identified as applicator displacement, organ motion in between the treatment planning and dose delivery.

Chapter 3: Treatment planning and Optimization

Most brachytherapy centers in the world have followed a traditional concept based on the Manchester or Fletcher loading patterns. The rationale behind the Manchester approach is to achieve a consistent dose rate at point A, by applying a set of strict rules with regard to position and activity of radium sources for the different combination of sizes for the uterine tandem and ovoids. With the introduction of HDR remote after loaders, the rules of Fletcher and Manchester systems were extended from the milligram radium equivalent activity distribution to a pattern of dwell positions where a single stepping source is positioned at programmable dwell times. Dose optimization is based on dose constraints for dose points or dose–volume parameters, which could be done either by manual forward planning or inverse optimization. Inverse planning algorithms was first introduced in brachytherapy for prostate. The major aim of the inverse planning algorithms was to improve the dosimetric results, make reproducible plans, and decrease the time to prepare a treatment plan. However, at this moment, these inverse planning algorithms were not robust enough to control the dosimetry especially for intracavitary brachytherapy. For example, the loading pattern resulting from these algorithms has a large deviation from the traditional pattern which may not be clinically acceptable. Dosimetric and clinical evidence have to be collected to obtain as much knowledge as possible which then will be integrated into future inverse planning tools.

There are two common inverse planning algorithms in brachytherapy, IPSA and HIPO. IPSA is an optimization algorithm that allows wider sampling and hill climbing to escape from a local minimum. This is required whenever the cost function is mathematically nonlinear and presents with multiple minimums. Simulated annealing (SA), first introduced by Kirkpatrick and other related algorithms can process cost functions with arbitrary boundary conditions with the statistical guarantee of finding an optimal solution/global minima [189]. HIPO, is a new inverse planning algorithm, wherein it combines both stochastic (simulated annealing-SA) and deterministic (DVH-based) optimization algorithms [196]. Taking the SA result as an initial input, the DVH-based inverse optimization algorithm optimizes the 3D dose distribution quickly for given dosimetric constraints. Three different clinical situations in IGABT have been investigated using IPSA and HIPO algorithms.

3.1. Standard loading pattern and inverse planning:

Twenty-eight consecutive patients who underwent MRI based HDR brachytherapy for cervix cancer was selected for this study. Three plans were calculated for each patient: 1) standard loading, 2) manual optimized, and 3) inverse optimized plan using HIPO. The target volumes were drawn based on GYN GEC ESTRO recommendations [83]. Dosimetric outcomes from these plans were compared based on dose–volume parameters. The ratio of Total Reference Air Kerma of ovoid to tandem $TRAK_{O/T}$ was used to compare the loading patterns.

The volume of HR CTV ranged from 9–68 cc with a mean of 41(±16.2)cc. Mean V_{100} for standard, manual optimized and inverse plans was found to be not significant (p = 0.35, 0.38, 0.4). Dose to bladder (7.8 ± 1.6 Gy) and sigmoid (5.6 ± 1.4 Gy) was high for standard plans; Manual optimization reduced the dose to bladder (7.1 ± 1.7 Gy p = 0.006) and sigmoid (4.5 ± 1.0 Gy p = 0.005) without compromising the HR CTV coverage. The inverse plan resulted in a significant reduction to bladder dose (6.5 ± 1.4 Gy, p = 0.002). TRAK was found to be 0.49(±0.02), 0.44(±0.04) and 0.40(±0.04)cGym^2 for the standard loading, manual optimized and inverse plans, respectively. It was observed that $TRAK_{O/T}$ was 0.82(±0.05), 1.7(±1.04) and 1.41(±0.93) for standard loading, manual optimized and inverse plans, respectively, while this ratio was 1 for the traditional loading pattern.

For standard plans, TRAK was independent of HR CTV volume while for manual optimized and inverse plans, TRAK was found to be linearly dependent on the volume of HR CTV. The reduced TRAK in inverse plan could be attributed to the dose sculpting used in the inverse plan. The increased weightage of ovoid loading in both the manual optimized and inverse plans, was attributed to the physical location of HR CTV which is situated around cervix. Another important finding of this study was that when dwell time gradient restriction was not used, a large variation in dwell time was observed, which may not be desirable. It was suggested that the deviation from the traditional loading pattern and the variation in the dwell time may be acceptable as long as the isodoses conform to the specific topography of the target and optimal reduction in the doses to OARs . However, a large deviation of the loading pattern/variations in the dwell time was not acceptable as it may increase the hotspots locally. In this study a dwell time gradient restriction was maintained at 0.5 for the inverse optimized plans, hence the accumulation of hotspots was minimized. Detailed analysis revealed that topography of the OAR with respect to HR CTV is the deciding factor for the loading pattern, for example, when the sigmoid dose was well below the dose constraint, tandem was heavily loaded to meet the

other constraints, such as coverage of HR CTV and dose to the bladder and rectum. Currently, it may be essential to respect the standard loading pattern, while practicing conformal brachytherapy using inverse planning, until sufficient clinical evidence becomes available.

3.2 Role of help structures and dwell time gradient restriction in inverse planning:

IPSA algorithm has been tested for MRI image based brachytherapy by the French group [147], and they concluded that, in the present form, it cannot be used to make clinically acceptable plans, as the variation in the dwell time is quite high. It was suggested the high dose regions can be controlled by the use of the help structures. Hence to analyze the role of help structures in IPSA, this investigation was carried out.

33 patients who underwent MR image-based HDR intracavitary-brachytherapy for cervix cancer based on GYN-ESTRO recommendations were selected for this evaluation. Help structures of diameter of 5 mm were drawn around the tandem/needles/ovoid and ring. Three plans were generated: manual optimized plan (MOPT), IPSA without help structures (IPSA_woHS) and IPSA with help structures (IPSA_wHS). Dose-volume parameters and the loading pattern were evaluated.

For tandem/ovoid applicator, the use of HS did not make significant impact in the dose-volume parameters and in the loading of tandem and ovoids, however steep variation was found in the individual dwell time. In case of Vienna applicator, inclusion of HS in the optimization made a significant impact in loading of needles. The percentage ratio of total time of needles to the tandem ($T_{N/T\%}$) was found to be 14 ± 2.5, 53 ± 9, 22 ± 6 for MOPT, IPSA_woHS and IPSA_wHS, respectively, which implies that in IPSA_woHS the dwell time in needles were half of the dwell time in the tandem, while in MOPT the needles were loaded only in 14%, and in IPSA_wHS it was 22% of the dwell time of tandem. Inclusion of HS in the optimization has reduced the contribution of dwell time of needle in IPSA_wHS. The individual variation of dwell time was also reduced in IPSA_wHS, however drawing of HS is a time consuming procedure and may not be practical for a routine practice.

The results of the present study indicate that inverse plans in general, produced significant sparing of bladder while maintaining the HR CTV coverage. IPSA has not made any significant variation in the dose to rectum and sigmoid for both T/O and Vienna applicator. However, the high dose regions V_{200} and V_{400} were significantly higher in IPSA as compared to MOPT. Detailed analysis of each patient's planned isodose distribution showed that, in case of T/O

applicator, the majority of high dose regions were found around the tandem and the ovoids. On the other hand, in case of Vienna applicator, the hot spots were found equally around the needles as that of tandem and ring. It was also found that the dwell weights of the tandem/ring and the needles were almost equal or even higher in certain patients. Here the dwell time near a sigmoid and the bladder was turned off, and the dwell weight of the needles was higher. In such cases, region of V_{200} and V_{400} was present around the needles as a continuous volume. When HS were included in the optimization with higher penalties for the HS of the needles, the high dose regions around the needles were reduced. The ratio of treatment time of tandem and ovoid/ring, $T_{T/O}$ and $T_{T/R}$ did not show any significant variation among the IPSA plans for both T/O and Vienna applicator. However, $T_{N/T}$ was as high as 53% for IPSA_ woHS, while it was 22% for IPSA_wHS. Hence, it may be considered that while using combinedintracavitary and interstitial (IC + IS) approach, help structures may be used during optimization and need not be used with intracavitaryapplication, as the benefit is negligible both in terms of dosimetric parameters and dwell time.

Based on the above findings, the use of IPSA is justified in the clinics for T/O application. Nevertheless, extreme caution is required in controlling the high dose regions. The benefit of using the HS is more in Vienna applicator as compared to T/O applicator. In case of Vienna applicator, the clinical consequences of the presence of high dose regions especially around the needles are unknown since they were nonexistent in time tested traditional loading pattern and manual after loading.

3.3 Inverse planning for interstitial implants:

Treatment planning concepts for interstitial implants differ very much from the intracavitary implants. Traditionally catheter based optimization is used for interstitial implants, viz dose point or geometric optimization. For volume implants, geometric optimization or dose point optimization is always used, as it produces a uniform distribution. In geometric optimization, the dwell times are determined such that dwell time in each dwell position, is inversely proportional to the dose contribution, of neighboring source positions**.** The data set of 10 consecutive patients was selected for this dosimetric study. For each patient, three plans were calculated: DPO, GrO, and IPSA. Dose volume parameters from the three plans were compared to analyze the dosimetric outcome.

Coverage of CTV with GrO and IPSA was significantly better (mean V_{100} of 88.8% and 89.1%; p=0.006) as compared with DPO (83.7%; p = 0.62). Similarly, mean D_{100} was same in both GrO and IPSA, 3.96± 0.23 and 3.96± 0.15 Gy, respectively. DPO plans were homogeneous with homogeneity index being 0.82 as compared with 0.68 ± 0.05 of GrO and 0.71±0.04 of IPSA. However, IPSA resulted in high conformity index of 0.78 as compared to 0.72 (p =0.001) and 0.68 (p = 0.001) for GrO and DPO plans, respectively. The dose to rectum (3.3±1.06 Gy) and bladder (3.17±0.5 Gy) was generally high for DPO. GrO reduced the dose to the rectum (2.91 ± 0.63; p = 0.011) and bladder (2.89 ± 0.63 Gy; p =0.003) significantly. IPSA resulted in a further reduction of the dose to rectum (2.79 ±0.67 Gy; p =0.046) and bladder (2.81 ± 0.67 Gy; p =0.035), however with no statistical significance as compared with GrO.

The results of this study have shown that, IPSA has resulted in superior plans in terms of CTV coverage, sparing of normal tissues and conformality as compared with DPO. However, this benefit came with a decrease in homogeneity. It was observed that, DPO plans were highly homogeneous; however, IPSA plans were associated with reduced homogenity. This is the only difference observed between the present study and the earlier investigations comparing IPSA with other algorithms, such as GO, and GrO[178]. It was also observed that the coverage was significantly low in DPO as compared with GrO and IPSA plan, which could be attributed to the location of the dose points. In the present study, the dose points were positioned inside the CTV and used a prescription isodose of 85-100%, which sufficiently covers the CTV. Alternatively, the dose points could be positioned around the CTV about 3-7 mm, in such a case the coverage may be superior, however, with an increased dose to the OARs, which may be partially rectified by positioning the dose points only laterally and not anterio-posteriorly or by differentially weighting or prescribing the dose points. The major conclusion of this study was that IPSA resulted in clinically acceptable plans for interstitial gynaecological implants using MUPIT template.

Chapter 4: Uncertainties of organ motion

In multi fractional brachytherapy, inter-application/fraction variations occur between different treatments/applicator insertions, both in terms of geometric and dosimetric parameters [233]. These parameters have been identified as bladder and/or rectal filling, movements of sigmoid colon, and variation in vaginal packing among others. The current practice of determining the D_{2cm3} cumulative dose to OARs during brachytherapy is based on what has previously been called ‘‘the worst-case scenario’’, which is the assumption that the D_{2cm3} regions

are located in the same anatomical part of the organ in each fraction [155]. This assumption implies that the cumulated brachytherapy dose can be calculated by adding D_{2cm3} values for each fraction. This approximation can lead to OAR dose overestimation when different organ parts are exposed to a high dose in different fractions. To study and investigate further, a systematic investigation has been undertaken in various multi-fractional brachytherapy situations: 2D orthogonal radiograph based dosimetry, IGABT using MR images with rigid and deformable image registration.

4.1 Uncertainties of organ motion in 2D orthogonal image based dosimetry:

The patients (n=27) who underwent intracavitary brachytherapy procedure using Fletcher-suit applicator (Nucletron) were taken up for this evaluation. Every patient had four applications each, as per institutional protocol. 2D orthogonal images were acquired in C-ARM (Siemens) located next to operating room with the appropriate dummy markers placed in the applicators. The images were transferred to treatment planning system (Oncentra, v 4.3) for further planning. Treatment planning was carried out as per departmental protocol. A dose of 7Gy was prescribed to point A. ICRU bladder and rectum point were identified according to ICRU 38 protocol (20). The inter-application dose variation of ICRU bladder and rectal point was carried out by evaluating the ICRU bladder and rectal point dose from each application. The inter application variation of spatial location of ICRU bladder and rectum was evaluated with flange of the applicator as the reference point. The polar coordinates of the ICRU bladder and rectal points also were evaluated for each of the application. The mean and standard deviation (SD) of dose and spatial location variation was evaluated for each patient. The mean dose variation with respect to the first application dose also was evaluated.

The mean (±SD) of inter-application dose variation of rectum and bladder with respect to the first application was found to be 10.9 (±7.9)% and 9.1(±5.3)% respectively. A dose variation of 10% is expected in cases where planning for only first application is being carried out without any further planning in subsequent applications. The mean of SD of inter application dose variation for rectum and bladder were 8.9 and 13.1 respectively, which indicates that ICRU rectal point has less inter application dose variation as compared to ICRU bladder point dose. The mean(±SD) of polar coordinates (r,θ) of rectal and bladder point with respect to the flange was found to be (2.7(±0.3),0) and (2.8(±0.4), 27(±13)). The mean of SD of inter application spatial location variation for rectum and bladder were 0.3(±0.1) and 0.4(±0.2) respectively, which indicates that ICRU rectal point has less inter application spatial location variation as

compared to ICRU bladder point dose. Based on these findings, we conclude that fractional replanning to be carried out for T/O applicator.

4.2 Uncertainties of organ motion in 3D MR image based dosimetry using rigid registration.

Twenty-seven patients treated with EMBRACE protocol were analyzed. Every patient had two applications, one week apart. For each application patient had undergone MR-imaging (MR-1 and MR-2), volume delineation, reconstruction, treatment planning (plan-1 and plan-2) and dose evaluation. Both the image series were then co-registered with applicator as the reference coordinate system (Eclipse planning system v8.6.14). Inter-application dose, volume and spatial location of D_{2cm3} variation were evaluated.

The largest inter-application systematic and random dose variations were observed for sigmoid as compared to rectum and bladder. The mean (±SD) of the relative D_{2cm3} variations were 0.6(±15.1)%, 0.9(±13.1)% and 11.9(±37.5)% for rectum, bladder and sigmoid respectively. The overlap of D_{2cm3} volumes was more than 50% in 16(59%), 8(30%) and 3(11%) patients for rectum, bladder and sigmoid, respectively. The inter fraction variation of bladder volume observed in the present study was low as compared to other studies reported in the literature which may be attributed to adherence to bladder protocol during imaging and delivery. The present study also indicates that the derived random uncertainties were lowest for bladder (13.1%) and rectum (15.1%) and highest for sigmoid (37.5%).

From the results, it could be inferred that 1) The spatial location of D_{2cm3} volume is stable for rectum, and 2) A dose variation of 15% per fraction was obtained, and hence imaging for every fraction may improve the accuracy of dose reporting as the dose variation may be significant if the doses are higher. These findings also validate the present concept of DVH addition where the dose received by the rectum may be directly additive in multi fractional brachytherapy.

4.3 Uncertainties of organ motion in 3D MR image based dosimetry using deformable image registration.

The major limitation of the above study is the use of rigid registration, where the registration was based on the applicator and not on the anatomy. This was also pointed out by the reviewers that the organ deformations like bladder-rectal filling, was not taken quantitatively

into account, due to which, it is not possible to locate the exact tissue where the dose D_{2cm3} dose was received previously. Hence, there could be a situation that can arise where the D_{2cm3} was not scored to have an overlap, but the tissue that receives the dose could be overlapping, which may overestimate the effect. One possible solution to overcome this issue is to use deformable registration algorithm, where the organ deformation is taken into account.

An analysis of 21 patients treated with MR image based brachytherapy under the EMBRACE protocol was carried out. The algorithm used in the present study for DIR is based on an optimized derivative of Lucas-Kanade Optic Flow, which works on mutual Information similarity function over a Radial Basis Function transformation model (Smart Adapt, Varian Medical Systems, Palo Alto).

In order to evaluate the impact of the registration on the dose accumulation, we made two registrations for each patient: from BT_1 to BT_2 and from BT_2 to BT_1. The 3D physical dose matrix was recalculated into 3D EQD_2 dose (voxel by voxel) by in-house software, and the BT_1 and BT_2 EQD_2 doses were added using the two transformations between the images established through DIR. Voxel wise deformed dose accumulation(DDA) was done for registrations in both directions: a) BT_1 deformed + BT_2 and b) BT_1 + BT_2 deformed. DVHs were calculated after DDA and D_{2cm3} of rectum and bladderwere compared with the DVH direct addition (DA). To compare the current DIR and DDA process to other approaches, we analyzed nine patients from Aarhus University Hospital who had previously been investigated using an in-house bio-mechanical algorithm for bladder dose accumulation. It was also evaluated whether the patients most in need of DIR-based dose accumulation could be identified based on the location of hotspots between the two BT fractions.

The mutual information DIR algorithm resulted in a larger mean deviation between DDA and DA as compared to the biomechanical DIR, but statistically insignificant ($p=0.32$). Biomechanical algorithm showed a systematic variation between DA and DDA based on the reference frame of bladder chosen for the deformable image registration. Such a systematic trend in the dose variation was not observed and found to be randomly varying in mutual information algorithm. There was a direct correlation between the registration difference and the DIR expansion/contraction for both rectum and bladder, which indicates that anatomically implausible DIRs were correlated with high discrepancy between two way registrations. Mean (±sd; range) percentage variation between DA and DDA were found to be 2.4 (±3.3; -1.8 to 11.5)% and 5.2 (±5.1; -1.7 to 16.5)% for rectum and bladder respectively. The differences

between the DA and DDA were found to be statistically significant for both rectum ($p=<0.005$) and bladder ($p<0.005$).

Chapter 5: Summary& Conclusion.

In this thesis, certain issues concerning technical and physical aspects of IGABT procedure with specific focus to treatment planning, newer algorithms such as inverse planning and uncertainties of organ motion were investigated. The summary of the results are as follows:

Inverse planning with HIPO and/or manual optimization offers improved plans in terms of OAR sparing and maintaining target coverage when compared to standard clinical plans. The average loading pattern was found to deviate from a traditional standard Fletcher loading. The tandem loading was decreased compared to the ovoids mainly due to high sigmoid dose. Inverse planning with IPSA resulted in plans with higher volumes of high dose regions for combined intracavitary and interstitial applicators. Without the help structures, the treatment time in the needles was high, which was significantly reduced when help structures were included. For Interstitial gynecological implants based on MUPIT template, IPSA resulted in significant sparing of normal tissues without compromising CTV coverage as compared with geometrically and graphically optimized plans.

For 2D orthogonal radiograph image based dosimetry, the inter application dose variation for ICRU rectum and bladder was found to be 10%. ICRU rectal point was more stable as compared to ICRU bladder point. Similarly, in MR image based dosimetry using rigid registration, the inter application variation of the spatial location of D_{2cm3} volumes was found to be most stable for rectum and to a large extent for bladder which implies that 'DVH addition' could be applicable to rectum and bladder. Minimal to moderate geometric changes in sigmoid are seen in majority of the patients resulting in maximal variation in spatial location of D_{2cm3} volumes which may lead to over estimation of doses during the DVH addition. The results of dose accumulation using deformable image registration also indicate that the direct addition provide a reasonable estimate to the dose to the OARs, as the current DIR algorithms are not robust enough to handle large deformations especially in high dose gradient region associated with brachytherapy dose distribution.

Future Direction:

In the uncertainty budget of IGABT, the largest component is the organ motion, of the order of 20-25%. In this thesis, the issues related to this uncertainty component have been addressed to some extent, and it was suggested that one of the ways to reduce this uncertainty component, is to have an access to imaging just before the delivery, followed by rapid re-planning according the organ anatomy at the time of treatment delivery.

Our results in the present study indicate that DDA based on intensity based DIR is less reliable than DIR based on a contour model. Intensity based DIR seems to be related with significant uncertainties and there is a lack of correlation between DDA estimated by intensity and contour based DIR. Other studies from external beam radiotherapy in various sites also indicate certain limitations with some algorithms. DIRs based on organ contours and incorporation of contour based models performs more accurately as compared to algorithms that depend only on the image intensities [290-291]. The DIR approach based on image intensity cannot specifically restrict deformations along organ walls to assure anatomically plausible registrations. Even when a deformable registration results in a good visual result with overlapping organ contours after deformation, there may be implausible deformations along the organ walls, which may not be readily detected through visual inspection of the quality of the deformed images. Furthermore, the present study is based on MR images, where the signal intensities/grey levels may be less reproducible as compared to electron densities associated with CT images. Use of DIR without detailed validation may result in large deviations, especially, if applied in the BT scenario with large dose gradients [292-293]. The contour based algorithm controls the deformations on the bladder wall and these are more consistent deformations, which result in less dose degradation induced by deformable registration. Future studies can be aimed at using CT images for intensity based algorithms, to investigate further, such that the uncertainties associated with the DIR can be reduced. In addition, newer algorithms can be developed such that the organ wall constraints can be taken into account.

List of figures:

24. Dose distribution of Intracavitary where the target is not adequately covered(left), the addition of interstitial needles helps to extend the dose coverage by 8mm, while sparing the OARs (right) . Dotted red line- HRCTV, Dotted Yellow line-GTV, Dotted Majenta-Bladder, contineous blue line – 7Gy, continuous red line – 9 Gy.
25. A typical DVH of a Brachytherpy application. The dose volume parameters quoted here refers for one BT application.
26. Flow chart depicting all the dose volume parameters to be reported for 2D and 3D image based brachytherapy.
27. Relationship of HR CTV volume and V_{100}, shows that they are inversely related.
28. Isodose distribution for standard Plan (a), manually optimized plan (b), inverse plan(c). Yellow:200%, 14Gy, green: 150%, 10.5Gy, red: 100%, 7Gy, blue:70% 4.9 Gy.
29. V_{100} is plotted for D2cc of bladder, rectum and sigmoid for standard, manually optimized and inverse plan. The dose to bladder and sigmoid is high in standard plan as compared to manually optimized and inverse plan. Optimization, both manual and inverse plan improved the sparing of OARs without compromising the target coverage.
30. Relationship of HR-CTV volume and TRAK, showing direct proportanality, standard loading delivers same amout of TRAK irrespecive of the HR CTV volume, while optimized plan reduced the TRAK for small volume tumours, which inturn will reduce the dose to OARs.
31. The isodose distribution of a representative patient for various plans, MOPT, IPSA woHS, and IPSA wHS using Vienna applicator.
32. (a)Individual dwell time of a tandem for three plans which are manual optimized(MOPT), IPSA plans done with help structures (IPSA_wHS) and IPSA plan without help structures(IPSA_woHS) for T/O applicator. **(b)** Individual dwell time of a needle for three planswhich are manual optimized (MOPT), IPSA plans done with help structures (IPSA_wHS) and IPSA plan without help structures(IPSA_woHS) for Vienna applicator.
33. Dose distribution of DPO, GrO, and IPSA plans of a representative patient. DPO 5 dose-point optimization; GrO 5 manual/graphical optimi- zation; IPSA 5 inverse planning simulated annealing.
34. Variation of dwell time in each catheter of a representative patient for DPO, GrO, and IPSA plan. DPO = dose-point optimization; GrO = manual/graphical optimization; IPSA = inverse planning simulated annealing.
35. DVH of DPO, GrO, and IPSA plan. DVH 5 dose-volume histogram; DPO = dose-point optimization; GrO = manual/graphical optimization; IPSA = inverse planning simulated annealing.
36. a) The obstruction of implant pathway because of the pelvic bone and (b) the usage of diverging needles that distort the implant geometry. DPO = dose-point optimization; GrO = manual/graphical optimization; IPSA = inverse planning simulated annealing.

37. An illustration of identifying the ICRU rectal and bladder point for inter- application variation of spatial location.
38. Deviation in reported mean ICRU rectal and bladder point doses with respect to that of first fraction.
39. Inter application dose variation of ICRU rectal point for every fraction and patient.
40. Inter application dose variation of ICRU bladder point for every fraction and patient.
41. Deviation in mean radial distance of ICRU rectal and bladder point doses with respect to that of first fraction.
42. Inter-application volume variation of rectum, bladder and sigmoid.
43. a,b,c: Inter application variation of spatial location of rectum and the hot spot- D_{2cm^3}region of various categories. (a) Volume of overlap of D_{2cm^3}region >50%, (b) volume of overlap of D_{2cm^3} region 10-50% (c) Volume of overlap <10% or no overlap.
44. Inter application variation of spatial locatoon of bladder and the hot spot- D_{2cm^3} region of various categories. (a) Volume of overlap of D_{2cm^3}region >50%, (b) volume of overlap of D_{2cm^3} region 10-50% (c) Volume of overlap <10% or no overlap.
45. a,b,c: Inter application variation of spatial locatoon of sigmoid and the hot spot- D_{2cm^3} region of various categories. (a) Volume of overlap of D_{2cm^3} region >50%, (b) volume of overlap of D_{2cm^3} region 10-50% (c) Volume of overlap <10% or no overlap .
46. A representative image of deformable image registration of rectum and bladder. Blue contours represent BT1, yellow BT2 and red represents the D_{2cm3} region.
47. Absolute change in $EQD2_{\alpha/\beta = 3}$ between DA and DDA for all patients for rectum (2a) and bladder (2b).
48. Percentage variation between DA and DDA for biomechanical (3a) and mutual information algorithm (3b). Registration with small and large bladder as the reference frame, and the mean of two registrations, are plotted.
49. The percentage dose difference between DA and DDA for biomechanical (x-axis) and Intensity based DIR (y-axis) algorithms. The correlation coefficient was $R^2 = 0.006$.
50. An example of patient images that shows implausible deformable image registration in rectum and bladder. Panel 5a & 5c : Rigid registration of BT1 and BT2 images for rectum and bladder, respectively. Panel 5b & 5d: Deformation map showing a maximum deformation of 10.7 /11.97mm in the region of anterior rectal/posterior bladder wall, The contour marked in red/magenta is the region of D_{2cm3} in rectum and bladder, respectively.

List of Tables:

Glossary

3D IGABT	Three Dimensional Image Guided Adaptive Brachytherapy
AAPM	American Association of Physicists in Medicine
ABS	American Brachytherapy Society
BED	Biological Equivalent Dose
BT	Brachytherapy
COIN	Conformity Index
CT	Computerized Tomography
CTV	Clinical Target Volume
CV	Coefficient of Variation
D0.1cc	Minimum dose to the most exposed 0.1 cm^3 region
D2cc	Minimum dose to the most exposed 2 cm^3 region
D90	Dose to 90% of HR CTV
DA	Direct Addition
DDA	Deformed Dose Accumulation
DIR	Deformable Image Registration
DPO	Dose Point Optimization
DSC	Dice Similarity Co-efficient
DVH	Dose Volume Histogram
EBRT	External Beam Radiotherapy
EUA	Examination Under Anesthesia
FSE	Fast Spin Echo
GO	Geometric Optimization
GrO	Graphical Optimization
GTV	Gross Tumour Volume
GYN GEC ESTRO	European Group of Curietherapie and the European Society for Therapeutic Radiology and Oncology

HDR	High Dose Rate
HI	Homogeneity Index
HIPO	Hybrid Inverse Planning Optimizatio
HR CTV	High Risk Clinical Target Volume
HS	Help structures
IPSA	Inverse planning Simulated Annealing
MOPT	Manual optimized plan.
MRI	Magnetic Resonance Images
MUPIT	Martinez Universal Perineal Interstitial Template
OAR	Organs At Risk
PDR	Pulse Dose rate
PET	Positron Emission Tomography
T/O	Tandem/Ovoid
T/R	Tandem/Ring
TMH	Tata Memorial Hospital
TRAK	Total Reference Air Kerma
V_{100}	Percentage of volume covering 100% of the dose,

Chapter 1

Introduction

1.1. What is Brachytherapy?

Brachytherapy (BT) is the delivery of radiation dose using radioactive sources positioned at close proximity to the tumour, for treatment of cancer. BT is also referred as curietherapy or endo-curietherapy, and it derives its name from the greek word “Brachus” means “near”. One of the advantages of BT as compared to external beam radiotherapy (EBRT) is that the dose is highly localized to the tumour with a sharp fall-off of dose to neighboring organs at risk (OAR). This was possible due to the physical property of the radioactive sources that follows the inverse square law principle. This property of the radioactive sources has been put in use, very well by brachytherapists, to deliver highly localized doses to the tumour while sparing neighboring critical structures. However, this advantage of brachytherapy also constitutes the very challenge, since large dose gradients give rise to inherent risk that geometric errors cause a large deviation between calculated and delivered doses. Thus, to achieve maximum therapeutic ratio of the treatment, precise localization and treatment planning of tumours is paramount in BT. Since 1900, its clinical use, research has been focused to address the above question, which resulted in the rapid evolution of BT that resulted in the safe delivery of radiation to the patients with modern tools in terms of new radioactive sources [1], applicators [2], imaging [3], dose fractionation [4] and delivery techniques [5] etc. Last decade especially has witnessed a great potential in imaging at the time of BT especially in gynecological tumours that enables visualization of the tumour volume, which improves our knowledge of dose delivered to the tumour and to the OARs.

1.2. History of Brachytherapy

The history of BT dates back to 1898, when Marie Curie extracted radium from pitchblende ore, for which she won Nobel prize in physics in the year 1903 [Fig 1].

Figure 1: Madam Curie and her husband Pierre Curie

Soon after, Radium was used to treat cancer patients. The first patient treated with radium was by Dr. Danlos at the hospital St.Louis in Paris, He treated cases of lupus with radium loaned by Marie Curie (1905). The first treatment of cervical cancer was treated in 1905 and prostate in 1911. After the First World War, BT for cancer patients has become popular with several different schools of practice were created around the world: The Radium Hemmet in Stockholm, the Memorial hospital in NewYork, and in Paris [6]. The Stockholm and Paris methods for intracavitary radiation were described in 1914 and 1919 and during 1930s, the rules of the Manchester system were published. For interstitial radium therapy, Patterson and Parker [7] and later Meredith [8] had developed dosimetric systems with the rules of distribution of radium that ensures uniform distribution. In 1934, artificial radioactivity was discovered by Pierre and Marie Curie's daughter, Irene Curie and her husband Joliot, which opened up a possibility of a new era of BT using artificial radio-nuclides. After the II world war, the access to nuclear reactors has made it possible to produce artificial radioactive sources on a large scale. The traditional Radium sources were replaced by Cobalt-60, Caesium-137, and Iridium-192. One of the advantages of these sources was that the specific activity (Ci/gm) was high, so that the sources could be miniaturized. Originally, Radium was used in pre-loaded needles, where radiation exposure to the personnel was high. Later, manual after loaders came into existence, which improved the implantation technique and also reduced the radiation exposure to the personnel. In the early 1980s, computer controlled remote after-loaders with treatment planning systems were introduced, which does not require manual handling of the radio-active sources. In remote after-loaders, the source is moved by a stepper motor, which completely eliminates the radiation exposure to the personnel. The important landmark in the

history of BT is the use of High dose rate (HDR), where the treatment time is reduced from few hours to few minutes, which improves the patient's comfort to a large extent [9]. Pulse Dose rate(PDR) also was introduced with the principle of delivering short pulses over hours/days in order to match the radiobiological advantages of low dose rate with after-loading capability to reduce the radiation exposure. One of the landmarks, in the BT evolution is the capability to optimize the dose by modulating the source positions and source dwell times. Modern imaging facilities allow more accurate delineation of target volume and the localization of adjacent normal tissue [10-12]. This together with computerized dosimetry and better knowledge of the radiobiology involved, have made BT much more accurate and safe in modern times as compared to the historical times. [13-17]

Image guidance in BT was first introduced using ultrasound images for prostate cancer in 1981[18], and later was used for cervical cancer using Computerized Tomography (CT) and Magnetic Resonance Images (MRI) in late 1980s. However it was performed only in few centers in Europe [19]. In early 2000, the image guidance technology was rapidly used in EBRT; however the use of image guidance in BT is sparse.

1.3. Brachytherapy of uterine cervical cancer:

Cancer of the uterine cervix is the leading cancer among the female population in India [20-21]. In recent decades, an increase of rapidly growing tumours was noticed even in young women. The human papilloma virus (HPV 16/18/31/33) plays an important role in the genesis of cervix cancer and is observed in 90% of all women with cervix cancer[22]. Symptoms are dependent on the stage of disease with no symptoms in early disease and various symptoms such as vaginal discharge and bleeding in advanced disease according to the individual tumour extension. The most important prognostic factors are tumour size, tumour extension and nodal involvement [23].

EBRT in combination with BT forms the mainstay of the treatment, especially BT plays a pivotal role in the management of carcinoma of the uterine cervix. One of the major advantages of using intracavitary BT for cervical cancer, is the implantation of uterine tandem and vaginal ovoids, in naturally occurring body cavities, in a particular geometric fashion so that a high dose is delivered to the tumour with sharp dose fall to spare rectum and bladder. High cure rates have been reported even in patients with locally advanced disease [24]. BT for cervical cancer is generally done using two techniques, largely using intracavitary procedure. Under some special circumstances, where intracavitary is not possible, where tumour is large extending upto the parametrium interstitial implantation is carried out. In the following section a brief description is given about each of this technique.

1.3.1 Intracavitary Brachytherapy:

Intracavitary BT in cervical cancer is based on the application of intravaginal and intrauterine sources in the naturally occurring body cavities [Figure 2]. Different schools have different traditions related to the implantation technique [25]. Some of the popular systems are being Manchester system, which uses Tandem/ovoid (T/O), Stockholm system with Tandem/Ring (T/R) and Paris system with individualized mould technique. The classical Manchester system introduced the famous dose prescription point A, while Stockholm and Paris system used mgRa-hr, (Milligram amount of radium implanted in the patient for a particular duration) for dose prescription. Both point A and mgRa-hr had limitations interms of dose

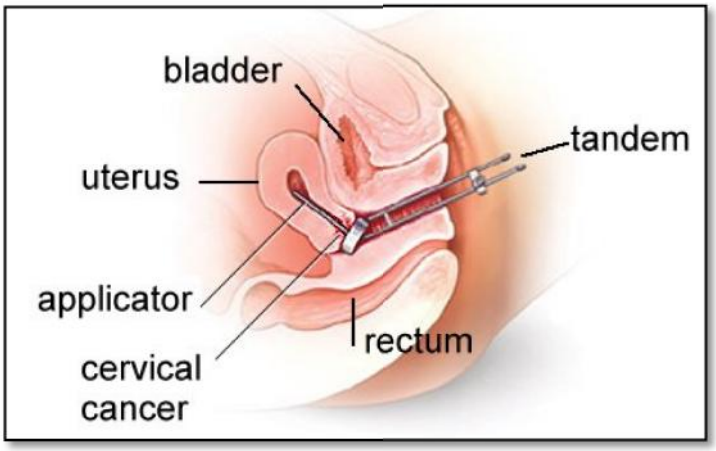

Figure 2: An example of Intracavitary implantation with tandem and ring positioned in the uterus, and the cervix. OARs anteriorly bladder and posteriorly rectum are also shown.

prescription, as it does not correlate to the spatial dose distribution of the dose in the tumour volume. In the year 1985, ICRU 38, report was published which introduced a new concept for dose reporting, 60 Gy volume, the volume covered by the 60Gy isodose line in both EBRT and BT[26]. In the following section, a brief description is given about these different schools of tradition of intracavitary BT.

1.3.1.a. Manchester system:

The Classical Manchester technique was based on using one intrauterine tube with a choice of two standard lengths (4cm and 6cm) and one non standard length (3.5cm) (each tube has a rubber flange at its cervical end to hold the tube in the correct position) and two vaginal ovoids ellipsoid in shape, two small (2cm), two medium (2.5cm), or large (3cm) in diameter held apart in the vagina by a washer or a spacer. Nowadays, uterine tubes with different lengths graduated in centimeters are commercially available allowing for adaptation according to the individual anatomy and angled at varying degrees to the vaginal component [Figure 3]. The classical Manchester system was governed mainly by three rules: a) Define treatment in terms of dose to a point representative of the target i.e., uterus, more or less reproducible from patient to patient. b) Design applicators and their loading to enable the same dose-rate to point 'A' regardless of which combination of applicators is used. c) Define a set of rules dictating the relationship, position, and activity of radium sources in the uterine and vaginal applicators to achieve the consistent dose rates. To define the actual dose delivered in "fixed mg-hr systems" in a more meaningful way, Todd and Meredith began to calculate the dose (in Roentgens) to various sites in the pelvis by defining a series of points anatomically comparable from patient to patient. Obvious sites for dose prescription, such as

Figure 3: Manchester applicator with tandem of different lengths, ovoids and spacers.

cervix itself, were not suitable due to the high dose gradient inherently present in that region. Limiting radiation dose was not the dose to the critical structures, such as the rectum or bladder, but to the area in the medial edge of the broad ligament where uterine vessels cross the ureter. To this pyramid shaped area, the base of which rests on the lateral vaginal fornices and apex curves around the ante-verted uterus, the name "Paracervical Triangle" was given. It was considered that the tolerance of this para-cervical triangle is the main limiting factor in the irradiation of uterine cervix which was the basis for the genesis of point A. The original definition of point A was defined as 2 cm lateral to the uterine canal and 2 cm from the mucous membrane of the lateral superior fornix of the vagina in the plane of the uterus.

The original, definition of point A, in 1938, used a line connecting the superior surfaces of the ovoids as the basis for finding point A [figure 4]. Although point 'A' was defined in relation to important anatomical structures, these cannot be revealed on a radiograph. So point 'A' definition was modified in 1953 and is sometimes denoted as Ao (o stands for external os) [25,27].

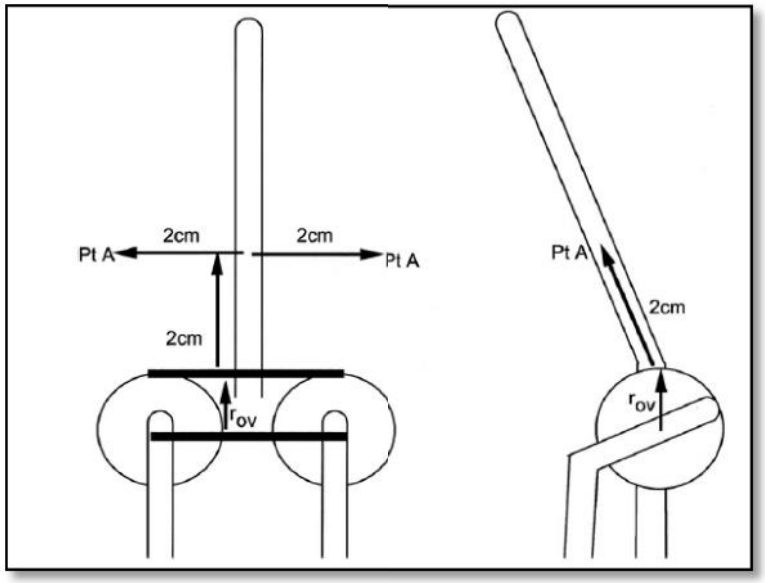

Figure 4: Definition of point A according to ABS recommendations (Picture courtesy: ABS report Reference:30)

Since then, external OS was began to be used as the basis for locating point A for applicators with no fixed relationship between the OS and the superior surface of the ovoids, such as the standard Fletcher applicator. Using the external cervical OS as the base for locating point A results in large variation of the dose at point A for patients undergoing very similar treatments [29]. For this reason, the American Brachytherapy Society (ABS) recommends that point A be defined in relation to the applicator, following the original Manchester definition, which is a more commonly used definition, and also is the recommended definition by the upcoming ICRU 88 [29]. The ABS, in its recommendations for low dose rate BT of cervical cancer retained original Manchester system point A denoted as Ao. For tandem and ovoids, localization of point A can be carried out using radiographs as follows: draw a line connecting the middle of the sources in the vaginal ovoids on the AP radiograph and move 2cm (plus radius of the ovoid), superiorly along the tandem from the intersection of this line with the intrauterine source line and then 2 cm lateral on either side of the tandem [30].

Apart from the para-cervical triangle, recto-vaginal septum and vagina were also considered as the major dose limiting structures in the Manchester system. The tolerance of vaginal mucosa is such that not more than about 40% of the total dose to point A can safely be delivered through the vaginal ovoids and this should be taken into account in planning the differential loadings. Dose to the recto-vaginal septum for any technique should be less than that at point A. Dose to this area can be reduced to less than 80% of the dose to point A by carefully

packing gauze to a thickness of at least 1.5 cm to pack ovoids away from the rectum. The loading pattern of classical Manchester system mimics the radium loading of 20mg, 15+10mg, 15+10+10mg in short, medium and long intrauterine tubes respectively; 22.5mg, 20mg, 17.5mg for large, medium and small ovoids respectively. When the new radioisotopes like ^{137}Cs, ^{192}Ir were used, the source loadings were mimicked for the radium equivalent standard loading pattern, which will be dealt in detail in chapter 3.

1.3.1.b Fletcher system:

In the early 1950s, Fletcher developed a system for Radium that combined a rigid metallic intrauterine tandem with cylindrical colpostats, the latter are positioned against the cervix perpendicular to the axis of the vagina [31]. Subsequently, this system was modified by Delclos and Suit for manual after-loading and then for remote after-loading [32]. The uterine length can be adjusted by an adjustable flange [Figure 5]. The intrauterine tandem is available in a variety of curvatures. The cylindrical colpostats are available in various diameters: 2.0, 2.5 and 3.0cm. Tungsten shielding was integrated into the anterior and posterior part of the standard colpostats to reduce the dose to bladder and rectum. The amount of radiation is expressed as a product of activity and treatment time and is limited by anatomical considerations and by the volume of disease and selected treatment schedule. Variations in the loadings selected for the tandem and colpostats are based on anatomical considerations. The doses to various points representing paracervical areas, regional node (Fletcher Trapezoid), vaginal mucosa, bladder, rectum and other structures were

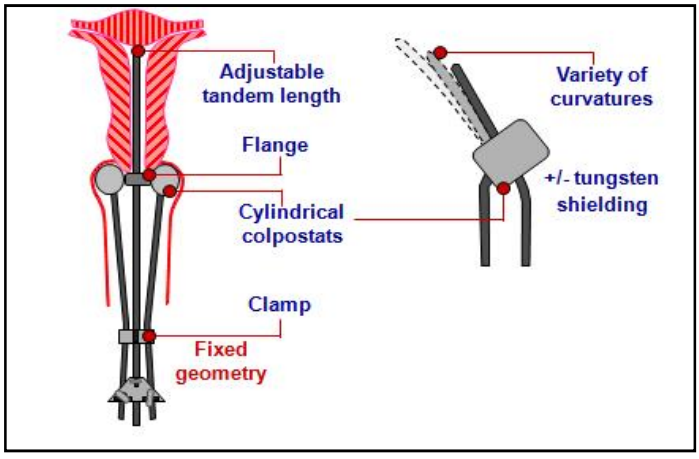

Figure 5: A typical Fletcher applicator showing tandem of various curvatures and ovoids with tungsten shielding. Picture courtesy: Primoz Petric, Ljubljana.

calculated from the orthogonal radiographs. With this system, the length of the intrauterine tandem, the size of the vaginal ovoids and the position of the system in the pelvis significantly influence the dose distribution. To maximize the depth dose, the whole length of the uterine canal is usually loaded with the largest ovoids that can be used without inferior displacements of the applicator and fitted in the vagina. The loading pattern is similar to Manchester loading pattern.

The modified Fletcher method follows the same dosimetry guidelines of the classical Fletcher system. However the dose is prescribed in terms of Total Reference Air Kerma (TRAK), which depends on the tumour volume and its location. An integral part of this system is to adapt the volume to take into account of dose volume relationships of organs at risk as well as of the target. A volume adaptation is performed for each individual patient. Knowledge of the dose distribution in a particular patient is based upon the anatomic, tumoural and implant parameters as identified on the two orthogonal films taken at the end of the implant. Dose is calculated at various points such as cervix, bladder, rectum nodes and pelvic walls. These parameters, in addition to 60Gy reference volume are recorded and reported according to ICRU 38 recommendations.

1.3.1.c. Stockholm system:

The classical Stockholm method was based on a flexible intrauterine tube and a flat box (plate) in the vagina pushed by an individual packing device against the cervix. The tube and the box were implanted independently of each other. Therefore no fixed geometry was present. The rigid uterine tandem with a ring applicator was developed during the 1960s as an after loading device [33]. The length and the curvature of the intrauterine tandem is chosen dependent on the size and the bending of the uterine cavity. The diameter of the ring which is perpendicular to the axis of the intrauterine tube is also chosen according to the individual anatomical situation

[Figure 6]. The ring is covered by a cap for reduction of the dose to the vaginal mucosa. The ring is fixed to the intrauterine tandem. The angle between the ring and the tandem is always 90°. The angle between the ring and the axis of the vagina is selected according to the angle between the axis of the vagina and the uterus. In this system, the standard loading pattern is based on the Manchester/Fletcher loading. The dose is prescribed to point A. ICRU 38 rectal and bladder point are considered as the dose limiting structures.

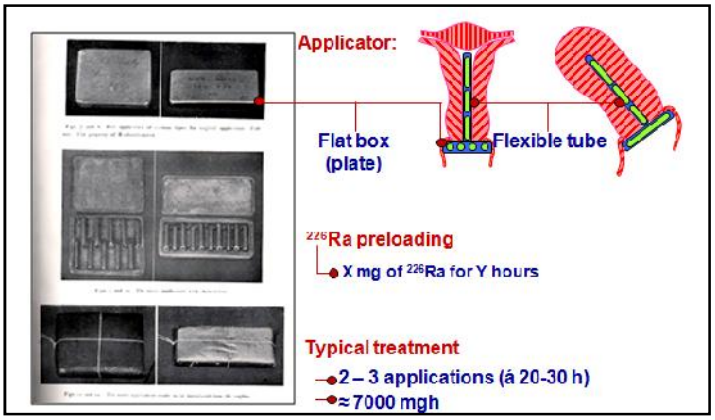

Figure 6: Stockholm system. Picture Courtesy: Primoz Petric, Liubliana

1.3.1. d. Paris system / Institut Gustave –Roussy technique:

The classical Paris method was based on two corks (ovoids) situated in each lateral fornix perpendicular to the intrauterine tube connected by a transverse metal spring and independent of this, a hollow gum elastic tube in the uterine cavity [figure 7] [34]. Later, a vaginal cork was sometimes used to ensure a more uniform dose distribution in the cervix. It typically uses three intrauterine tubes (10 +10 +15 mg) and 2 vaginal tubes (15 +15 mg), and the application lasted for six days. The ratio of the total activity of the vaginal sources to the total activity of the uterine sources should be 1 (with variations between 0.66 and 1.5). As far as the method of application is concerned, the historical Paris system does not imply any

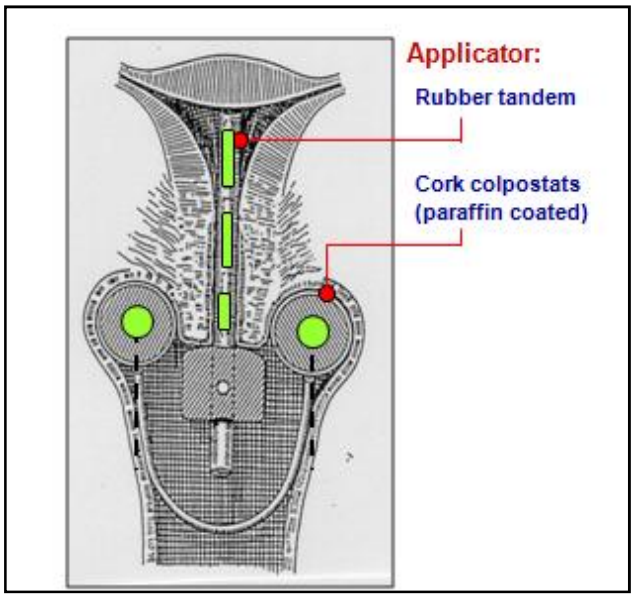

Figure 7: Paris system applicator showing the tandem and the vaginal colpostats.

fixed distance between the vaginal and uterine sources.

The Manchester and Fletcher based techniques are in regard to their application techniques related to the original "Paris Method". The other technique developed in Paris have much advanced and individualized approach called the moulage (molded) applicator [Figure 8]. This method developed at the IGR has four basic aims: personalized tailored irradiation, perfect knowledge of dose distribution, total radiation protection, and good tolerance by the patient. A brief description of the fabrication of the mould is as follows: First the cervico vaginal impression is taken by inserting the liquid paste into the vagina. It is then removed from the vagina after the solidification. This was used for making the acrylic mold. Vaginal catheters are placed in this mold by taking into account the tumour topography. The two catheters must be parallel to the anterior superior surface of the mould (parallel to the surface of the cervix) lateralized to the left and the right part of the cervical lip, parallel to each other, and separated by a distance equal to the mean length of the two vaginal sources. The two vaginal catheters are introduced and fixed on the internal surface of the molded applicator. The final preparation of the mould includes, one hole for the cervical OS, an indication for the external meatus of the urethra, and other perforations to fix the mold to the vaginal wall and to allow circulation of the liquid antiseptics for the daily vaginal irrigation with liquid antiseptics. These perforations eliminate the risk of displacement of the device, the vaginal mucosa hernitaes through each perforation. No vaginal packing is necessary, as the packing is integrated into the mould applicator keeping the catheters in place at the same position and keeping the same topography throughout the treatment duration. With this

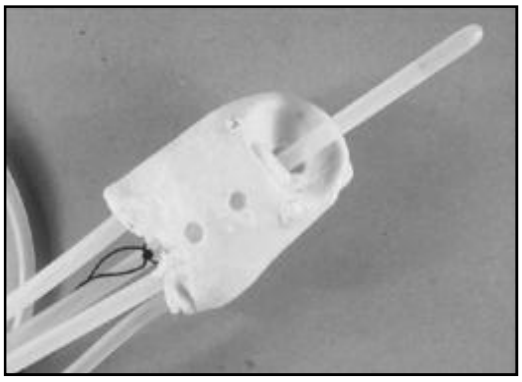

Figure 8: A typical mould applicator showing the tandem and the customized vaginal impression with plastic catheters. Courtesy: GEC ESTRO Handbook of Brachytherapy.

applicator, the patient can move out of the bed without risk of displacement of the material and the complications of prolonged bed rest.

The positioning of the sources is dictated by the anatomy of the patient and the topography of the tumour. Individually selected lengths are used for the sources, from 16-88mm with steps of 8mm. The vaginal sources most often used are 34, 32, and 40mm. Position and length can be modified when check films are taken. The decision of treatment duration depends on the applicator geometry, patient anatomy, tumour topography and the dose to critical organs and ICRU points. A dose of 60Gy is delivered to the reference isodose. TRAK is reported for the entire treatment BT treatment.

1.3.2. Interstitial Brachytherapy:

Interstitial BT refers to the implantation of radioactive sources directly into the affected tissue. Interstitial BT used in various sites eg. prostate, soft tissue sarcoma, head and neck etc. In gynaecological BT, interstitial technique is used when intracavitary is not possible for various indications such as narrow vagina, large tumour with parametrial extension, prior hysterectomy primary or recurrent vaginal cancer [35-40].

The aim of this technique is to tailor the dose of irradiation to the anatomy of the patient with a better target volume coverage, especially at the center of the implant with the intracavitary component, while delivering the homogeneous dose to the lateral parametrium. This technique can be done with or without the central tandem in place. Originally, interstitial implants were performed with free-hand placement of the radioactive needles [41]. The development of trans-perineal [35] or trans-vaginal [36] templates resulted in a better needle positioning. Different templates were designed in order to get a better target volume coverage. Two main perennial templates types have been used: the Martinez Universal Perineal Interstitial Template (MUPIT)

[43] Syed Neblett [37] . The use of Syed Neblett template is slowly declining with the use of HDR machines, while MUPIT template has become popular.

Newer imaging techniques including fluoroscopy [44], CT [45], trans-abdominal or trans-rectal ultrasound [46], MRI [47], have improved the needle placement accuracy. Despite an improvement in the technological approach of these techniques, the potential benefit of interstitial BT in gynecological malignancies has not been clearly demonstrated. This technique is associated with a potential increase in the risk of complications as compared to Intracavitary BT [48]. One reason for this is, in interstitial BT, the sources are in direct contact with the tissue, and hence it is important to keep the volume of high dose region to a minimum to avoid tissue necrosis. High dose volumes and dose homogeneity within the implant can be controlled by rules laid down by some of the popular systems like Paterson parker, Quimby [49] and Paris [50]. It is very important to follow these rules to produce a uniform distribution, and to keep the high dose region minimum, which is clinically acceptable. In the following section, we will see in brief about each of these applicators, its benefits, limitation and challenges associated with them.

1.3.2.a: MUPIT applicator:

The MUPIT [43] [Figure 9] was designed to treat not only gynecological malignancies but also prostatic, ano-rectal and perinneal tumours. This applicator consists of two acrylic cylinders, one acrylic template and a cover plate. The template has arrays of holes used as guides for the needles. Guide holes are designed to allow the inserted trocars lie in parallel horizontal planes, perpendicular to the template plane, insuring an adequate geometry of the application. The planes are spaced vertically one cm apart. The distal guide holes are angled 13° laterally, outward to allow a wider coverage of the external part of the tumour, especially parametrial involvement. The 17-gauge needles are stainless steel with a blinded end. Lateral, anterior and posterior limits of the tumour are determined with the corresponding selection of the location of

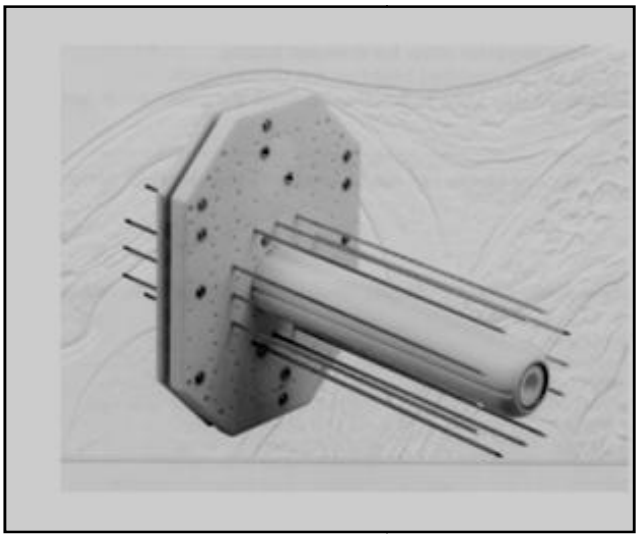

Figure 9: MUPIT applicator, Courtesy: GEC ESTRO Handbook of Brachytherapy

the guide holes in the template. The superior and inferior tumoural limits determine the depth to which the guide needles must be inserted. The cylinder length in the vagina is identified according to physical examination.

The implants are done under spinal anesthesia in the operating room. Hollow plastic/stainless steel catheters are inserted through the perineum, guided with ultrasound or fluoroscopy to fully encompass the tumour. The catheter placement is secured by a rubber template which is sutured against the perineum to ensure positioning accuracy of the template with respect to the anatomy. The patient is transferred to the recovery room and following recovery, transported to the CT simulation room, followed by treatment planning and delivery. In the MUPIT template system, the loading depended on the extent of the tumour.

Historically, the treatment planning was carried out based on the pair of orthogonal radiographs. Last decade, the introduction of CT imaging in radiotherapy departments has contributed to image based treatment planning for MUPIT based interstitial BT, which has improved the dosimetry and quality of treatment planning to a great extent. Dose prescription points are defined considering the Paris system rules, where the dose points/normalization points are considered as basal points. The dose is normalized on these points followed by geometric/dose point optimization, which delivers the uniform dose distribution in the implanted volume. Erickson et al [36] described a technique based on CT images allowing the definition of criteria to select an appropriate reference isodose. These criteria included: to avoid a dose rate gradient across the implant greater than 20%, in the central plane the isodose surface (whose

value is <125% of the reference isodose) should not be contiguous and its dimensions should be less than two by two cm, the diameter of the hyperdose sleeve (two times the reference isodose) should be less than one cm. With this approach, dose rate gradients higher than 20% across the central plane of the implant were avoided in the majority of the implants. The details of new optimization tools, inverse planning for interstitial BT are dealt in detail in chapter 3.

1.3.2.b: Combined intracavitary and Interstitial Brachytherapy:

Conventionally, for cervix cancer BT, only intracavitary applicators were used, which produce dose coverage of 4cm width at the level of point A. However, if the tumour is large, more than 4cm at the level of point A at the time of BT, then, the dose coverage is inadequate if a standard intracavitary plan with prescription to point A is applied. Adaptations to larger volumes can partly be performed but are limited to the fact that prescription to a larger volume will increase the dose to the OARs. By inserting interstitial needles through predefined holes in the ring applicator, the dose could be further shaped allowing, an increase of dose in the proximal to middle third of the parametrial space without significantly increasing the dose to the organs at risk. For appropriate coverage of tumours, which are larger at the time of BT, a novel system of intracavitary and interstitial applicator was introduced by Kirisits et al [2] [Figure 10]. This applicator has a facility to implant additional needles along with intracavitary component, which can treat a tumour of up to 6.5cm in width at the level of point A, while respecting the OAR tolerance.

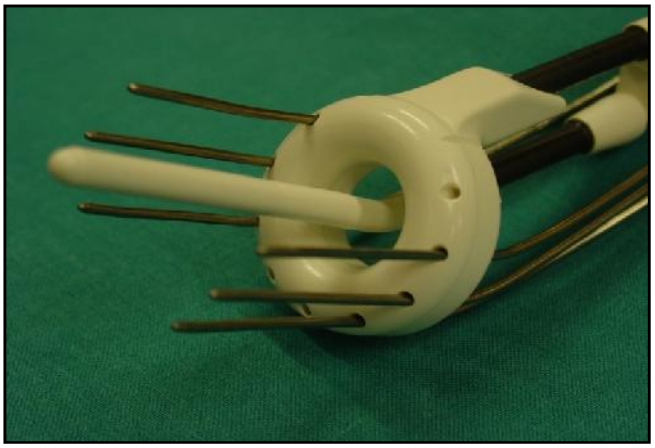

Figure 10: Vienna applicator with additional needles placed in the ring. Courtesy: Christian Kirisits, MUW.

This device is based on a commercially available CT/MRI compatible tandem ring set Nucletron, Veenendal, The Netherlands). This applicator has holes of 2-mm diameter

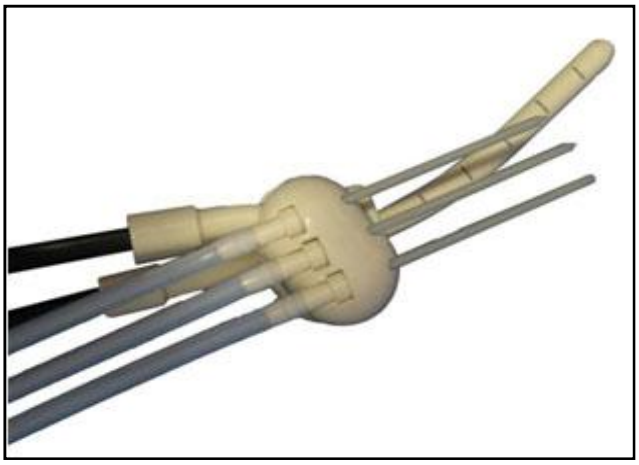

Figure 11: Utrecht applicator with catheters inserted in ovoids. (Picture Courtesy: Nucletron, An Elekta company)

drilled parallel to the ring axis with their axis at a distance of 2 mm from the outer ring surface. The number of holes drilled depends on the ring diameter: six holes are drilled for the 26-mm ring (outer diameter, 38.5 mm) and nine holes for the 30- and 34-mm ring (outer diameter, 42.5 mm and 46.5 mm). In terms of a clockwise representation, this corresponds to needle positions at 8, 9, 10, 11, 12, 1, 2, 3, 4 o'clock (8, 10, 11, 1, 2, and 4 o'clock for the 26-mm ring). At the 5 and 7 o'clock positions, no hole has been drilled; instead, an incision was drilled to guide the needle along the outer ring surface. Figure 10 shows an image of the tandem/ring with needles and a drawing for a 34-mm nominal diameter ring. The needles used in this approach are made of titanium with a length of 20 cm (Acrostak Corp., Winterthur, Switzerland). The tip of each needle has to be blunt and not trocar tip. The use of such a type of needle in combination with an open MRI has been described by Popowski *et al.* [47]. A similar applicator design was made by University Medical Center Utrecht in cooperation with Nucletron Veenendaal, The Netherlands for T/O applicator type [51][figure 11]. This applicator is a renewed version of the CT/MR applicator (tandem-ovoid) and provides the additional possibility to apply MRI-compatible plastic bold/sharp needles. These MRI compatible applicators are without internal shielding, unlike the original Fletcher technique. A needle guiding system, consisting of guiding tubes anchored in drilled holes through the ovoids, is used for needle placement. Each ovoid (having different sizes with 20, 25, or 30 mm of distance between the source channels) contains five needle holes in a 15 angle so that the needles are more or less parallel to the tandem. As many as 10 needles can be inserted, and insertion depth is variable.

Chapter 2

Literature Review and Transition from 2D to 3D Image based Brachytherapy.

2.1. Limitation of 2D orthogonal radiograph based dosimetry and rationale for transition:

Conventionally, BT planning was carried out by means of a pair of orthogonal radiographs [Figure 12] The major limitation of the conventional imaging modalities is the lack of information on the tumour volumes and OARs, however in MRI the tumour and the OARs can be visualized clearly [Figure 13]. In ICRU 38, point doses are calculated for rectum and bladder according to ICRU 38 recommendations, which uses surrogate markers to locate these points. But, these point doses may not represent the dose received by the volume of the organs [52-58]. Due to which the doses to the OARs were not known accurately, hence the treatment related side effects / toxicities were high [59]. In addition, tumour cannot be seen in the radiographs, hence local control of the disease also was a challenge especially in large tumours[60]. Another major limitation of conventional BT planning is that the treatment strategy is not individualized based on the response of the tumour. However, with the new imaging modalities, it is now possible to adapt the dose by assessing the tumour response and individually tailor the dose to the patients. In the following section, the limitation of 2D BT is described in detail.

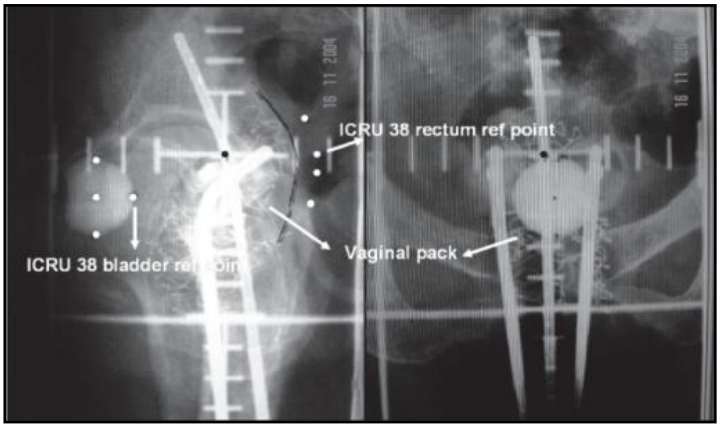

Figure 12: A pair of orthogonal radiographs where ICRU 38 bladder and rectal reference point are shown.

2.2. Dose to the tumour volume:

Conventionally, Point A was used as a dose prescription point, which is considered as the representative point of the tumour volume. However this point has many limitations to be clinically used, for example, point A is related to the source and not to any specific anatomic

structure. Point A does not take into account the tumour volume, depending on the size of the cervix, point A may be inside or outside the tumour. Further, Point A is very sensitive to position of ovoid sources relative to tandem, which should not be deciding factor in deciding on the implant duration.

On the other hand, in 3D image based dosimetry, the dose is sculpted to the tumour volume – (High Risk Clinical Target Volume HR CTV) which represents more accurately the dose delivered to the residual tumour at the time of BT. The relation between the dose to point A and the HR-CTV D_{90} depends largely on the HR-CTV volume [61-63]. For small tumours, the point A dose is lower than the HR-CTV D_{90}, whereas for large tumours the point A dose is higher than the HR-CTV D_{90}. The HR-CTV D_{90} typically varies between 60% and 150% of the point A dose. Although the point A dose cannot be used to predict the target dose in individual patients, it provides a reasonable estimate of the average HR-CTV D_{90} for a large patient population. Therefore, it is recommended to report the dose received by point A, while prescribing the dose to HR-CTV in 3D image based BT. In complicated 3D IGABT (Three Dimensional Image Guided Adaptive Brachytherapy) intracavitary and interstitial plans, standard loading point A plan would be the starting plan followed by optimization. Point A also allows comparison between different approaches, it also acts as a link to non-3D image based approaches, serves as a quality assurance parameter along with TRAK. Since point A is a good representation of "an average position" of the tumour, it is possible to make a safe transition from 2D to 3D without any

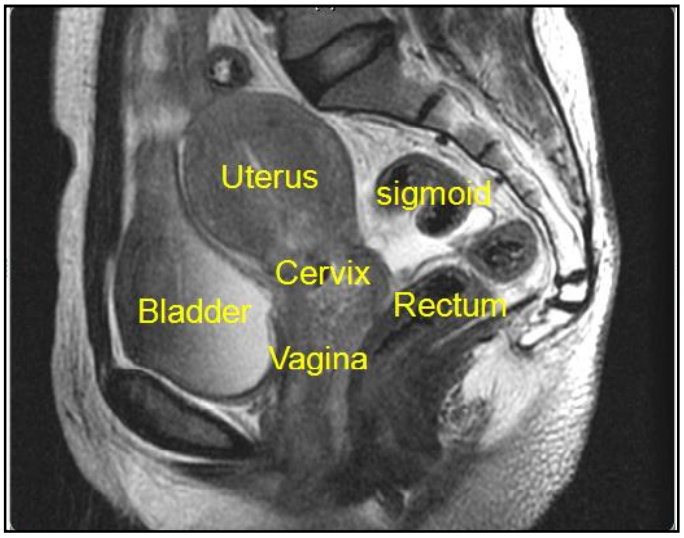

Figure 13: A typical saggital view of a MR image where visualization of the tumour, OARs is superior as compared to conventional imaging modality – orthogonal radiographs/CT.

major changes in the dose prescription system. In some traditional systems, the dose was prescribed to a reference isodose volume, or 60Gy isodose line, which would be equivalent to dose to Intermediate Risk Clinical Target Volume (IR CTV) in 3D IGABT [64]. This further indicates that all conventional systems will have a parameter, which could be comparable with the new concepts, which will improve the confidence while implementing the new dose prescription methods.

Concerning the dose to the lymph node, the dose delivered through the external beam radiotherapy is high as compared to BT. According to Manchester system, the dose delivered to the lymph nodes by BT, is represented by point B, which is located 3cm lateral to the point A. However point B poorly correlates to the dose received by the lymph nodes [66]. In the year 1985, ICRU 38, published new recommendations of dose reporting to the pelvic wall points and lymphatic trapezoid from the orthogonal radiographs. However, these points were not popular and scarcely reported.

2.3: Dose to the OARs

The most common OARs in 2D BT are rectum and bladder, which are identified by means of surrogate points in radiographs. Other OARs like sigmoid [58] and small bowel cannot be visualized in radiographs. In 3D IGABT, the common OARs include, rectum, bladder and sigmoid. However, in some patients, part of the small bowel also is considered as the OAR. Very, recently, the research is focused on the dose to the vagina [67-76]. New recommendations regarding dose reporting points, uncertainties associated with it have been published [77]. The ICRU 38 rectal and bladder point have been very popular, due to its simplicity of identifying in the radiographs, reproducibility, and most importantly, represent the dose received by the organs, although bladder point underestimates the dose marginally.

The rectal reference point was located at 5mm behind the posterior vaginal wall on the anterio-posterior line drawn from the center of the vaginal sources. The posterior vaginal wall may be visualized by means radio-opaque gauze packed in the vagina or by vaginal retractor. Rectal markers inserted in the rectum may not accurately estimate the dose received by the anterior rectal wall [78]. The bladder is point is identified by means of a foleys catheter filled with 7cc of radio opaque fluid. The catheter is pulled outwards and fixed to bring the balloon in contact with the bladder neck.

2.3.a. Dosimetric evaluation of rectum and bladder using CT planning and orthogonal radiographs:

One of the major advantages of 3D IGABT is the accurate quantification of doses received by various volumes of OARs. However, it must be acknowledged that the traditional methods of planning such as 2D orthogonal dosimetry have yielded high control rates of the tumour and acceptable complications of the normal tissues. However, a more accurate understanding of the doses received by the dose-limiting structures may contribute in improving the therapeutic ratio, both in terms of treatment outcome and reducing the complications further. In addition, with three-dimensional planning, it may be possible to evaluate the dose-volume response relationship by assessing the composite doses of both EBRT and BT. It has been reported that the ICRU point doses do underestimate doses received by the rectum and bladder [52-58]. The ratio of maximum dose to the rectum and bladder from the CT planning to that obtained from radiograph-based planning has a wide range [52-58]. In order to document, validate and compare volume based doses to rectum and bladder with the conventional standard ICRU 38 rectal and bladder points, we undertook this dosimetric study [57] as a part of the transition from 2D to 3D BT at Tata Memorial Hospital (TMH).

Patients with FIGO stage IIB or IIIB of carcinoma of uterine cervix treated between May 2004 and February 2005 with radical radiation therapy and HDR BT were studied. Twenty-two applications consisting of 12 IIB and 10 IIIB of HDR ICA were analyzed. Four patients of IIB and 6 patients of IIIB were included in this study. All the patients were treated with standard dose of external beam radiotherapy, followed by HDR BT according to the institutional protocol.

Orthogonal radiographs were taken on a conventional simulator (Varian, Palo Alto, USA) with radio-opaque markers in the applicators. Orthogonal radiographs were reconstructed and the treatment planning was done using PLATO planning system (BT v14.3, Nucletron, Veneendal, The Netherlands). Source positions were loaded according to the standard loading pattern and point-A plan was generated. Bladder and rectal reference points were identified according to ICRU 38 recommendations [26]. In addition to the ICRU rectal reference point, two additional rectal points were defined at 1 cm superior and inferior to the ICRU rectal reference point based on our earlier report [79]. Dwell positions were optimized to minimize the dose to rectal and bladder points.

Table 1: Dose received by ICRU reference point from orthogonal radiograph based plan and D_{2cc} from image based CT plan for bladder and rectum.

Organ	Volume (cm^3)	D_{2cc} (Gy)	Dose to ICRU point (Gy)	V_2 (cm^3)	D_{2cc}/Dose to ICRU ratio
Rectum	60 (±28)	5.2 (±1.2)	4.6(±1.3)	6 (±1.7)	1.11(±0.2)
Bladder	138 (±41)	7.1 (±1.9)	4.6(±1.4)	20.8(±6)	1.56 (±0.6)

D_{2cc} is the dose received by the $2cm^3$ of the volume of the critical structure receiving maximum dose in CT based planning and V_2 is the volume of the critical structure receiving dose more than the ICRU reference point dose.

All the patients were simultaneously taken up for CT planning. CT scans of 5-mm slice-thickness were obtained. Rectum, bladder and sigmoid were delineated. Treatment planning was carried out using PLATO (BT v 14.3, Nucletron, The Netherlands) planning system. Point A, ICRU rectal and bladder reference points were identified on CT planning. For each

application, the corresponding optimized source positions used in radiograph-based planning were duplicated for CT image-based planning. For quality assurance purposes, shift in point A, location of dwell positions in tandem and ovoids with respect to the applicator origin (flange) were evaluated. A variation of ±2 mm shift was set as acceptability criteria.

The dose volume parameters D_{5cm3}, D_{2cm3}, $D_{0.1cm3}$, were evaluated for rectum and bladder and were compared with ICRU rectal and bladder point. The results of this dosimetric study indicate that, the dose to ICRU rectal point from the radiograph-based planning was similar to that of CT planning [Figure 14].

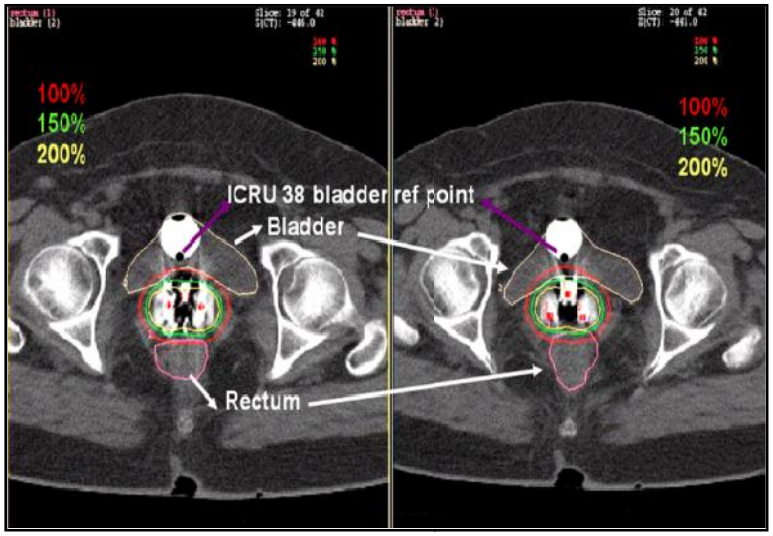

Figure 14:Figure showing that theICRU bladder point underestimates the maximum dose received by the bladder wall.

Mean D2cc of rectum was found to be 1.11 ± 0.2 times the mean ICRU rectal reference point, suggesting that there was no significant difference between the radiograph based ICRU rectal point and CT-based estimation of the parameter D_{2cc} (Table 1)[54, 80] . For bladder, the results of the present study suggest that the ICRU bladder reference point does not correlate with the maximum dose from the CT planning. Mean D_{2cc} of bladder was found to be 1.56 ± 0.6 times the mean ICRU bladder reference point. These results agree with the other studies published in the literature, where the ICRU bladder reference point underestimated the maximum dose by two to three times [12, 15, 16, 19].

2.3.b. Dosimetric evaluation of sigmoid using CT planning and orthogonal radiographs:

Patients treated with 2D orthogonal based BT for cervical cancer have been reported with high symptomatic grade III radiation proctitis and cystitis which are difficult to manage. The incidence of mild to severe late rectal toxicities ranges from 5 to 30% in HDR BT series [82].

This is dependent on doses to rectal point/s and the incidence is higher when the doses delivered are more than 100 Gy (BED-Biological Equivalent dose). However, despite rectal doses within tolerance limits and reduction in BT doses, many patients still develop symptomatic radiation proctitis [84]. Endoscopy in these patients invariably shows telangiectasia or ulceration of rectal/recto-sigmoid mucosa of varying grades. These changes are usually seen at a higher level than the ICRU 38 rectal point/s, challenging the conventional point-based BT dosimetry practice [85]. It is well recognized that sigmoid and upper rectal part of the anatomy is not visible in the radiographs [86]. So, it is imperative to identify and modify parameters, which directly predict or correlate with late toxicities in long-term survivors. This was the motivation behind this investigation where we identified additional rectal and sigmoid points and document doses to these points on CT based ICA-HDR BT planning, with an aim to explore a reproducible upper rectal and sigmoid point in orthogonal radiograph based dosimetry and to study and review the intracavitary dosimetry planning strategy.

Patients with stage IIB or IIIB cervical cancers treated with radical radiation therapy and HDR BT were studied. A total of 15 HDR BT applications that had undergone both conventional orthogonal X-ray and CT based planning were selected and studied. Routine orthogonal radiographs were taken for planning and treatment (Sunrise Plato Planning System (Nucletron). Planning was done conventionally and dose was prescribed to point A with 7 Gy per fraction. On the orthogonal films, the dose points (point A, bladder and rectal points) were

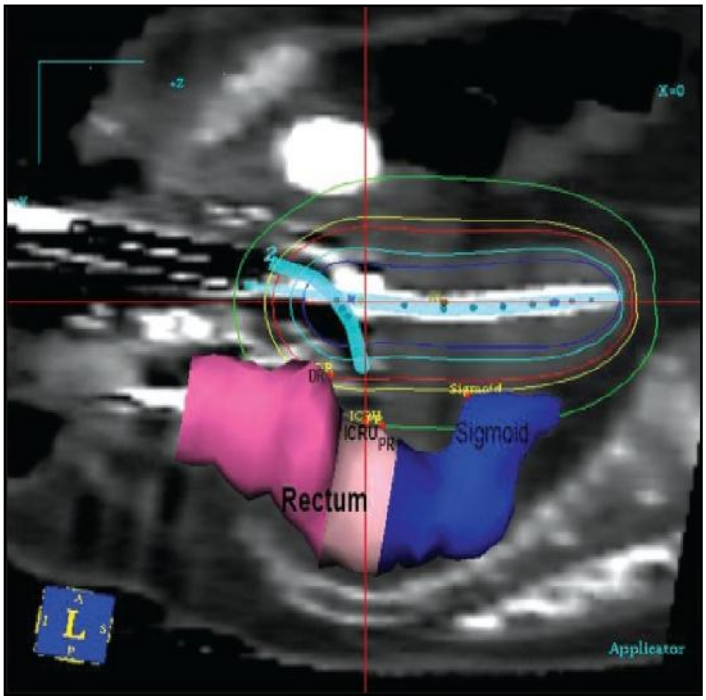

Figure 15: 3D view of catheter reconstruction showing International Commission on Radiation Units and Measurement rectal, additional rectal and sigmoid points.

defined by the ICRU 38 recommendations. All the patients underwent CT imaging followed by treatment planning in 3D PLATO BT V 14, (Nucletron). After catheter reconstruction, for each application, the corresponding optimized dwell positions and dwell times used in 2D planning were duplicated for 3D planning. The external contour of the OAR, viz. rectum and sigmoid in the pelvis, was delineated CT images . In addition to the ICRU 38 recommended rectal and bladder points, additional proximal and distal rectal and sigmoid points in the high-dose regions on dose volume histogram (DVH) and in close proximity to the uterus were digitized randomly on each axial CT slice. Of all these points, the maximum dose point/s were identified, compiled and compared. We also identified the most commonly appearing high-dose region points in rectal (other than ICRU point) and sigmoid regions and document their spatial distribution in relation to the flange (at the level of external os) [Figure 15] . The locations were tabulated in x, y and z axes, with the applicator flange as the origin of these three axes. The x axis represents left (+) or right (-) of the applicator central axis, the y axis denotes posterior (+) or anterior (-) to the uterine tandem, while the z axis represents cranial (+) or caudal (-) to the applicator flange.

In an attempt to define the high-dose point regions with respect to the HDR BT applicator, we compiled and extracted these points receiving maximum dose for proximal rectal (PR), distal rectal (DR) and sigmoid for each application [Table 2]. The additional DR points were located in the median position without any lateral displacement, 20 mm (mean) (range -24.6 to 29.5 mm) posterior to the applicator axis and -9 mm (range -14.5 to -5.8 mm) caudal to the flange of uterine tandem. Similarly, the additional PR points were situated within a mean of 30 mm (range 20.8-41.0 mm) posterior to the uterine axis and 2 mm (range -11.4 to 15.9 mm) cranial to the flange without any lateral displacement, while the sigmoid points were at a mean of -8 mm (range -23 to 10.4 mm) lateral, 10 mm (range -15.9 to 27.8 mm) posterior and 31 mm (range 8.1-62.9mm) cranial from the applicator flange. The mean ICRU rectal point dose did not significantly differ from the PR and DR point doses ($p=0.076$ and $p=0.337$, respectively).

However, the mean sigmoid point dose was significantly higher than the ICRU rectal point doses (p=0.001), the PR (p=0.000) and DR point doses (*p*=0.000). This pattern can be explained by the relative fixed anatomy of rectum and close anatomical proximity of sigmoid to the intrauterine sources, as evident in Figure 16. The sigmoid point doses were higher in more than 90% of the applications, suggesting a need to optimize the BT plans to reduce sigmoid doses.

We also attempted to identify the exact location and reproducibility of these sigmoid points in relation to the flange for extrapolation to orthogonal radiographs. In our dosimetric analysis, the sigmoid points were at a mean of -8 mm (range -22.95 to 10.43 mm) lateral, 10 mm (range -15.87 to 27.82 mm) posterior and 31 mm (range 8.08-62.91 mm) cranial from the applicator flange. But the wide variation and no specific reproducible point limits our endeavor to extrapolate these on orthogonal planning radiographs[Figure 16]. Identification of these sigmoid points on conventional orthogonal X-rays still remains a challenge. Sigmoid points receive significantly higher doses. No definite conclusion on reproducible spatial distribution on orthogonal X-rays could be achieved. To document and reduce sigmoid doses, some form of 3D image based planning for BT is necessary.

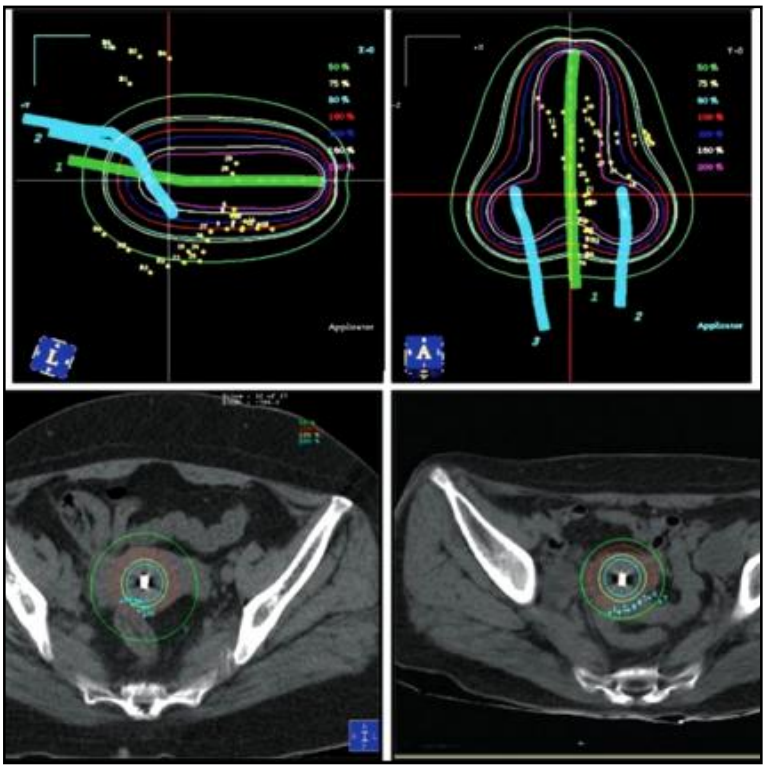

Figure 16: Pear-shaped isodose distribution, ICRU rectal, additional rectal and sigmoid point doses.

None of the reports in the literature address the issue of sigmoid points, their doses and spatial distribution on X-ray based

dosimetric studies although it has been addressed to some extent by DVH parameters and clinical outcome recently [63,87].To validate our findings of high doses to these additional rectal and sigmoid points, we are doing a retrospective analysis of detailed endoscopic findings of patients with grade III radiation proctitis and BT planning details.

***Table 2**: Spatial distribution of additional proximal and distal rectal and sigmoid points receiving maximum in two dimensional orthogonal radiographs. (PR and DR are proximal and distal rectal points).*

Points	Mean (mm)	Median (mm)	Range (mm)
Distal rectal (mm)			
DR_x	0	0	0
DR_y	20	21	-24.6 to 29.5
DR_z	-9	-9	-14.5 to -5.8
Proximal rectal			
PR_x	0	0	0
PR_y	30	30	20.8 to 40.97
PR_z	2	2	-11.4 to 15.9
Sigmoid			
Sigmoid_x	-8	-7	-22.95 to 10.4
Sigmoid_y	10	13	-15.9 to 27.8
Sigmoid_z	31	30	8.1 to 62.9

2.3.c: Dosimetric evaluation of vaginal doses

The vaginal wall, as an organ at risk, is a new concept, was not within the scope of most of the literature of modern times [67-76] . Conventionally, according to Fletcher system, the tolerance dose to the vaginal mucosa was 100-120 Gy. However, there is no general dose dependence structure for vaginal morbidity, such as fibrosis, vaginal atrophy, thinning, telengeectasia, and decrease in elasticity.

Finding applicable dose limits to this organ can improve the quality of life for patients. This could be of even more importance when changing the practice from 2D to 3D image based BT that includes changes in the dose prescription, applicators etc. Traditionally, T/O applicators are used in TMH. When T/R applicator was procured we carried out this study, to estimate the

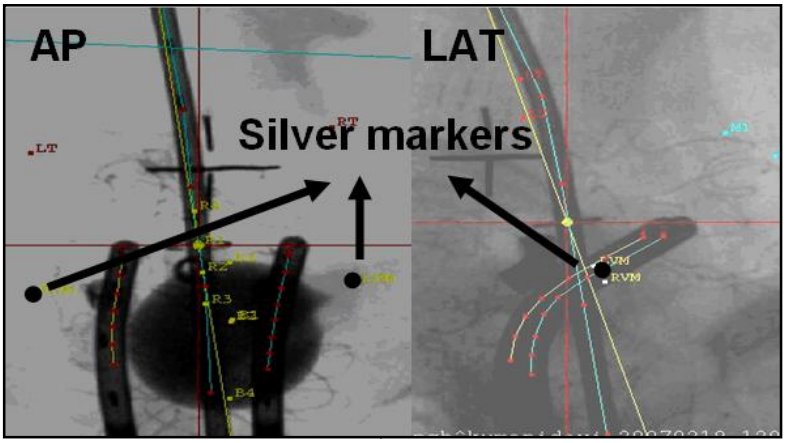

Figure 17 : Vaginal implanted markers on the surface of the ovoid visible on the ortzhogonal radiographs.

dose to the vagina. Although, used in routine clinical practice, there is a general thinking that vaginal doses with T/R applicator are higher with reported literature sparse. With an aim to estimate and compare vaginal mucosal doses received by T/R with T/O applicator we undertook this dosimetric study.35 patients treated with HDR Intracavitary BT using Nucletron standard T/O and T/R applicators for carcinoma of cervix were evaluated retrospectively. The nominal length of the tandem was 40mm, 50mm and 60mm with diameter of the ovoid 15mm, 20mm and 25mm, while T/R applicators with tandem length of 40 mm, 60 mm and ring diameter of 26 mm, 30 mm, and 34 mm with various curvatures (30°, 45°, 60°) was used. Silver markers were placed on the centre of each of the ovoid and the lateral surface of the ring before each procedure as shown in [figure 17&18]. Point A normalized plan was carried out for all the applications. Orthogonal radiographs based planning was carried out for T/R applicator on sunrise Plato (Nucletron) planning system. Doses to the vaginal mucosa for T/O applicator were assessed using the silver markers placed on the ovoid. Doses to the vaginal mucosa for T/R applicator were assessed by defining three points symmetrically on the surface of the

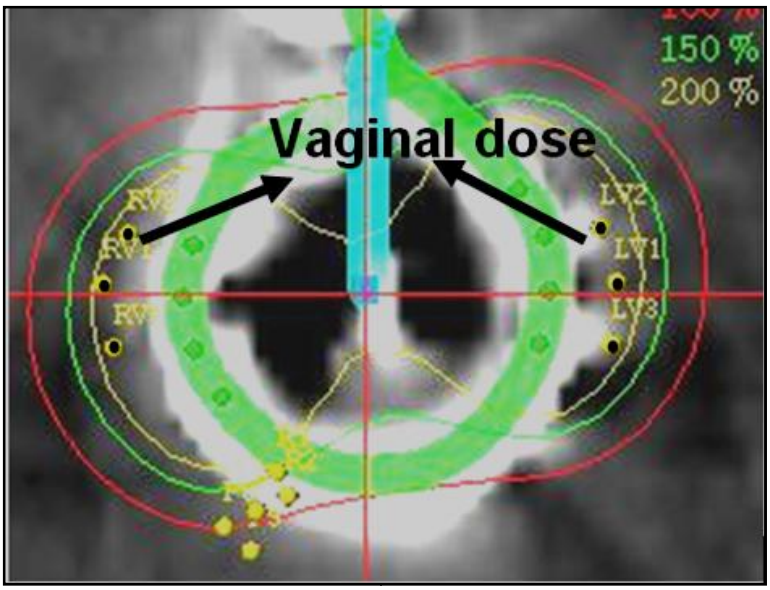

Figure 18: Vaginal dose points marked at the surface of the ring.

ring cap where the dose to the vaginal mucosa would be maximum. The mean vagina dose for both the T/O and T/R were determined and the ratio of point A to mean vagina dose was calculated. A dose of 7Gy was prescribed to point A. ANOVA test was performed with a significance level of 5%. A Total of 55 fractions were evaluated, out of which 41 fractions were T/O and 14 fractions were T/R applications. The mean vaginal dose for ovoid diameter 25 mm, 20mm and 15 mm for T/O applicator were 10Gy (9.2-11.3Gy), 11.5Gy (9.6-13.4Gy), and 13.5Gy (11.4-21.6 Gy) respectively. The mean vagina dose for 34 mm and 26mm of T/R applicator were 19.6Gy (18.5-20.8Gy), 19 Gy(17.7-21.5 Gy) respectively. In summary mean vaginal dose for T/O was 11.7 Gy while for T/R it was 19.3 Gy ($p<.001$).The ratio of mean vaginal dose to the prescription dose was found to be 1.7 and 2.8 for T/O and T/R applicator respectively. This could be attributed to the short distance between source channel and the cap which is about 6mm for all rings, while for ovoid the distance is 7.5mm, 10mm, and 12.5 mm for 15mm, 20mm and 25mm of ovoid respectively. The dose to the vagina decreases with the increase in the diameter of the ovoid, however, no significant change in the dose to the vagina was observed with the variation in the ring diameter.

From this, dosimetric study, it was found that the lateral vaginal mucosal doses are significantly higher with T/R applications as compared to standard T/O application. The doses reduce as the ovoid diameter increases which is not seen with T/R application. Also, three dimensional vaginal dose volume parameters (0.1, 1, 2 and 3cc doses) is being estimated and compared on CT/MR applications. Vaginal dose documentation and reporting with IGABT and correlation with vaginal morbidity would be key in future studies in carcinoma cervix. Reporting vaginal dose at points has a lot of uncertainty due to geometric shift and high dose gradient[68].

2.4: Processes of transition:

In the recent past, the advent of advanced imaging modalities such as MRI and availability of CT / MR compatible applicators have paved the way for IGABT. Various imaging modalities like ultrasound [88-94], CT, MRI [95-102] and Positron Emission Tomography (PET) [103-114] scan etc. have been explored. Among all the imaging modalities, MR imaging is becoming increasingly popular for diagnosis and treatment planning for EBRT and BT for cervical cancer. Promising results in terms of increased local control and reduced toxicities have been reported which made this technique popular during the last decade [115-123].

In the year 2004, GYN GEC ESTRO first published its recommendations, which describes the concepts and terms used in 3D IGBT [83,124]. Various definitions of Gross Tumour Volume (GTV) and Clinical Target Volume (CTV) were proposed, which are now widely accepted. In Multi fractionated BT, a new dimension, time is added in to the process, as imaging and treatment planning is carried out for each fraction, and the inter application/fraction variation has been a major concern during dose accumulation. The organ deformation by means of bladder filling, tumour shrinkage has resulted in large uncertainty in the process of dose reporting of this process. Since, the fourth dimension is also being used in the treatment planning, a term called IGABT has been introduced. During this PhD thesis, clinical implementation of 3D image based BT for cervical cancer was implemented in TMH. We are also a part of an ongoing multi-centric collaborative trial IntErnational study on MRI-guided BT in locally advanced cervical cancer (EMBRACE) which will reveal more information on the dose effect relationship on local control/morbidity of the tumour and toxicities of OARs. Although IGABT is widely practiced in many centers across the globe, it is still in its infancy in India. The implementation of IGABT in India and other developing countries is a big challenge due to the resources, expertise and financial constraints. Nevertheless, with the successful

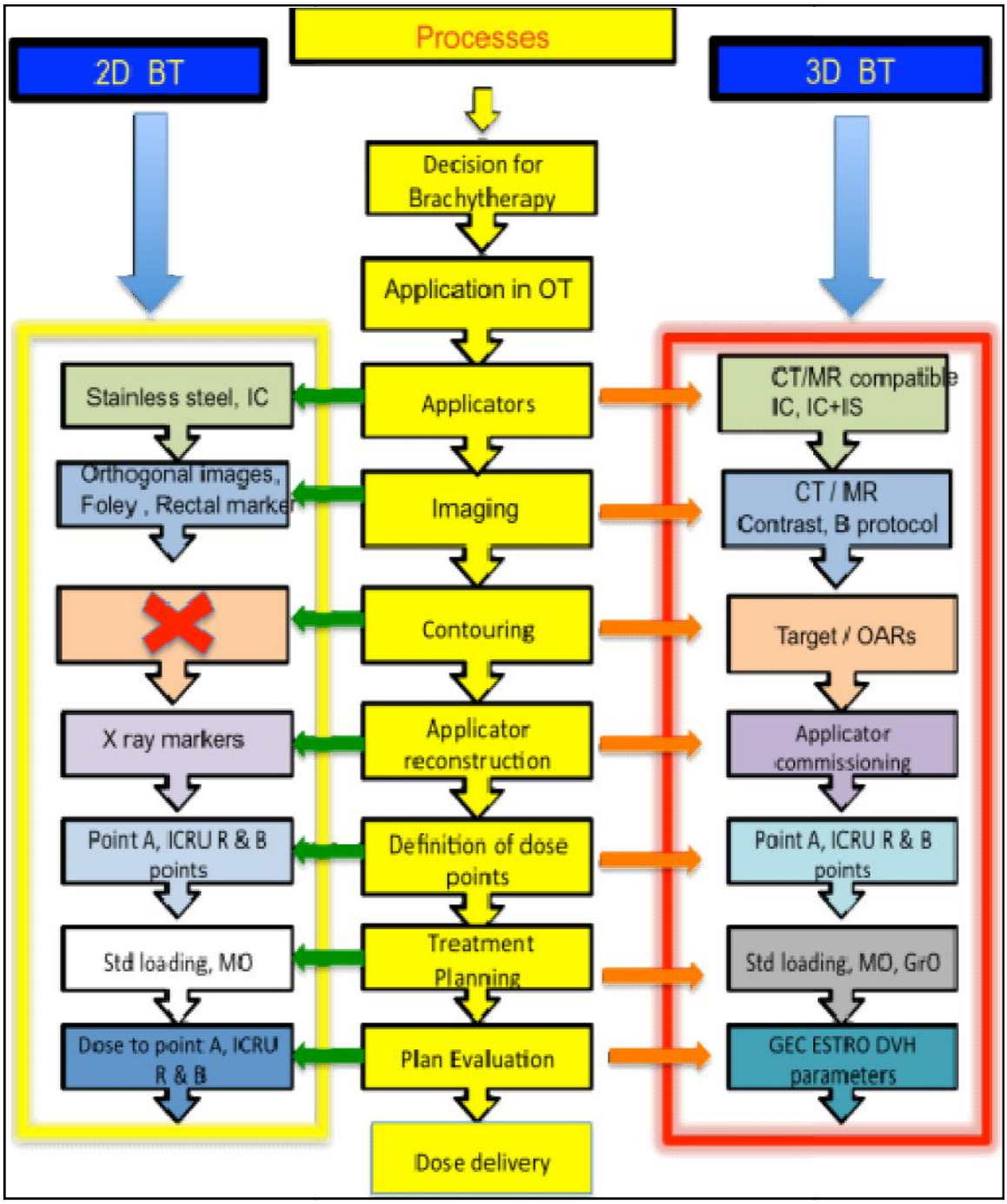

Figure 19: Typical workflow of the 2D Orthogonal radiograph planning and 3D MR image based Brachytherapy.

implementation of Three Dimensional Conformal Radiotherapy, Intensity Modulated Radiotherapy and Image Guided Radiotherapy in routine clinical practice, there is a growing interest in IGABT in cervical cancers in India. As any other advanced techniques,

IGABT too requires systematic clinical implementation that includes familiarization of the processes. In-appropriate implementation of IGABT and change of clinical practice based on this could be damaging to the patients. The contouring procedure has been shown to carry some of the most significant uncertainties in the IGABT procedure [125, 126]. Therefore, specific training in contouring remains one of the most important pre-requisites for IGABT. Further, in the past, lack of proper treatment planning system quality assurance procedures has led to some serious accidents [128]. Unlike treatment delivery errors, which are usually random in nature, the errors from the TPS and applicator commissioning are more often systematic and can be avoided. During this thesis period, we made this transition of 2D to 3D MR Image BT in TMH. The successful implementation of 3D image based BT in to clinical routine which is of international standard, is the basis of this thesis.

In the following section, a brief discussion has been included which will cover the salient features of the practical implementation of IGABT in clinical practice, There are various steps in the process of IGABT such as applicator selection, contouring, imaging, treatment planning and optimization that may quite differ from the conventional BT planning [Figure 19]

2.4.a. Clinical benefits of IGABT and rationale for transition:

In past 10-15 years, MR Image based adaptive BT approach has been standardized with many mono-institutional series of clinical outcome being reported now [115-123] (Table 3). Potter at el have published their single institution experience with MRI based IGABT, where they reported three year pelvic control rate of 96% for tumours 2-5cm in diameter, and 90% for tumours >5cm in diameter with a three year actuarial rate of grade 3-4 bowel and urinary toxicity of 2% as compared to the historical series [128]. The French STIC trial that compared 2D vs 3D concludes that 3DBT results in improved local control with half toxicity observed with 2D

dosimetry. They concluded that for patients with advanced tumours, it is necessary to improve coverage of target volumes without increasing the toxicity [129].

Table 3: Literature survey of Clinical outcome of MRI based IGABT.

Authors	Imaging modality	Number of patents	Median follow up (months)	HR CTV value	HR CTV D90 (EQD2 Gy)	LC	PFS	OS	Grade 4 morbidity
Nomden et al, 2013	MR	46	41	57	84	93	74	65	9.5%
Haie-Meder et al 2010	MR	84	53	48	79	89.2	52(DFS)	57	13%
Haie-Meder et al 2010	MR	156	42		93	95	74(CSS)	68	7%
Beriwal et al, 2011	MR	44	3	29.3	83.3	88	85 (DSS)	86	0%
Tan LT et al, 2009	CT	28	23		74	96	81(CSS)		11%
Lindegaard et al 2012	MR	145	31	29.6	91	91	86 (CSS)	78	5%

2.4.b. Applicators /Selection:

IGABT mandates use of CT/MR compatible applicators that do not throw artifacts and interfere with the CT or MRI signal such that tumour visualization is possible. A wide range of CT/MR compatible applicators ranging from simple tandem-ovoids/ring for intracavitary alone to ovoids/rings with titanium needles/plastic tubes for intracavitary + interstitial applications are commercially available. The applicators are made up of titanium/carbon material for CT/MR compatibility making them expensive as compared to applicators made of stainless steel material.

In TMH, T/O is the most commonly used BT applicator, as compared to T/R applicator. Ring allows greater flexibility of source dwell positions as compared to T/O applicator, it also offers fixed geometry as compared to T/O applicator. However, T/R application results in higher doses to vagina than ovoids when the standardized "Fletcher" loading is used [130].The clinical significance of higher doses at surface of T/R applicator and its impact on vagina in terms of late toxicities is unclear [131]. Levin et al, and Tuncell N et al evaluated the dosimetric differences in T/O and T/R applicators [132,133]. They reported that there were no significant differences between T/O and T/R applicators in doses to prescription points or OARs, however, there were significant differences in treated volumes and total treatment time. T/O treated larger volumes over a longer time. At the moment there is no data supporting the clinical benefit of either of the applicator type.

2.4.c. Imaging

Imaging is an important component of the IGABT process. In TMH, 2D radiographic localization is generally used for BT, however in the recent past, with an additional CT scanner in the department, CT planning also is being carried out for selected patients. However, access to MRI for BT planning is limited only to a few selected patients enrolled in trial. Studies were undertaken to compare the contouring in CT and MR which showed that the tumour volume can be significantly over estimated in CT images as compared to MR. No systematic differences in the volume or in the dose to OARs were found, although MRI has in general better visualization of OARs [100,134]. The overestimation of tumour width in CT results in reduced tumour coverage D_{90}, and resulting dose escalation in D_{90}, which would result in increased dose to OARs. At the moment, MR is considered as gold standard in IGABT, as it provides good soft tissue contrast that enables the depiction tumour regression in great detail.

Gyn GEC ESTRO recommendations for MRI imaging has been published which describe in detail all the issues pertaining to imaging [135]. A brief summary of which is as follows:

Generally, applicators used for IGABT are MRI compatible, made up of either polymer or titanium. The plastic/polymer applicators do not infere with the magnetic field and appear as black voids in the images, however titanium applicators, produces susceptibility artifacts particularly in the regions of considerable material thickness which is typically at the end of the tandem, needle, ovoid, and ring channels. In particular with 3Tesla MRI, titanium applicators may compromise the image quality due to susceptibility artifacts. The titanium artifacts depend on image sequence and may extend beyond 5–10 mm on 3T T2-weighted sequences whereas they may be less than 3–5 mm on 3T T1-weighted MRI [136]. The impact of spatial distortions will directly translate into dose calculation uncertainties as the BT dose gradient is about 5–10% per mm [137]. Distortion is quite significant at the field edges and minimal at the center, which is the region of interest in IGABT. Yet, quantification of these distortions needs to be carried out, as the dose gradient is quite high in BT. A 1mm distortion may cause a dose variation of 5-10%

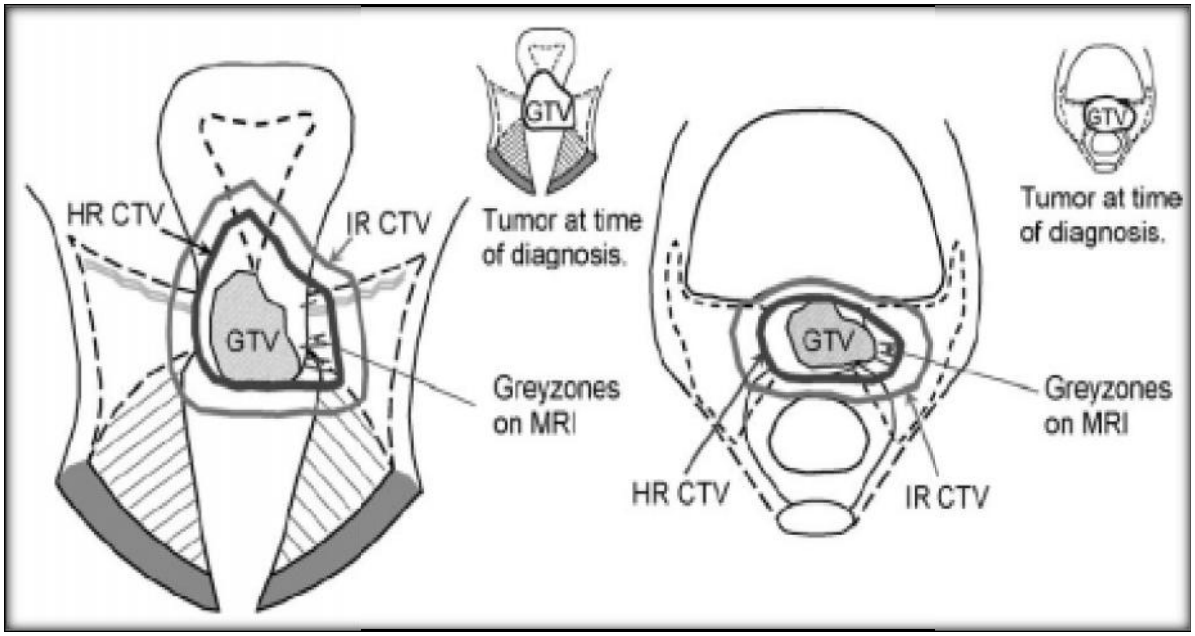

Figure 20: Schematic diagram of cervix cancer with coronal and axial sections representing the volumes recommended by GEC ESTRO (124)

in the region of point- A. Susceptibility distortions are field dependent, but it has so far been proven that these distortions are acceptable for magnetic field strengths up to 1.5Tesla [138] and 3Tesla [136]. Geometric distortions are sequence dependent and have to be taken into account when choosing MRI-sequences. Fortunately the geometric stability of standard T2-weighted spin-echo and turbo spin-echo sequences is fairly robust to susceptibility artifacts.

Gyn GEC ESTRO working group IV recommendations tabulates all the sequences of pre RT and BT MRI scans required [135]. Out of which the mandatory scans, include minimum of T2 FSE(Fast Spin Echo) paraxial (in the axis of the uterus), para-saggittal and para- coronal sequences that covers the entire uterine body, inferior border of symphysis pubis, entire vagina- if vagina is involved and pelvic side wall. A slice width of 3-5mm is recommended. It also lists all the protocols that tabulate the sequence parameters such as time of repetition, time of Echo, Echo train length, slice width etc for quick reference. These parameters as a starting point and further customization of these parameters that are machine specific produce the best image quality.

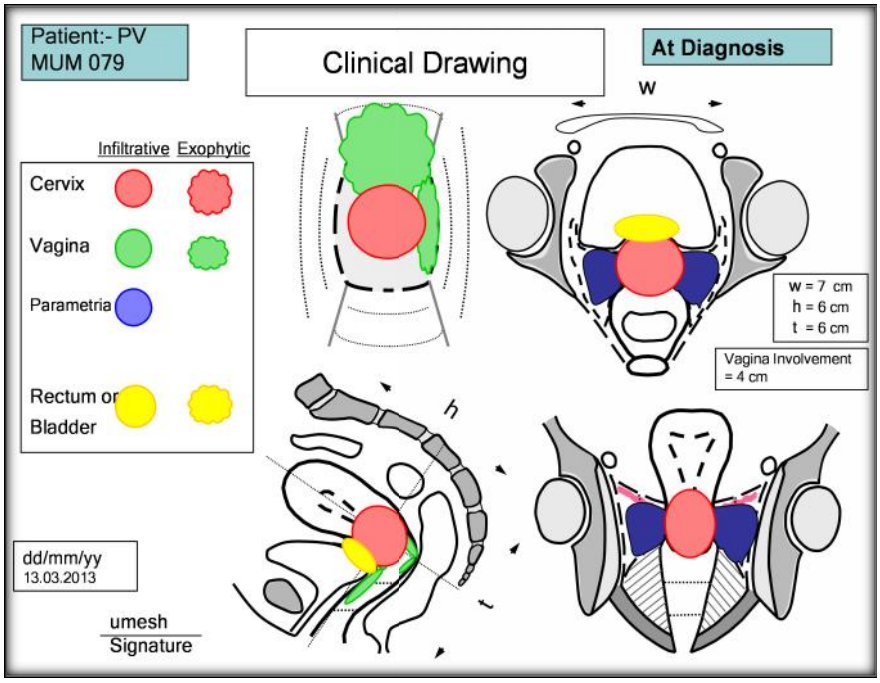

Figure 21: Documentation of Clincal findings

In the year 2004, GYN GEC ESTRO first publisheditsrecommendations, which describes the concepts and terms for defining and reporting various volumes with the use of MR image guided BT planning, which are now widely accepted [124] [Figure 20]. It is

recommended that clinical examination findings have to be documented and can also be used as a guide while reading the MRI images for various target volume delineation. [Figure 21].

2.4.d. Volume delineation:

Gross tumour volume (GTV-D) at BT: GTV at the time of BT represents the macroscopic tumour as visible and palpable on clinical examination and detectable on T2-weighted MRI as high signal intensity lesion in the cervix and surrounding structures namely uterus, parametria or vagina or other organs [Figure 20]

High-risk Clinical Target Volume (HR-CTV): The HR- CTV is assumed to carry a high density of tumour cells and is characterized by a high risk of recurrence. It includes the GTV as described above, whole cervix, and areas of low-signal intensity (gray zones) in the parametria corresponding to the topography of initial tumour spread [Figure 20]

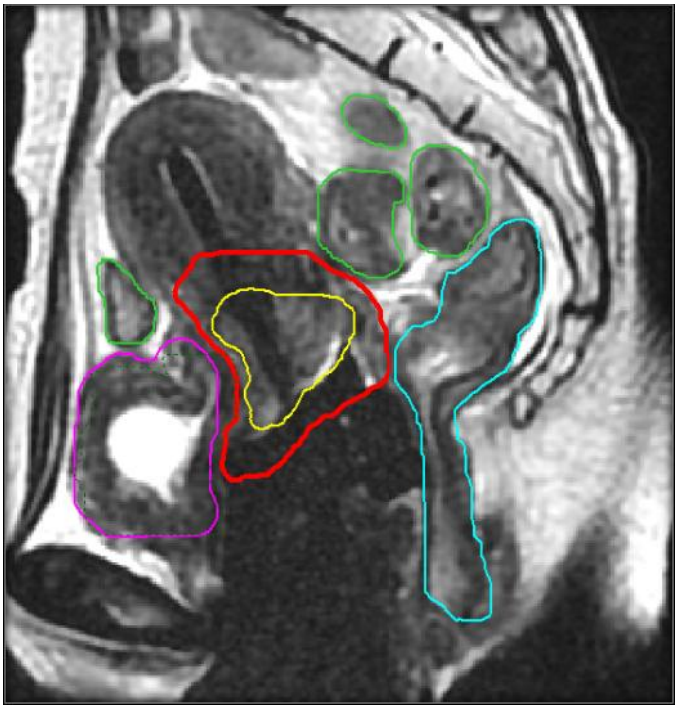

Figure 22: *Figure illustrates the target volumes and OARs drawn as per GYN GEC ESTRO recommendations. yellow-GTV, red- HR CTV, magenta-Bladder, Green-Sigmoid, cyan-rectum.*

Intermediate risk CTV (IR-CTV): The IR-CTV is assumed to carry a significant microscopic tumour load. It is characterized by an intermediate risk of local recurrence. This includes HR-CTV with anisotropic margins ranging from 5-15 mm depending on the initial tumour extent and respecting the anatomical boundaries for tumour spread.

Organs at risk: The most commonly delineated OAR's are urinary bladder,

rectum, and sigmoid colon. Depending on different clinical situations, other OAR's like small bowel, urethra, vagina that is not part of the target volumes, anal sphincter etc. may also be contoured and doses documented. Recently a new proposal for documenting the vaginal doses has been published [77] [Figure 22].

2.4.e. Applicator reconstruction:

The accuracy in applicator reconstruction is crucial due to the inherent steep dose gradients present in BT. A dose variation of 8-10 % was found per mm of applicator displacement for target and OAR doses [139] . Applicator reconstruction with CT images is more straightforward as compared to MRI. In CT images, source channels can be visualized by means of dummy markers with predefined source positions. For MR based reconstruction, catheters containing copper sulfate [140], water [141], glycerine or ultrasound gel (vitamin D) when inserted in the applicator give hypo / hyper intense signal on T1/T2 MR sequences such that the source channel could be reconstructed. However, for titanium needles / applicators, these channels cannot be visualized, as titanium is known to cause susceptibility artifacts [140]. In such cases, the

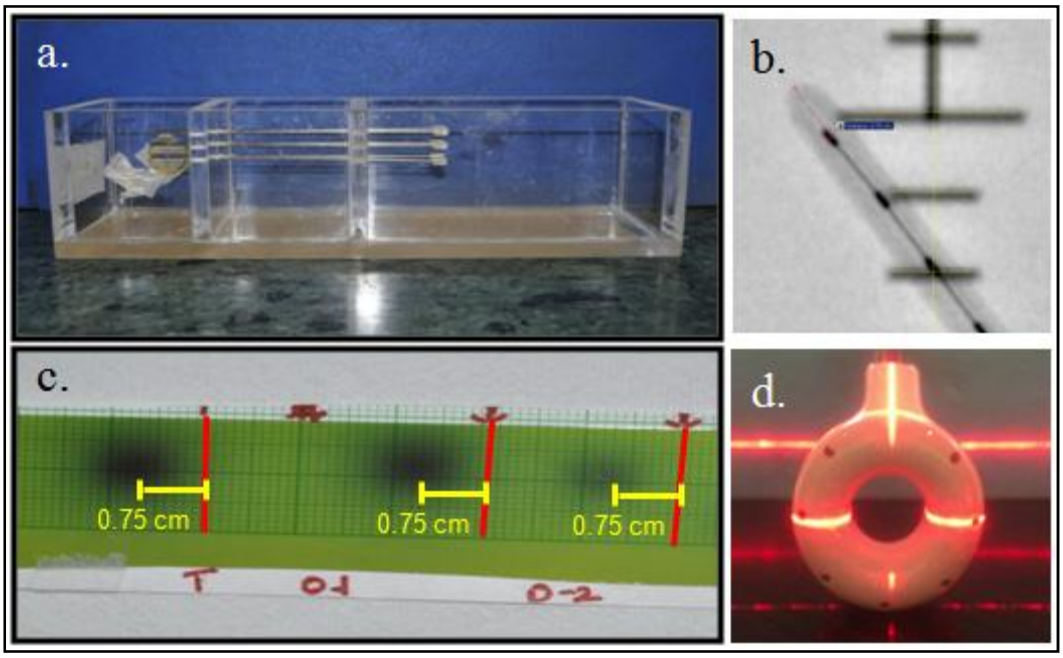

Figure 23: Figure showing various processes of the quality assurance procedures for applicator commissioning 23a: In house made phantom 23b &23c : Auto radiograph and the radiograph to determine the offset for first dwell position. 23d: Ring applicator positioned during the CT scan.

applicator landmarks such as needle holes, cavities can be used to aid the process of reconstruction [142,143]. Also, optimal MR axial slice thickness is an important parameter for accurate reconstruction and a slice thickness of ≤5 mm was recommended as reported by Hellebust et al [144] .

GEC-ESTRO recommendations for applicator reconstruction have been published which describe in detail the reconstruction procedure [145]. A brief summary of the report is as follows: The commissioning process includes the verification of the location of clinically relevant source positions in relation to the outer surface of the applicator and/or in relation to reference points in the applicator, which includes for example, the distance from the tip of a tandem applicator or a needle to the first dwell position, distance from the top of a ring applicator to the level of the source. Traditionally the commissioning has been performed using X-ray images. However, with wide availability of CT scanners now in the clinics, CT images can be used to commission the applicators. The correct method of reconstruction should be verified using auto-radiographs from which the true location of the dwell positions is found. Extra care should be taken using curved applicators, e.g. the ring applicator or ovoids.

An In-house phantom with the fiducials/markers with the known geometry was fabricated which can house the applicator in fixed geometry [Figure 23a]. To produce good contrast of the applicators the phantom was filled with agarose gel. Images of both CT and MRI of various sequences, which will be used clinically, were obtained. The MR images have been compared with the corresponding CT images by means of image registration to quantify the artifacts and spatial distortion. Further, the applicator was positioned on the CT table in such a way that the relevant part of the applicator can be visualized in one image, followed by autoradiography with the known dwell positions[Figure 23a, b, c, d]. The dwell positions were identified in relation to reference points in the applicator or to the outer surface of the applicator, which should be within the specified tolerance.

2.4. f. .Treatment planning / optimization:

Historically, Manchester / Fletcher dosimetry systems were used, which consist of standard radium loadings in tandem, ovoid/ring that produced a classical pear shaped dose distribution. With the introduction of remote after loaders and stepping source technology, standard loading pattern were followed that resembles the traditional radium loading which produced similar pear shape dose distribution. The dose prescription/normalization was to point A. Although in IGABT, where we can visualize the tumour and the OARs clearly, the optimization procedure is still conservative, where, the starting point is to follow a standard loading pattern, followed by normalization to point A, minimal optimization such that there is no large deviation in the loading pattern while, reducing the dose to OARs without compromising the target coverage. In IGABT, the dose prescription and reporting is on HR-CTV, however, it is recommended to report the dose to point A.

Generally, it is advisable, that large deviation from the standard loading pattern or the pear shape dose distribution is avoided. If Interstitial + intracavitary approach is being used, it is important to maintain the loading of the interstitial needles to not more than 20-30% so that the major part of the dose is delivered from the intracavitary applicator and the high dose region remains inside the uterus/ GTV [2]. By means of optimization the prescription isodose can be expanded typically by 5mm in intracavitary applications [146] . By introduction of additional interstitial needles parametrial involvement can be targeted and it is possible to provide prescription depth upto 15mm from point A without increasing the dose to OARs significantly[146] [Figure 24]. In larger tumours, optimized plans resulted in better OARs sparing with good target coverage as compared to standard plans [62].

Inverse planning is not widely used in clinics, and had to be done with caution as certain algorithms are known to produce large variation among the dwell times, it is important to understand how these algorithm works in a certain clinical situation [147,148] . To optimize the

resources, two fractions of treatments per application, one on the day of the implantation and the other after 12 hours gap could be implemented which is practiced in few centers [146,121]. The DVH parameters recommended for reporting is given in Figure 26[83].

The recent publications of dose response relationship with DVH parameter validate the prescription concept and dose levels followed by most of the institutions practicing IGABT in the last decade [150-152, 128]. There are no recommendations or guidelines for dose limits to target or OAR's. However, with the clinical experience evident there are reports to suggest certain parameters which when achieved can obtain optimal results in terms of local control and morbidity. For eg.: D_{90} of at least 85 Gy (EQD_2) to HRCTV and 60 Gy EQD_2 to IR CTV achieve optimal local control rates. Similarly, for OAR's restricting the doses to 85 Gy (EQD_2) for bladder, 70–75 Gy (EQD_2) for rectum and sigmoid as minimal doses to the most exposed D_{2cm3} resulted in in <5% long term morbidity. The evidence is quite clear for rectum but less for bladder and sigmoid. It is important to document both D_{2cm3} and $D_{0.1cm3}$ for the OARs, as these parameters are found to correlate various toxicities, for instance, in the case of rectum, $D_{0.1cm3}$ level may be relevant for the development of ulceration, necrosis, and fistula and the D_{2cm3} for telangiectasia [151] . Due to difficulties in defining the vagina on images and the

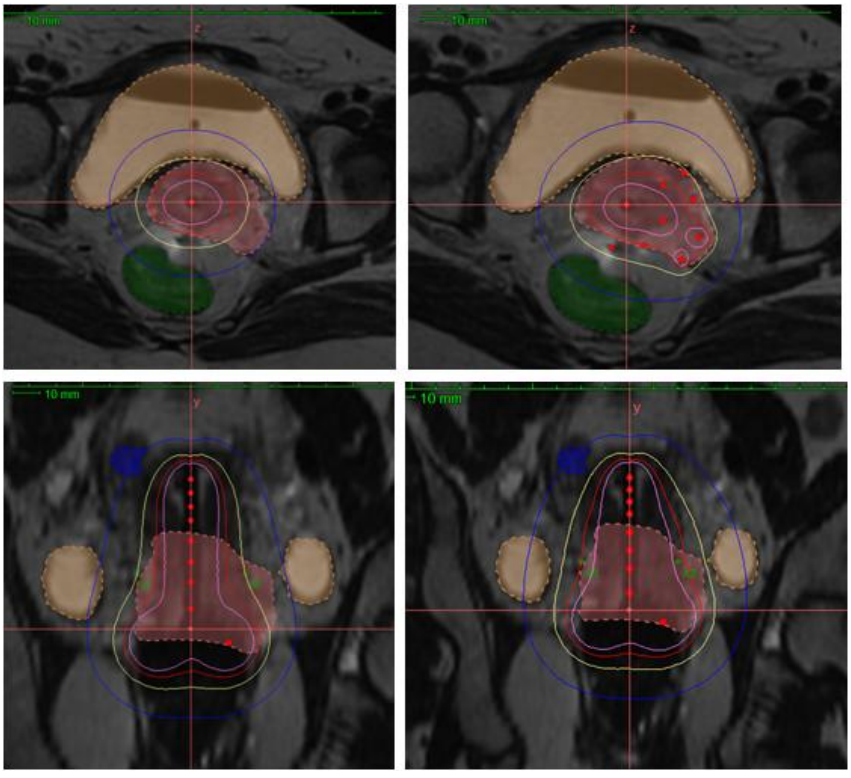

Figure 24 : Dose distribution of Intracavitary where the target is not adequately covered(left), the addition of interstitial needles helps to extend the dose coverage by 8mm, while sparing the OARs (right) . Dotted red line-HRCTV, Dotted Yellow line-GTV, Dotted Majenta-Bladder continuous blue line – 7Gy, continuous red line – 9 Gy.

steep dose gradients with very close proximity to BT sources, a meaningful DVH analysis and correlation of dose to vaginal morbidity have so far been impossible [68]. An ongoing collaborative trial EMBRACE will reveal more information on the dose effect relationship on local control/morbidity of the tumour and toxicities of OARs.

2.4.g. Dose reporting:

Unlike 2D orthogonal image based planning, in IGABT, we are dealing with the 3D images in both EBRT and BT, and hence, it is now possible to evaluate a cumulative dose distribution for target and OARs. However, the radio-biological basis of combining EBRT and BT dose is too complicated. The steep dose gradients associated in BT dose distribution and the estimation of cumulative dose of various volumes which change in time has lot of uncertainties.

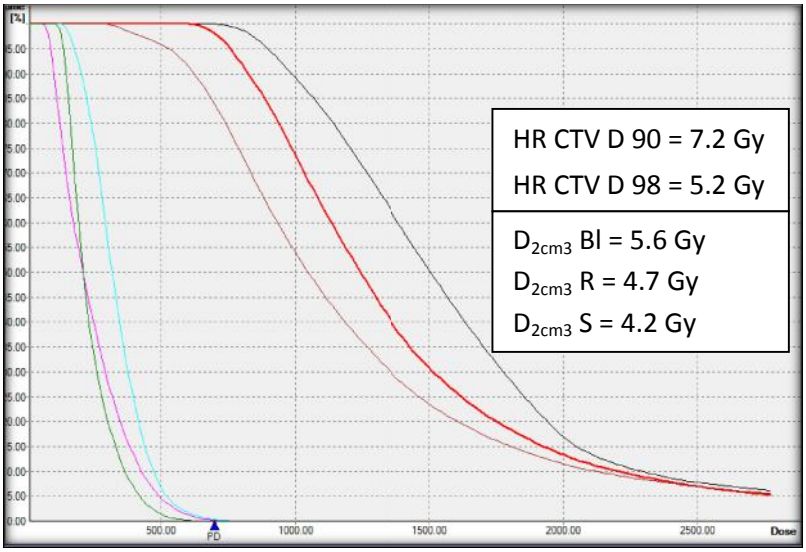

Figure 25: A typical DVH of a Brachytherpy application. The dose volume parameters quoted here refers for one BT application.

Combining EBRT and BT dose distribution by means of simple registration methods based on 3D physical voxel model may not have information about the changes in the organ or its biological impact. To keep the addition of doses simple, LQ model is adopted, where the dose is converted to equivalent of 2Gy (EQD_2) taking into account repair half time of 1.5 h, α/β of 10 for tumour and 3 for organs at risk is assumed [149]. The formulae for converting the physical dose to EQD_2 dose are as follows:

$$BED = D_{IsoE}\left(1 + \frac{2}{\alpha/\beta}\right)$$

$$D_{IsoE} = \frac{BED}{1 + \frac{2}{\frac{\alpha}{\beta}}} = EQD_2$$

$$D_{IsoE,Total} = D_{IsoE,External} + D_{IsoE,Brachy}$$

There are no recommendations or guidelines for dose limits to target or OAR's. However, with the clinical experience evident there are reports to suggest certain parameters which when achieved can obtain optimal results in terms of local control and morbidity. For eg.: D_{90} of at least 85 Gy (EQD_2) to HRCTV and 60 Gy EQD_2 to IR CTV achieve optimal local control rates. Similarly, for OAR's restricting the doses to 85 Gy (EQD_2) for bladder, 70–75 Gy (EQD_2) for rectum and sigmoid as minimal doses to the most exposed D_{2cm3} resulted in in <5% long term morbidity. The evidence is quite clear for rectum but less for bladder and sigmoid. It is important to document both D_{2cm3} and $D_{0.1cm3}$ for the OARs, as these parameters are found to correlate various toxicities, for instance, in the case of rectum, $D_{0.1cm3}$ level may be relevant for the development of ulceration, necrosis, and fistula and the D_{2cm3} for telangiectasia [151] . Due to difficulties in defining the vagina on images and the steep dose gradients with very close proximity to BT sources, a meaningful DVH analysis and correlation of dose to vaginal morbidity have so far been impossible[53] .However, recently, a new formalism for reporting vaginal doses have been published [77] .

2.4.h. Dose Delivery / Inter-intra fraction/application variation:

With increasing conformity of dose it becomes important that the delivery of dose is in accordance with what is planned on the TPS. Optimal source geometry, timing and stability are prerequisites for safe delivery of optimized BT. Both patient related factors and technical issues associated with the BT equipment can give rise to uncertainties in the delivered dose. It is well recognized that equipment related quality assurance has to be conducted periodically to prevent the dose delivery errors. Patient related factors are being identified as applicator

Figure 26, gives the dose reporting parameters in 2D and 3D image based brachytherapy.

displacement, organ motion in between the treatment planning and dose delivery. In this thesis, some of the unresolved issues related to inter application variation has been investigated and discussed in chapter 4.

Chapter 3

Treatment planning and Optimization

3.1. Treatment planning

Most BT centers in the world have followed a traditional concept based on the Manchester or Fletcher loading patterns. The rationale behind the Manchester approach is to achieve a consistent dose rate at point A, by applying a set of strict rules with regard to the position and activity of radium sources for the different combination of sizes for the uterine tandem and ovoids. With the introduction of HDR remote after loaders, the rules of Fletcher and Manchester systems were extended from the milligram radium equivalent activity distribution to a pattern of dwell positions where a single stepping source is positioned at programmable dwell times. With the introduction of computers and sophisticated mathematical models, HDR BT has brought in more advances in to field of BT. One such advance in the process of treatment planning is the application of optimization algorithms in HDR BT, which offers a great flexibility in shaping the desired dose that adequately covers the tumour and minimizes the dose to normal tissues.

The objective of any treatment planning in radiotherapy is to deliver the maximum dose to the tumour and minimum elsewhere. One of the basic pre requisite to meet this objective is the knowledge of the spatial location of tumour volume with respect to OARs. In 2D orthogonal images, the OARs with respect to the target volumes were not clearly seen and hence the toxicities were reported to be high, although most of the series reported with good clinical results [154-158]. The integration of CT or MR imaging for treatment planning in 3D IGABT serves the purpose of identifying the target volumes in 3D geometry [54, 63, 81, 146,159, 160]. The introduction of IGABT, has also added a new dimensions in terms of both volume to the target and OAR and how these volumes change with time, providing an improved understanding compared with the limited information available with radiographic localization [63, 81, 119,147,159, 160, 161, 162,163,].

The dose effect curves for OAR may be steep depending on the endpoint. Recent publication from the Vienna group shows that the dose volume correlations for late rectal morbidity treated with MR IGABT, where a steep dose effect is evident, especially when D_{2cm3} is used as a predictor for the dose delivered to the rectum [164,165]. The historical series based on the clinical experience and radiobiology also shows steep dose effect relationship [166, 167-169]. Moreover, the steep dose gradients in BT demands for an optimized dose distribution, where the tumour is adequately irradiated with sharp fall off of dose in OARs [150,151]. Hence, it is imperative to obtain a best possible treatment plan that satisfies the above conditions [146, 83]

The second pre-requisite to meet the planning objective in BT treatment planning, is to achieve certain dose volume parameters or constraints, which are considered as the dose tolerance for the organs. The method to achieve these constraints in HDR BT may be termed as optimization. Optimization in HDR BT is nothing but adjusting the dwell positions and dwell times in an iterative process until the best compromise for target and OAR constraints is achieved. This chapter summarizes the theoretical and practical aspects of treatment planning for both intracavitary and interstitial cervical BT with a specific focus to various planning methods such as forward and inverse planning and various optimization techniques such as stochastic and deterministic methods.

3.1.1 Forward Planning

In this method, the user wants to achieve a dose distribution, which meets certain criteria by adjusting iteratively the dwell times. These adjustments can be done either manually or by graphical tools. Graphical optimization tools are often considered as not safe and hence have to be used with caution. Forward planning generally includes simple tools such as, addition or deletion of dwell positions, adjusting the individual dwell time to improve the target coverage or to reduce the dose to OARs and overall scaling of the dose distribution. After the physicist has changed the dwell times, the dose distribution is recalculated followed by an evaluation to find

out whether the plan meets the dose volume criteria. The whole process is repeated until the physicist is satisfied with the resulting treatment plan. Such a method of trial and error makes the whole procedure sometime time-consuming and dependent on the experience of the physicist [171]. However, in gynecological BT, forward planning is considered as the state of the art method for treatment planning.

3.1.2. Inverse Planning

Inverse planning algorithms was first introduced in BT for prostate [172,173, 174, 175, 176]. The major aim of the inverse planning algorithms was to improve the dosimetric results, to make reproducible plans, and decrease the time to prepare a treatment plan. In inverse planning, the user defines the objective and the dose constraints for the target volume and the OARs. The mathematical algorithms determine an optimal set of dwell times that best meets the objectives of the user. The user therefore does not anymore need to do the manual adjustments. The resulting plan will be used immediately for treatment. Optimization according to this model is referred to as inverse planning [177]. However, at this moment, these inverse planning algorithms were not robust enough to control the dosimetry especially for intracavitary BT. For example, the loading pattern resulting from these algorithms has a large deviation from the traditional pattern, which may not be clinically acceptable, which was the main investigative component of this thesis [147]. The use of inverse planning based on volumetric parameters in BT has currently been mainly reported for interstitial BT [177, 178]. The literature of inverse planning on intracavitary BT has been sparse. This thesis adds to the literature with some significant findings, which will be summarized at the end of this chapter.

3.2. Optimization

Optimization in HDR BT broadly refers to an algorithm, which searches through potential solutions to find one that best minimizes the objective function. The potential solution is in terms of a distribution of source dwell positions and dwell time, hence the variables in the

optimization problem is source location, source strength/dwell time. Mathematically, optimization refers in minimizing the variance of the doses Di at points i on the PTV surface from the prescription dose Dp.

$$\text{Minimize } f = \sum (D_i - D_p)^2$$

Where f is a simple objective function

In the literature, several mathematical techniques in the domain of BT are used to optimize the dose distribution. These optimization techniques can be broadly divided into exact and heuristic methods. In general, heuristics are indeed more suitable in solving real problems. They do not necessarily provide the optimal solution to a problem, but are looking for a result that is close to the optimal solution and within a reasonable computation time [179]. Heuristics methods can be further divided into stochastic and deterministic.

3.2.1 Exact Methods

Exact methods guarantee an optimal solution to a problem, unlike heuristics. The exact methods are solved by linear programming problem, where the objective function and constraints are linear expressions of the decision variables [180]. This means that the problem is said to have met the solution provided it meets certain hard constraints. Hard constraints are constraints, which cannot be violated. However, in reality, hard constraints cannot be achieved, as the problem may not have any solution when hard constraints are applied. Therefore the hard constraints are often replaced by a cost function, with higher costs involving lower quality of the treatment plan. These constraints are called soft constraints, which reduce the quality of the plan. Exact methods primarily consist of two optimization techniques: Dose point and GO, which have been used extensively in the clinics for optimizing the HDR dwell time dose distribution. A brief summary of these methods is given in the following section.

3.2.1.a Dose Point optimization (DPO):

DPO has been developed by van der Laarse and Prins [181,182]. In DPO, the desired dose at a number of dose points at a certain distance from the catheter is defined. The optimal set of dwell times is obtained using the least squares method. The sum of squares of the difference between the actual and prescribed dose at each dose point and the difference between the successive dwell times is minimized by setting the derivative of the objective function to each dwell time equal to zero. In this way, a system with as many equations as there are dwell locations is obtained, and therefore that is mathematically easy to solve. However, when there are a lot of dwell locations, the computation time can become high and a large memory is required. To prevent this, the dwell times can be approximated using a polynomial function. This leads to a system with a smaller number of equations and the parameters as unknowns. This type of dose-point optimization is known as distance polynomial optimization. This type of optimization is generally used in single plane implants such as soft tissue sarcoma, buccal mucosa etc. Clinically dose point optimized implants are generally acceptable, as they provide uniform distribution throughout the implanted volume.

3.2.1. b Geometric Optimization (GO)

In GO, the dwell locations themselves act as dose points. The dwell time in a dwell location is inversely proportional to the sum of the inverse squares of the distances to the other dwell positions. This sum is an approximation of the dose contribution of other dwell positions. When the dwell positions in the same catheter are taken into account, it is refereed as geometric distance optimization. When they are not taken into account, it is called GO on volume. GO is generally works best for volume implants such as breast – Accelerated Partial Breast Irradiation and any large volume implants of 2-3 planes. Kolkman-Deurloo et al, [183] investigated the effect of geometrical optimization in regular and irregular implants. Kestin et al. [184] apply a correction

of the dwell times to decrease the under-dosing of the lumpectomy cavity with a self-developed algorithm, after GO.

3.2.1. c. Combination of Dose point and GO.

In some rare clinical situation, DPO and GO can also be applied together. In polynomial optimization on volume [185], for example, GO on volume is first applied to obtain the overall dwell time for each catheter. Thenpolynomial optimization is used, with the additional objective that the overall dwell time for each catheter from the GO is preserved. In other studies [172, 186, 183, 173] both optimization methods are used in the first phase of an inverse planning method. These methods indicate the optimization potential. In a subsequent phase, objectives for the target volume and critical organs are specified. Finally, the optimal dose distribution is determined by an inverse optimization technique.

3.2.1 d. Graphical optimization (GrO):

GrO is the last method among exact methods. In using GrO, the isodose curves of the radiation plan the computer displays are changed manually with the mouse. Isodose curves are curves that indicate a similar radiation dose. After manual adjustment, the algorithm calculates the exact corresponding dwell times. Tanderup et al for example, use GrO, and compare the results with those of GO [187].

3.2.2 Heuristic methods:

3.2.2.a Stochastic Heuristics - Simulated Annealing

Stochastic heuristics have a probability aspect in their search process, converge towards a global optimum and usually have a longer computation time than deterministic heuristics [188]. Simulated annealing is the first example of a heuristic that solves the optimization problem in a stochastic manner. The heuristic is based on the influence of the physical cooling process on the properties of metals. With slow cooling, the atoms change into a perfect crystal structure [189]. For example, Lessard and Pouliot [190] have developed IPSA, an inverse planning algorithm. In

IPSA, the objective function is a cost function associated with dose objectives for each target volume and critical organ. Before the optimization, the physicist needs to specify the lower and upper limits of the acceptable dose in the dose points for each tissue type and the weights associated with exceeding these limits. A dose outside the range is linearly penalized. The cost function is minimized using simulated annealing and the result is an optimal set of dwell times. At the start, the dwell times are set at an arbitrary value. The objective function value changes by allowing the dwell times to increase or decrease randomly in each iteration by a random value. A new set of dwell times resulting in a better objective function is always accepted. A less suitable value of the objective function will only be accepted at a certain level of probability. In this way it is possible to escape from local minima. The probability of acceptance decreases as the search process progresses. To this end, the temperature parameter in each iteration is reduced. The search process is stopped if the objective function does not change for many iterations.

3.2.2.b. Deterministic Heuristics

Deterministic heuristics are typically used in the literature for variance-based objectives. Milickovic et al. [191], for example, compare the results of evolutionary algorithms with the results of the deterministic algorithms. The deterministic algorithms optimize the weighted sum based on the dose variance objectives for dose points in and on the target volume. The optimization is repeated several times, each time with different weights. Because the solution space is convex here, the deterministic heuristics converge rapidly towards a global Pareto front. They use two gradient methods, namely the Broyden-Fletcher-Goldfarb-Shanno (BFGS) quasi-Newton algorithm and the Fletcher-Reeves-Polak-Ribiere (FRPR) algorithm. Gradient methods apply the first derivative of the objective function to the decision. The decision variables are the square roots of the dwell times. By taking the square root of the dwell times, negative times are avoided. This way, no additional constraint for positive dwell times should be added to the model. They also use a method that does not include gradient information, namely the adapted

Powell algorithm. When the objectives for the critical organs are also included in the aggregated objective function, there may be local minima. Milickovic, Lahanas, Papagiannopoulou and Baltas [192] conclude, however, that deterministic heuristics also lead to global solutions in their research, in the presence of objectives for critical organs. Shwetha et al. [193] use another deterministic algorithm that requires no derivatives: Nelder-Mead simplex. The optimization aims at a specific dose to be delivered to one or more anatomical structures, and the physicist must start to indicate the objectives for each structure.

3.2.2.c Hybrid Heuristics

Hybrid Inverse Planning and optimization (HIPO) [186, 194, 195,196, 197-199] is a hybrid inverse planning method that uses both a stochastic and a deterministic heuristic. The objective function is the weighted sum of objectives for different anatomical structures. Dose values for the target volume that are above or below a dose limit are penalized. For the critical organs and normal tissue, only the dose values above a dose limit are penalized. HIPO optimizes not only the dwell times of the dwell location in each catheter, but also the position of the catheters. In this respect, it differs from all other techniques. HIPO starts from a random catheter position or a catheter position indicated by the physicist. It uses simulated annealing to change the catheter positions and limited-memory Broyden-Fletcher-Goldfarb-Shanno (LBFGS) to optimize the dwell times. HIPO can also be used if the position of the catheters is already fixed [194, 199]. In this situation the algorithm optimizes only the dwell times. The physicist again fixes a number of parameters before the optimization.

HIPO offers a dwell time gradient restriction filter in order to account for clinical constraints within the catheters. In other words, high values of this filter are expected to produce solutions with smooth changes of dwell times/weights along each catheter and prevent solution swith dominating source dwell positions. The dwell time gradient restriction acts practically as a

dose modulation restriction filter. This enables the creation of better security in the delivery of dose distributions without having to compromise to the optimization performance.

3.3 Application and evaluation of Inverse Planning:

The application of inverse planning in EBRT is very common, however in BT it is still not commonly practiced in the clinics. In the last 4-5 years, the application of inverse planning has been practiced in prostate BT, however, its use in gynaecological BT is sparse. One of the major reason for this, is the use of standard loading pattern, which originates from the traditional schools that resulted in excellent results [167]. Any deviation from these standard loading patterns was not well taken. In this chapter, three major clinical scenarios were investigated, viz, Tandem ovoid application, Tandem/ring application, combined Intracavitary and interstitial implants – Vienna applicator and MUPIT Interstitial applicator.

3.3.1. Standard loading pattern and Inverse planning algorithm (HIPO) for Tandem and ovoid applicator:

3.3.1.a. Purpose:

The inverse planning algorithms, employing sophisticated mathematical formulations expected to result in better plans as compared to manual trial and error method. Although, it produced good plans, the loading pattern of these algorithms in comparison with traditional systems was not similar [147]. This may be attributed to the fact that the traditional systems were based on the applicator geometry such as the length of the tandem and the size of the ovoid, while the more modern planning concepts are based on the tumour and the topography of the OARs with respect to the applicator. Hence, we have decided to study in detail, the change in the loading pattern of inverse planning algorithm for T/O applications. The specific purpose of

this study was to compare standard plans, manual optimized plans and inverse generated plans. The comparison was based on dose–volume parameters and the loading pattern for these plans.

3.3.1.b Materials and methods:

Twenty-eight patients who underwent MRI based HDR IGABT for cervix cancer was selected as the data set for this retrospective study. This set was made up of eleven IIIB, fourteen IIB, two IIA and one IB2 patients. A dose of 46–50 Gy was given as the EBRT dose. Nucletron standard tandem-ovoid CT/MR compatible applicators with tandem lengths of 5 or 6 cm and ovoid diameters of 2 or 1.5 cm were used. 1.5 Tesla T2 weighted MRI scans (GE Healthcare) were obtained after implantation. HR CTV, rectum, bladder, and sigmoid were contoured based on the GYN GEC ESTRO recommendations [83,124]. MRI findings at the time of diagnosis and BT, and clinical examination were used for target volume delineation. Treatment planning was performed using the Oncentra GYN (v0.9, Nucletron, Veneendal, Netherlands) TPS. The applicator geometry was reconstructed using data from a library of various applicators. The reconstruction tool uses the outer applicator shape and the known source path. This allows positioning of the applicator directly on the MRI series [142]. The Oncentra GYN includes tools such as bar graphs and online DVH monitors to facilitate fast graphical/manual optimization planning. The dose computation algorithm is based on the TG 43 as recommended by the American Association of Physicists in Medicine (AAPM) [200].

Three plans were calculated for each patient: (1) standard loading plan, (2) manual optimized plan, and (3) inverse optimized plan. A dose of 7Gy was prescribed to Point A for standard plans and to the HR CTV for manual and inverse optimized plans. The loading pattern of the standard plan was based on the Fletcher system. Although the dwell weights are equal in all the dwell positions, the dwell positions are arranged in such a manner that it resembles the Fletcher loading pattern. It consists of three positions in the ovoid and 7 or 8 positions in the tandem with a 2.5 mm step size. Table 4 provides the details of the dwell positions and other

parameters. In manual optimized plans, the dwell positions were changed and the individual dwell weights were manipulated. The plan objective for optimization was to maximize the HR CTV coverage while minimizing the dose to the OARs. The manual optimization was carried out by changing the dwell weights manually and also by using the GrO tool for fine-tuning, with careful monitoring of the resulting dose distribution. Inverse optimization was based on the Hybrid Inverse Planning Optimization (HIPO) [196]. The plan objectives were same as those for the manual optimized plans. The relative importance factors were tuned to obtain an optimal plan that meets the dose constraints of HR CTV and OARs. The dwell time gradient restriction was maintained at a constant value of 0.5. The dose constraints for optimization were as follows. The dose to the most exposed $2cm^3$ volume,,D_{2cm3} of bladder was 6.2 Gy while D_{2cm3} of rectum and sigmoid was 4.4 Gy. For HR CTV, the dose to 90% of HR CTV, D_{90}, was optimized to aim for a value of at least 7 Gy. Assuming 4 fractions of 7 Gy in BT and 45 Gy of external beam, these doses correspond to 90 Gy for bladder, 70 Gy for rectum and sigmoid and at least 84 Gy for the HR CTV based on the EQD_2, equivalent dose in 2 Gy per fraction [83,124, 159,203]. The dosimetric outcomes obtained from these three plans were compared qualitatively and quantitatively. The dose volume reporting parameters of the GYN GEC ESTRO recommendations were evaluated [83,124]. As the high dose region is a cause of concern whenever inverse plan or manual optimization is used, the volume receiving 200% of the prescription dose, V_{200}, was also evaluated to characterize the high dose region. A two sided paired t test with a level of significance of 0.05 was used to determine the statistically significant differences of parameters between plans. The comparison of the loading patterns between the standard plan, manual optimized plan and inverse plan was performed based on the following methodology: For each plan, the value of the TRAK was calculated. While the TRAK presents the total loading, the ratio of the loading was calculated, based on TRAK, from positions in the ovoid versus positions in

the tandem TRAK. This ratio, O/T was calculated for each patient and compared between the plans.

Table 4: Details of various plans generated for each patient in the current study.

Dwell positions	Standard plan	Manually optimized plan	Inverse plan
Ovoid Lt	4,5,6	1-6 (variable)	1,2,3,4,5,6
Ovoid Rt	4,5,6	1-6 (variable)	1,2,3,4,5,6
Tandem 5cm	1,3,5,7,10,13,16	1,3,5,7,10,13,16	1,3,5,7,10,13,16
Tandem 6cm	1,3,5,7,10,13,16,20	1,3,5,7,10,13,16,20	1,3,5,7,10,13,16,20
Dwell weights	Equal	unequal	unequal
Optimization	optimization	manual + graphical	inverse

3.3.1. c Results:

3.3.1. c.1 Dose to HR CTV: The volume of HR CTV ranged from 9 to 68 cc with a mean of 41(±16) cc at the time of BT. The relationship between the total volume of HR CTV and the percentage covered by the prescribed dose (V_{100}) for the standard plan and inverse plan is shown in Fig. 27. Mean D_{90} was the highest (6.5 ± 1.8 Gy) in standard plans as compared to manual optimized (6.2 ± 0.5 Gy) and inverse plans (6.3 ± 0.6 Gy). Mean V_{100} values for standard plan, manual optimized and inverse plan were 83.9 ± 8.9%, 83.5 ± 5.1% and 83.5 ± 4.9%, respectively, and not statistically significant (p = 0.35, 0.38, 0.4) [Table 5, Figure 28] . The coverage of HR CTV decreases with increase in volume. Both standard plan and inverse plan

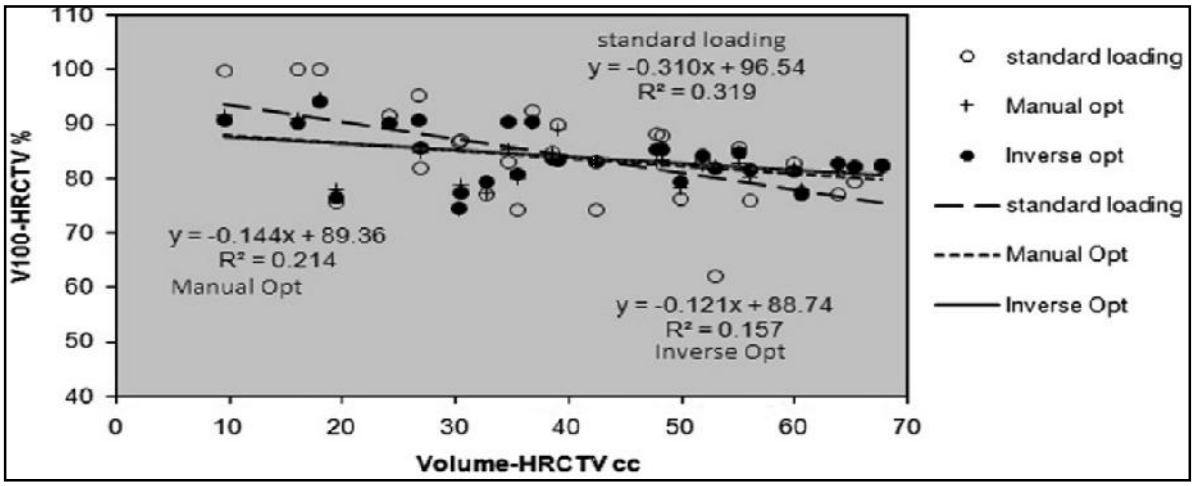

Figure 27: Relationship of HR CTV volume and V_{100}, shows that they are inversely related

showed negative slope, however the slope was different. For standard plan, the slope was -0.31 as compared to -0.12 for inverse plan, which points to the fact that large volume tumours were not adequately covered by both standard and inverse plans.However, for optimized plans this effect could be partially compensated for, resulting in a more flat relationship. It was found that for relatively smaller tumours (<35 cc), standard plans produced high HR CTV coverage with a mean V100 value of 88 ± 4%, while the inverse plan resulted in a significant reduction in coverage due to increased sparing of OARs (85.9 ± 6% p = 0.005). In the cases of large tumours (>35 cc), however, inverse plan was found to be slightly superior in terms of coverage (80.3 ± 7% vs 81 ± 7% p = 0.1), albeit of no statistical significance. This may be attributed to the tradeoff between the dose volume constraints to sufficiently cover the HR CTV while reducing the dose to the OARs. It was also found that for 7/28 patients, the HR CTV coverage was poor (mean V100 = 75 ± 5% manual/inverse optimization). Neither manual nor inverse optimization made any substantial impact on the coverage. These patients had tumours with lateral and posterior extension.

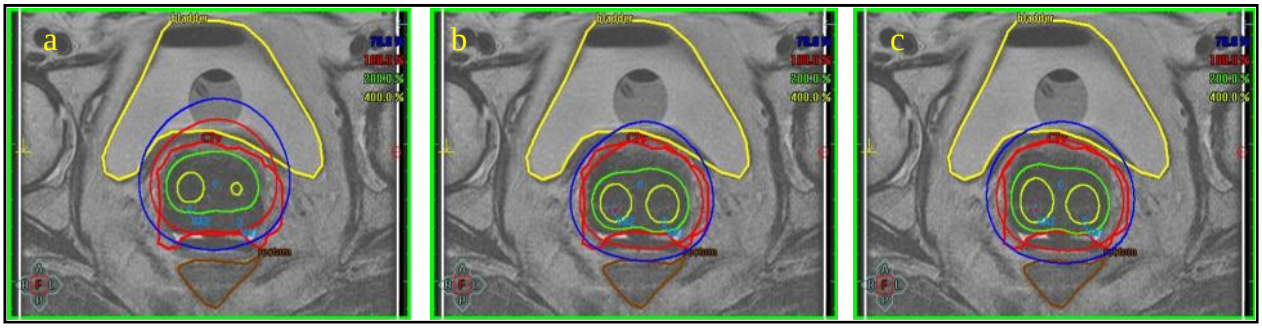

Fig 28: Isodose distribution for standard Plan (a), manually optimized plan (b), inverse plan(c).Yellow:200%, 14Gy, green: 150%, 10.5Gy, red: 100%, 7Gy, blue:70% 4.9 Gy.

3.3.1.c.2 Dose to OARs

Fig. 29a, b and c show the relationship of D_{2cm3} of bladder, rectum and sigmoid with respect to V_{100} of standard, manual optimized and inverse plans. Mean values of V_{100}, D_{90}, $D_{2cm}{}^{3}$ of bladder, rectum and sigmoid are presented in Table 5. It was observed that dose to bladder (mean 7.8 ± 1.6 Gy) and sigmoid (mean 5.6 ± 1.4 Gy) was generally high for standard plans; however, dose to rectum (mean 3.7 ± 0.7 Gy) was well within the tolerance limits. Manual optimization reduced the dose to bladder (mean 7.1 ± 1.7 Gy p = 0.006) and sigmoid (mean 4.5 ± 1.0 Gy p = 0.005) without compromising the HR CTV coverage. However, dose to rectum increased with a mean of 4.1 ± 1.0 Gy (p = 0.07). Inverse plan resulted in a significant reduction of dose to the

Table 5: Dose volume parameters of standard plan, manually optimized and inverse plan.

Parameter	Standard plan	Manually optimized plan	Inverse plan	P value Std.vs Manual	StdVs. Inverse	Manual vs Inverse
V_{100} %	83.9 ± 9.0	83.5±5.1	83.5±4.9	0.35	0.38	0.4
D_{90} Gy	6.6 ± 1.8	6.2±0.5	6.3±0.6	0.25	0.23	0.35
Bl D_{2cc} Gy	7.8±1.6	7.1±1.7	6.5±1.4	0.006	0.001	0.005
R D_{2cc} Gy	3.7±0.7	4.1±0.9	4.3±1.0	0.07	0.06	0.15
Sig D_{2cc} Gy	5.6±1.4	4.5±1.0	4.6±1.0	0.005	0.001	0.38
V_{200}%	36.4±11.2	33.5±9.3	28.9±8.3	0.24	0.003	0.02
Point A Gy	7.0±0	6.1±1.1	6.1±1.2	0.007	0.006	0.41
TRAK cGy m^{-2}	0.49±0.02	0.44±0.04	0.4±0.04	0.03	0.005	0.01

bladder (6.5 ± 1.4 Gy, p = 0.002). All the other dose–volume parameters between the manual and the inverse plans were statistically not significant (Table 5). Mean value of V200 was also highest in the standard plan (36.4 ± 11.2%) as compared with other plans. Neither the inverse plan nor the manual optimized plan resulted in larger high dose regions. Mean dose to point A

was reduced to 6.1 Gy (p = 0.007) for both the manual optimized and inverse plans as compared to 7.0 Gy for the standard plan.

3.3.1.c.3. Loading pattern:

TRAK was found to be 0.49(±0.02), 0.44(±0.04) and 0.40(±0.04)cGym^2 for the standard loading, manual optimized and inverse plans, respectively. [Figure 30] illustrates the relationship between TRAK and the HR CTV volume. It was found that for standard plans, TRAK is independent of HR CTV volume while for manual optimized and inverse plans, TRAK is found to be linearly dependent on the volume of HR CTV. It was also observed that TRAK for the inverse plan is less than for the standard and manual optimized plans. This could be attributed to the dose sculpting used in the inverse plan. It was observed that the ratios $TRAK_{O/T}$ were 0.82(±0.05), 1.7(±1.04) and 1.41(±0.93) for the standard loading, manual optimized and inverse plans,respectively. To compare TRAK with traditional systems, the loading of Fletcher was considered, where in tandem 15, 10, 10 mgRa was usedwhile 22.5/20/17.5 mgRa was used in ovoids depending on size. In our clinical situation, the majority of the applications consist of small ovoid, hence 17.5 mgRa of loading was considered for ovoid for the sake of comparison, while 35 mgRa was considered to be in tandem (15 + 10 + 10). Hence $TRAK_{O/T}$ for the traditional loading pattern was taken as 1, (17.5 x 2/15 + 10 + 10 mgRa). It was observed in this study that ovoids were more loaded in both the manual optimizedand inverse plans. It was also observed that the loading patterns in the manual optimized and inverse plans were not reproducible, which is quite evident from the standard deviation of TRAK Standard deviation was 1.04 and 0.93 for the manual and inverse plans, respectively, as against 0.05 for standard plan.

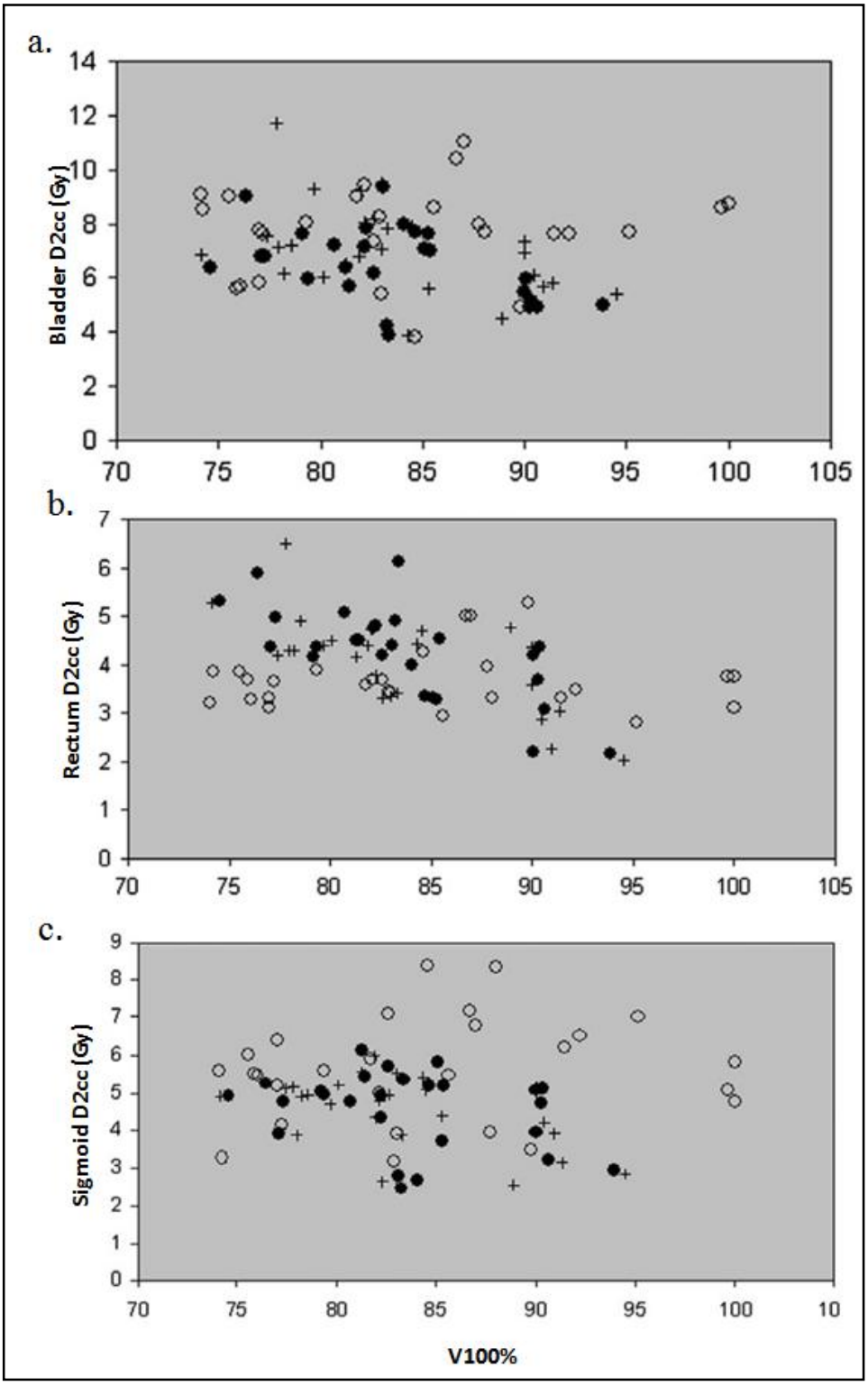

Figure 29 (a-c) :V_{100} is plotted for D2cc of bladder(a), rectum(b) and sigmoid(c) for standard(empty circle), manually optimized(plus) and inverse plan (dots).

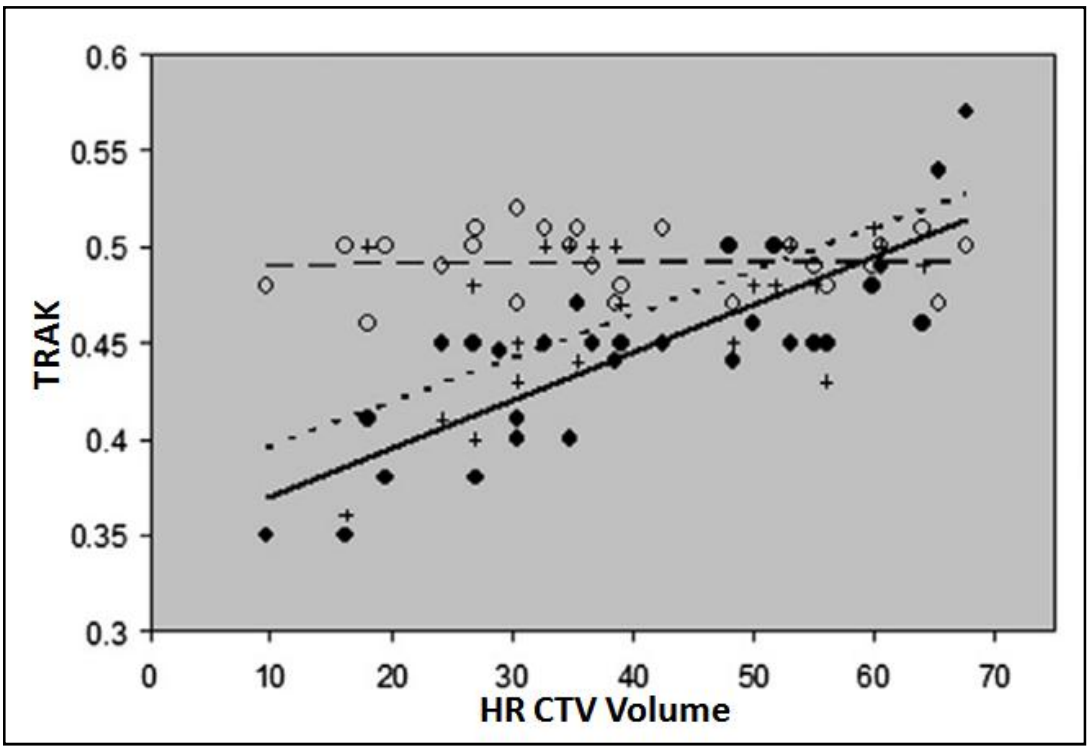

Fig 30: Relationship of HR-CTV volume and TRAK, showing direct proportanality for manually optimized(plus) and inverse plans (dots) but independent for standard plan (empty circle).

3.3.1. d Discussion:

There have been a lot of studies, which have compared the standard plan with the optimized (manual or inverse) one and reported that the optimized plan produces superior coverage and sparing of OARs [62, 63,147, 202-205]. Irrespective of the type of applicator (ovoid/ring) and the dose rate (HDR/PDR), optimization produces better results. In our experience, the standard plan produces optimal HR CTV coverage in the case of limited HR CTV size with good sparing of rectum, however dose to bladder and sigmoid are quite high. Optimization reduces the dose to the bladder and sigmoid significantly, while maintaining the HR CTV coverage [Fig. 29a, b]. However, HR CTV volumes of more than 35 cc were not adequately covered even by inverse optimization. Here it is important to emphasize that no adaptation of the application technique (e.g. addition of needles) was performed, and therefore the mean dose to the target could not be increased substantially. In many cases it even had to be reduced to achieve the dose limits for OAR. This has to be decided on an individual case basis by looking at target coverage and organ sparing at the same time. It implies that the application technique needs to be modified

to sufficiently treat such large tumours. It has been reported that the combined intracavitary and interstitial Vienna applicator can deliver prescription doses of up to 15 mm lateral to point A [2]. Similar approaches for ovoids have been reported [51, 206]. It was also found that for standard loading plans, TRAK is independent of HR CTV volume, while for manual optimized and inverse plans, TRAK is directly proportional to the volume of HR CTV, which could be attributed to the adaptation of dose to HR CTV in inverse optimized plans. This is in agreement with the findings published by Tanderup et al [61].

Between the manual optimized and inverse plans, only bladder dose was reduced significantly ($p = 0.005$), while all the other dose–volume parameters which were taken into consideration did not show any statistical significance. This study is the first to use the optimization tools in the Oncentra GYN, such as bar graphs and online DVH monitors. This might have improved the dosimetric results for the manual plans, with the resulting effect of reducing the differences between the manual and inverse optimization plans. However, this observation is limited to intracavitary plans, with a limited degree of freedom for dwell time optimization, and it does not take into account the time factor. Inverse planning may decrease the duration of planning time as compared to manual treatment planning.

A major experience noted from this work is that the average loading for the whole patient cohort was found to deviate from the original Fletcher loading. The difference in loading pattern is expected, due to the difference in the basic philosophy of the plans: the standard loading plan utilizes the same dwell loading while the inverse/manual plans are optimized such that the tumour is covered while normal tissues are optimally spared. Manual optimization is generally carried out by tweaking dwell weights, hence the change in loading pattern is expected to deviate from the standard loading pattern, and the planner is aware of the changes, while on the other hand inverse plans are based on mathematical cost functions to achieve local minima. In this study, the loading pattern of the manual optimized plan showed more deviation ($TRAK_{O/T}$= 1.7 ±

1.04) than the inverse plan (TRAK= 1.41 ± 0.93). This may be attributed to the HIPO algorithm that employs dwell time gradient restriction, which plays a major role in limiting the variation of dwell time [198].

It was found that the loading in the ovoid is high, for both manual and inverse plans. This could be attributed to the physical location of HR CTV, which is situated around cervix. The traditional Manchester system was designed to give the same dose to point A for various combinations of intra-vaginal and intrauterine source combinations, whereas the aim of inverse and manual plans is to cover HR CTV, while minimizing the dose to OARs. Dose to point A was not considered during optimization. Deviation from the traditional loading pattern and the variation in the dwell time may be acceptable as long as the isodoses conform to the specific topography of the target and optimal reduction in the doses to OARs [63,147]. However, a large deviation of the loading pattern/variations in the dwell time was not acceptable as it may increase the hotspots locally. In this study a dwell time gradient restriction was maintained at 0.5 for the inverse optimized plans, hence the accumulation of hotspots was minimized. It has been reported that volumes of 5 mm diameter were drawn around the catheter to reduce the variation in the dwell time [147]. There are no clear rules of how much of a deviation from the traditional loading systems is acceptable or on the amount of variation acceptable for dwell times. In clinical practice, the plans are generally evaluated based on the dose–volume parameters and the dose distribution. In the era of 3D treatment planning, dose prescription has seen a paradigm shift from point A to tumour volume. The dose distribution is individualized based on the location of the tumour with respect to the OARs, rather than the standard loading pattern. The loading pattern or the variation of dwell times has never been a major criterion for rejecting a plan in the clinics. It has also been suggested by Pötter et al. that in addition to DVH parameters considered at present, additional constraints and concepts are necessary to reduce high dose areas. This is particularly applicable to structures, which have not yet been contoured, such as vagina, vessels,

nerves, and connective tissue [153]. Currently, it may be essential to respect the standard loading pattern, while practicing conformal BT using inverse planning, until sufficient clinical evidence becomes available. Detailed analysis revealed that topography of the OAR with respect to HR CTV is the deciding factor for the loading pattern. When the sigmoid dose was well below the dose constraint, tandem was heavily loaded to meet the other constraints, such as coverage of HR CTV and dose to the bladder and rectum. In this case, the ovoid loading was less, which results in lower dose to the vagina, while the hotspot around the tandem increases. Hence careful evaluation of hotspots around the tandem is warranted when the sigmoid dose is well below the tolerance. When the bladder dose is very high, the contribution from the ovoid is increased to meet the constraints rather than increasing the loading of the tandem. In such a case, the hotspot in the vagina may well be a cause for concern.

For about 50% of our patients, the topography of the sigmoid shows that it lies close to the tandem superiorly. This may be attributed to the vaginal packing and rectal separator that displaces the rectum posteriorly and hypothetically pushes the sigmoid anteriorly close to the tandem. The situation for other centers may be different. In Vienna, fewer patients showed sigmoid in such a vicinity to the treated volume as compared to the rectum. This fact may be related to different application procedures or different patterns of tumour and OAR topography. There, in contrast to this study, the optimization results in lower dose from the ring than the tandem. This requires further investigation and comparison with other institutions' implantation and packing techniques with lower sigmoid doses, which is beyond the scope of the current study. The preliminary evaluation of our data of 3D image-based BT indicates that the dose to the upper rectum and sigmoid is higher than to the rectum [58]. This is consistent with other published data [152, 207,208]. Dose to the vagina has not been analyzed in this study. Trnkova et al. found that the HIPO algorithm also used in the current study was able to lower the vaginal dose compared to manual treatment plans [199]. In the present study ovoids have been used instead of

rings. A clear comparison between ovoid and ring dose distributions and their relationship to clinical endpoints is absent [68].

3.3.1.e Conclusion

Inverse planning with HIPO and/or manual optimization offers improved plans in terms of OAR sparing and maintaining target coverage when compared to standard clinical plans. For large and/or unfavorable targets, coverage cannot be achieved with either manual or inverse optimization if no adaptation of the application technique is included. The average loading pattern for the whole patient cohort was found to deviate from a traditional standard Fletcher loading. For our patient cohort, the tandem loading was decreased compared to the ovoids mainly due to high sigmoid dose.

3.3.2 Role of help structures in reducing the variation of dwell time using Inverse planning algorithm (IPSA):

3.3.2.a Purpose

The use of inverse planning is popularized with its application for BT [172-176]. Very few investigating groups have studied the use of inverse optimization algorithm in cervical cancer BT [209-211, 202, 147, 198]. Although successful in prostate BT, its use in GYN BT is still not common, due to various issues, which have been reported. Chajon *et al.* [147] reported that a large variation of dwell times was observed with IPSA for T/O application and suggested the use of help structures to reduce the variation. Further it was reported by Trnkova *et al.* [198] that HIPO algorithm produces plans without high dose regions for both T/R and Vienna applicator and concluded that modulation restriction, which is used in HIPO plays an important role in obtaining a distribution, without much of heterogeneity as compared to IPSA. A recent study by Mavroids *et al.* [197] for prostate BT investigates the use of modulation restriction and concludes that modulation restricted optimization gives similar results as compared to optimization without modulation restriction; however, it may slightly improve the dose distributions.

One of the typical qualities of manual optimization as compared to inverse planning algorithms is that it did not deviate very much from the standard loading pattern. The traditional pear shaped dose distribution was maintained, except for a few minor changes that improve the target coverage and OAR sparing. On the other hand, the inverse optimization changes the dwell time gradient to a large extent. These issues with inverse planning especially in intracavitary BT need to be clearly understood for various situations and how much the result deviates from the clinically acceptable standard, i.e. the standard loading pattern or manual optimization, before implementing into clinical practice. To study the effect of modulation restriction we made IPSA plans with and without help structures for two types of applicators used in TMH which are T/O and Vienna applicators.

The purpose of this study was to objectively compare the dosimetric outcome of IPSA, with the focus on the use of help structures during optimization for T/O and Vienna applicators.

3.3.2.b Materials and Methods:

The data of thirty-three patients who underwent MRI image based HDR intracavitary BT for cervix cancer was selected for this retrospective study. There were eleven IIIB, fourteen IIB, two IIA and one IB2 patients. A dose of 50 Gy was given as external beam radiotherapy dose. Out of 33 patients, 23 patients were treated with intracavitary approach (I/C) using Nucletron standard T/O CT/MR compatible applicators with tandem lengths of 5 or 6 cm and ovoid diameters of 2 or 1.5 cm. Ten patients were treated with combined intracavitary and interstitial approach (I/C + I/S) with Vienna applicator [2]. All patients were transferred to the MRI scanner soon after completion of the application in operation theatre. The in-house built MRI dummies filled with water were inserted in the catheters to visualize central tandem, ovoid and ring in the scans. T2 weighted fast spin echo MRI scans (GE, Signa, Excite, 1.5T) were obtained in the axial, coronal, and sagittal orientations. The scans were taken with 3 mm thickness and 0mm spacing. These scans were transferred to the Oncentra contouring workstation (Nucletron, Netherlands) where HR CTV, bladder, rectum and sigmoid were contoured in accordance with GEC ESTRO recommendation [83, 124]. Direct applicator reconstruction was carried out on the MR images using multi-planner reconstruction [142]. The dose computation algorithm was based on TG 43 as recommended by the AAPM (200). Treatment planning was carried out with the PLATO Sunrise planning system (Nucletron, Netherlands).

Three plans were generated for T/O and Vienna applicator: manual optimized plan (MOPT), IPSA without help structures (IPSA_woHS) and IPSA with help structures (IPSA_wHS). Prescription dose of 7 Gy was used for these three plans.MOPT plans were generated by applying manual optimization to the standard plan, which was based on Fletcher standard loading system. Manual optimization, also called GrO, was done by altering dwell

times/dwell weights or by dragging the isodose lines using mouse in MRI images. The dwell positions outside the HR CTV were not switched off during manual optimization to retain the pear shaped distribution. The dwell positions contributing to the coverage was increased and the dwell positions contributing to the dose to OARs were reduced appropriately. In case of the Vienna applicator, the loading of the needles were kept at about 15-20% as compared to the tandem and the ring [2].

Two inverse plans were completed: IPSA_woHS and IPSA_wHS. For IPSA_woHS, HS around tandem, ovoid/ring and needles were ignored during inverse optimization, whereas for IPSA_wHS they were taken into account. The dose volume objectives used for inverse plan are shown in Table 6. All the plans were started with the dose volume objectives presented in the table. Based on the results of the previous plan, the objectives were changed by trial and error until an optimal plan was obtained. The dose volume constraints used for IPSA were similar to MOPT. The DVH was calculated with the upper dose limit factor of 3 and 100,000 sampling points in the volume of interest.

The dose volume parameters recommended by GEC ESTRO GYN were analyzed for comparison: V_{100}, D_{90}, D_{2cc} and $D_{0.1cc}$ of bladder, rectum and sigmoid. For the evaluation of high dose region, the volume receiving 200% of the prescription dose was also evaluated. Dose to point-A and TRAK were documented. Conformity index (COIN) was calculated using the followingformula:

$$COIN = [(V_{ptv,ref}/V_{ptv}] \times [V_{ptv,ref}/V_{ref}]]$$

Where $V_{ptv,ref}$ is the target volume received by reference isodose line, *Vptv* is the volume oftarget volume , *Vref* is the volume of the implant received by reference isodose line. The data was analyzed using paired sample t-test. The test was performed with a significance level of 5%.

Table 6: Dose volume constraints used to obtain inverse plans.

VOI	Margin(mm) dose control	Margin(mm) catheter activation	Min surface dose weight	Min surface dose (cGy)	Max surface dose (cGy)	Max surface dose weight	Min volume dose weight	Min volume dose (cGy)	Max volume dose (cGy)	Max volume dose weight
HR CTV	5	2	100	700	750	100	150	700	750	150
Help structure	0	0	20	1500	2700	5	20	1500	2700	5
Bladder	0	0	0	500	500	30	0	500	500	30
Rectum	0	0	0	420	420	20	0	420	420	20
sigmoid	0	0	0	420	420	30	0	420	420	30

Table 7: Dose volume parameters of HR CTV and OARs for T/O applicator

	Dose volume parameter	MOPT	IPSA_woHS	IPSA_wHS	p-value MOPT vs woHS	p-value MOPT vs wHS	P-value wHS vs woHS
HR-CTV	Volume (cc)			41±12			
	D_{90} (Gy)	6.2±0.9	6.1±0.5	6.0±0.4	0.19	0.22	0.25
	V_{100} (%)	85±7	86.5±3.4	86.0±4.1	0.54	0.50	0.64
	$V_{200\%}$(cc)	11.2±4.3	15±1.9	13.7±1.9	0.000	0.001	0.01
	$V_{400\%}$(cc)	3.1±1.8	7.6±1.5	5.4±1	0.000	0.001	0.01
	Point A (Gy)	6.6 ±1.9	6.7 ±1.4	6.7 ±0.9	0.22	0.21	0.30
	TRAK	0.48±.09	0.42±.08	0.43±.06	0.001	0.000	0.30
	COIN	0.34±.08	0.42±.08	0.41±.05	0.000	0.000	0.35
Bladder	D_{2cc} (Gy)	6.5±1.3	6.0±1.4	6.1±1.4	0.001	0.001	0.29
Rectum	D_{2cc} (Gy)	3.9±1.2	4.1±1.4	4.0±1.4	0.26	0.54	0.50
Sigmoid	D_{2cc} (Gy)	4.9±1.1	4.8±1.3	4.8±1.3	0.40	0.45	0.59

3.3.2.c Results

The isodose distribution of Vienna applicator of a representative patient for various plans is presented in Figure. 31.

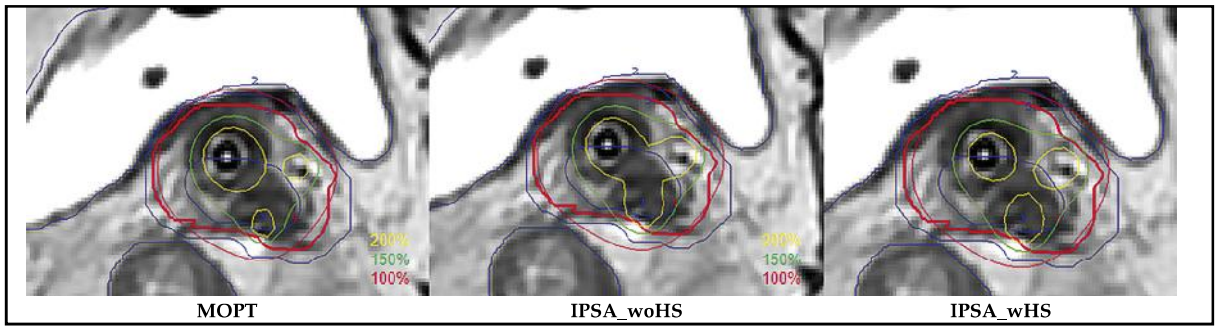

Figure 31: The isodose distribution of a representative patient for various plans, MOPT, IPSA woHS, and IPSA wHS using Vienna applicator.

3.3.2.c.1 T/O applicator

Table 7 illustrates the dose volume parameters for the HR CTV and OARs. No significant variation was observed with dose volume parameters for HR CTV among the three plans. Similarly, IPSA did not offer significant improvement in sparing the OARs, as compared to MOPT, except for the bladder dose. The D2cc bladder dose was significantly less in inverse plans as compared to MOPT plan (p = 0.001). The dose to rectum was within tolerance limits (3.9 ± 1.2 Gy) in MOPT, but an increased dose was observed in both inverse plans, though not significantly (0.26). It was observed that V200 and V400 was significantly high in both the IPSA plans as compared to MOPT, however in IPSA_wHS, reduced volume was observed and the p-value was towards non significance. Similarly, the TRAK was significantly lower in IPSA as compared to MOPT (p = 0.001), which may suggest that dose distribution from IPSA plans were customized to the individual tumour shape without maintaining the conventional pear shaped dose distribution as in case of MOPT. In terms of conformity, IPSA plans scores over MOPT plan, as IPSA plans were significantly conformal as compared to MOPT (p = 0.000).

3.3.2.c.2 Vienna applicator

The dose volume parameters of HR CTV showed statistical significance in favour of IPSA as compared to MOPT (Table 8). However, it is to be noted that in addition to a considerable improvement in D90 and V_{100} of HR CTV, the high dose regions V200 and V400 had also increased significantly in inverse plans as compared to MOPT plans. It is also worth noting that IPSA plans were more reproducible as compared to the MOPT plan, as the standard deviation of all the dose volume parameters of IPSA was smaller as compared to MOPT plans. TRAK and COIN showed statistical significance in favour of IPSA, which could be attributed to the individual adaptation of IPSA to tumour volume, as against standard loading pattern in case of MOPT (p = 0.001). However, amongst OARs, only the bladder dose was significantly improved with IPSA, as compared to the rectum and sigmoid. The dose volume parameters of both HR CTV and OARs between IPSA_woHS and IPSA_wHS were found insignificant for all the dose volume parameters and significant for the high dose regions, V200 and V400.

3.3.2.c.3 Loading pattern and treatment time

For the T/O applicator, the ratio of dwell time of tandem to ovoid (T/O) was found to be 0.93 ± 0.2, 0.64 ± 0.15, 0.66 ± 0.17 for MOPT, IPSA_woHS and IPSA_wHS, respectively. For both the inverse plans, the ratio showed significant deviation as compared to MOPT plan. On the other hand, for the Vienna applicator, the ratio of dwell time of tandem and ovoid was found to be 1.02 ± 0.15, 0.94 ± 0.1, 0.98 ± 0.08 for MOPT, IPSA_woHS and IPSA_wHS, respectively. However, the ratio of total time of needles to the tandem) was found to be 14 ± 2.5, 53 ± 9, 22 ± 6 for MOPT, IPSA_woHS and IPSA_wHS, respectively (Table 9), which implies that in IPSA_woHS the dwell time in needles were half of the dwell time in the tandem, while in MOPT the needles were loadedin 14% and in IPSA_wHS it was 22% of the dwell time of tandem.

Table 8: Dose volume parameters of HR CTV and OARs for Vienna applicator.

	Dose volume parameter	MOPT	IPSA_woHS	IPSA_wHS	p-value MOPT vs woHS	p-value MOPT vs wHS	p-value wHS vs woHS
HR-CTV	Volume (cc)			39±14			
	D_{90} (Gy)	7.6±0.6	7.8±0.4	7.7±0.2	0.001	0.002	0.38
	V_{100} (%)	93.8±3.3	98±1.8	98.5±2	0.005	0.006	0.64
	$V_{200\%}$(cc)	13.5±0.9	21±0.5	15.8±0.4	0.000	0.001	0.003
	$V_{400\%}$(cc)	4.3±0.5	12±0.3	7±0.3	0.000	0.001	0.000
	Point A (Gy)	7.3 ±1.9	7.6 ±0.5	7.5 ±0.4	0.002	0.006	0.30
	TRAK	0.43±.06	0.39±.03	0.40±.02	0.001	0.001	0.30
	COIN	0.32±.08	0.42±.06	0.43±.04	0.000	0.000	0.5
Bladder	D_{2cc} (Gy)	5.4±0.9	5.0±0.5	5.1±0.4	0.000	0.001	0.25
Rectum	D_{2cc} (Gy)	3.6±1	3.7±0.5	3.6±0.3	0.51	0.52	0.51
Sigmoid	D_{2cc} (Gy)	3.4±0.8	3.5±0.6	3.3±0.5	0.50	0.52	0.55

It was observed that IPSA_woHS had highest contribution from needles, while help structures in IPSA_wHS has significantly reduced the dwell time contribution from the needles (p= 0.000). It could be noted that the ratio T ($T_{N/T}$ %) is comparable with each other for the three plans for Vienna applicator, while in case of T/O applicator both IPSA plans showed significant variation as compared to MOPT, which may be attributed to the involvement of needles. It was observed that the contribution from the needles is highest in IPSA_woHS. Inclusion of the HS in the optimization reduced the contribution of dwell time of the needles in the IPSA_HS plan and was of the same order as the MOPT plan. During manual optimization it was considered that most of the dose came from the intracavitary Vienna applicator with the needles having very low loading only to cover the missing parts of the HR CTV, which was not possible to cover with the intracavitary alone [2]. With respect to individual variation in dwell time for the T/O applicator, IPSA resulted in steep variation in the dwell time in the catheters, which resulted in-homogeneous plans, as compared to MOPT. It was also observed that in IPSA, the dwell time next to a critical structure was turned off completely, while long dwell times were noticed where no critical structures were present. Figure 32a & b shows the individual dwell time of catheters

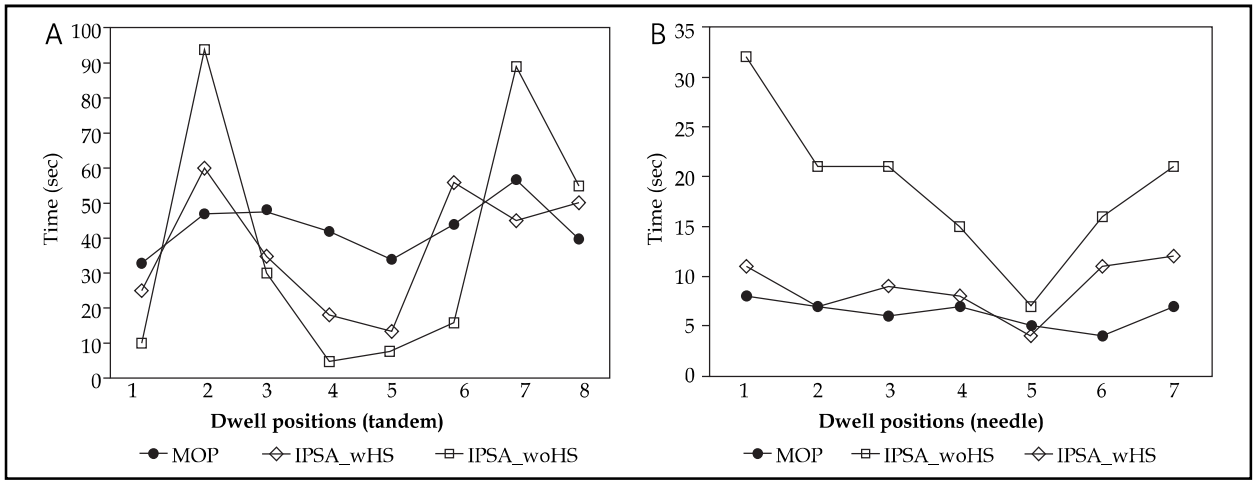

Fig 32 (a) *Individual dwell time of a tandem for three plans which are manual optimized(MOPT), IPSA plans done with help structures (IPSA_wHS) and IPSA plan without help structures(IPSA_woHS) for T/O applicator.* ***(b)*** *Individual dwell time of a needle for three plansfor Vienna applicator.*

for MOPT, IPSA_woHS and IPSA_wHS plans of a representative patient for T/O and Vienna applicator.

3.3.2.c.4 Planning time

The planning time for MOPT plan was 15-20 minute, while planning time for IPSA was about 10 min. Changing the constraints and re-evaluating the dose volume parameters to arrive at an optimal plan was indeed a time consuming factor for IPSA plans as well. However, it took about 20 minutes to arrive at an optimal MOPT plan for a Vienna applicator by an experienced physicist. Changing the individual dwell weights, manually dragging the isodose lines using a mouse and evaluation of dose volume parameters was a time consuming process during MOPT plans. Drawing of help structures was also found to be a time consuming process, although we did not quantify the time.

3.3.2.d Discussion:

In intracavitay BT, inverse planning is not a popular concept due to various factors. One is the reluctance to change from traditional practice, which produced excellent results as the pear shaped distribution has been used for decades which resulted in good clinical outcomes [154-158]. Inverse planning in intracavitary BT is always seen with a doubt, due to various factors. The clinical implication of changing the standard loading pattern is not known. Similarly, the variation of dwell time across the catheters due to the absence of modulation restriction in certain algorithm was debated [147, 197,199,212]. Although, it is proved beyond doubt that IPSA produces superior dose distribution in terms of improved and highly conformal target coverage and reduced dose to OARs, it is still unclear whether the variation of dwell time across the catheters due to the absence of modulation restriction plays a role in toxicities. While this information is missing it is still believed that pear shaped distribution should be maintained as far as possible. Chajon et al have proposed defining help structures around the applicator to obtain homogenous dwell time distributionand to overcome the problemof variationof dwelltime

Table:9: The absolute dwell time in seconds of T/O and Vienna applicator for MOPT: Manual plan, wHS: IPSA plan with help structures, woHS: IPSA plan without help structures.

T/O applicator				p value		
Dwell time	MOPT	woHS	wHS	MOPT vs woHS	MOPT vs wHS	wHS vs woHS
Tandem(sec)	340±38	253±65	270±45	0.000	0.040	0.015
Rt ovoid(sec)	180±26	228±71	210±38	0.003	0.025	0.021
Lt ovoid(sec)	185±45	170±52	198±54	0.005	0.010	0.000
Total time(sec)	705±49	651±81	678±51	0.003	0.020	0.008
Total ovoid(sec)	365±41	398±47	408±49	0.004	0.002	0.330
Tandem/Total ovoid	0.93±0.2	0.64±0.15	0.66±0.17	0.000	0.002	0.370
Vienna applicator						
Tandem(sec)	361±29	270±46	320±42	0.001	0.150	0.030
Ring(sec)	353±38	286±69	325±37	0.002	0.180	0.028
Needles(sec)	51±15	143±105	70±39	0.000	0.130	0.000
Total time(sec)	765±59	699±64	715±59	0.003	0.100	0.007
Needles / Tandem time (%)	14±2.5	53±9	22±6	0.000	0.150	0.000
Tandem/Ring	1.02±0.15	0.94±0.1	0.98±0.08	0.170	0.200	0.350

while using IPSA, with GYN application [147]. However, the generation of such dummy structures would be time consuming in a busy clinical centre especially in the case of IC+IS approach. Hence we carried out a study, to find if the help structures really help in reducing the variation of dwell time and its impact on the dose volume parameters.

The results of the current study implies that the use of help structures have not made any significant impact over the dose volume parameters, on the other hand, irrespective of the help structures, both the inverse plans resulted in superior plans as compared to MOPT. In the case of T/O applicator, IPSA produced significantly reduced bladder dose without compromising the HR CTV coverage, it also produces highly conformal dose as compared to MOPT. Similarly, in the case of Vienna applicator, it has produced significant improvement in the HR CTV coverage in addition to bladder sparing and conformity. It also showed no significant increase in high dose regions V200 and V400 for T/O applicator. However, in the case of Vienna applicator, the high dose regions were significantly higher.

The ratio of $T_{T/O}$ and $T_{T/R}$ did not show any significant variation among the IPSA plans for both T/O and Vienna applicator, however, $T_{N/T}$ was as high as 53% for IPSA_woHS, while it was 22% for IPSA_wHS. This may imply that the benefit of using the help structures during optimization is more when the number of catheters is more than two/three catheters as against T/O or T/R applicator. Hence it may be considered that while using combined intracavitary and interstitial (IC+IS) approach, help structures may be used during optimization and need not while using intracavitary application as the benefit is negligible both in terms of dosimetric parameters and dwell time. It is not very clear as to why, during IC approach, the help structures are not as beneficial as IC+IS approach. However, it may be attributed to the number of degrees of freedom associated with the interstitial approach. Caution is therefore, required while using IPSA in the case of IC+IS approach, as it may lead to overloading of needles and variation of

dwell time especially in the needles. However, during routine clinical work, we found that this approach of drawing help structures in the case of Vienna applicator is not very practical, as it is a time consuming process, although, it produces superior dose distribution, as compared to MOPT plan.

In a recent publication Trnkova et al has compared HIPO and IPSA algorithm and concluded that HIPO optimization offers better dose distribution as compared to IPSA, interms of controlling the high dose regions, as HIPO employs dwell time gradient restriction [198]. It is still unclear, how this is going to translate clinically. However, recent clinical results are encouraging and justify the use of IPSA in the clinics [212]. Kim et al had presented clinical outcomes of image-guided BT using IPSA high dose rate BT boost of 51 patients of cervical cancer with two year follow up. They concluded that IPSA HDR BT is well tolerated and achieves excellent local control of disease. However, it should be noted that this study was based on IC and not IC+IS approach. The results of the current study also justify the use of IPSA in the clinics for T/O application without any modification, such as drawing of HS. The findings of the present study shows that drawing of HS around the tandem, ring and the needles help in reducing the hotspot around the needles. Now the question is that, in the case not using these HS during optimization, what would be the clinical consequences if any due to the variation of dwell time or low volumes of high dose regions outside the uterus, which was nonexistent in time-tested traditional loading pattern and manual after loading. Mavroids et al has carried out a radiobiological evaluation of the influence of dwell time modulation restriction in prostate BT using HIPO, and concluded that modulation restricted optimization gives on average similar results with the optimization without modulation restriction [197]. Optimization with modulation restriction gives only a minor improvement in the effectiveness of plans. While this is true for prostate BT, further investigation may be required for GYN BT, where

traditionally, the high dose is restricted inside the uterus and may emphasize the need for further investigation of the clinical implication of modulation restriction.

3.3.2.e Conclusion:

IPSA plans were compared with manually optimized plan for T/O and Vienna applicator, it was found that IPSA produced superior plans with respect to HR CTV coverage and sparing of OARs. IPSA also produced conformal plans as compared to MOPT. For T/O applicator, it was found that the use of HS did not make any impact both in the dose volume parameters and in the loading of tandem and ovoids, however in the case of Vienna applicator, inclusion of HS in the optimization made a significant impact in the loading of needles. Without the HS, the optimizer loaded the needles heavily, which drastically came down when HS were included. HS may be included in the optimization while using IC+IS, and may not while using just intracvaitray approach.

3.3.3 Inverse planning algorithm (IPSA) for interstitial implants in Gynaecological BT:

3.3.3.a Purpose:

When pelvic anatomy is suboptimal because of narrow vagina or the absence of uterus postoperatively, interstitial BT using template plays an important role especially in advanced stage or recurrent diseases [35-40]. Various template systems have been developed for treatment of pelvic malignancies [37, 43]. Among them, MUPIT for BT was first devised by Martinez for prostate, and was later adapted to cervix, vagina, female urethra, perineum, and ano-rectal region. The review of literature shows the evolution of this technique over the years, overcoming a number of limitations with advanced imaging modalities [215,216] and dose optimization [209-211, 202, 147, 198].

Three-dimensional treatment planning uses images of CT/ MR to visualize target volumes and critical structures with respect to the implanted needles to produce customized dose distributions that may improve local control and reduce complications relative to conventional BT treatment planning for MUPIT using orthogonal images [213,214]. Further, CT/MR imaging provides excellent soft tissue definition such that delineation of target and OARs in relation to the applicator is possible. It enables to accurately assess the dose received by the target and the OARs. With the advances in imaging, the optimization methods also have improved. IPSA has been found to be superior with respect to target coverage and normal tissue sparing as compared with traditional optimization methods for prostate [174-178], and gynecologic malignancies [209-211, 202, 147, 198].

The purpose of this study was to objectively compare the dosimetric outcome of inverse planning algorithm as compared to traditional dose-point optimized (DPO) plan and manual optimized plan/GrO plan. This was the first independent assessment of IPSA algorithm in clinical practice for interstitial gynecologic malignancies using MUPIT.

3.3.3.b. Methods and materials

The data set of 10 consecutive patients of gynecologic cancers (post-op cervix: 3, vault recurrence: 4, and carcinoma vagina: 3) who underwent routine external radio- therapy and high-dose rate interstitial boost using MUPIT were selected for this dosimetric study. The external radiation dose was 50 Gy at the rate of 2.0 Gy/fraction followed by 20 Gy in 5 Gy/fraction (2 fractions/day) of interstitial BT. The details of the BT procedure have been based on the departmental protocol [215]. To summarize, a pelvic examination under anesthesia was done followed by marking the boundaries of the residual disease using silver makers. The urinary bladder was catheterized with 7 mL of diluted urograffin pushed into its bulb, followed by the insertion of vaginal cylinder; the template then was placed and held to the perineum using 18 gauge needles with closed and blunt tips. Ultrasound imaging was used in a few patients as guidance for the placement of needles. Patients were then taken for imaging and planning.

3.3.3.b.1 Dosimetry and optimization

Image acquisition for treatment planning was done on the same day after the implant using axial CT scans of 3 mm slice thickness was taken on Somatom Emotion CT scanner (Siemens Medical Systems, Germany). The images were transferred to the BT Planning System (PLATO-Sunrise v.14. 3, Nucletron B.V., Veenendaal, The Netherlands) via local area network. The dose computation algorithm in the treatment planning system is based on Task Group 43 as recommended by the AAPM [200]. The radiation oncologist delineated the CTV using pretreatment clinical extent, imaging (pretreatment and post-EBRT), intraoperative findings, and radio-opaque silver markers placed during the procedure. The OAR's, the rectum, bladder, and urethra were contoured. Reconstruction of the implant geometry was carried out using multi-planar reconstruction. This algorithm enables the planner to track the catheters in axial, coronal, and sagittal planes. A negative offset of 9 mm was given for each needle to compensate for the dead space (5.5 mm) and the source clearance (3.5 mm). The dwell positions were loaded based

on the CTV, with an extra margin of 5 mm across the CTV. For each patient three plans were generated.

3.3.3.b.2 Dose Point Optimized plan

The dose points were placed between the catheters in accordance with the stepping source dosimetry system throughout the CTV. The dose points were created using the option of creating basal points in the treatment planning system. In our case, generally square geometry was used. The plans were dose-point optimized on volume. The dose was prescribed on the dose points. The prescription isodose line was 85-100% line, variable from patient to patient based on the coverage.

3.3.3.b.3 Graphical Optimized plan

The DPO plans were manually optimized, wherein the active dwell weights were changed. This could be done by clicking the isodose line with the mouse dragging it to the desired location. Alternately, the dwell weights of those positions contributing to the dose to the OARs were reduced and the dwell weight of those positions contributing to the CTV coverage was increased. This was done repeatedly until a satisfactory plan was obtained with respect to CTV coverage, sparing of OARs, homogeneity, and conformity in that order. The plan objective for optimization was to maximize the CTV coverage, whereas minimizing the dose to the OARs. Because GrO/manual forward planning is operator dependent, to maintain uniformity among the manually optimized plans, emphasis was given to adequately cover the CTV, while trying to reduce the dose to the OARs to the predetermined dose objective parameters. The dose objective parameters for the OARs were as follows. Dose to the most exposed volume, D2cc of bladder and rectum was 3.0 and 2.5 Gy, respectively whereas D1cc of urethra was 3.0 Gy. For CTV, dose to 90%, D90 of 4 Gy was considered.

3.3.3.b.4 Inverse plan

IPSA was used to generate an inverse plan, where the dwell positions were maintained similar to DPO plans. The plan objectives were similar to that of GrO plan. The relative importance factors and the dose constrains were changed until an optimal plan was obtained that meets the dose objective parameters of both CTV and the OARs. Table 6 provides a representative set of dose objective parameters used to obtain an IPSA plan.

3.3.3.b.5 Plan evaluation

Dosimetric outcome from these three different plans were compared. For quantitative analysis, cumulative DVH was calculated for every plan with 25 mm margins around the implanted volume in all directions with 100,000 calculation points randomly placed in the volume of interest. For the CTV, D_{90}, the dose covering 90% of the CTV volume, and V_{100}, the percentage volume covered by 100% of the CTV volume were evaluated. V200, the absolute volume covered by 200% of the prescription isodose, was evaluated. For OARs, D_{2cm3}, minimal dose received by the most irradiated $2cm^3$ volume of bladder and rectum were compiled [146]. For urethra, dose to 1 cc volume was considered. In addition, V_{75}, the volume receiving 75% of the prescription dose was evaluated for rectum, bladder, and urethra. Dose-volume indices, including homogeneity index (HI) and conformity number were evaluated [216]. HI is the fraction of CTV receiving a dose between 100% and 150% of the reference dose. To evaluate the statistical significance, we made an analysis of the descriptive statistics (mean, standard deviation, and 95% confidence interval) of dosimetric parameters for the three optimization techniques. The parameters were compared for the three groups using paired t test. The level of significance was set at 0.05.

3.3.3.c Results:

All 10 applications were evaluable for this dosimetric outcome. The average number of implanted needles was 23 ± 6 (range, 18-25). The dose distribution of DPO, GrO, and IPSA

plans of a representative patient is shown in Figure 33. Table 10 illustrates the dose-volume parameters of all the plans. The mean (standard deviation) volume of CTV was 123.97 ± 40.57 cc (range, 68.04-190.48 cc). The mean volume of rectum and bladder was 43.76 ± 18 and 121.05 ±59.18 cc, respectively. Coverage of the CTV with GrO and IPSA was significantly better (mean V100 of 88.8% and 89.1%; p = 0.006) as compared with DPO plan (83.7%). Similarly, mean D90 was same in both GrO and IPSA plan, namely, 3.96± 0.23 and 3.96 ± 0.15 Gy, respectively. Although both plans have resulted in similar D_{90}, it was observed that IPSA plans were more reproducible as compared with GrO plan. This could be observed from the standard deviation of the IPSA plan, 0.15 Gy as compared with GrO plan 0.23 Gy (p =0.003). Mean volume receiving 150% of dose was 25.6% and 26.9% for GrO and IPSA as compared with 15.3% of DPO plan, which is reflected in HI. DPO plans were more homogeneous with HI being 0.82 as compared with 0.68± 0.05 of GrO and 0.71 ± 0.04 of IPSA.

Table 10: Dose volume parameters of DPO, GrO, and IPSA plan

Parameters	DPO	GrO	IPSA	p value (IPSA vs GrO)	P value (IPSA vs DPO)
D_{90} (Gy)	3.7 (±0.21)	3.96 (±0.19)	3.96(±0.18)	0.75	0.001
D_{100} (Gy)	2.4 (±0.3)	2.3(±0.23)	2.24(±0.2)	0.4	0.003
$V_{100\%}$(%)	83.73 (±4.6)	88.81(±3.9)	89.14(±3.0)	0.62	0.001
$V_{150\%}$ (cc)	18.8(±6.3)	30.57(±8.07)	33.38(±1.5)	0.48	0.000
V_{200} (cc)	6.92 (±0.33)	10.51(±0.72)	9.88 (±1.74)	0.12	0.001
HI	0.82(±0.03)	0.68(±0.05)	0.71 (±0.04)	0.1	0.000
COIN	0.68 (±0.08)	0.72(±0.06)	0.78(±0.05)	0.001	0.001
TRAK (cGy)	0.27(±0.06)	0.29(±0.06)	0.27(±0.06)	0.006	0.524
RD_{2cc} Gy	3.3(±1.06)	2.91(±0.63)	2.79(±0.67)	0.046	0.011
BD_{2cc} Gy	3.17(±0.5)	2.89(±0.63)	2.81(±0.67)	0.035	0.003
BV_{75cc}	3.69(±0.05)	2.33(±1.1)	1.95(±0.98)	0.004	0.001
UD_{1cc} Gy	2.53(±0.9)	2.45(±0.6)	2.37(±0.8)	0.04	0.03

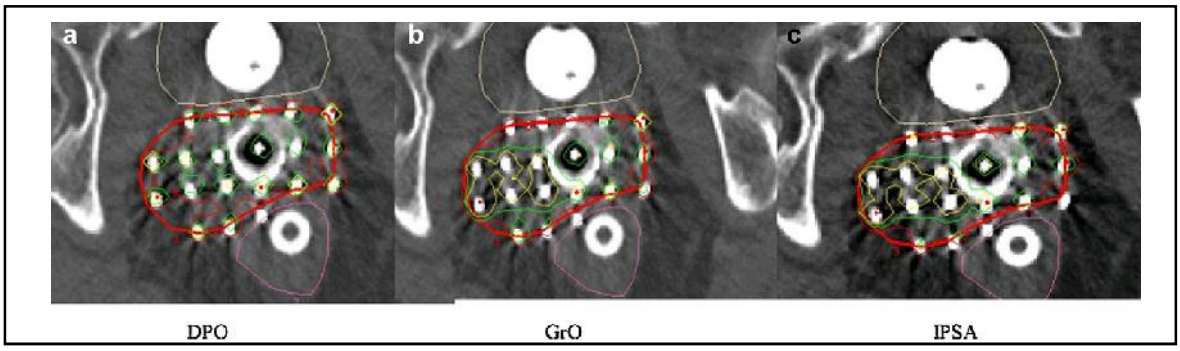

Figure 33: Dose distribution of DPO, GrO, and IPSA plans of a representative patient. DPO = dose-point optimization; GrO =manual/graphical optimization; IPSA= inverse planning simulated annealing.HRCTV shown as thick red contour. Dose levels 150%(yellow), 100%(green) and 85%(thin red)are also shown.

However, IPSA plans resulted in high conformality with conformity index of 0.78 as compared with 0.72 (p = 0.001) and 0.68 (p = 0.001) for GrO and DPO, respectively. Total reference air kerma of DPO and IPSA plans were 0.27 ±0.06 cGy, whereas for GrO it was 0.29 ±0.06 cGy. Figure 33 a-c illustrates the relation between the dose to the OAR (D_{2cm3}) with respect to CTV coverage (D_{90}), for DPO, GrO, and IPSA plan. The lower right quadrant represents the dose limits of the OAR without compromising the CTV coverage. It could be seen that rectum is the dose limiting factor [Fig. 33a], and none of the DPO plans could satisfy the dose-limiting criteria. For IPSA and manual optimization, it was observed that most of the patients were approaching toward the lower right quadrant, which confirms that optimization plays a major role in reducing the dose to the OARs, while maintaining CTV coverage. The dose to rectum (D_{2cm3} : 3.3 ±1.1 Gy) and bladder : 3.2± 0.5 Gy) was generally high for DPO plans. However, dose to urethra (D_{1cm3}: 2.5 ± 0.9) was well within the tolerance limits. GrO reduced the dose to the rectum (2.9± 0.6 Gy; p 50.0) and bladder (2.9 ± 0.6 Gy; p =0.003) significantly. IPSA resulted in a further reduction of the dose to the rectum (2.79± 0.67 Gy; p =0.046) and bladder (2.8± 0.7 Gy; p = 0.035), however with no statistical significance as compared with GrO.

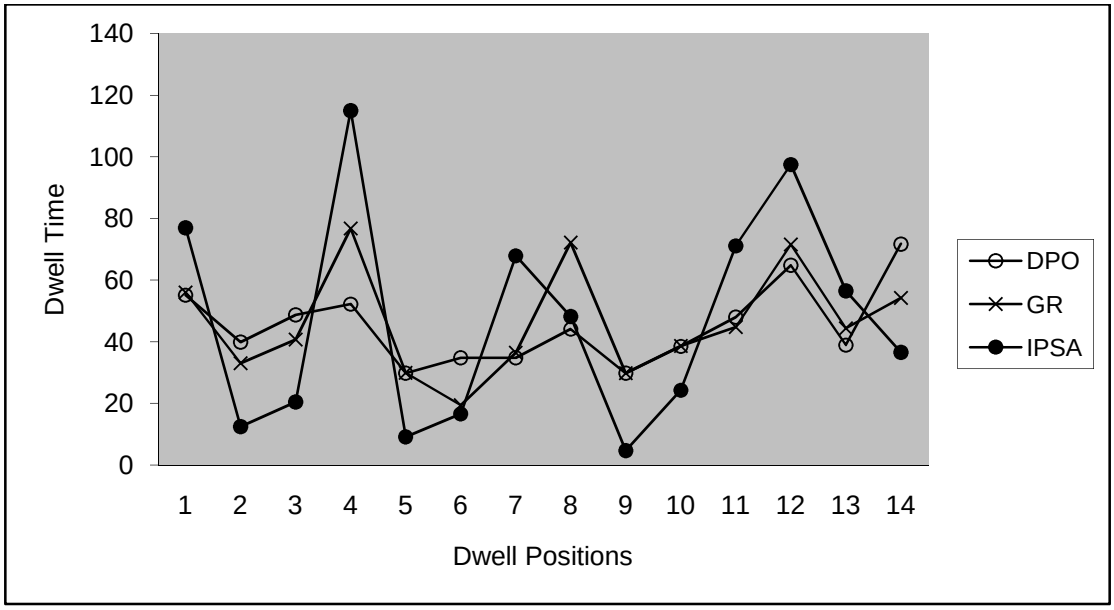

Figure 34: Variation of dwell time in each catheter of a representative patient for DPO, GrO, and IPSA plan. DPO = dose-point optimization; GrO = manual/GrO; IPSA = inverse planning simulated annealing.

Figure 34 shows the individual dwell time of catheters for DPO, GrO, and IPSA plans of a representative patient. DPO plans showed a smooth variation between the dwell time in the catheters, which resulted in highly homogeneous plans. On the other hand, both IPSA and GrO plans resulted in steep variation in dwell time, which could be seen from the DVH. The long tail in the DVH of CTV represents the low volumes of high dose regions [Fig. 35]. It was observed that in DPO, none of the dwell times were completely turned off even if the dwell position is next to a critical structure; however, in IPSA and in GrO the dwell time next to a critical structure were turned off, whereas long dwell times were noticed where no critical structures were present. The optimization time for DPO plan was 1-2 min, whereas planning time for IPSA was about 10 min. changing the constraints and reevaluating the dose-volume parameters to arrive at an optimal plan was indeed a time consuming factor for IPSA plans too. Each GrO plan had taken about 15-20 min to arrive at an optimal plan by an experienced physicist. Changing the individual dwell weights or manually dragging the isodose lines using a mouse and evaluation of dose-volume parameters was a time consuming process during GrO plans.

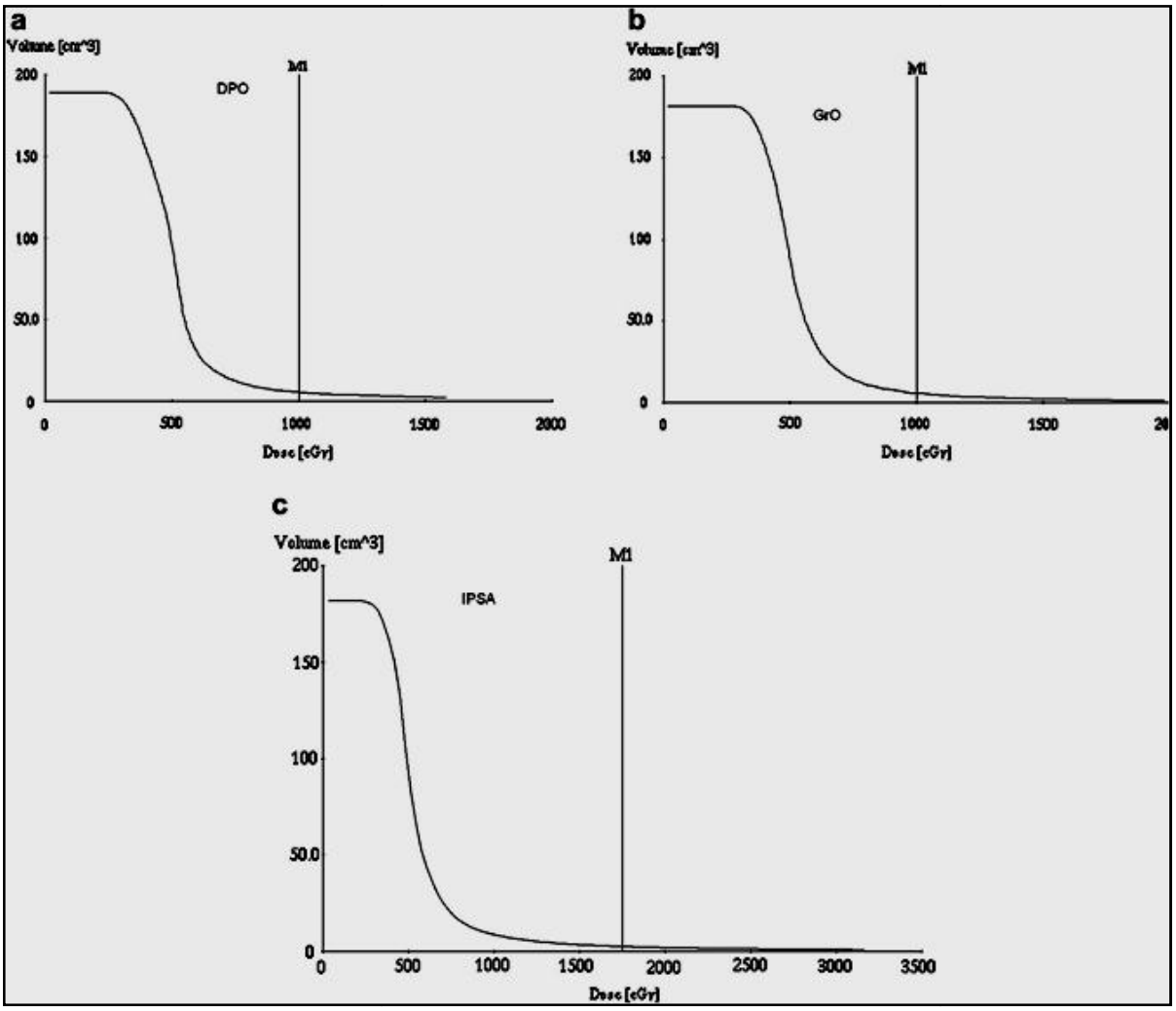

Figure 35:DVH of DPO, GrO, and IPSA plan. DVH 5 dose-volume histogram; DPO = dose-point optimization; GrO = manual/graphical optimization; IPSA = inverse planning simulated annealing

3.3.3.d Discussion:

The results of the present study have shown that IPSA has resulted in superior plans in terms of CTV coverage, sparing normal tissues and conformality as compared with DPO algorithm. However, this benefit came with a decrease in homogeneity. In our study, DPO plans were highly homogeneous; however, IPSA plans were associated with reduced HI. This is the only difference observed between the present study and the earlier investigations comparing IPSA with other algorithms, such as GO, DPO, and GRO [176, 216, 217, 218]. Most of the earlier investigations were carried out in prostate, using template technique [176, 216, 217, 218].Although the site is different, we expected the results to be similar because of the similar implantation

technique and dose calculation algorithm. The reduction of homogeneity in IPSA plans may be attributed to the geometry of the implant, where the needles are placed laterally to cover the parametrial region, where as in prostate implants, the needles are positioned in a circular fashion. Moreover, in gynecologic implants, achieving a good geometry was limited with the usage of diverging needles to avoid the converging of needles in the parametrium laterally, which may distort the geometry of the implant and in turn homogeneity.

Diverging needles are also used in a situation where the implant pathways are obstructed because of pubic bones [Figure 36]. Another reason could be large CTV volumes associated with the gynecologic implants as compared with prostate implants. The mean CTV volume in the present study was 124 cc, whereas the prostate volumes reported in the literature has a mean CTV volume of the order of 30-50 cc [176, 217], except Lachance et al.[219] who reported large prostate volume of 102.84 cc. Hence, our results did not compare well with other studies of IPSA with regard to homogeneity; however, with regard to CTV coverage and OAR sparing, it agrees well with the others [176, 216, 217, 218]. It is unclear whether dose homogeneity is a necessity in gynecologic implants, as long as the CTV is covered adequately with optimal sparing of OARs. However, it may be a cause of concern especially during dose escalation and simultaneous boost. Vikram et al. [221] reported that the relationship between the hot spot and the complication rate is

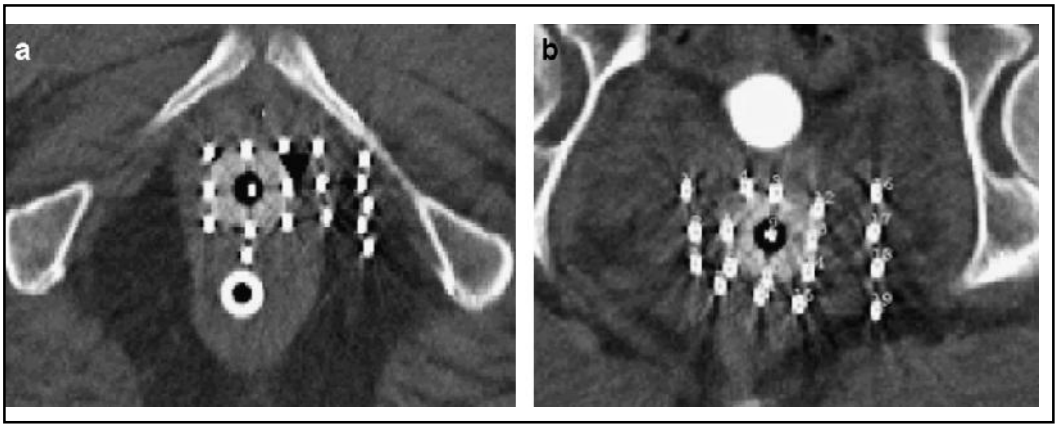

Figure 36: a) The obstruction of implant pathway because of the pelvic bone and (b) the usage of diverging needles that distort the implant geometry

insignificant for high-dose rate interstitial BT implants, so the hotspots need not preclude optimization to ensure adequate coverage of the CTV. Hence, reduction of HI is acceptable during inverse and GrO for adequate CTV coverage. In some implants, it was observed that because of large geometrical irregularities, the HI becomes reduced [214]. In another publication, Wazer et al. [222] reported that the size of high-dose regions correlates to necrosis for breast implants, and the reduction of high-dose volumes may reduce the normal tissue complication. Although there is limited data available correlating the hot spots and its consequences for gynecologic implants, the use of inverse and GrO to obtain good CTV coverage in implants with geometrical irregularities has to be done with caution [223].

It was also observed that the coverage was significantly low in DPO as compared with GrO and IPSA plan, which could be attributed to the location of the dose points. In our case, we have positioned the dose points inside the CTV and used a prescription isodose of 85e100%, which sufficiently covers the CTV. Alternatively, the dose points could be positioned around the CTV about 3e7 mm, in such a case the coverage may be superior, however, with an increased dose to the OARs, which may be partially rectified by positioning the dose points only laterally and not anterio-posteriorly or by differentially weighting or prescribing the dose points. GrO is a powerful tool as it provides an interface, which allows the planner to drag isodoses on the computer screen to the desired position. In the absence of inverse planning softwares, we had routinely used GrO for our implants and found these plans to be clinically acceptable, providing optimal sparing of OARs, while maintaining adequate CTV coverage. It is worth mentioning here that the planning process of GrO requires skill and experience from the planner point of view. It is laborious and time consuming as compared with other optimization algorithms. At sometimes, unacceptably large amount of hot spots may occur at some cross section, which can go unnoticed even by DVH analysis. Evaluation of isodose distribution in each cross section, DVH analysis, and evaluation of quality indices may be warranted in arriving at an optimal plan

when using GrO. Even an experienced planner can take about 20-30 min to arrive at an optimal plan, whereas IPSA can be generated in 5-10 min. Another advantage of IPSA is that once a class solution is made, it can be recalled for every patient that reduces the planning time; on the other hand, GrO plan is patient-specific, which has to be obtained by individually looking at CTV coverage and organ sparing at the same time. Although GrO produces clinically acceptable plans that are comparable with IPSA, attempts at GrO should be undertaken with a little caution keeping in mind all the possible variations of isodose distributions resulting from the GrO.

3.3.3.e Conclusion

IPSA resulted in significant sparing of normal tissues without compromising CTV coverage as compared with DPO. However, IPSA did not show any significant improvement either in CTV coverage or in normal tissue sparing as compared with GrO. IPSA plans were found to be superior in terms of homogeneity and conformity as compared with GrO.

3.4 Summary:

Forward planning with manual optimization is the current standard of practice in the clinics. The results of the above investigations summarize that inverse planning offers improved plans in terms of OAR sparing while maintaining target coverage when compared to standard clinical plans. However, the average loading pattern was found to deviate from a traditional standard Fletcher loading. For our patient cohort, the tandem loading was decreased compared to the ovoids mainly due to high sigmoid dose. This deviation also changes the conventional pear shaped distribution. In IC+IS implants the needles were loaded as that of the tandem. Due to which the dose to unknown critical structures like nerves, vessels, vagina, ureter, urethra may receive a higher dose. Hence they need to be contoured; however, the dose constraints and the contouring process of these above structures are still not known and not commonly practiced. It was also observed that, the variation of dwell time is large across the catheter, which can be minimized with the use of help structures drawn around the catheters. For T/O applicator, it was

found that the use of HS did not make any impact both in the dose volume parameters and in the loading of tandem and ovoids, however in the case of Vienna applicator, inclusion of HS in the optimization made a significant impact in the loading of needles. Without the HS, the optimizer loaded the needles heavily, which drastically came down when HS were included. In interstitial implants, IPSA plans were found to be superior in terms of homogeneity and conformity as compared with GrO. It was also found that for large and/or unfavourable targets, coverage cannot be achieved with either manual or inverse optimization if no adaptation of the application technique is included.

Chapter 4

Uncertainties of Organ Motion.

4.1 Introduction

BT has evolved into a high-technology modality of radiotherapy incorporating advanced imaging modalities such as CT, MR, US and intelligent optimization and planning methods as standards of care. However, BT uncertainties that could have a direct impact on the clinical treatment and therefore the outcome have not been adequately addressed. While uncertainties related to 3D image based EBRT have been investigated in detail during decades [224-231], there has so far been a limited knowledge of uncertainties related to 3D volumetric image based BT. There have been ‘‘dogmas’’ that uncertainties in BT are negligible based on the observation that the applicator, tumour and surrounding tissues represent a stable system. However, BT dose gradients are significant and geometric uncertainties can potentially lead to significant uncertainties which cannot be neglected [232, 233]. IGABT is subjected to uncertainties in each step of the entire process: Source calibration [234], imaging [29, 235-238], contouring [239,240], applicator reconstruction[139, 143, 241], dose and DVH calculation [242-244], dose delivery [245] and anatomical variations [246]. It is essential to identify these uncertainties, their magnitude, and their impact on the overall uncertainty of dose delivery to the patient. Having this knowledge may provide correct dose assessment, dose effect modeling, and subsequently improved clinical outcome when using better planning aims with dose and volume constraints. The table 11 lists the uncertainties that have been quantified: Uncertainties related to source strength, dose calculation, and dwell position accuracy is of the order of 2-4%. Uncertainties related to contouring have been quantified as 9% (target) and 5–11% (OARs) [240]. Intra- and inter-fraction uncertainties related to organ and applicator changes taking place in between imaging and dose delivery have been analyzed [241, 247-251] and quantified to be 20-25% which is the largest.

Table 11: Uncertainty budget (SD) for one intracavitary BT fraction. The overall uncertainty for the entire treatment course is depending on the fractionation schedule and level of verification. (Table reproduced from Tanderup et al, Ref: 232)

Parameter	Target (HR CTV D_{90})	OARs ($D2_{cm3}$)
Source strength	2%	2%
Dose and DVH calculation	3%	3%
Dwell position uncertainty(reconstruction and source positioning)	4%	4%
DVH addition across fractions (previously called worst case assumption)	NA	1-7%
Contouring (Inter observer)	9%	5-11%
Intra- and Inter-fraction (Intra application) uncertainties	11%	20-25%
Total	12%	21-26%

This indicates that organ motion is the major contribution to OAR dose uncertainties. In summary, physics uncertainties related to dosimetry and geometry are in general more limited as compared to the pronounced clinical uncertainties related to contouring and organ motion. Contouring is by far the largest contributor to uncertainties for target, whereas organ motion has the major impact on uncertainties in OARs. This was the motivation to study in detail about the quantification of uncertainties of inter fraction variation and dose accumulation of dose to OARs in this part of the thesis.

In this chapter, we have analyzed the uncertainties of organ motion in 2D orthogonal radiograph image based dosimetry and 3D volumetric MR image based BT using both rigid and deformable image registration.

4.2: Uncertainties of organ motion in 2D orthogonal image based dosimetry:

4.2.a. Purpose:

Conventionally, BT planning was carried out by means of a pair of orthogonal radiographs. In the recent past, the introduction of newer imaging modalities such as CT, MR and US has brought a paradigm shift in the practice of BT. While the benefit of image based BT is quite evident, the clinical implementation of the same poses a great challenge especially in the resource constraint countries, including India. Expensive CT/MR compatible applicators, inaccessibility of 3D imaging (CT/MR) in or near the operating room, large amount of patient load, lack of expertise, are some of the challenges faced by the radiotherapy community in the poor income countries during the implementation of image based BT. 2D orthogonal image based dosimetry is still largely practiced including TMH, India. The current protocol in our hospital, for intracavitary BT planning is to carry out imaging for each application, whether 2D or 3D dosimetry, followed by treatment planning and delivery. However, in some special situations, for example, when the imaging unit is non-functional, heavy patient load, it may not be possible to image the patient for every application. In such situations, cost effective alternative methods have to be explored, without compromising the treatment quality, which was the primary motivation of this investigation.

In multi-fractional BT, the inter-application variation may occur due to various reasons such as bladder filling, rectal gas filling, movement of sigmoid colon, variation in vaginal packing due to the application, especially in non-fixed applicator such as T/O applicators. Although it is recommended to use imaging for each application to reduce the uncertainties, in certain situations as described above, it may not be possible to image each application. There could be a scenario, where the first application plan may have to be used for subsequent fraction/s. In such situations, although the dose to target may not exhibit a large variation, especially, in point-A prescribed plans, the dose to OARs may vary to a large extent. Hence,

we need to identify, and systematically quantify these uncertainties to take them into account. The inter application/fraction variation and uncertainty analysis for image based BT for cancer of uterine cervix has been well documented by various groups [233, 248, 252], however, the inter-application variation for 2D orthogonal radiograph based dosimetry has not been documented in detail [253], which is still largely practiced in our hospital.

The purpose of this study was to investigate the inter-application variation, for dose to ICRU rectal and bladder point and their spatial location with respect to first fraction using 2D orthogonal image based dosimetry in BT of cancer of uterine cervix.

4.2.b. Materials and methods:

Twenty-seven patients diagnosed with cancer of uterine cervix, who underwent intracavitary BT application, were taken up for this evaluation. All patients had received EBRT of 50Gy/25 fractions followed by four fractions of 7Gy HDR BT as per institutional protocol. The BT applications were carried out after the completion of EBRT one week apart. All patients were implanted with Fletcher-suit standard applicator (Nucletron, An Elekta company). After the application, patients were wheeled into a imaging & treatment room located next to the operating room. X ray dummy markers (1cm apart) were inserted in each applicator to aid in the reconstruction process. 2D orthogonal X-ray images were acquired using C-ARM (Siemens) which were then transferred to treatment planning system (Oncentra, v 4.1). Applicator reconstruction was carried out, followed by point-A prescription plan based standard loading pattern. ICRU rectal and bladder point were identified and the doses were documented. If the dose to the OARs is not acceptable as per the departmental protocol, manual optimization of dwell position and dwell weights were carried out, which will not deviate very much from the standard loading. According to the standard protocol of TMH, each application/fraction has to be imaged and planned individually. However for this evaluation, the plan of image -1 (day 1)

was overlayed on image-2, 3, and 4, the plan parameters were compared with the actual plan of the day.

In addition, inter application variation in dose to rectum and bladder point and their spatial location was investigated. In order to evaluate the inter-application variation of ICRU rectal and bladder point doses, dose received by these points were recorded for each fraction. To evaluate the variation in spatial location of ICRU rectal and bladder points, saggital image was used as a reference image. Polar coordinates were evaluated with the centre of flange as the origin. The following parameters were evaluated from the saggital images: (a) r (bladder): radial distance between ICRU bladder point and center of flange, (b) r (rectum): radial distance between ICRU rectum point and center of flange, (c) a: perpendicular distance between ICRU bladder point and vertical axis. (d) Φ: angle between r (bladder) and vertical axis and is given by $\Phi = \sin^{-1}\frac{\text{r bladder}}{a}$. The angular coordinate (θ) of ICRU bladder point is given as $\theta = 270^0 - \Phi$. The angular coordinate for ICRU rectal point was assumed to be zero, as ICRU rectal point was on the flange level, which was the reference point for all the measurements [Fig.37].

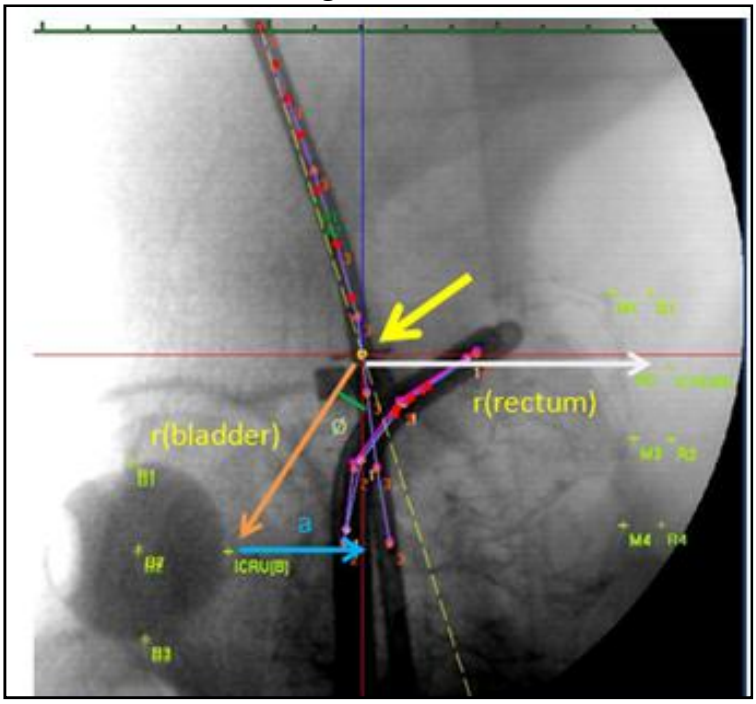

Figure 37: An illustration of identifying the ICRU rectal and bladder point for inter- application variation of spatial location.

The Inter-application dose variation was quantified by means of coefficient of variation (CV). It can be expressed as a percentage and is defined as the ratio of the standard deviation to the mean.

$$\%CV = (\text{Std. Dev/Mean}) * 100.$$

It is a normalized measure of dispersion of a probable distribution, in other words, it shows the extent of variability in relation to mean of the population. In addition to %CV, average absolute change and average relative change of dose respect to fraction-1 was evaluated.

4.2.c. Results:

Inter-application variation in doses to ICRU rectal and bladder points:

The mean (±sd, range) CV% was 32.6(±16.9, 0.3-67.9) and 24.3(±12.5, 6.9-64.4) for bladder and rectum respectively. The mean (±sd, range) average absolute change was -2.6(±3.0, 0.1-8.5)$Gy_{\alpha/\beta=3}$ and 1.3(±0.8, 0-3.2) $Gy_{\alpha/\beta=3.}$ The inter-application variation in doses to ICRU rectal and bladder points with respect to the first fraction were found out to be 9.1±5.3% and 10.4±7.9% respectively. 16/27 (60%) patients had variation less than 10% for ICRU rectal point, while 11/27 had variation less than 20%. However in the case of ICRU bladder, 16/27, 6/27 and 5/27 patients had variation of upto 10%, 20% and 30% respectively. While in case of ICRU bladder point 16 out of 27 cases (60%) have variation less than 10%, 23 out of 27 cases(85%) have variation less than 20% and in 27 out of 27 cases(100%) have variation less than 30% [Fig. 38-40].

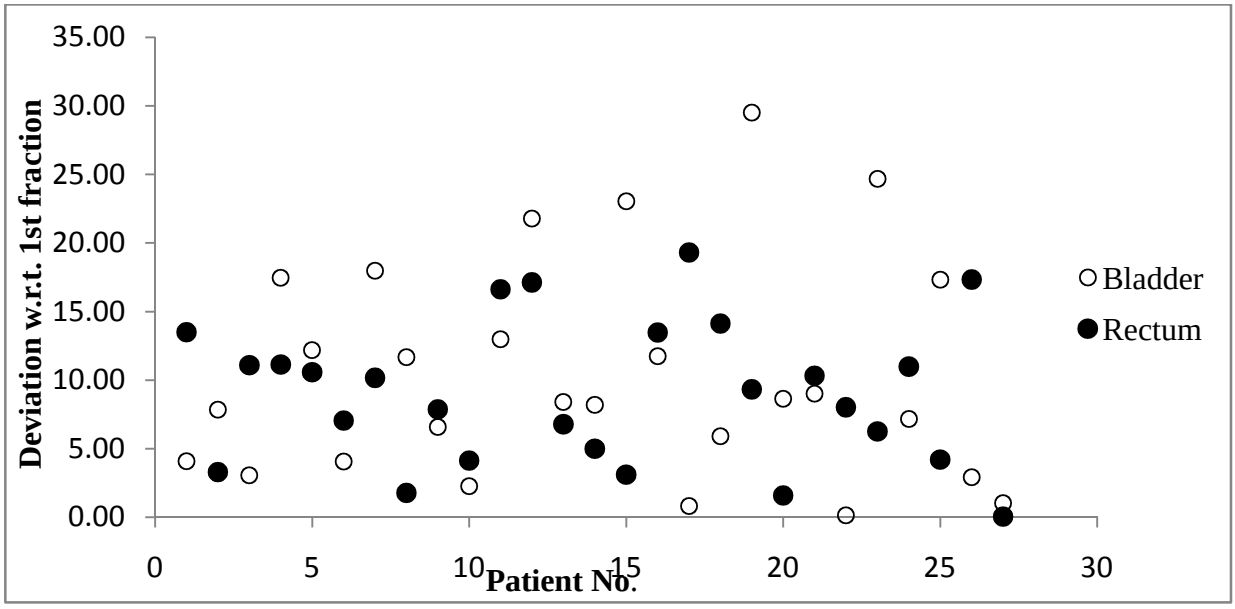

Fig 38. Deviation in reported mean ICRU rectal and bladder point doses with respect to that of first fraction.

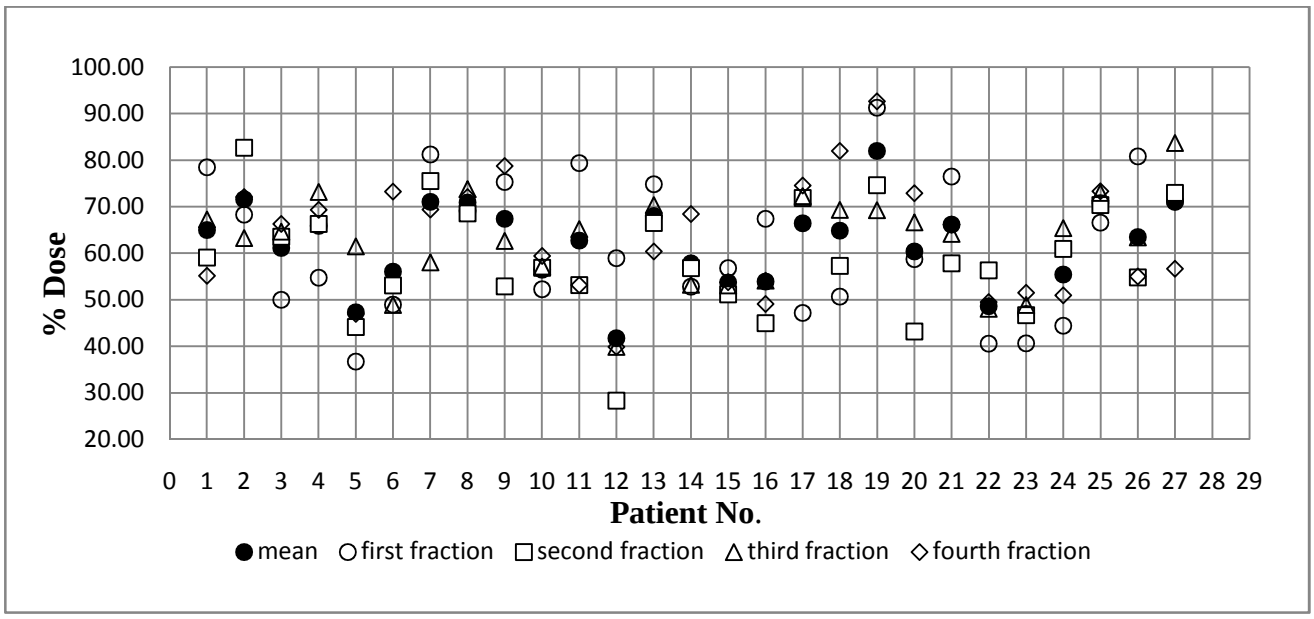

Fig 39: Inter application dose variation of ICRU rectal point for every fraction and patient.

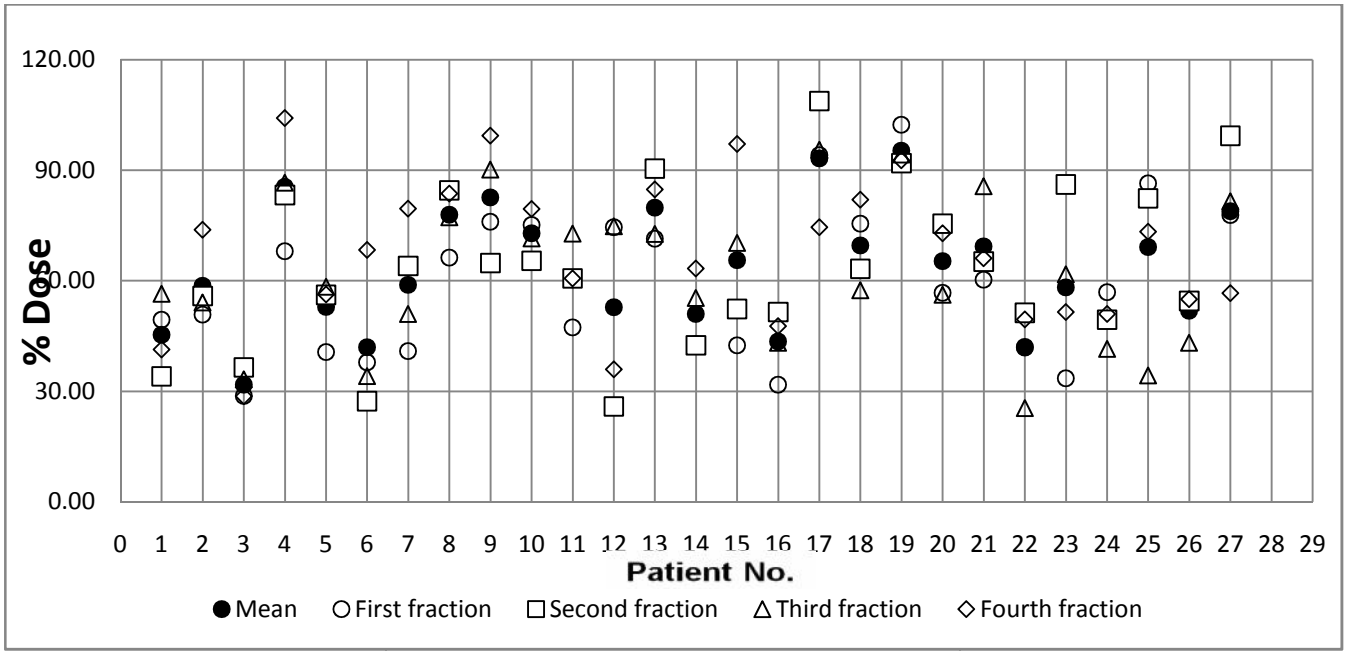

Fig 40 : Inter application dose variation of ICRU bladder point for every fraction and patient.

Inter-application variation in spatial location of ICRU rectal and bladder point: The mean position of bladder point in polar coordinates (r cm, θ^0), was found to be ($2.8\pm0.4, 27^0\pm13^0$) while the mean radial distance of ICRU rectal point from the center of the flange was found to be 2.7±0.3 cm. The angular coordinate of ICRU rectal point was 0^0 as level of flange was the reference. The inter-application variation in spatial location of ICRU rectal and bladder points with respect to the first fraction was found to be ($0.3\pm0.3, 0^0\pm0^0$) and ($0.4\pm0.2, 6^0\pm5^0$) respectively. 17/27 (63%), 7/27(26%) and 3/27(11) patients had variation of less than 3mm, 5mm and 7mm in ICRU rectal point respectively. A similar pattern was found for ICRU bladder point, 16/27 (59%), 6/27(22%) and 5/27(19) patients had variation of less than 3mm, 5mm and 7mm in ICRU bladder point respectively [Figure 41]

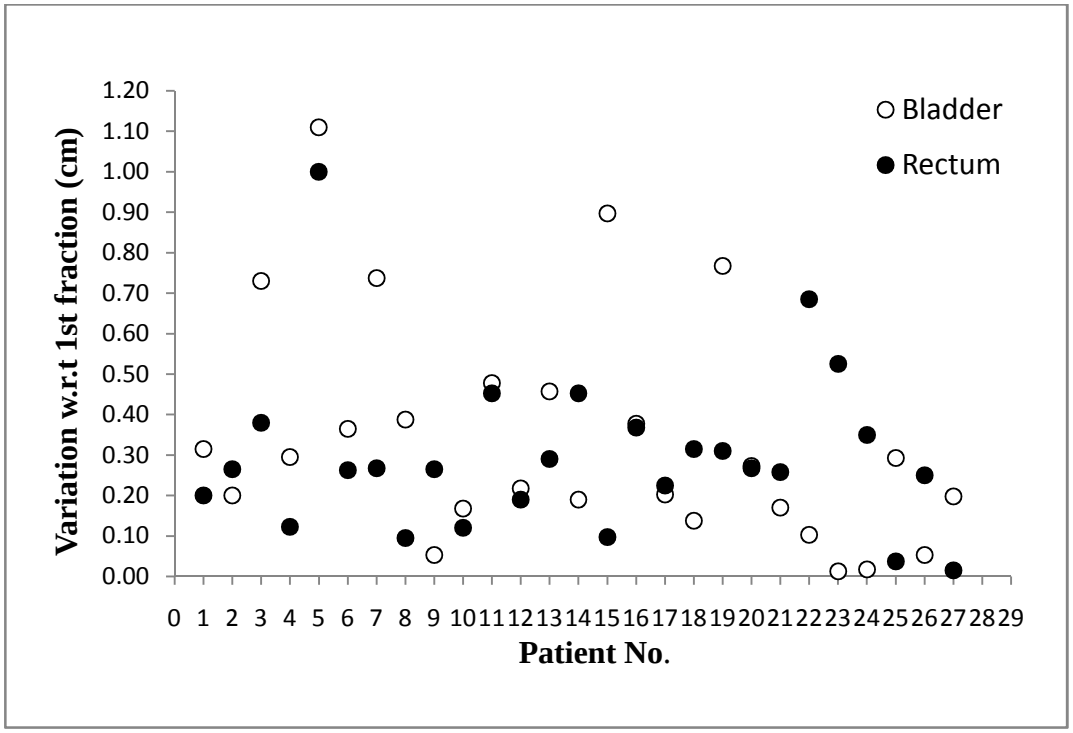

Fig 41. *Deviation in mean radial distance of ICRU rectal and bladder point doses with respect to that of first fraction.*

4.2.d. Discussion:

The impact of inter-application anatomical variation on dosimetric parameters such as ICRU rectal and bladder point in 2D orthogonal radiograph image based BT was investigated. These effects have been studied very much in detail in EBRT [224-231], however in BT, there are seldom publications addressing this issue [253, 246, 252, 248, 254-265]. The objective of this study was to quantify the variation, to find out, if re-planning is necessary in the subsequent fractions for 2D orthogonal image based dosimetry for gynaecological HDR BT.

Several dosimetric studies, investigated the benefit of fractional re-planning, using 3D image based dosimetry [246,252,248,254-266], however very few have used the 2D image based planning [253] and there are some contradicting results [254-266]. In the current study, the clinical plans were made with standard loading pattern followed in our hospital, followed by point A prescription; hence we did not find any variation in the dose to point A.

Kirisits et al. [266] and Mohamed et al. [248] pointed out that re-planning of individual fractions is advisable for consecutive applicator insertions when interstitial needles are added to the intra-cavitary applicator, however for intra-cavaitary application, re-planning may not be necessary. However, the results of the present study indicate that the fractional re-planning is necessary in the intracavitary application. This difference could be attributed to the difference in the applicator used by these studies. Kirisits and Mohamed have used a fixed ring applicator, while in the present study we have used the non fixed applicator tandem/ovoid [266, 248].

Yaparpalvi et al. analyzed the inter-fraction variations of applicator insertion, as well as the fluctuations in bladder and rectal volumes, which have led to variations of bladder and rectal doses; they concluded that the dose to OARs should be assessed on individual fraction basis [261]. Consequently, each fraction should be image-based, in order to achieve an accurate and complete dosimetric assessment of the treatment. However, other investigators stated that the small inter-fraction variation in doses to the bladder and rectum do not support treatment planning and reporting doses to the OARs beyond the first fraction [267-269].

The OARs dose can vary considerably from fraction to fraction during the course of HDR BT. A number of patient-based and technique-based factors, as: changes in bladder and rectum filling, inconsistencies in patient orientation, and differences in ovoid position within the vagina may contribute to this variation [262, 270]. Siddiqui et al. showed that over a series of patients, such variations result in an increased rectum volume receiving a percentage of the prescribed dose, but over the course of multiple fractions for an individual patient, this effect is dosimetrically averaged out [262].

While Symon et al., analysing 44 paired BT plans, showed that individual fraction optimization is important, in order to minimize doses to critical structures, Zhou et al. concluded that there is no advantage of re-planning for each fraction, analysing the ICRU 38 points dose for rectum and bladder, in a recent dosimetric study over 9 paired BT plans [255,259].

Our data demonstrate a larger variation in the bladder doses in both mean and standard deviation as compared to rectal dose, if fractional re-planning is not performed. This may be attributed to the non-adherence of bladder protocol in some patients. It should also be noted that the foley's catheter should be pulled such that it lies in the trigone of the bladder. In the present study, we have found that the inter-application variation is mainly attributed to the ovoid size and the gap between the ovoids. Hence clinical vaginal examination may play a major role, where the physician examines the patient and decide the size of the ovoid that best fits the vaginal mucosa of the patient during the first application. In addition to that, it is important to consider reproducing the vaginal packing. In the present study, we have found that 8/27 patients had different ovoid size implanted in the subsequent fractions, and also variation in the gap between the ovoids. So whenever possible, it is recommended to reproduce the locking of the applicator to retain the consistency of the applicator geometry.

Other factors attributed to the inter application variation in the present stud includes the variation in the implant geometry interms of uterine tandem length & angle, ovoid size has to be consistent. It should also be recognized that the implant geometry has to be consistent, which can be achieved by maintaining certain parameters such as following the bladder filling protocol, rectal packing, and ovoid gap.

One current limitation of our study is the use of only two parameters, ICRU rectum and bladder point as a representative parameter for the anatomical variations of OARs. Future research can be considered with more number of points representing the organs. The current clinical and dosimetric evidence shows that the ICRU bladder point does not correlate well with the maximum dose received by the bladder wall, unlike the ICRU rectal reference point, which correlates well with the maximum dose received by the rectal wall, hence the dose to the bladder must be quantified appropriately [52-58]. If the dose to the bladder is high in the first fraction, and if the implant geometry is found to be high, then re-planning may be carried out to avoid large

variation in the ICRU bladder point. It should also be observed that the standard deviation was high in the variation of bladder point as compared to rectal point, hence replanning may be considered as and when it is required based on the variation in the implant geometry.

4.2.e. Conclusion: For HDR intracavitary BT application based on 2D orthogonal radiograph images, the present data showed marked differences in rectum and bladder dose point, and therefore recommend individual fraction re-planning.

4.3 Uncertainties of organ motion in 3D MR image based dosimetry using rigid registration.

4.3.a. Purpose:

One of the recommendations for the implementation of image based BT is the use of MR imaging for every application to adapt to the tumour shrinkage and to estimate the doses to the OARs accurately, however, this may act as a limiting factor in resource constrain settings [152,153]. Imaging before every application will certainly reduce the uncertainties associated with the organ motion and applicator movements during or in between planning process and delivery. However, it is important to quantify the uncertainties to understand these factors and its possible impact on implementation in clinical practice.

In multi fractional BT, inter-application / fraction variations occur between different treatments / applicator insertions, both in terms of geometric and dosimetric parameters[152,153, 271]. Inter-fraction variation has been defined as change between fractions without removal of the applicator, while Inter-application variation is the variation between different applications after reinserting the applicator [152].The current practice of determining the D_{2cm^3}cumulative dose to OARs during BT is based on what has previously been called “the worst-case scenario”, which is the assumption that the D_{2cm^3}regions are located in the same anatomical part of the organ in each fraction [235]. This assumption implies that the cumulated BT dose can be calculated by adding D_{2cm^3}values for each fraction. Various parameters such as bladder and/or rectal filling, movements of sigmoid colon, and variation in vaginal packing have been identified for inter-fraction / inter application variation[83]. The available data on inter fraction/application variation documents dose variation of target structures and the OARs quantitatively, but do not take into account the spatial (topographic) location of the high dose region of OARs [250,266]. However, analysis of local recurrences in cervical cancer patients in the setting of image-guided BT was attempted by comparing spatial dose distribution within a matched-pair analysis [272].

To study and investigate further, the inter application variation of spatial location and D_{2cm^3}dose volumes and the topography of OAR's, we undertook this study.

4.3.b Methods & Materials:

An analysis of 27 patients treated with MR image based intracavitary BT for carcinoma cervix under EMBRACE protocol was carried out. The treatment protocol of EMBRACE including application, imaging, volume delineation, and planning and dose evaluation was discussed in our previous publication in detail [121]. Briefly, patients undergoing MR image based BT are transferred to MRI (1.5T, GE signa), and FSE TI axial, FSE T2 true axial, para coronal and para saggital sequences with 3-4mm slice thickness and 0-1mm gap were acquired [135]. Contouring was done on Oncentra (V 3.1.2.9, Nucletron) using the GYN GEC ESTRO guidelines [83]: HR-CTV, rectum, bladder and sigmoid. The outer contours (including the mucosa and the muscle layer) of bladder, rectum and sigmoid were contoured on each axial slice at least 2cm below the HR-CTV to 2cm above the uterus. Clinical examination, examination under anesthesia (EUA) and MRI findings were taken into account for target volume delineation [83].

Reconstruction was done using multi-planer images [145]. Plans were obtained such that optimal dose was delivered to the HR CTV while respecting the tolerance dose to OARs. The dose prescription and constraints followed in our institution are as follows: total D_{90} for the HR CTV was 45 Gy of external plus 4 * 7 Gy BT dose. The EQD_2 dose to the OARs was limited by dose constraints of total 90 Gy, 75 Gy and 75 Gy for bladder, rectum, and sigmoid, respectively. Every patient had two applications, one week apart with 2 fractions of 7 Gy each delivered per application. For each application patient had undergone MR- imaging (MR-1, MR-2), volume delineation, reconstruction, treatment planning (Plan-1 & Plan-2) and dose evaluation.

In the present study, the evaluation of the inter application variation of OARs consists of three parts (a). Inter - application volume variation (b) Inter - application dose variation (c). Inter application variation of spatial location of D_{2cm^3}volumes.

For each application, a clinical plan was obtained using the respective MR imaging (plan-1 on MR-1 and plan-2 on MR-2) which was used for patient treatment. Both the image series were then exported to Eclipse planning system (V 8.6.14, Varian Medical Systems) and was co-registered with applicator as the reference coordinate system using rigid registration algorithm. Both point based and the pixel data based algorithm was used to perform rigid registration. Three points were used for point-based registration: tip of the tandem, point at 4cm from the tandem tip and first dwell position of the ring. To fine tune the accuracy of the registration the pixel data-algorithm was used.

The point based registration is used as a starting orientation-pre alignment. Using the VOI tool, a smaller volume within the image set was used to perform the registration using pixel data. This algorithm samples the pixel data in the images and measures the amount of mutual information in the pixel values of the images. Automatic image registration searches for a spatial transformation between the frames of references of the images that maximizes the amount of mutual information. The greater the amount of mutual information, better the registration. The accuracy of the registration was verified manually and fine-tuning was done by using the manual matching tools (translate & rotate).

4.3.b.1 Inter application of volume variation:

The volumes of each of the OARs in plan 1 & 2 were evaluated and compared. The common / overlapping volume between the two image series for each of the OAR was contoured and evaluated.

4.3.b.2 Inter application dose variation:

For quantification of inter-application dose variation, plan-1 of MR-1, was applied to MR-2, without modifying the reconstruction on MR-2. This corresponds to a clinical scenario where only one treatment plan (plan-1) is applied for both BT (BT) applications. Dose was recalculated in MR-2, with plan-1. Mean and standard deviations of the relative dose differences of plan-1 on MR-2 as compared to plan-2 on MR-2 were calculated in order to distinguish between systematic and random variations. Total BT dose and EBRT+BT dose was calculated according to the linear quadratic model as biologically equivalent doses in 2Gy fractions (EQD2) using α/β=3 Gy for OAR and α/β = 10 Gy for target [5]. The percentage dose variation for total BT was calculated as follows: (2*plan1+2*plan2true) – (2*plan1+2*plan2) / (2*plan1+2*plan2true)*100, where plan2true is the dose obtained from clinical plan on MR2. To obtain the total (EBRT + BT) variation, the EQD2 dose of EBRT was added to total BT dose, and the percentage variation was calculated.

4.3.b.3 Inter application variation of spatial location of D_{2cm^3}volumes:

The volume receiving the dose $D_{2cm^3}$was contoured in both MR-1 and MR-2 for OARs from plans 1 & 2 respectively viz rectum, bladder and sigmoid. The D_{2cm^3}volumes were analyzed for spatial overlap between the applications. In the absence of deformable registration the overlap region was determined qualitatively by assessing visually whether the $D_{2cm^3}$was spatially situated in the same anatomical part of the organ in each application. The size of the overlap regions of the D_{2cm^3}volumes was scored according to three categories: major overlap (>50%), partly overlapping (> ~10% and <50%), and minimal (<~10%) or no overlap. Paired t test was used to evaluate the inter application volume and dose variation in rectum, bladder and sigmoid.

4.3.c. Results:

4.3.c.1 Inter-application volume variation:

Inter application volume variation was not found to be significant for any of the OARs. The percentage overlap of the whole organ was found to be 55±30%, 60±30% and 24±44% for rectum, bladder and sigmoid respectively. Figure 42 shows the inter application volume variation for various OARs. It was observed that that the inter-application volume variation of rectum was minimal as compared to bladder and sigmoid. It should be noted that all patients investigated in the present study, were under bladder protocol of maintaining empty, followed in our institution. The scoring of the geometric changes of sigmoid was carried out using the guidelines followed in EMBRACE protocol. Sigmoid changes were moderate in 15/27 patients, 11/27 patients had minimal change while no patient was in the category of complete change or no change. Hence, more than 90% of patients had minimal or moderate changes in sigmoid.

4.3.c.2. Inter application dose variation:

The largest inter application systematic (mean values) and random dose variations (standard deviation) were observed for sigmoid as compared to rectum and bladder. The mean (±SD) of the relative D_{2cm^3} physical dose variations were 0.6 (±15.1)%, 0.9 (±13.1)% and 11.9 (±37.5)% for rectum, bladder and sigmoid respectively for inter application variation. Positive values suggest that the dose values were higher than in the reference image. P value of 0.17 for rectum vs sigmoid, and 0.14 for bladder vs sigmoid and 0.93 for bladder vs rectum shows no statistical

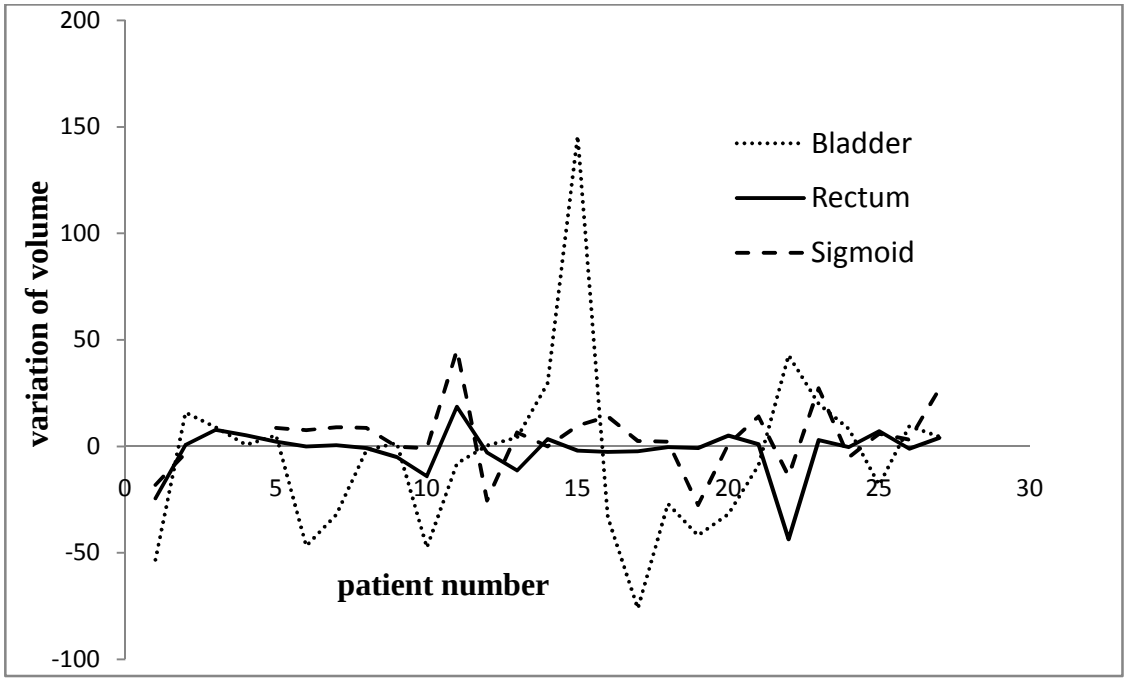

Figure 42: Inter-application volume variation of rectum, bladder and sigmoid.

significance. Extrapolating to total BT (BT) EQD2 dose, the mean (±SD) of the relative D_{2cm^3}dose variations were -3.0±14.7%, -2.6±11.2% and 9.2±37.9% for rectum, bladder and sigmoid, respectively, which was equal to a variation of -1.4±4.1Gy, -1.4±5.6Gy and 0.8±4.5Gy in terms of absolute EQD2 dose. Further extrapolating the variations to total dose (BT+EBRT), the mean (SD) were -1.6±5.3%, -1.4±5.8% and 1.4±7.3% for rectum, bladder and sigmoid respectively (Table 12).

Table 12: Mean and SD of inter-application dose variation of OARs.

Inter application variation	Rectum	Bladder	Sigmoid
Variation per BT fraction Physical dose (%)	0.6±15.1	0.9±13.1	11.9±37.5
Variation for total BT dose EQD2 dose (%)	-3.0±14.7	-2.6±11.2	9.2±37.9
Variation for total EBRT + BT EQD2 dose (%)	-1.6±5.3	-1.4±5.8	1.4±7.3
EQD2 variation for total BT dose(Gy)	-1.4±4.1	-1.4±5.6	0.8±4.5

4.3.c.3 Inter application variation of spatial/topographic location of D_{2cm^3}volumes:

The overlap of D_{2cm^3}volumes was more than 50% in 16(59%), 8(30%) and 3(11%) patients for rectum, bladder and sigmoid respectively. This clearly implies that the inter application spatial variation is minimal for rectum as compared to bladder and sigmoid. Table 13 gives the number of patients and the different categories of patients with the overlap of $D_{2cm^3}$for various OARs. Fig 43-45 a,b,c shows representative images of these three categories of patients for rectum, bladder and sigmoid respectively. More than 50% overlap of D_{2cm^3}volumes was maximum for

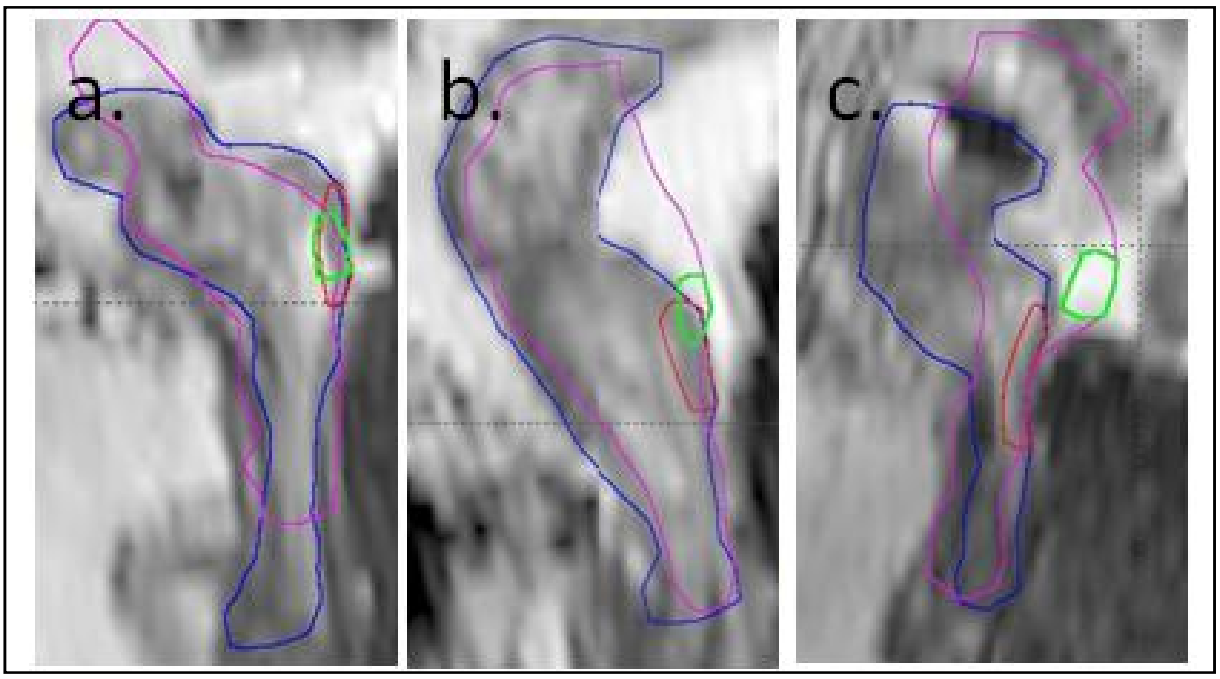

Figure 43 a,b,c: Inter application variation of spatial location of rectum and the hot spot- D_{2cm^3}region of various categories. (a) Volume of overlap of D_{2cm^3}region >50%, (b) volume of overlap of D_{2cm^3} region 10-50% (c) Volume of overlap <10% or no overlap. Application1 rectum-blue, Application2 rectum-magenta, Application1 D_{2cm^3} region-red, Application1 D_{2cm^3} region-green

Categories	Rectum (n=27)	Bladder (n=27)	Sigmoid (n=27)
1. Overlapping region>50%	16	8	3
2. Overlapping region 10-50%	7	14	9
3. Overlapping region<10% / no overlap	4	5	15

Table 13: Summary of results of spatial location of D_{2cm^3}hot spot region for each of the OAR.

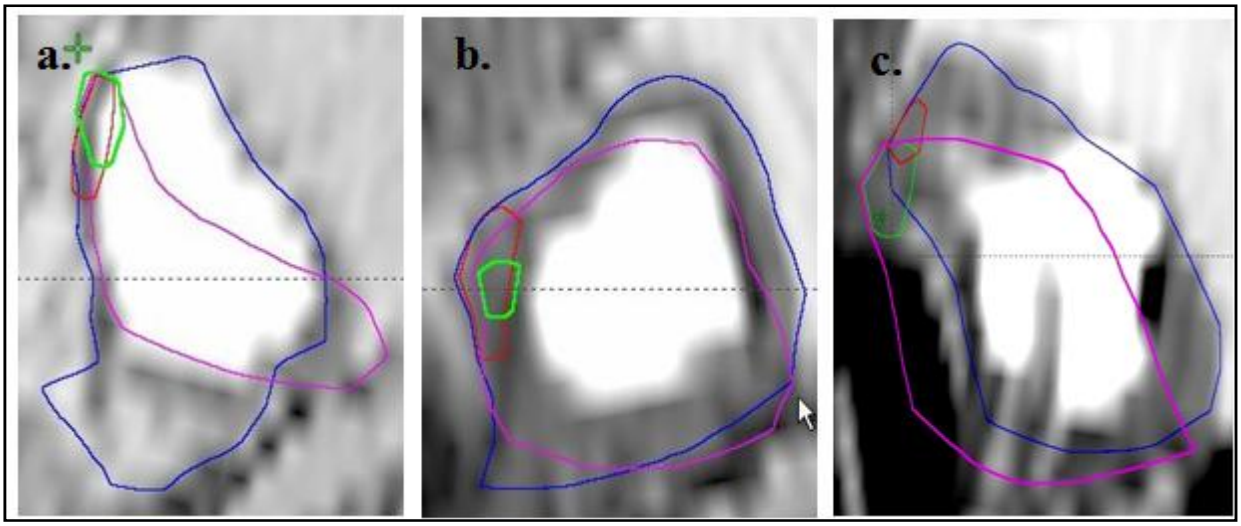

Figure 44 a,b,c: Inter application variation of spatial locatoon of bladder and the hot spot- D_{2cm^3} region of various categories. (a) Volume of overlap of D_{2cm^3}region >50%, (b) volume of overlap of D_{2cm^3} region 10-50% (c) Volume of overlap <10% or no overlap. Application1 rectum-blue, Application2 rectum-magenta, Application1 D_{2cm^3} region-red, Application1 D_{2cm^3}region-green.

rectum (16/ 27 patients) and least for sigmoid (3/27 patients) while <10% overlap/ no overlap of D_{2cm^3}volumes was maximum for sigmoid (15/ 27 patients) and least for rectum (4 / 27 patients), suggesting that variation in spatial location of D_{2cm^3}volume for rectum is minimal while large for sigmoid. For bladder D_{2cm^3}volumes, 10-50% overlap was observed in 14/ 27 patients (52%), 8 patients with >50% overlap while <10% overlap / no overlap seen in 5 patients. This implies that the DVH addition for assessment of cumulative dose could be true for rectum and to some extent bladder but not for the sigmoid.

4.3.d Discussion:

The current practice of dose assessment in IGBAT has certain assumptions that are conservative and may result in over estimation of OAR doses and hence may limit certain situations like dose escalation to the tumour. However, various factors such as organ motion, tumour shrinkage, bladder filling, variation in the applicator geometry with respect to anatomy and other undefined uncertainties may contribute to the variation in the cumulative dose delivered to the tumour and the OARs. It is important to understand these uncertainties in more detail to understand the correlation of dose-volume parameter with the clinical endpoints such as toxicities. We report here to study and understand the implications of inter application / inter

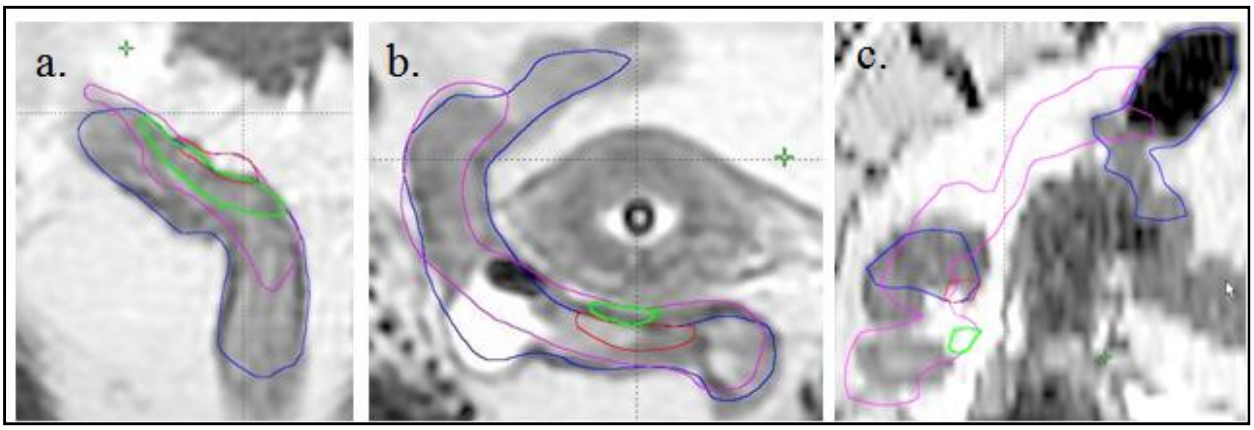

Figure 45 a, b, c: Inter application variation of spatial locatoon of sigmoid and the hot spot- D2cm³ region of various categories. (a) Volume of overlap of D2cm³ region >50%, (b) volume of overlap of D2cm³ region 10-50% (c) Volume of overlap <10% or no overlap. Application1 rectum-blue, Application2 rectum-magenta, Application1 D2cm³ region-red, Application1 D2cm³ region-green.

fraction dose variation and variation in the spatial location of D_{2cm^3}volumes of OARs during MR Image Based IGABT.

4.3.d.1 Inter application volume variation:

The inter fraction variation of bladder volume observed in the present study is low as compared to other studies reported in the literature which may be attributed to adherence to bladder protocol during imaging and delivery endorsing the conclusion of a study reported by Kirisits et al that a bladder filling protocol could reduce the variations substantially [250,266]. The inter-application volume variation of rectum is less as compared to bladder in the present study [figure 42]. It is interesting to note that although the inter-application volume variation is less for rectum as compared to bladder, the spatial overlap of the organ-rectum is less as compared to bladder, which may attribute to the variation in vaginal packing which may shift the whole organ rectum. Despite the spatial overlap as a whole organ is less in rectum, the spatial location of $D_{2cm^3}$is quite stable.

4.3.d.2 Inter application dose variation:

Hellebust et al investigated the inter fraction variation using the CT images and concluded that every fraction has to be imaged for obtaining reliable DVH parameters [250]. More recently Kirisits et al investigated inter application variation [266]. The findings revealed a

systematic increase in OAR and target dose when using the same dose plan for succeeding applications which can be attributed to the tumour shrinkage in a schedule where BT was started rather early during EBRT. Our study did not find any systematic increase in dose for rectum and bladder by applying the same treatment plan for several applications, however, for sigmoid it was found that variation of 11.9% was observed, which is approaching towards the statistical significance. This may be explained by BT being administered after EBRT completion and the tumour shrinkage between BT fractions after completion of EBRT being minimal as reported [151]. The present study indicates that the derived random uncertainties were lowest for bladder (13.1%) and rectum (15.1%) and highest for sigmoid (37.5%). This could be attributed to the high mobility of sigmoid as compared to more stable structures like rectum and bladder (with some protocol for filling) with respect to the applicator. The clinical impact of such uncertainties depend much on the dose level, as e.g. 13-30% can be critical if the dose is close to an OAR or target constraint, whereas it may be of less relevance in case of low OAR or high target doses. In summary, the feasibility of applying the same treatment plan for several fractions depends on the dose level in an individual patient.

4.3.d.3. Inter application variation of spatial location of D_{2cm^3} region:

The major observation about rectum, was that the inter application variation of the spatial location of the D_{2cm^3}region is minimal as compared to bladder and sigmoid. The variation is minimal probably due to bowel preparation prior to each application despite contributing factors like variation in vaginal packing, applicator rotation etc. Many reports available in the literature trying to correlate the dose received by rectum and the occurrence of late complications. Georg et al reported that in MR image guided adaptive BT the parameters $D_{2cm^3}$and D_{1cm^3}have a good predictive value for rectal toxicity and a D_{2cm^3}higher than 75Gy may result in rectal toxicities [152]. From the present study, it could be inferred that 1) the spatial location of D_{2cm^3}volume is stable for rectum, and 2) A dose variation of 15% per fraction was obtained, and hence imaging

for every fraction may improve the accuracy of dose reporting as the dose variation may be significant if the doses are higher. Also, these findings validates the present concept of DVH addition where the dose received by the rectum may be directly additive in multi fractional BT,

For bladder, Georg et al demonstrated that $D_{2cm^3}$of bladder might predict bladder toxicity in MR Image based BT [273]. In the present study, the overlap volume for bladder was between 10-50% in 14/27 patients, and more than 50% in only 8/27 (29%) patients as compared to 16/27 (58%) in rectum. However, even with only partial overlap, DVH addition may be a good approximation as concluded in a study on dose accumulation in the bladder based on deformable registration [274].

In the case of sigmoid, most of the patients had minimal to moderate topographical changes. However, in majority of patients there was minimal / no overlap in the spatial location of D_{2cm^3} region. These observations imply that inter-application / inter-fraction variation is maximal for sigmoid 2cm³ dose volume spatial locations and the dose to the sigmoid may be overestimated if the doses are directly added according to what has previously been called the "worst case scenario". In these situations, it may be useful to critically evaluate the image series and spatial location of the D_{2cm^3}volumes visually between the applications / fractions and decide on additive model to obtain the cumulative dose. Georg et al reported that no dose effect relationship could be postulated for the sigmoid [273].

4.3.d.4. Limitations of this study:

The major limitation of this study is the use of rigid registration, where the registration was based on the applicator and not on the anatomy. In the present study, the organ deformations like bladder-rectal filling, deformation of organs was not taken quantitatively into account. Due to which, it is not possible to locate the exact tissue where the dose D2cc dose was received previously. Hence, in the present study, there could be a situation that can arise where the D2cc was not scored to have an overlap, but the tissue that receives the dose could be

overlapping. So the result described in the present study as “not overlapping” may actually be overestimating this effect. One possible solution to overcome this issue is to use deformable registration algorithm, where the organ deformation is taken into account

4.3.e Conclusion:

The spatial location of D_{2cm^3}volumes is most stable for rectum and to a large extent for bladder which implies that ‘DVH addition’ could be applicable to rectum and bladder. Minimal to moderate geometric changes in sigmoid are seen in majority of the patients in between applications resulting in maximal variation in spatial location of D_{2cm^3} volumes which may lead to over estimation of doses during the DVH addition. However, studies in larger cohort of patients and more importantly correlation with the actual toxicities is required to validate these findingsfurther.

4.4. Uncertainties of deformable image registration for dose accumulation of high-dose regions in bladder and rectum in locally advanced cervical cancer

4.4.a. Introduction:

MRI image-based BT have brought a paradigm shift in the radio-therapeutic management of cervical cancer. Mono institutional series showed promising results in favor of MR image based BT in terms of increased local control and reduced toxicities [118, 119, 123, 128]. Georg et al. investigated a possible correlation between the dose volume parameters D_{2cm3}, D_{1cm3} and $D_{0.1cm3}$ and morbidity for rectum and urinary bladder in IGABT for cervix cancer patients, and they found that these parameters predictive for grade 2 toxicity and have reported a consistent dose effect curve for complications [273]. There are many uncertainties in the process of IGABT which has been systematically reported, recently including contouring [239,240], applicator reconstruction[139,143,241], planning [242-244], inter fraction variation [246] and overall uncertainties[233]. Many groups have been working and reporting on these uncertainties and possible solutions. One of the uncertainties is deformation of organs [246] which has an impact on the dose accumulation in OARs. These clinical uncertainties may introduce uncertainties in endorsing the dose response relationship.

In a fractionated BT schedule, the absolute dose to OAR volumes is derived by adding (DVH parameters from each fraction. The underlying assumption is that the high- dose region is located in the exact same part of the organ in each BT fraction. This approach has previously been called the ‘‘worst case assumption’’ in the GEC ESTRO recommendations, since DVH parameter addition will overestimate the dose if the high- dose region moves to a new location [146].

Inter-application variations result in deformation of organs, which may lead to uncertainties in dose accumulation while directly adding the DVH parameters. To provide better

estimates of accumulated doses, deformable image registration (DIR) algorithms have been introduced in the recent past, to take into account the variation in the anatomy such as bladder filling and organ motion [275-277]. The DIR relates the registered images to a common reference frame, and the dose distributions of the registered images can then be mapped to this reference frame, which enables calculation of the cumulative dose. In the recent past, dose accumulation based on deformable image registrations has been reported for bladder dose accumulation [275]. However, dose accumulation for rectum is not reported yet and in general the literature is sparse for multi fractionated IGABT.

The purpose of this investigation was to estimate and compare, the dose accumulation for bladder and rectum by deformable image registration and direct addition of DVH parameters in a multi-fractionated HDR MR IGABT schedule.

4.4.b. Materials and methods:

4.4.b.1. Patient material:

An analysis of 21 patients treated with MR image based BT for carcinoma cervix under the EMBRACE protocol was carried out. The treatment protocol of EMBRACE including application, imaging, volume delineation, and planning and dose evaluation was discussed in our previous publication in detail [121]. Reconstruction was done using multi-planar images [145]. Plans were optimized for a high dose to the HR-CTV while respecting the tolerance dose to OARs. We aimed for a total D_{90} for the HR CTV of at least 84Gy EQD_2, which corresponds to 45 Gy of EBRT plus 4 x 7 Gy BT dose. The EQD_2 dose to the OARs was limited by dose constraints of total 90 Gy, 75 Gy and 75 Gy for bladder, rectum, and sigmoid, respectively. Every patient had two applications, one week apart with 2 fractions of 7 Gy each delivered per application. For each application, the patient had undergone MR-imaging (MR_1, MR_2), volume delineation, reconstruction, treatment planning (BT_1 and BT_2) and dose evaluation.

4.4.b.2. Deformable Image Registration (DIR) and Dose Accumulation:

The algorithm used in the present study for DIR is based on an optimized derivative of Lucas-Kanade Optical Flow [278], which minimizes the mutual Information similarity metric [279-281] over a Radial Basis Function (RBF) transformation model (Smart Adapt, Varian Medical Systems, Palo Alto). The algorithm is solely driven by image intensities and does not apply any constraints related to organ contours or anatomical landmarks. In this manuscript, this algorithm is henceforth referred as "Intensity based DIR"

Initially, we performed a rigid registration based on the applicator, followed by DIR of a region of interest (ROI), which included rectum and bladder. Since the automatic DIR did not align the organ walls perfectly, a manual deformation tool available in the DIR software was applied after automatic DIR to align the organ walls. In this study, since the dose to D_{2cm3} (minimum dose to the most exposed region) of bladder and rectum is of interest, the manual deformation of anterior rectal and posterior bladder wall of the contour was prioritized while other regions of the organs such as posterior rectal wall and anterior bladder wall were not modified to a large extent by manual adaptation.

In order to evaluate the impact of the registration on the dose accumulation, we performed two registrations for each patient with the reference frame being BT_1 and BT_2, respectively. The 3D physical dose matrix was recalculated into 3D EQD_2 dose (voxel by voxel) by in-house software (MatLab R2013a), and the BT_1 and BT_2 EQD_2 doses were added using the two transformations between the images established through DIR. Voxel-wise deformed dose accumulation (DDA) was done for registrations in both directions: a) BT_1 deformed + BT_2 and b) BT_1 + BT_2 deformed. DVHs were calculated after DDA and D_{2cm3} of rectum and bladder were compared with the DVH direct addition (DA).

Deformation vector fields along the organ walls were evaluated in the D_{2cm3} region. The expansion/contraction of the organ wall was assessed as the difference between maximum and minimum deformation in the D_{2cm3} region. In order to evaluate the expansions/contractions from the deformable registration, a simplified estimation of expected expansions/contractions was performed by assuming a uniform isotropic spherical (bladder) or cylindrical (rectum) expansion/contraction as caused by the volume change of rectum and bladder from BT_1 to BT_2. When assuming a spherical shape of the bladder a volume increase of x% will cause the circumference to increase by $(x\%)^{1/3}$, since the volume of a sphere is proportional to r^3 while the circumference is proportional to r, where r is radius. Likewise, assuming a cylindrical shape of the rectum a volume increase of y% will cause the circumference to increase by $(y\%)^{1/2}$, since the volume is proportional to r^2 while the circumference is proportional to r.

It was evaluated whether the variability of high- dose location had impact on the difference between DA and DDA. By visual inspection we scored the patients in two groups, based on whether the spatial location of D_{2cm3} was in the same region of bladder and rectal wall. Group 1: D_{2cm3} region not overlapping defined as the overlap of high- dose region <50%. Group 2: D_{2cm3} region overlapping, defined as overlapping volume being more than 50%.

4.4.b.3. Comparison with contour based DIR:

To compare the intensity based DIR to other DIR approaches, we analyzed nine patients from Aarhus University Hospital who had previously been investigated using an in-house contour based algorithm for bladder dose accumulation [275]. The contour based, bio-mechanical algorithm has been previously described in detail [275]. In short, the algorithm is based on surface registration, which utilizes a surface mesh registration technique that establishes a mapping from one bladder mesh surface onto another based on energy minimization of an elastic surface membrane. During an iterative optimization algorithm, the moving surface was constrained to

map onto the fixed surface through a 2D parameterized ‘‘constraint’’ – while the elastic energy term was evaluated in 3D. Registrations were aided by manually placed landmarks on the bladder surface. A landmark matching force was included in the surface membrane energy minimization scheme. The contour based algorithm was developed for bladder registration, and therefore validation was performed for bladder only. In the validation data set, two - way registrations were performed with both intensity based and contour based DIR.

4.4.b.4. Statistical analysis:

Paired two sided Student’s T- test was used to evaluate the variation between the DDA and DA. Significance level p value less than 0.05 was considered. The variation was also evaluated in terms of percentage variation. Unpaired t-test was used, when the data was not paired. The quality of the DIR of the entire organ was evaluated by Dice Similarity Co-efficient (DSC) [282].

4.4.c. Results:

4.4.c.1. Deformable Image Registration (DIR) and Dose Accumulation:

4.4.c.1a. Intensity based DIR:

Intensity based DIR could be carried out in all 21 patients for rectum and bladder. Representative intensity based DIR for rectum and bladder is shown in fig 46 (a&b). The mean (±sd; range) DSC was 0.61(±0.14; 0.31 to 0.83) and 0.63 (±0.1; 0.43 to 0.77) for rectum and bladder, respectively. The organ walls were aligned within ±1mm in the region of anterior rectal and posterior bladder wall. The other regions of rectum (posterior wall) and bladder (anterior wall) were not aligned to such a high degree due to the strategy of applying as small manual corrections as possible and mainly focusing on matching the region of the D_{2cm3}.

The mean (±sd; range) absolute D_{2cm3} difference between the two reference frame registrations was 5.6% (±6.2%; 0-22%) for rectum and 6.6% (±5.1%; 0-20%) for bladder, respectively.

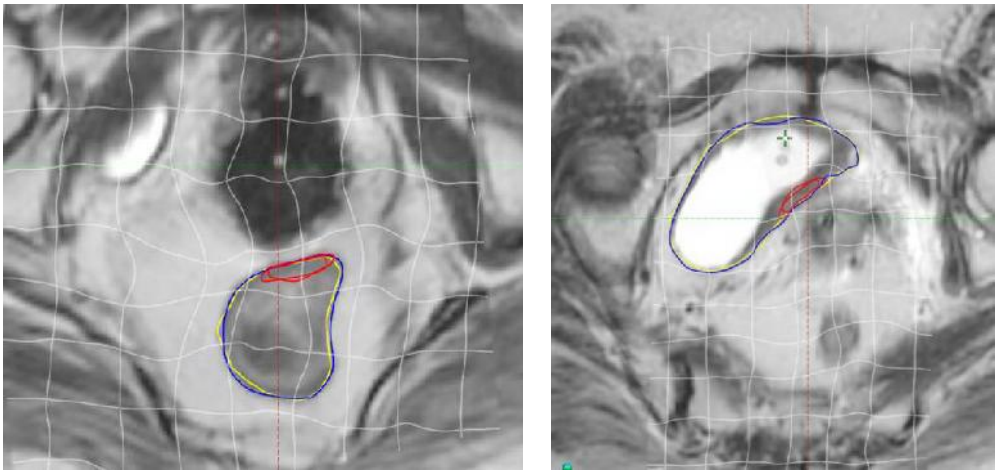

Fig 46 a&b: *A representative image of deformable image registration of rectum and bladder. Blue contours represent BT1, yellow BT2 and red represents the D_{2cm3} region.*

Expansions and contractions over the high-dose region varied between 1 and 26mm with mean(±sd) of 6.3(±6.5)mm and 7.5(±4.8)mm for rectum and bladder respectively. Mean estimated isotropic expansions/contractions were 2.7(±1.9)mm and 4.5(±4.0)mm for typical high-dose region sizes of 30mm(rectum), 40mm (bladder), respectively, which was significantly smaller (p=0.01) for rectum and borderline significantly smaller for bladder (p=0.06). Contractions/expansions predicted by DIR and by isotropic expansion were not correlated (R^2 = 0.005 for rectum and 0.081 for bladder), which indicates that DIR based expansions/contractions were not related to volume changes of the organs. In particular, a significant number, of anatomically implausible expansions were found: 33% (5/15) and 50%(4/8) of the patients were found to have small volume changes of less than 10cc but large organ wall expansions/contractions larger than 6mm and up to 18mm and 12mm for rectum and bladder respectively.

4.4.c.1b. Deformable Dose Accumulation

Mean (±sd; range) percentage variation between DA and DDA were found to be 2.4(±3.3;-1.8 to 11.5)% and 5.2(±5.1;-1.7 to 16.5)% for rectum and bladder respectively. The differences between the DA and DDA were found to be statistically significant for both rectum (p=<0.005) and bladder (p<0.005). The dose in DA was larger than the dose obtained by DDA in most of the patients, 16/21 and 19/21 patients for rectum, and bladder respectively [figure 47 (a&b)]. The mean (±sd; range) difference in dose between DA and DDA per BT fraction was

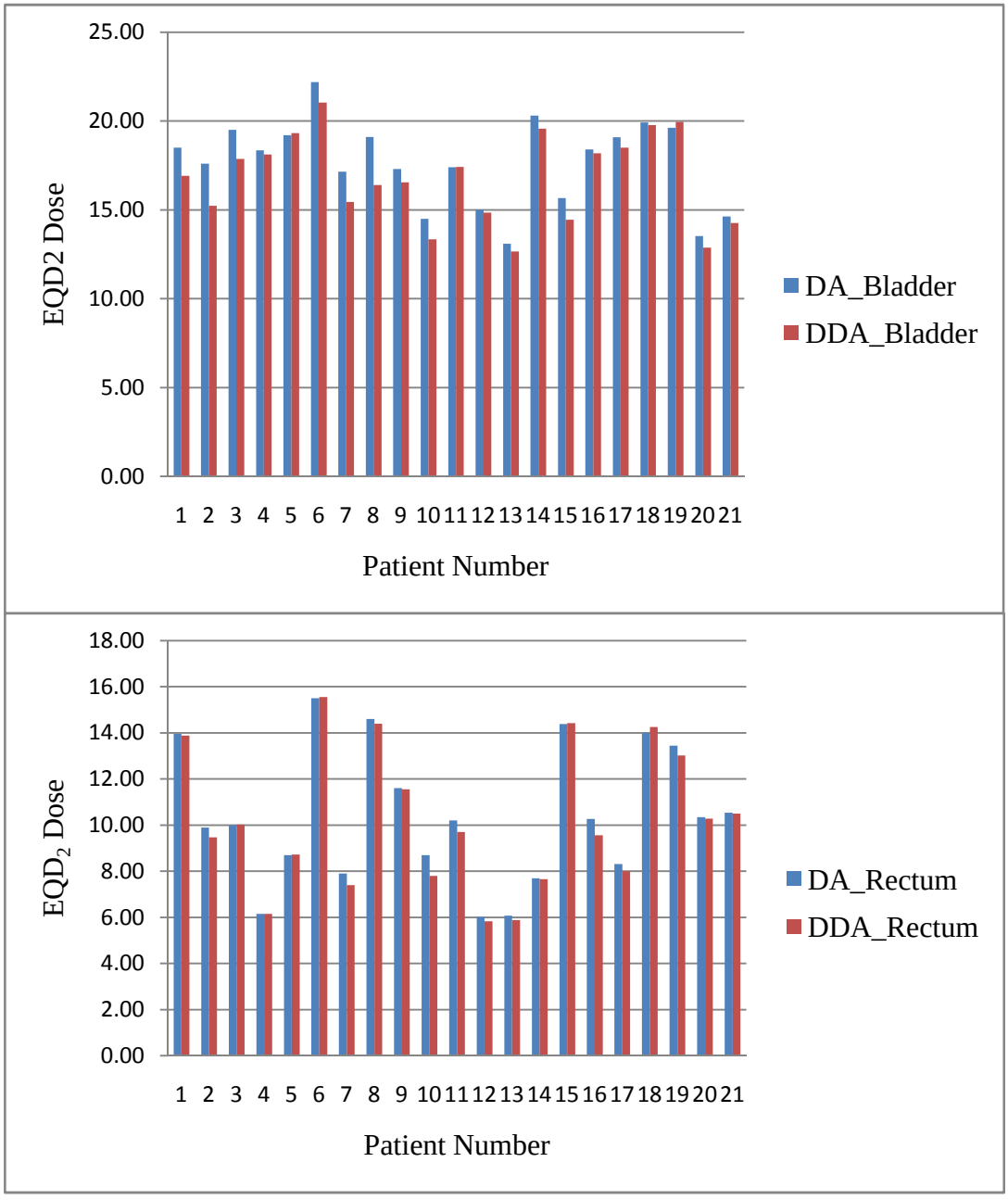

Fig 47a: *Absolute change in $EQD2_{\alpha/\beta=3}$ between DA and DDA for all patients for rectum (47a) and bladder (47b).*

found to be 0.2(±0.3; -0.25 to 0.9)$Gy_{\alpha/\beta=3}$ and 0.8 (±0.8; - 0.34 to 2.7)$Gy_{\alpha/\beta=3}$ for rectum and bladder, respectively. Considering the entire BT schedule which consists of 4 such fractions of 7Gy each, the dose difference between DA and DDA was amounted to 0.8(±1.1; -1 to 3.6)$Gy_{\alpha/\beta=3}$ and 3.2 (±3.3; - 1.3 to 10.8)$Gy_{\alpha/\beta=3.}$

4.4.c.1c: Spatial location of D_{2cm3} region and DIR

In general, most of the patients in this series belonged to group-2, where the D_{2cm3} region was in the same spatial region in BT_1 and BT_2. Only, 3 and 5 out of 21 patients were found to belong to group 1 for rectum and bladder respectively. The group mean percentage variation between DA and DDA was evaluated for each group, and it was found that the variation was similar in rectum irrespective of the group, and statistically insignificant (p=0.94), however for bladder, the variation in group-1 was twice as that of group-2 and borderline significant (p=0.08) (table 14).

4.4.c.1d: Comparison with contour based DIR

In the patient sample where both intensity based and contour based DIR was performed, the intensity based DIR algorithm resulted in a larger mean deviation between DDA and DA as compared to the contour based DIR, although statistically insignificant (p=0.32). The mean±sd

Table 14: *Patient scoring results based on the location of D2cm3 region. Group1-patients with different D_{2cm3} location Group-2 patients with same D_{2cm3} location.*

	Number of patients		% variation		P value
	Group 1	Group 2	Group 1	Group 2	
Rectum	3	18	2.5±1.8	2.4±3.5	0.941
Bladder	5	16	7.6±3.9	3.6±4.3	0.084

of the difference between DDA and DA was 2.4±2.0% and 1.3±1.2%, for intensity based and contour based DIR, respectively. The difference between the two reference frame registrationswas 7.4(±5.4)% for the contour based algorithm and 3.7±3.8% for intensity based DIR, although the difference was not statistically significant (p=0.14) [Figure 48(a&b)]. The contour based

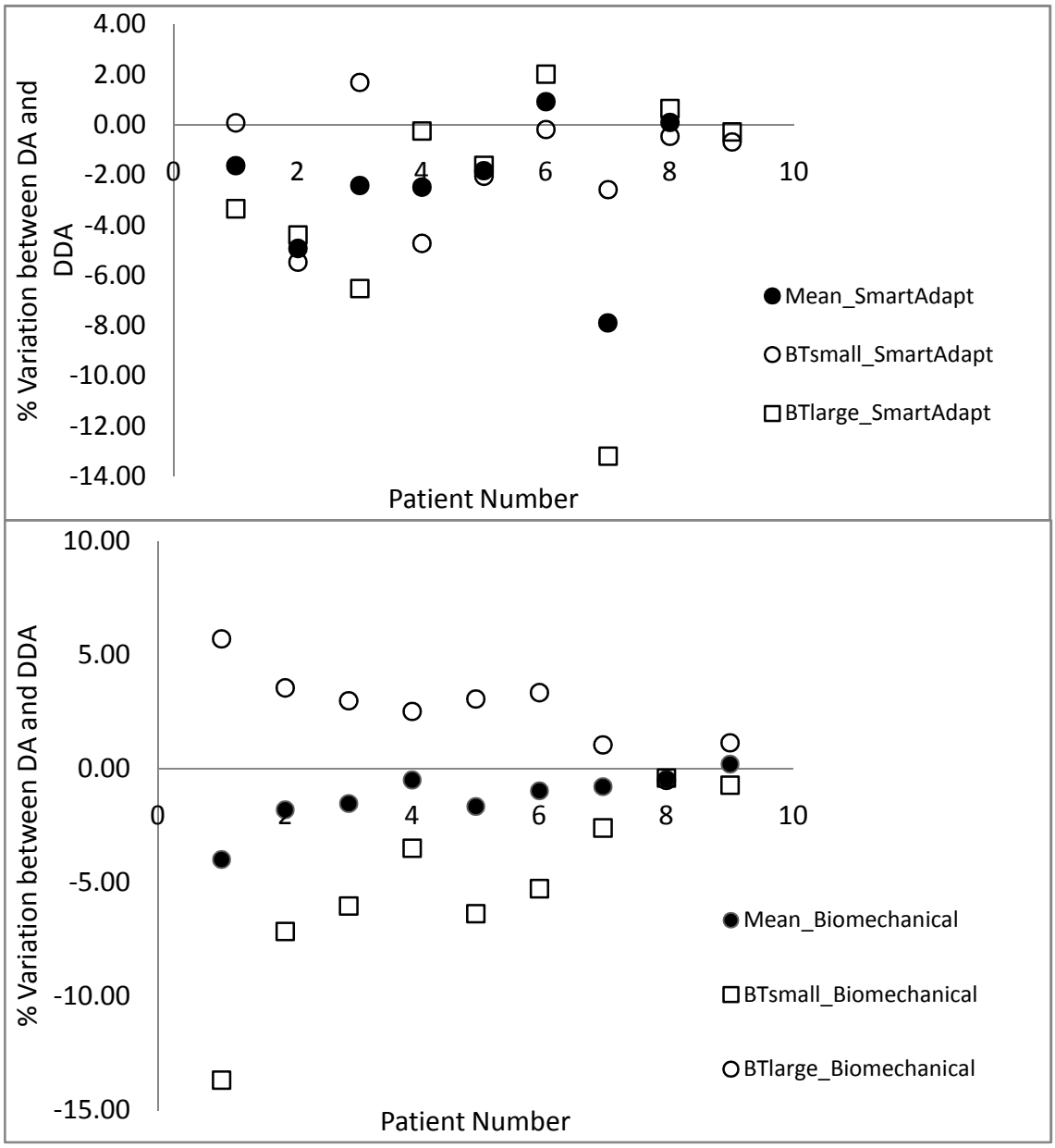

Figure 48: *Percentage variation between DA and DDA for biomechanical (48a) and mutual information algorithm (48b). Registration with small and large bladder as the reference frame, and the mean of two registrations, are plotted*

algorithm showed a systematic variation between DA and DDA according to the bladder volume on the reference frame. DDA was systematically lower than the DA, when the small bladder was registered to the large bladder, [Fig 48a], and higher than DA, when the large bladder was registered with the small bladder. The DDA average of the two reference frames was slightly smaller than the DA. This systematic effect was not observed for the intensity based algorithm [Fig 48b]. It was also observed that the difference between DA and DDA assessed by contour and intensity based was not correlated (R^2 =0.006) [Fig 49]

4.4.d: Discussion

Generally, the accumulated dose in multi-fractional BT is calculated by directly adding the DVH parameters from the treatment plan obtained from the image of each application/fraction. It is however, acknowledged that the patient anatomy may change with time, and this may introduce uncertainties in the accumulated dose. It has been suggested that reducing the uncertainty associated with the accumulated dose, may give rise to a more accurate dose response accounts for organ deformations have been introduced in radiotherapy, and this has created a lot of interest in anatomic deformations and their dosimetric consequences both in relationship for the OARs [233]. In the recent past, newer algorithms which external beam radiotherapy [282-285] and BT [275,277], however with only few investigations in BT. The challenge in using DIR based dose accumulation in BT, is the inherent high dose gradient associated with BT as compared to external beam radiotherapy. In the present study,the comparison between intensity based and contour based DIR resulted in two major observations a) there was no correlation between the high dose region dose degradation predicted by intensity and contour based DIR, b) the difference between DA and DDA depended systematically and consistently on organ volume difference between the reference frames for the contour based DIR, unlike intensity based which showed random variations. As argued by Andersen et al [275] there is a

systematic effect that DIR-based dose accumulations to the reference frame with the largest bladder results in D_{2cm3} values greater than dose accumulations to the reference frame with the smaller bladder. In the present study, this systematic effect was not reproduced with the intensity based DIR. our results in the present study, indicate that DDA based on intensity based DIR is less reliable than DIR based on a contour model. Intensity based DIR seems to be related with significant uncertainties and there is a lack of correlation between DDA estimated by intensity and contour based DIR. Other studies from external beam radiotherapy in various sites also indicate, certain limitations with some algorithms. Yeo et al, compared the Demons (Thirion) and the original H.S. optical flow (Horn & Scunck) algorithms for lung images. Both these algorithms were based on a differential approach that relies on information from image intensities and gradients. They concluded that the the original Horn & Schunck optical flow algorithm is more accurate than the Demons algorithm [286]. Thörnqvist S et al compared two demons algorithms for prostate images, one with predefined setting from the manufacturer,and

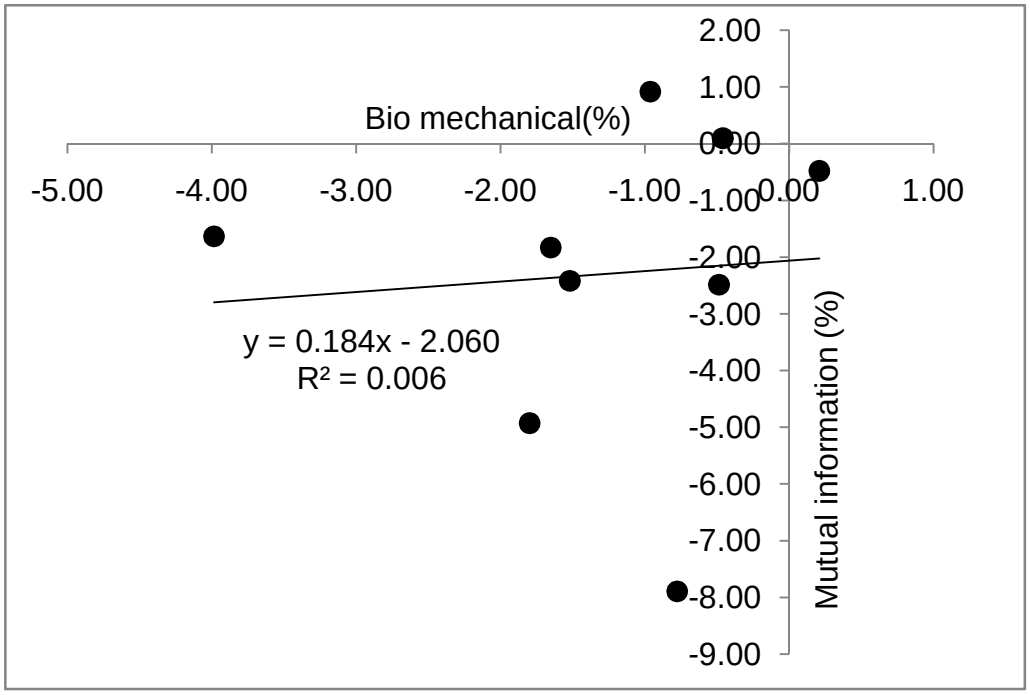

Fig 49: *The percentage dose difference between DA and DDA for biomechanical (x-axis) and Intensity based DIR (y-axis) algorithms. The correlation coefficient was* $R^2 = 0.006$.

the other where the user was given a possibility to choose an anatomical region for matching and concluded that the former was superior than later, although neither performed adequately for contour propagation of the contours [287]. Zhong H et al, evaluated the performance of the Demons and B-Spline algorithms and concluded that the accuracy is closely related to the intensity gradients of the underlying images, the DIR algorithms produce much lower errors inheterogeneous lung regions relative to homogeneous (low intensity gradient) regions, suggests that feature-based evaluation of DIR accuracy must be viewed cautiously [288]. Brock KK et al, compared various algorithms for lung, liver and prostate patients and concluded that DIR was accurate in sites which has high contrast as compared to anatomical sites that has less contrast variation [289].

On the other hand, DIRs based on organ contours and incorporation of contour based models performs more accurately as compared to algorithms that depends only on the image intensities [290-291]. The DIR approach based on image intensity cannot specifically restrict deformations along organ walls to assure anatomically plausible registrations. Even when a deformable registration results in a good visual result with overlapping organ contours after deformation, there may be implausible deformations along the organ walls, which may not be readily detected through visual inspection of the quality of the deformed images. Furthermore, the present study is based on MR images, where the signal intensities/grey levels may be less reproducible as compared to electron densities associated with CT images. Use of DIR without detailed validation may result in large deviations, especially, if applied in the BT scenario with large dose gradients [292-293].

In this study, a large variation was observed between the registrations performed according to different reference frames. Thus, we reconfirm the findings of Andersen et al, that it is necessary to perform DIR based dose accumulation to both the reference frames and to

estimate accumulated D_{2cm3} as the mean of two dose accumulations [275]. Using only one reference DIR and dose accumulation instead of two registrations and the mean, may introduce significant uncertainties in the estimation of DDA. These variations are partly related to evaluation of DVH parameters in terms of absolute volume (e.g. D_{2cm3}) [275]. DDA for DVH parameters based on relative volume (e.g. $D_{2\%}$) depend less on choice of reference frame. Andersen et al. reported a mean variation of 1.8% (SD) of $D_{98\%}$, $D_{66\%}$, $D_{33\%}$ and $D_{2\%}$ by change of reference frame for bladder dose accumulation in prostate radiotherapy, which is significantly lower than the inter-frame variation of 7% evaluated in this study [283]. A more advanced algorithm specifically modeling the walls, special processing of the images that include the mechanical properties of the walls would be needed to resolve this issue [275]. However, when the mean of dose accumulations based on two reference bladder registrations is taken into account, the dose difference between DDA and DA is reduced significantly. Hence, to reduce the uncertainty in the estimation of dose accumulation of BT D_{2cm3} high-dose region, it is necessary to perform registrations based on different reference frames.

Successful deformable image registration is an essential pre-requisite for any deformable dose accumulation especially in BT, where the dose gradient is high. To reduce the uncertainty of DIR, as described in the previous section, we carried out two registrations, (BT_1 deformed+BT_2& BT_2 deformed+BT_1). The maximum percentage variation in deformed dose between the registrations was found to be 22.2% and 19.5% for rectum and bladder respectively. 4/21 patients had large deformed dose deviation of more than 10% between the registrations for both rectum and bladder. Analysis of the size of deformations revealed that large expansions/contractions were found in the high dose region and many of them anatomically implausible [Fig 50]. The discrepancy in dose between the registrations had direct correlation with the size of expansion/contraction. This indicates that the dose degradation seen with DIR based dose accumulation may be largely influenced by implausible registrations. This

observation is also supported by the comparison of intensity based dose accumulation with the contour based algorithm. The contour based algorithm controls the deformations on the bladder wall and these are more consistent deformations, which result in less dose degradation induced by deformable registration.

Generally, the DDA resulted in lower doses as compared to DA, as the D_{2cm3} region will vary between the fractions due to relocation of the high-dose region dose. It was observed in the present study that the high-dose region dose degradation was larger in the bladder as compared to rectum. The percentage difference between DA and DDA was 2.4(±3.3)% and 5.2(±5.1)% for

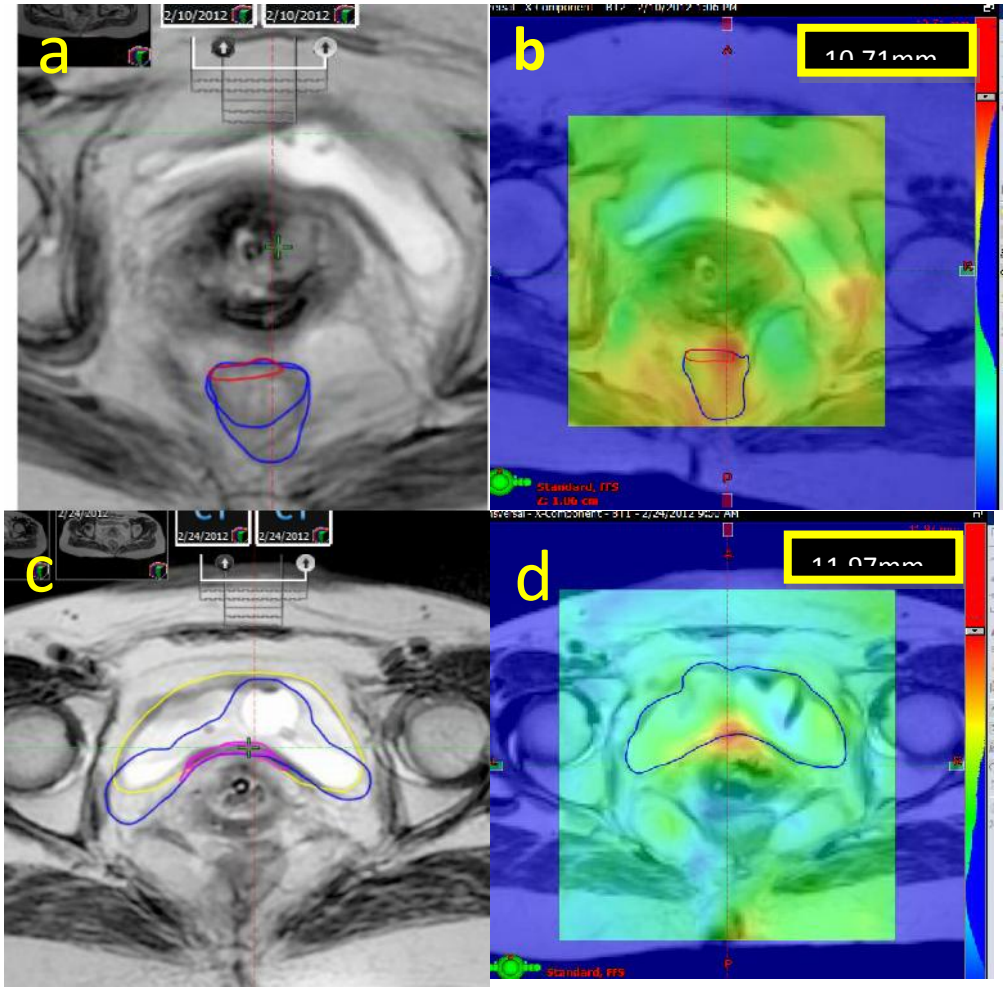

Figure 50: *An example of patient images that shows implausible deformable image registration in rectum and bladder. Panel 5a & 5c : Rigid registration of BT1 and BT2 images for rectum and bladder, respectively. Panel 5b & 5d: Deformation map showing a maximum deformation of 10.7 /11.97mm in the region of anterior rectal/posterior bladder wall, The contour marked in red/magenta is the region of D_{2cm3} in rectum and bladder, respectively.*

rectum and bladder respectively. The maximum percentage difference was 11.5% and 16.5% for rectum and bladder respectively. For bladder, the location of $2cm^3$ volume varied significantly in some patients, which also correlated with larger dose difference between DA and DDA. It seems therefore that the intensity based DIR could predict dose degradation in case of high-dose region relocation. However, the above-mentioned uncertainties of intensity based DIR indicate that it is difficult to discriminate whether any predicted dose degradation is due to a real effect or induced by implausible DIR.

Inter-and intra-fraction organ movements constitute the major uncertainty component in IGABT with mean dose variations of 15-30% for bladder, rectum and sigmoid [12]. In addition, organ contouring also is a significant source of uncertainty [235,294-295]. Kirisits et al. reported inter-observer variation up to 7% and 12% for D_{2cm3} of a simple geometrical structure representing the bladder [235]. Other sources of variation in image-guided BT are geometrical uncertainties regarding source positioning and applicator reconstruction. Tanderup et al. investigated uncertainties stemming from applicator reconstruction, and found that when avoiding systematic errors the uncertainty in DVH parameters could be kept below 10% in 90% of the patients [139]. Direct addition of DVH parameters, without taking into account the deformation due to organ filling may also add some uncertainty in the DVH parameter reporting. However this uncertainty is small as compared to the other uncertainties discussed above [275]. Efforts to reduce this uncertainty should not introduce new uncertainties in terms of DIR related uncertainties in the process. In general, the findings of the present study, indicate that for the majority of patients, DIR based dose evaluation is unlikely to result in substantial improvement of bladder and rectal dose reporting compared to direct addition of DVH parameter D_{2cm3}, and intensity based DIR may even add uncertainties in dose assessment. This is consistent with conclusions from a study performed in vaginal cuff BT, where the authors also recommend DA for BT dose accumulation [277].

4.4.e: Conclusion:

As expected from relocation of high-dose region between BT fractions, DIR based dose accumulation degrade the high-dose region dose as compared to direct DVH addition. However, there was significant discrepancy between hotspot dose degradation predicted by DIR algorithms based on image intensity as compared to contour based method. Intensity based DIR on MR images resulted frequently in implausible deformations, since it was not regulated by mechanical properties of organ walls. Based on the results of the present study, we conclude that the direct addition of DVH parameters provides a reasonably good estimate to the dose to the OARs, and that DIR based on image intensities may lead to systematic underestimation of dose due to implausible DIR.

4.5. Summary

In this chapter, intra- and inter-fraction uncertainties related to organ and applicator changes taking place in between imaging and dose delivery have been analyzed. In T/O applicator, it was found that the inter-application variation was mainly attributed to the ovoid size and the gap between the ovoids. Hence clinical vaginal examination may play a major role, where the physician examines the patient and decide the size of the ovoid that best fits the vaginal mucosa of the patient during the first application. In addition to that, it is important to consider reproducing the vaginal packing. It should also be recognized that the implant geometry has to be consistent, which can be achieved by maintaining certain parameters such as following the bladder filling protocol, rectal packing, and ovoid gap. For HDR intracavitary BT application based on 2D orthogonal radiograph images, our data show marked differences in rectum and bladder dose point, and therefore recommend individual fraction re-planning.

The current practice of determining the D_{2cm^3}cumulative dose to OARs during BT is based on what has previously been called “the worst-case scenario”, which is the assumption that the D_{2cm^3}regions are located in the same anatomical part of the organ in each fraction [235]. This assumption implies that the cumulated BT dose can be calculated by adding D_{2cm^3}values for each fraction. The available data on inter fraction/application variation documents dose variation of target structures and the OARs quantitatively, but do not take into account the spatial (topographic) location of the high dose region of OARs [250,266]. The results of our study indicate that the spatial location of D_{2cm^3}volumes is most stable for rectum and to a large extent for bladder which implies that ‘DVH addition’ could be applicable to rectum and bladder. Minimal to moderate geometric changes in sigmoid are seen in majority of the patients in between applications resulting in maximal variation in spatial location of D_{2cm^3} volumes which may lead to over estimation of doses during the DVH addition.

The major limitation of this study is the use of rigid registration, where the registration was based on the applicator and not on the anatomy. One possible solution to overcome this issue is to use deformable registration algorithm, where the organ deformation is taken into account**.** It was found that, DIR based dose accumulation degrade the high-dose region dose as compared to direct DVH addition. However, there was significant discrepancy between hotspot dose degradation predicted by DIR algorithms based on image intensity as compared to contour based method. Intensity based DIR on MR images resulted frequently in implausible deformations, since it was not regulated by mechanical properties of organ walls. It was concluded that that the direct addition of DVH parameters provides a reasonably good estimate to the dose to the OARs, and that DIR based on image intensities may lead to systematic underestimation of dose due to implausible DIR.

Chapter 5

Summary, Conclusion and Future direction

5.1. Summary

In the recent past, the advent of advanced imaging modalities such as MR and availability of CT / MR compatible applicators have paved the way for IGABT. Various imaging modalities like ultrasound CT, MRI and PET scan etc. have been explored. Among all the imaging modalities, MR imaging is becoming increasingly popular for diagnosis and treatment planning for EBRT and BT for cervical cancer. Promising results in terms of increased local control and reduced toxicities have been reported which made this technique popular during the last decade.

In the year 2004, GYN GEC ESTRO first published its recommendations, which describes the concepts and terms used in 3D IGBAT. Various definitions of GTV and CTV were proposed, which are now widely accepted. In Multi fractionated BT, a new dimension, time is added in to the process, as imaging and treatment planning is carried out for each fraction, and the inter application/fraction variation has been a major concern during dose accumulation. The organ deformation by means of bladder filling, tumour shrinkage has resulted in large uncertainty in the process of dose reporting of this process. Since, the fourth dimension is also being used in the treatment planning; a term called IGABT- Image Guided Adaptive BT has been introduced. During this PhD thesis, clinical implementation of 3D image based BT for cervical cancer was implemented in TMH. We are also a part of an ongoing multicentric collaborative trial International study on MRI-guided BT in locally advanced cervical cancer (EMBRACE) which will reveal more information on the dose effect relationship on local control/morbidity of the tumour and toxicities of OARs.

Although IGABT is widely practiced in many centers across the globe, it is still in its infancy in India. The implementation of IGABT in India and other developing countries is a big challenge due to the resources, expertise and financial constraints. Nevertheless, with the successful implementation of 3D-CRT, IMRT and IGRT in routine clinical practice, there is a growing interest in IGABT in cervical cancers in India. As any other advanced techniques,

IGABT too requires systematic clinical implementation that includes familiarization of the processes. In-appropriate implementation of IGABT and change of clinical practice based on this could be damaging to the patients. The contouring procedure has been shown to carry some of the most significant uncertainties in the IGABT procedure. Further, in the past, lack of proper TPS QA procedures has led to some serious accidents. Unlike treatment delivery errors, which are usually random in nature, the errors from the TPS and applicator commissioning are more often systematic and can be avoided. During this thesis period, we made this transition of 2D to 3D MR Image BT in TMH. The successful implementation of 3D image based BT in to clinical routine which is of international standard, is the basis of this thesis.

5.1.1. Treatment planning and Optimization:

Most BT centers in the world have followed a traditional concept based on the Manchester or Fletcher loading patterns. The rationale behind the Manchester approach is to achieve a consistent dose rate at point A, by applying a set of strict rules with regard to the position and activity of radium sources for the different combination of sizes for the uterine tandem and ovoids. With the introduction of HDR remote after loaders, the rules of Fletcher and Manchester systems were extended from the milligram radium equivalent activity distribution to a pattern of dwell positions where a single stepping source is positioned at programmable dwell times. With the introduction of computers and sophisticated mathematical models, HDR BT has brought in more advances in to field of BT. One such advance in the process of treatment planning is the application of optimization algorithms in HDR BT, which offers a great flexibility in shaping the desired dose that adequately covers the tumour and minimizes the dose to normal tissues.

The objective of any treatment planning in radiotherapy is to deliver the maximum dose to the tumour and minimum elsewhere. One of the basic pre requisite to meet this objective is

the knowledge of the spatial location of tumour volume with respect to OARs. In 2D orthogonal images, the OARs with respect to the target volumes were not clearly seen and hence the toxicities were reported to be high, although most of the series reported in good clinical results. The integration of CT or MR imaging for treatment planning in 3D IGABT serves the purpose of identifying the target volumes in 3D geometry. The introduction of IGABT, has also added a new dimensions in terms of both volume to the target and OAR and how these volumes change with time, providing an improved understanding compared with the limited information available with radiographic localization.

The dose effect curves for OAR may be steep depending on the endpoint. Recent publication from the Vienna group shows that the dose volume correlations for late rectal morbidity treated with MR IGABT, where a steep dose effect is evident, especially when D2cc is used as a predictor for the dose delivered to the rectum. The historical series based on the clinical experience and radiobiology also shows steep dose effect relationship. Moreover, the steep dose gradients in BT demands for an optimized dose distribution, where the tumour is adequately irradiated with sharp fall off of dose in OARs. Hence, it is imperative to obtain a best possible treatment plan that satisfies the above conditions. The second pre-requisite to meet the planning objective in BT treatment planning, is to achieve certain dose volume parameters or constraints, which are considered as the dose tolerance for the organs. The method to achieve these constraints in HDR BT may be termed as optimization. In the recent past newer algorithms such as inverse planning have been introduced in the clinic.

The application of inverse planning in external beam radiotherapy is very common; however in BT it is still not commonly practiced in the clinics. In the last 4-5 years, the application of inverse planning has been practiced in prostate BT; however, its use in gynaecological BT is sparse. One of the major reasons for this is the use of standard loading pattern, which originates from the traditional schools that resulted in excellent results. Any

deviation from these standard loading patterns was not well taken. In this thesis, three major clinical scenarios were investigated, viz, Tandem ovoid application, Tandem/ring application, combined Intracavitary and interstitial implants – Vienna applicator, Interstitial applicator-Martinex Universal Interstitial Perinneal Template (MUPIT) and prostate implants.

The inverse planning algorithms, employing sophisticated mathematical formulations expected to result in better plans as compared to manual trial and error method. The results of our study concludes that although, inverse planning algorithms produced good plans interms of dose volume parameters, the loading pattern of these algorithms in comparison with traditional systems was not similar. This may be attributed to the fact that the traditional systems were based on the applicator geometry such as the length of the tandem and the size of the ovoid, while the more modern planning concepts are based on the tumour and the topography of the OARs with respect to the applicator. Inverse planning with HIPO and/or manual optimization offers improved plans in terms of OAR sparing and maintaining target coverage when compared to standard clinical plans. For large and/or unfavorable targets, coverage cannot be achieved with either manual or inverse optimization if no adaptation of the application technique is included. The average loading pattern for the whole patient cohort was found to deviate from a traditional standard Fletcher loading. For our patient cohort, the tandem loading was decreased compared to the ovoids mainly due to high sigmoid dose.

One of the typical qualities of manual optimization as compared to inverse planning algorithms is that it did not deviate very much from the standard loading pattern. The traditional pear shaped dose distribution was maintained, except for a few minor changes that improve the target coverage and OAR sparing. On the other hand, the inverse optimization changes the dwell time gradient to a large extent. IPSA plans were compared with manually optimized plan for T/O and Vienna applicator; it was found that IPSA produced superior plans with respect to HR CTV coverage and sparing of OARs. IPSA also produced conformal plans as compared to

MOPT. For T/O applicator, it was found that the use of HS did not make any impact both in the dose volume parameters and in the loading of tandem and ovoids, however in the case of Vienna applicator, inclusion of HS in the optimization made a significant impact in the loading of needles. Without the HS, the optimizer loaded the needles heavily, which drastically came down when HS were included. HS may be included in the optimization while using IC+IS, and may not while using just intracavitary approach.

5.1.2. Uncertainties due to Organ motion:

BT has evolved into a high-technology modality of radiotherapy incorporating advanced imaging modalities such as CT, MR, US and intelligent optimization and planning methods as standards of care. However, BT uncertainties that could have a direct impact on the clinical treatment and therefore the outcome have not been adequately addressed. While uncertainties related to 3D image based EBRT have been investigated in detail during decades, there has so far been a limited knowledge of uncertainties related to 3D volumetric image based BT. There have been ‘‘dogmas’’ that uncertainties in BT are negligible based on the observation that the applicator, tumour and surrounding tissues represent a stable system. However, BT dose gradients are significant and geometric uncertainties can potentially lead to significant uncertainties, which cannot be neglected. IGABT is subjected to uncertainties in each step of the entire process: Source calibration, imaging, contouring, applicator reconstruction, dose and DVH calculation, dose delivery and anatomical variations. It is essential to identify these uncertainties, their magnitude, and their impact on the overall uncertainty of dose delivery to the patient. Having this knowledge may provide correct dose assessment, dose effect modeling, and subsequently improved clinical outcome when using better planning aims with dose and volume constraints.

Intra- and inter-fraction uncertainties related to organ and applicator changes taking place in between imaging and dose delivery have been analyzed and quantified to be 20-25% which is

the largest. This indicates that organ motion is the major contribution to OAR dose uncertainties. In summary, physics uncertainties related to dosimetry and geometry are in general more limited as compared to the pronounced clinical uncertainties related to contouring and organ motion. Contouring is by far the largest contributor to uncertainties for target, whereas organ motion has the major impact on uncertainties in OARs. This was the motivation to study in detail about the quantification of uncertainties of inter fraction variation and dose accumulation of dose to OARs in this part of the thesis.

Detailed analysis was carried out to investigate the uncertainties of organ motion in 2D orthogonal radiograph image based dosimetry and 3D volumetric MR image based BT using both rigid and deformable image registration.In multi-fractional BT, the inter-application variation may occur due to various reasons such as bladder filling, rectal gas filling, movement of sigmoid colon, variation in vaginal packing due to the application, especially in non-fixed applicator such as tandem/ovoid applicators. Although it is recommended to use imaging for each application to reduce the uncertainties, in certain situations, it may not be possible to image each application. There could be a scenario, where the first application plan may have to be used for subsequent fraction/s. In such situations, although the dose to target may not exhibit a large variation, especially, in point-A prescribed plans, the dose to OARs may vary to a large extent.

In the present study, we have found that the inter-application variation is mainly attributed to the ovoid size and the gap between the ovoids. Hence clinical vaginal examination may play a major role, where the physician examines the patient and decide the size of the ovoid that best fits the vaginal mucosa of the patient during the first application. In addition to that, it is important to consider reproducing the vaginal packing. So whenever possible, it is recommended to reproduce the locking of the applicator to retain the consistency of the applicator geometry. Other factors attributed to the inter application variation in the present study includes the variation in the implant geometry in terms of uterine tandem length & angle, ovoid size has to be

consistent. It should also be recognized that the implant geometry has to be consistent, which can be achieved by maintaining certain parameters such as following the bladder filling protocol, rectal packing, and ovoid gap. For HDR intracavitary BT application based on 2D orthogonal radiograph images, our data show marked differences in rectum and bladder dose point, and therefore recommend individual fraction re-planning.

The current practice of determining the D_{2cm^3}cumulative dose to OARs during BT is based on what has previously been called “the worst-case scenario”, which is the assumption that the D_{2cm^3}regions are located in the same anatomical part of the organ in each fraction. This assumption implies that the cumulated BT dose can be calculated by adding D_{2cm^3}values for each fraction. Various parameters such as bladder and/or rectal filling, movements of sigmoid colon, and variation in vaginal packing have been identified for inter-fraction / inter application variation. The available data on inter fraction/application variation documents dose variation of target structures and the OARs quantitatively, but do not take into account the spatial (topographic) location of the high dose region of OARs.

To study and investigate further, the inter application variation of spatial location and D_{2cm^3}dose volumes and the topography of OAR’s, we undertook this study. The results of our study indicate that the spatial location of D_{2cm^3}volumes is most stable for rectum and to a large extent for bladder which implies that ‘DVH addition’ could be applicable to rectum and bladder. Minimal to moderate geometric changes in sigmoid are seen in majority of the patients in between applications resulting in maximal variation in spatial location of D_{2cm^3} volumes which may lead to over estimation of doses during the DVH addition. However, studies in larger cohort of patients and more importantly correlation with the actual toxicities is required to validate these findings further.

The major limitation of this study is the use of rigid registration, where the registration was based on the applicator and not on the anatomy. In the present study, the organ

deformations like bladder-rectal filling, deformation of organs was not taken quantitatively into account. Due to which, it is not possible to locate the exact tissue where the dose D2cc dose was received previously. Hence, in the present study, there could be a situation that can arise where the D2cc was not scored to have an overlap, but the tissue that receives the dose could be overlapping. So the result described in the present study as “not overlapping” may actually be overestimating this effect. One possible solution to overcome this issue is to use deformable registration algorithm, where the organ deformation is taken into account Inter-application variations result in deformation of organs, which may lead to uncertainties in dose accumulation while directly adding the DVH parameters. To provide better estimates of accumulated doses, deformable image registration (DIR) algorithms have been introduced in the recent past, to take into account the variation in the anatomy such as bladder filling and organ motion. The DIR relates the registered images to a common reference frame, and the dose distributions of the registered images can then be mapped to this reference frame, which enables calculation of the cumulative dose. In the recent past, dose accumulation based on deformable image registrations has been reported for bladder dose accumulation. However, dose accumulation for rectum is not reported yet and in general the literature is sparse for multi fractionated IGABT.

With an aim to estimate, compare and report, the dose accumulation for bladder and rectum by deformable image registration and direct addition of DVH parameters in a multi-fractionated HDR MR IGABT schedule, we undertook this study. As expected from relocation of high-dose region between BT fractions, DIR based dose accumulation degrade the high-dose region dose as compared to direct DVH addition. However, there was significant discrepancy between hotspot dose degradation predicted by DIR algorithms based on image intensity as compared to contour based method. Intensity based DIR on MR images resulted frequently in implausible deformations, since it was not regulated by mechanical properties of organ walls. Based on the results of the present study, we conclude that the direct addition of DVH

parameters provides a reasonably good estimate to the dose to the OARs, and that DIR based on image intensities may lead to systematic underestimation of dose due to implausible DIR.

5.2 Conclusion

5.2.1. Treatment planning and Optimization:

The inverse planning algorithms, employing sophisticated mathematical formulations expected to result in better plans as compared to manual trial and error method. The results of our study concludes that although, inverse planning algorithms produced good plans in terms of dose volume parameters for intracavitary applications, the loading pattern of these algorithms in comparison with traditional systems was not similar. Inverse planning with HIPO and/or manual optimization offers improved plans in terms of OAR sparing and maintaining target coverage when compared to standard clinical plans. For large and/or unfavorable targets, coverage cannot be achieved with either manual or inverse optimization if no adaptation of the application technique is included. The average loading pattern for the whole patient cohort was found to deviate from a traditional standard Fletcher loading. For our patient cohort, the tandem loading was decreased compared to the ovoids mainly due to high sigmoid dose. One of the typical qualities of manual optimization as compared to inverse planning algorithms is that it did not deviate very much from the standard loading pattern. The traditional pear shaped dose distribution was maintained, except for a few minor changes that improve the target coverage and OAR sparing. On the other hand, the inverse optimization changes the dwell time gradient to a large extent. For T/O applicator, it was found that the use of HS did not make any impact both in the dose volume parameters and in the loading of tandem and ovoids, however in the case of Vienna applicator, inclusion of HS in the optimization made a significant impact in the loading of needles. Without the HS, the optimizer loaded the needles heavily, which drastically came down when HS were included. HS may be included in the optimization while using IC+IS,

and may not while using just intracavitary approach. For interstitial MUPIT applicator IPSA resulted in significant sparing of normal tissues without compromising CTV coverage as compared with dose point optimized plan. However, IPSA did not show any significant improvement either in CTV coverage or in normal tissue sparing as compared with graphically optimized plan. IPSA was found to be superior in terms of homogeneity and conformity as compared with graphically optimized plan.

5.2.2 Uncertainties due to Organ motion:

For HDR intracavitary BT application based on 2D orthogonal radiograph images, the data showed marked differences in rectum and bladder dose point, and therefore recommend individual fraction re-planning.

In multi fractional BT based on MRI image based planning using rigid registration, the spatial location of D_{2cm^3}volumes was found to be the most stable for rectum and to a large extent for bladder which implies that 'DVH addition' could be applicable to rectum and bladder. Minimal to moderate geometric changes in sigmoid are seen in majority of the patients in between applications resulting in maximal variation in spatial location of D_{2cm^3} volumes which may lead to over estimation of doses during the DVH addition.

In multi fractional BT based on MRI image based planning the dose accumulation carried out using deformable image registration algorithm revealed that the relocation of high-dose region between BT fractions, degrade the high-dose region dose as compared to direct DVH addition. However, there was significant discrepancy between hotspot dose degradation predicted by DIR algorithms based on image intensity as compared to contour based method. Intensity based DIR on MR images resulted frequently in implausible deformations, since it was not regulated by mechanical properties of organ walls. Based on the results of the current study, It was concluded that the direct addition of DVH parameters provides a reasonably good

estimate to the dose to the OARs, and that DIR based on image intensities may lead to systematic underestimation of dose due to implausible DIR.

5.3. Future Directions:

5.3.1 On line imaging

With increasing conformity of dose, and the inherentproperty of BT of high dose gradients, it becomes important that the delivery of dose is in accordance with what is planned on the TPS. Optimal source geometry, timing, and stability are prerequisites for safe delivery of optimized BT. Both patient‐related factors and technical issues associated with the BT equipment can give rise to uncertainties in the delivered dose. It is well‐recognized that equipment‐related uality assurance has to be conducted periodically to prevent the dose delivery errors. Patient‐related factors are being identified as applicator displacement, organ motion, between the treatment planning and dose delivery.However, what is finally missing is dose delivery verification as we have in EBRT, with portal imaging, cone‐beam CT, and tools for off‐line/on‐line correction. In contrast to EBRT, in BT, we miss verification systems that provide the proof that the source reaches its planned position, or by mistake no transfer tubes were exchanged or any other variation in anatomy and applicator geometry. This will be the logical next step to be developed and integrated. After successful implantation, no other treatment modality will be able to deliver such high doseswith such high accuracy. However, it is, especially, very important, that in addition to the management of variations, mistakes should be avoided. It is often seen in centers who start with IGABT, most focus is on the new planning methods, while the basic quality assurance is becoming of less importance. It is essential to perform appropriate commissioning and constancy checks.

5.3.2 Dose accumulation using deformable image registration using CT images.

Our results in the present study indicate that DDA based on intensity based DIR is less reliable than DIR based on a contour model. Intensity based DIR seems to be related with significant uncertainties and there is a lack of correlation between DDA estimated by intensity and contour based DIR. Other studies from external beam radiotherapy in various sites also indicate certain limitations with some algorithms. DIRs based on organ contours and incorporation of contour based models performs more accurately as compared to algorithms that depend only on the image intensities [290-291]. The DIR approach based on image intensity cannot specifically restrict deformations along organ walls to assure anatomically plausible registrations. Even when a deformable registration results in a good visual result with overlapping organ contours after deformation, there may be implausible deformations along the organ walls, which may not be readily detected through visual inspection of the quality of the deformed images. Furthermore, the present study is based on MR images, where the signal intensities/grey levels may be less reproducible as compared to electron densities associated with CT images. Use of DIR without detailed validation may result in large deviations, especially, if applied in the BT scenario with large dose gradients [292-293]. The contour based algorithm controls the deformations on the bladder wall and these are more consistent deformations, which result in less dose degradation induced by deformable registration. Future studies can be aimed at using CT images for intensity based algorithms, to investigate further, such that the uncertainties associated with the DIR can be reduced. In addition, newer algorithms can be developed such that the organ wall constraints can be taken into account.

5.3.3. Investigation of low cost imaging modalities:

One of the major limitations of the clinical implementation of MR image based BT for cervical cancer is the non availability of MR scanners, especially in the developing countries. In

the absence of MR and CT scanners, the low cost imaging modality like ultrasound may be an alternative to practice image based BT. Conventionally, trans-abdominal ultrasound used during difficult intracavitary applications to avoid uterine perforation. However, recently, It has been reported that the correlation of ultrasound with the MRI images were good particularly for the size and the shape of the uterus. No reported literature so far in using the ultrasound images as the primary modality, in conjunction with CT/2D radiographs without the use of MRI for target delineation. One of the proposal could to be to use the CT/MR image based planning for the first application and the use of ultrasound images for the subsequent applications may reduce the cost of the implementation of the image based BT for the cervical cancer.

References:

1. Henschke U, Hilaris BS, Mahan GD. Afterloading in interstitial and intracavitary radiation therapy. Am J Roentgenol 1963; 90:386-95.
2. Kirisits C, Lang S, Dimopolous J et al. The Vienna applicator for combined intracavitary and interstitial brachytherapy of cervical cancer: design, application, treatment planning and dosimetric results. Int J Radiat Oncol Biol Phys 2011; 80:947–55.
3. Dimopoulos JC, Schard G, Berger D, et al. Systematic evaluation of MRI findings in different stages of treatment of cervical cancer: potential of MRI on delineation of target, pathoanatomic structures, and organs at risk. Int J Radiat Oncol Biol Phys. 2006; 64:1380–8.
4. Orton C. High dose rate brachytherapy may be radiobiologically superior to low dose rate due to slow repair of late responding normal tissue cells. Int J Radiat Oncol Biol Phys. 2001; 49:183–9.
5. Patel FD, Sharma SC, Negi PS, et al. Low dose rate vs. high dose rate brachytherapy in the treatment of carcinoma of the uterine cervix: a clinical trial. Int J Radiat Oncol Biol Phys.1993; 28:335–41.
6. Pierquin B, Wilson JF, Chassagne D, Modern Brachytherapy 1987; NewYork: Masson.
7. Paterson R, Parker HM. A dosage system for interstitial radium therapy. Br J Radiol 1938; 1: 252-340.
8. Meredith WJ. Radium Dosage: The Manchester System. Edinburgh: Livingston 1967.
9. Simon N. Radium substitutes in the interstitial implantation of tumours with particular reference to iridium-192. J Okla State Med Assoc.1963;56:371-6.
10. Auer T, Hensler E, Eichberger P et al. 3D navigation for interstitial stereotaxic brachytherapy. Strahlenth Onkol 1998; 174:82-7.
11. Thomas I, Chemin A, Lasbareilles O et al. MRI and CT scan imaging during pulsed dose rate intracavitary brachytherapy in carcinoma of the cervix. Radiother Oncol 1998;47(suppl.1):8
12. Martel MK, Narayana V, Brachytherapy for the next century: use of image based treatment planning. Radiat Res 1998; 150:178-88.
13. Brenner DJ. Radiation biology in brachytherapy. J Surg Oncol 1997; 65:66-70.
14. Dale RG, Jones B. The clinical radiobiology of brachytherapy. Br J Radiol 1998; 71:465-83.
15. Joslin CAF, Flyn A, Hall EJ (eds). Principles and practice of brachytherapy 2001;London: Arnold.
16. Steel GG, Basic Clinical Radiobiology 1997;London; Edward Arnold.
17. Turesson I, Radiobiological aspects of continuous low dose rate irradiation and fractionated high dose rate irradiation. Radiother Oncol 1990; 19:1-16.
18. Holm HH, Juul N, Pedersen JF, Hansen H, Stroyer I, Transperineal 125Iodine seed implantation in prostate cancer guided by transrectal ultrasonography. J. Urol 1983;130:283-6.
19. Potter R, Kirisits C, Fidarova EF et al. Present status and future of high precision image guided adaptive brachytherapy for cervix carcinoma. ActaOncol 2008; 47:1325-36.
20. Nandakumar A. National Cancer Registry programme, Indian Council of Medical Research, consolidated report of the population based cancer registries. New Delhi, India; 1990–96. p. 60.
21. Dinshaw KA, Rao DN, Ganesh B. Tata Memorial Hospital cancer registry annual report. Mumbai, India; 1999. p. 52.

22. Bergeron C, Barrasso R, Beaudenon S, et al. Human papilloma viruses associated with cervical intraepithelial neoplasia. Great diversity and distinct distribution in low and high grade lesions. Am J Surg Pathol 1992; 16(7):641-9.
23. Perez CA, Grigsby PW, Nene SM, et al. Effect of tumour size on the prognosis of carcinoma of the uterine cervix treated with irradiation alone. Cancer 1992; 69:2796-806.
24. Perez CA, Camel HM, Kuske RR et al. Radiation therapy alone in the treatment of carcinoma of the uterine cervix: A 20 year experience. Gynecol Oncol 1986;23:127-40.
25. TOD M, Meredith WJ, Treatment of cancer of the cervix uteri, a revised Manchester method. Br J Radiol 1953;26:252-7.
26. International commission on Radiation Units and measurements (ICRU) Report 38: Dose and volume specification for reporting intracavitary brachytherapy in gynaecology: 1985.
27. Tod M, Meredith WJ. A dosage system for use in the treatment of cancer of the uterine cervix. Br J Radiol. 1938; 11:809-824.
28. Potish R, Gerbi B, Engler GP. Dose prescription, dose specification, and applicator geometry in intracavitary therapy. In: Williamson J, Thomadsen, B., Nath, R., ed. Brachytherapy Physics. Madison, WI: Medical Physics Publishing; 1995:379-410.
29. Pötter R., Kirisits C. Upcoming ICRU/GEC ESTRO recommendations for brachytherapy in cancer of the cervix (1 &2) Radiother Oncol. 2012; 103(Suppl. 2):42-43.
30. Viswanathan AN, Thomadsen B. American Brachytherapy Society consensus guidelines for locally advanced carcinoma of the cervix. Part I: general principles. Brachytherapy. 2012; 11:33-46.
31. Fletcher GH, Hamburger AD. Female pelvis squamous cell carcinoma of the Uterine cervix. In GH Fletcher (ed): Text book of radiotherapy. Philadelphia: Lea and Febiger, 3rd edition 1980; 720-89.
32. Delclos L, Fletcher GH, Moore EB, Sampiere VA. Minicolpostats, dome cylinders, other additions and improvements of the Fletcher – Suit afterloadable system: Indications and limitations of their use. Int J Radiat Oncol Biol Phys 1980; 6:1195-206.
33. Walstam R. A remotely controlled afterloading apparatus. Acta Radiol; (Suppl) 326:84-100.
34. Gerbaulet A, Maher M, Haie-Meder C, et al. Cancer of the cervix (K Morita). The Paris Method. In: Vahrson HV(ed). Rad Oncol Gynecol Cancer . NewYork: Springer, 1997;198-205.
35. Leung S. Perineal template techniques for interstitial implantation of gynaecological cancers using the Paris system of dosimetry. Int J Radiat Oncol Biol Phys 1990; 19:769-74.
36. Erickson, B., Albano, K., and Gillin, M. CT-guided interstitial implantation of gynecologic malignancies, Int J Radiat Oncol Biol Phys 1996;36: 699-709.
37. Syed, A. M., Puthawala, A. A., Abdelaziz, N. N., el-Naggar, M., Disaia, P., Berman, M., Tewari, K. S., Sharma, A., Londrc, A., Juwadi, S., Cherlow, J. M., Damore, S., and Chen, Y. J. Long-term results of low-dose-rate interstitial-intracavitary brachytherapy in the treatment of carcinoma of the cervix, Int J Radiat Oncol Biol Phys 2002; 54: 67-78.
38. Beriwal, S., Bhatnagar, A., Heron, D. E., Selvaraj, R., Mogus, R., Kim, H., Gerszten, K., Kelley, J., and Edwards, R. P. High-dose-rate interstitial brachytherapy for gynecologic malignancies, Brachytherapy 2006; 5: 218-222.
39. Beriwal, S., Demanes, D. J., Erickson, B., Jones, E., De Los Santos, J. F., Cormack, R. A., Yashar, C., Rownd, J. J., and Viswanathan, A. N. American Brachytherapy Society consensus guidelines for interstitial brachytherapy for vaginal cancer, Brachytherapy 2012; 11: 68-75.

40. Viswanathan, A. N., Erickson, B. E., and Rownd, J. Image-based approaches to interstitial brachytherapy, 2011; 247-259, In Gynecologic Radiation Therapy. Novel Approaches to Image-Guidance and Management (Springer-Verlag, Berlin Heidelberg).
41. Abbe R. The use of radium in malignant disease. Lancet 1913; 2:524-7.
42. Choy D, Wong RL, Sham J. Vaginal template implant for cervical carcinoma with vaginal stenosis or inadvertent diagnosis after hysterectomy. Int J Radiat Oncol Biol Phys.1993; 28:457-62.
43. Martinez A, Cox RS, Edmunson GK. A multiple site preineal applicator (MUPIT) for treatment of prostatic, anorectal and gynecological malignancies. Int J Radiat Oncol Biol Phys.1984; 10: 297-305.
44. Nag S, Martinez –Monge R, Ellis R. The use of fluoroscopy to guide needle placement in interstitial gynaecological brachytherapy. Int J Radiat Oncol Biol Phys.1998; 40: 415-20.
45. Erickson B, Albano K, Gillin M. CT guided interstitial implantation of gynaecological malignancies. Int J Radiat Oncol Biol Phys.1996; 36: 699-709.
46. Erickson B, Foley WD, Gillin M, Ultrasound guided transperineal interstitial implantation of pelvic malignancies. Endocurie Hypertherm Oncol 1995; 11:107-13.
47. Popowski Y, Hiltbrand E, Joliat D. Open magnetic resonance imaging using titanium-zirconium needles: improved accuracy for interstitial brachytherapy implants? Int J Radiat Oncol Biol Phys.2000; 47: 759-65.
48. The GEC ESTRO Hand book of radiotherapy. Ed Gerbaulet A, Potter R, Mazeron JJ et al, 2002.
49. Quimby EH, Castro V. The calculation of dosage in interstitial radium therapy. Am J Roentgenol Radium TherNucl Med 1953; 70: 739-49.
50. Pierquin B, Dutreix A, Paine CH, Chassagne, Marinello G, Ash D. The Paris system in interstitial radiation therapy. Acta Radiol Oncol Radiat Phys Biol 1978; 17:33-48.
51. Nomden CN, de Leeuw AA, Moerland MA et al. Clinical use of the Utrecht applicator for combined intracavitary/interstitial brachytherapy treatment in locally advanced cervical cancer. Int J RadiatOncolBiol Phys. 2012; 82:1424-30.
52. Kim RY, Pareek P. Radiography based treatment planning compared with computed tomography (CT) based treatmet planning for intracavitary brachytherapy in cancer of the cervix: Analysis of dose volume histograms. Brachytherapy. 2003; 2: 200–6.
53. Fellner C, Potter R, Knocke TH, Wambersie A. Comparison of radiography and computed tomography based treatment planning in cervix cancer in brachytherapy with specific attention to some quality assurance aspects. Radiother Oncol. 2001; 58:53–62.
54. Viswanathan CE, Palmer M, Chronowski GM, et al. Comparison between CT-Based volumetric calculations and ICRU reference point estimates of radiation doses delivered to bladder and rectum during intracavitary radiotherapy for cervical cancer. Int J Radiat Oncol Biol Phys. 2005; 62:131–7.
55. Shin KH, Kim TH, Cho JK, et al. CT guided intracavitary radiotherapy for cervical cancer: Comparison of conventional point A plan with clinical target volume based three dimensional plan using dose volume parameters. Int J Radiat Oncol Biol Phys. 2006; 64:197–204.
56. Datta NR, Srivastava A, Maria Das KJ, et al. Comparative assessment of doses to tumour, rectum, and bladder as evaluated by orthogonal radiographs vs. computer enhanced computed tomography-based intracavitary brachytherapy in cervical cancer. Brachytherapy. 2006; 5:223–9.
57. Jamema SV, Saju S, Mahantshetty U et al. Dosimetric evaluation of rectum and bladder using image based CT planning and orthogonal radiographs with ICRU 38 recommendations in intracavitary brachytherapy. Journal of Medical Physics 2008; 33:1-7.

58. Mahantshetty U, Tiwana MS, Jamema S Additional rectal and sigmoid mucosal points and doses in high dose rate intracavitary brachytherapy for carcinoma cervix: a dosimetric study. J Cancer Res Ther. 2011; 7:298-303.
59. Katz A, Eifel PJ. Quantification of Intracavitary Brachytherapy parameters and correlation with outcome in patients with carcinoma of the cervix. Int J Radiat Oncol Biol Phys 2000; 48:1417-1425.
60. Shrivastava SK, Mahantshetty U, Narayan K, Principles of radiation therapy in low-resource and well-developed settings, with particular reference to cervical cancer. International Journal of Gynecology & Obstetrics 2012; 119; S155–S159.
61. Tanderup K, Nielsen SK, Nyvang GB et al. From point A to the sculpted pear: MR image guidance significantly improves tumour dose and sparing of organs at risk in brachytherapy of cervical cancer. Radiother Oncol. 2010; 94:173-80.
62. De Brabandere M, Mousa AG, Nulens A, et al. Potential of dose optimisation in MRI-based PDR brachytherapy of cervix carcinoma. Radiother Oncol. 2008; 88:217–26.
63. Lindegaard JC, Tanderup K, Nielsen SK, et al. MRI-guided 3D optimization significantly improves DVH parameters of pulsed-dose-rate brachytherapy in locally advanced cervical cancer. Int J Radiat Oncol Biol Phys. 2008; 71:756–64.
64. Haie-Meder C et al. MRI-based brachytherapy (BT) in the treatment of cervical cancer: experience of the Institut Gustave-Roussy. Radiother Oncol. 2007; 83 Suppl 1:S11–2.
65. Lee LJ, Sadow CA, Russell A, Viswanathan AN. Correlation of point B and lymph node dose in 3D-planned high-dose-rate cervical cancer brachytherapy. Int J Radiat Oncol Biol Phys. 2009; 75:803-809.
66. Au SP, Grigsby PW (2003). The irradiation tolerance dose of the proximal vagina. Radiother Oncol ;67: 77-85.
67. Bahng AY, Dagan A, Bruner DW, et al (2012). Determination of prognostic factors for vaginal mucosal toxicity associated with intravaginal high-dose rate brachytherapy in patients with endometrial cancer. Int J Radiat Oncol Biol Phys; 8: 667-73.
68. Berger D, Dimopoulos J, Georg P, et al (2007). Uncertainties in assessment of the vaginal dose for intracavitary brachytherapy of cervical cancer using a tandem-ring applicator. Int J Radiat Oncol Biol Phys; 67: 1451-9
69. Fidarova EF, Berger D, Schussler S, et al (2010). Dose volume parameter D2cc does not correlate with vaginal side effects in individual patients with cervical cancer treated within a defined treatment protocol with very high brachytherapy doses. Radiother Oncol; 97: 76-9.
70. Frumovitz M, Sun CC, Schover LR, et al (2005). Quality of life and sexual functioning in cervical cancer survivors. J Clin Oncol; 23: 7428-36.
71. Greimel ER, Kuljanic Vlasic K, Waldenstrom AC, et al. The European Organization for Research and Treatment of Cancer (EORTC) Quality-of-Life Questionnaire Cervical Cancer Module: EORTC QLQ-CX24. Cancer2006; 14, 1812-22.
72. Grover S, Hill-Kayser CE, Vachani C, et al. Patient reported late effects of gynecological cancer treatment. Gynecol Oncol 2012; 124, 399-403.
73. Haie-Meder C, Kramar A, Lambin P, et al. Analysis of complications in a prospective randomized trial comparing two brachytherapy low dose rates in cervical carcinoma. Int J Radiat Oncol Biol Phys 1994; 29: 953-60.
74. Jensen PT, Groenvold M, Klee MC, et al. Early-stage cervical carcinoma, radical hysterectomy, and sexual function. A longitudinal study. Cancer 2004;100: 97-106.

75. Nout RA, Putter H, Jürgenliemk-Schulz IM, et al. Quality of life after pelvic radiotherapy or vaginal brachytherapy for endometrial cancer: first results of the randomized PORTEC-2 trial. J Clin Oncol2009; 27: 3547-56.
76. Nout RA, Putter H, Jürgenliemk-Schulz IM, et al. Five-year quality of life of endometrial cancer patients treated in the randomized post operative radiation therapy in endometrial cancer (PORTEC-2) trial and comparison with norm data. Eur J Cancer 2012; 48:1638-48.
77. Westerveld H , Potter R, Berger D, et al. Vaginal dose point reporting in cervical cancer patients treated with combined 2D/3D external beam radiotherapy and 2D/3D brachytherapy. Radiother Oncol 2013; 107:99-105.
78. Tanderup K, Christensen JJ, Granfeldt J, et al. Geometric stability of intracavitary pulsed dose rate brachytherapy monitored by in vivo rectal dosimetry. Radiother Oncol. 2006; 79:87-93.
79. Deshpande DD, Shrivastava SK, Pradhan AS, et al. Dosimetry of Intracavitary applications in carcinoma of the cervix: Rectal dose analysis. Radiother Oncol. 1997; 42:163–6.
80. Van den Bergh F, Meerteens H, Moonen L, et al. The use of a transverse CT image for the estimation of the dose given to the rectum in intracavitary brachytherapy for carcinoma of the cervix. Radiother Oncol. 1998; 47:85–90.
81. Barillot I, Horiot JC, Maingon P, et al. Maximum and mean bladder dose defined from ultrasonography: Compariosn with the ICRU reference in gynaecological brachytherapy. Radiother Oncol. 1994; 30:231–8
82. Ling CC, Schell MC, Working KR, et al. CT assisted assessment of bladder and rectum dose in gynecological implants. Int J Radiat Oncol Biol Phys.1987; 13:1577–82.
83. Pötter R, Haie-Meder C, Limbergen EV, et al. Recommendations from Gynaecological (GYN) GEC ESTRO working group (II): Concepts and terms in 3D image-based treatment planning in cervix cancers brachytherapy-3D Dose volume parameters and aspects of 3D image-based anatomy, radiation physics, radiobiology. Radiother Oncol 2006; 78:67-77.
84. Uno T, Itami J, Aruga M, Otaka KK. High dose rate brachytherapy for carcinoma of the cervix: Risk factors for late rectal complications. Int J Radiat Oncol Biol Phys 1998; 40:615-21.
85. Den Hartog Jager FC, Van Haastert M, Batterman JJ, et al. The endoscopic spectrum of late radiation damage of the rectosigmoid colon. Endoscopy 1985; 17:214-6.
86. Chun M, Kang S, Kil H, Oh Y, et al. Rectal bleeding and its management after irradiation for uterine cervical cancer. Int J Radiat Oncol Biol Phys 2004; 58:98-105.
87. Potter R, Dimopoulos J, George P, et al. Clinical impact of MRI assisted dose volume adaptation and dose escalation in brachytherapy of locally advanced cervix cancer. Radiother Oncol 2007; 83:148-55.
88. Van Dyk S, Narayan K, Fisher R, et al. Conformal brachytherapy planning for cervical cancer using transabdominal ultrasound. Int J Radiat Oncol Biol Phys. 2009; 75:64–70.
89. Van Dyk S, Kondalsamy-Chennakesavan S, Schneider M, et al. Comparison of measurements of the uterus and cervix obtained by magnetic resonance and transabdominal ultrasound imaging to identify the brachytherapy target in patients with cervix cancer. Int J Radiat Oncol Biol Phys. 2014; 88:860–865
90. Schmid MP, Pötter R, Brader P, et al. Feasibility of transrectal ultrasonography for assessment of cervical cancer. Strahlenther Onkol. 2013 ; 189:123-8.
91. Mahantshetty U, Khanna N, Swamidas J, et al. Trans-abdominal ultrasound (US) and magnetic resonance imaging (MRI) correlation for conformal intracavitary brachytherapy in carcinoma of the uterine cervix. Radiother Oncol. 2012; 102 :130-4.

92. Davidson MTM, Yuen J, D'Souza PD, et al. Optimization of high-dose-rate cervix brachytherapy applicator placement: the benefits of intraoperative ultrasound guidance. Brachytherapy 2008; 7:248–53.
93. Erickson B. MRI and ultrasound guide gynecologic brachytherapy. Diagn Imaging 2000; 192:78–83.
94. Van Dyk S, Narayan K, Fischer R, Bernshaw D. Conformal brachytherapy planning for cervical cancer using trans-abdominal ultrasound. Int J Radiat Oncol Biol Phys 2009; 75:64–70.
95. Wachter-Gerstner N, Wachter S, Reinstadler E, Fellner C, Knocke TH, Potter R. The impact of sectional imaging on dose escalation in endocavitary HDR-brachytherapy of cervical cancer: results of a prospective comparative trial. Radiother Oncol 2003; 68:51– 9.
96. Dimopoulos JC, Schard G, Berger D, Lang S, Goldner G, Helbich T, et al. Systematic evaluation of MRI findings in different stages of treatment of cervical cancer: potential of MRI on delineation of target, pathoanatomic structures, and organs at risk. Int J Radiat Oncol Biol Phys 2006; 64:1380– 8.
97. Kim SH, Choi BI, Lee HP, Kang SB, Choi YM, Han MC, et al. Uterine cervical carcinoma: comparison of CT and MR findings. Radiology 1990; 175:45– 51.
98. Yu WS, Sagerman RH, Chung CT, King GA, Dalal PS, Bassano DA, et al. Anatomical relationships in intracavitary irradiation demonstrated by computed tomography. Radiology 1982; 143:537 –41.
99. Schoeppel SL, Fraass BA, Hopkins MP, La Vigne ML, Lichter AS, McShan DL, et al. A CT-compatible version of the Fletcher system intracavitary applicator: clinical application and 3-dimensional treatment planning. Int J Radiat Oncol Biol Phys 1989; 17:1103– 9.
100. Viswanathan AN, Dimopoulos J, Kirists C, et al. Computed tomography versus magnetic resonance imaging based contouring in cervical cancer brachytherapy: result of a prospective trial and preliminary guidelines for standardised contours. Int J Radiat Oncol Biol Phys 2007; 68:491–8.
101. Eskander RN, Scanderbeg D, Saenz CC, et al. Comparison of computed tomography and magnetic resonance imaging in cervical cancer brachytherapy target and normal tissue contouring. Int J Gynecol Cancer 2010; 20:47– 53.
102. Krishnatry R, Patel FD, Singh P, et al. CT or MRI for image-based brachytherapy in cervical cancer. Jpn J Clin Oncol. 2012; 42:309-13.
103. Hobbs RF, Le Y, Armour E, et al. Voxelized Dose--FDG-PET Response in HDR Brachytherapy of Rectal Cancer. Pract Radiat Oncol. 2013 ;3(2 Suppl 1):S28-9
104. Miller TR, Grigsby PW. Measurement of tumour volume by PET to evaluate prognosis in patients with advanced cervical cancer treated by radiation therapy. Int J Radiat Oncol Biol Phys. 2002; 53:353–9.
105. Grigsby PW. PET and PET/CT in Cervical and Uterine Cancer. In: Wahl RL, Beanlands RSB, editors. Principles and Practices of PET and PET/CT. 2nd ed. Philadelphia: Lippincott; 2008. 348–54.
106. Showalter TN, Miller TR, Huettner P et al. 18F-fluorodeoxyglucose-positron emission tomography and pathologic tumour size in early-stage invasive cervical cancer. Int J Gynecol Cancer. 2009 ; 19:1412-4.
107. Grigsby PW, Dehdashti F, Siegel BA. FDG-PET evaluation of carcinoma of the cervix. Clinical Positron Imaging. 1999; 2:105–9.
108. Lin LL, Mutic S, Malyapa RS, et al. Sequential FDG-PET brachytherapy treatment planning in carcinoma of the cervix. Int J Radiat Oncol Biol Phys. 2005; 63:1494–501.

109. Lin LL, Mutic S, Low DA, et al. Adaptive brachytherapy treatment planning for cervical cancer using FDG-PET. Int J Radiat Oncol Biol Phys. 2007;67:91–6.
110. Malyapa RS, Mutic S, Low DA, et al. Physiologic FDG-PET three-dimensional brachytherapy treatment planning for cervical cancer. Int J Radiat Oncol Biol Phys. 2002;54:1140–6.
111. Mutic S, Malyapa RS, Grigsby PW, et al. PET-guided IMRT for cervical carcinoma with positive para-aortic lymph nodes-a dose-escalation treatment planning study. Int J Radiat Oncol Biol Phys. 2003;55:28–35.
112. Esthappan J, Chaudhari S, Santanam L, et al. Prospective clinical trial of positron emission tomography/computed tomography image-guided intensity-modulated radiation therapy for cervical carcinoma with positive para-aortic lymph nodes. Int J Radiat Oncol Biol Phys. 2008;72:1134–9.
113. Esthappan J, Mutic S, Malyapa RS, et al. Treatment planning guidelines regarding the use of CT/PET-guided IMRT for cervical carcinoma with positive paraaortic lymph nodes. Int J Radiat Oncol Biol Phys. 2004;58:1289–97.
114. Grigsby PW, Dehdashti F, Siegel BA. FDG-PET evaluation of carcinoma of the cervix. Clinical Positron Imaging. 1999;2:105–9.
115. Petrič P, Hudej R, Rogelj P et al. Uncertainties of target volume delineation in MRI guided adaptive brachytherapy of cervix cancer: a multi-institutional study. Radiother Oncol. 2013; 107:6-12.
116. Fokdal L, Tanderup K, Hokland SB et al. Clinical feasibility of combined intracavitary/interstitial brachytherapy in locally advanced cervical cancer employing MRI with a tandem/ring applicator in situ and virtual pre-planning of the interstitial component. Radiother Oncol. 2013 ;107:63-8.
117. Potter R, Dimopoulos J, George P, et al. Clinical impact of MRI assisted dose volume adaptation and dose escalation in Brachytherapy of locally advanced cervix cancer. Radiother Oncol 2007;83:148-55.
118. Nomden CN, De Leeuwa AA, Roesinka JM et al. Clinical outcome and dosimetric parameters of chemo-radiation including MRI guided adaptive brachytherapy with tandem-ovoid applicators for cervical cancer patients: A single institution experience. Radiother and Oncol 2013;107: 69–74.
119. Haie-Meder C, Chargari C, Rey A, Dumas I, Morice P, Magne N. MRI-based low dose-rate brachytherapy experience in locally advanced cervical cancer patients initially treated by concomitant chemoradiotherapy. Radiother Oncol 2010;96:161–5.
120. Beriwal S, Kannan N, Kim H, et al. Three-dimensional high dose rate intracavitary image-guided brachytherapy for the treatment of cervical cancer using a hybrid magnetic resonance imaging/computed tomography. approach: feasibility and early results. Clin Oncol (R Coll Radiol) 2011;23:685–90.
121. Mahantshetty U, Swamidas J, Khanna N, et al. Reporting and validation of gynaecological Groupe Euopeen de Curietherapie european society for therapeutic radiology and oncology (ESTRO) Brachytherapy recommendations for MR image-based dose volume parameters and clinical outcome with high dose-rate brachytherapy in cervical cancers: a single institution initial experience. Int J Gynecol Cancer 2011;21:1110–6
122. Tan LT, Coles CE, Hart C, Tait E. Clinical impact of computed tomography-based image-guided brachytherapy for cervix cancer using the tandem-ring applicator – the Addenbrooke's experience. Clin Oncol (R Coll Radiol) 2009;21:175–82.
123. MRI-guided adaptive radiotherapy in locally advanced cervical cancer from a Nordic perspective. Lindegaard JC, Fokdal LU, Nielsen SK, Juul-Christensen J, Tanderup K. Acta Oncol. 2013;52:1510-9.

124. Haie-Meder C, Pötter R, van Limbergen E, et al. Recommendations from the Gynaecological (GYN) GEC ESTRO Working Group. Concepts and terms in 3D image based 3D treatment planning in cervix cancer brachytherapy with emphasis on MRI assessment of GTV and CTV. Radiother Oncol 2004; 74: 235–45.
125. Petrič P, Hudej R, Rogelj P et al. Uncertainties of target volume delineation in MRI guided adaptive brachytherapy of cervix cancer: a multi-institutional study. Radiother Oncol. 2013; 107:6-12.
126. Hellebust TP, Tanderup K, Lervåg C et al. Dosimetric impact of interobserver variability in MRI-based delineation for cervical cancer brachytherapy. Radiother Oncol. 2013 ;107:13-9.
127. International Commission on Radiological Protection, Prevention of Accidental Exposures to Patients Undergoing Radiation Therapy, Publication 86, Pergamon Press, Oxford and New York (2000).
128. Pötter R, Petra G, Johannes CAD, et al. Clinical outcome of protocol based image (MRI) guided adaptive brachytherapy combined with 3D conformal radiotherapy with or without chemotherapy in patients with locally advanced cervical cancer. Radiother Oncol 2011;100:116–23.
129. Charra-Brunaud C, Harter V, Delannes M, et al. Impact of 3D image-based PDR brachytherapy on outcome of patients treated for cervix carcinoma in France: results of the French STIC prospective study. RadiotherOncol2012;103:305–13.
130. Mai J, Erickson B, Rownd J, et al. Comparison of four different dose specification methods for high dose rate intracavitary radiation for treatment of cervical cancer. Int J RadiatOncolBiol Phys. 2001;51:1131–41.
131. Au SP, Grigsby PW. The irradiation tolerance dose of the proximal vagina.RadiotherOncol. 2003;67:77–85.
132. Levin D, Menhel J, Rabin T et al. Dosimetric comparison of tandem andOvoids Vs. tandem and ring for intracavitary gynecologic applications. Med Dosim. 2008;33:315-20.
133. Tuncell N, Toy A, Demiral AN, et al. Dosimetric comparison of ring and ovoid applicators. J BUON. 2009 ;14:451-5.
134. Erickson B, Albano K, Gillin M, et al. CT guided interstitial implantation of gynaecologic malignancies. Int J Radiat Oncol Biol Phys 1996;36:699-709.
135. Dimopoulos J, Petrow P, Tanderup K, et al. Recommendatiosn from Gynaecological (GYN) GEC ESTRO working group (IV): Basic principles and parameters for MR imaging within the frame of image based adaptive cervix cancer brachytherapy. Radiother Oncol 2012;103:113–22.
136. Kim Y, Muruganandham M, Modrick JM, Bayouth JE. Evaluation of artifact and distortions of titanium applicators on 3.0-Tesla MRI: feasibility of titanium applicators in MRI-guided brachytherapy for gynecological cancer. Int J Radiat Oncol Biol Phys 2011;80:947–55.
137. Fransson A, Andreo P, Potter R. Aspects of MR image distortions in radiotherapy treatment planning. Strahlenther Onkol 2001;177:59-73.
138. Moerland MA, Beersma R, Bhagwandien R et al. Analysis and correction of geometric distortions in 1.5 T magnetic resonance images for use in radiotherapy treatment planning. Phys Med Biol. 1995;40:1651–4.
139. Tanderup K, Hellebust TP, Lang S, et al. Consequences of random and systematic reconstruction uncertainties in 3D image based brachytherapy in cervical cancer. Radiother Oncol 2008;89:156–63.
140. Haack S, Nielsen SK, Lindegaard JC et al. Applicator reconstruction in MRI 3D image based dose planning of brachytherapy for cervical cancer. Radiother Oncol. 2009;91:187-93.

141. Perez Calatayud J, Kuipers J, Ballester F, et al. Exclusive MRI based tandem and colpostats reconstruction in gynaecological brachytherapy treatment planning. RadiotherOncol. 2009;91:181-6.
142. Berger D, Dimopoulos J, Potter R, Kirisits C et al. Direct reconstruction of the Vienna applicator on MR images. Radiother Oncol. 2009;93:347-51.
143. Wills R, Lowe G, Inchley D, et al. Applicator reconstruction for HDR cervix treatment planning using images from 0.35 T open MR scanner. Radiother Oncol. 2010;94:346-52.
144. Hellebust TP, Tanderup K, Bergstrand ES, Knutsen BH, Røislien J, Olsen DR. Reconstruction of the ring applicator set using CT imaging; impact of reconstruction method and applicator orientation. Phys Med Biol 2007;52:4893–904.
145. Hellebust T P, Kirisits C, Berger D et al. Recommendations from Gynaecological (GYN) GEC-ESTRO Working Group: Considerations and pitfalls in commissioning and applicator reconstruction in 3D image-based treatment planning of cervix cancer Brachytherapy. Radiother and Oncol. 2010; 96: 153–160.
146. Kirisits C, Potter R, Lang S et al. Dose and volume parameters for MRI based treatment planning in intracavitary brachytherapy for cervix cancer. Int J Radiat Oncol Biol Phys 2005;62:901-11.
147. Chajon E, Dumas I, Touleimat M et al.Inverse planning approach for 3-D MRI-based pulse-dose rate intracavitary brachytherapy in cervix cancer. Int J Radiat Oncol Biol Phys. 2007;69:955-61.
148. Jamema SV, Kirisits C, Mahantshetty U et al. Comparison of DVH parameters and loading patterns of standard loading, manual and inverse optimization for intracavitary brachytherapy on a subset of tandem/ovoid cases. Radiother Oncol. 2010;97:501-6.
149. Lindegaard JC, Potter R, Limbergan EV et al. Clinical aspects of treatment planning. Chapter 10. Gynaecologic Brachytherapy. Publisher: Springer.
150. Dimopoulos JC, Lang S, Kirisits C, Fidarova EF, Berger D, Georg P, et al. Dose-volume histogram parameters and local tumour control in magnetic resonance image-guided cervical cancer brachytherapy. Int J Radiat Oncol Biol Phys. 2009;75:56–63.
151. Dimopoulos JC, Potter R, Lang S, Fidarova E,Georg P, Dorr W, et al. Dose-effect relationship for local control of cervical cancer by magnetic resonance image-guided brachytherapy. Radiother Oncol. 2009;93:311–5.
152. Georg P, Kirisits C, Goldner G, Dorr W, Hammer J, PotziR,et al. Correlation of dose-volume parameters, endoscopic and clinical rectal side effects in cervix cancer patients treated with definitive radiotherapy including MRI-based brachytherapy. RadiotherOncol. 2009;91: 173–80.
153. Pötter R, Dimopoulos J, Kirisits C, Lang S, Haie-Meder C, Briot E, et al. Recommendations for image-based intracavitary brachytherapy of cervix cancer: the GYN GEC ESTRO Working Group point of view: in regard to Nag et al. Int J Radiat Oncol Biol Phys. 2004;60:1160–72. Int J Radiat Oncol Biol Phys. 2005 ;62 :293–5.
154. Tanderup K, Georg D, Pötter R. Adaptive management of cervical cancer radiotherapy. Semin Radiat Oncol 2010:121–9.
155. Potter R, Kirisits C, Fidarova EF et al. Present status and future of high precision image guided adaptive brachytherapy for cervix carcinoma. Acta Oncol 2008;47:1325-36.
156. Eifel, P. J., Thoms, W. W., Jr., Smith, T. L., Morris, M., and Oswald, M. J. The relationship between brachytherapy dose and outcome in patients with bulky endocervical tumours treated with radiation alone, Int J Radiat Oncol Biol Phys. 1994; 28: 113-118.
157. Gerbaulet, A., Pötter, R., Mazeron, J. J., Meertens, H., and Van Limbergen, E. The GEC ESTRO Handbook of Brachytherapy, 2002, ESTRO, Brussels.

158. Horiot, J. C., Pigneux, J., Pourquier, H., Schraub, S., Achille, E., Keiling, R., Combes, P., Rozan, R., Vrousos, C., and Daly, N. Radiotherapy alone in carcinoma of the intact uterine cervix according to G. H. Fletcher guidelines: a French cooperative study of 1383 cases, Int J Radiat Oncol Biol Phys.1988; 14: 605-611.
159. Perez, C. A., Grigsby, P. W., Chao, K. S., Mutch, D. G., and Lockett, M. A. Tumour size, irradiation dose, and long-term outcome of carcinoma of uterine cervix," Int J Radiat Oncol Biol Phys. 1998; 41: 307-317.
160. Pernot M., Hoffstetter, S., Peiffert, D., Carolus, J. M., Guillemin, F., Verhaeghe, J. L., Marchal, C., Luporsi, E., Beckendorf, V., Stines, J., and et al. Statistical study of a series of 672 cases of carcinoma of the uterine cervix. Results and complications according to age and modalities of treatment. Bull Cancer. 1995; 82: 568-581.
161. Kirisits, C., Lang, S., Dimopoulos, J., Berger, D., Georg, D., and Potter, R. The Vienna applicator for combined intracavitary and interstitial brachytherapy of cervical cancer: design, application, treatment planning, and dosimetric results. Int J Radiat Oncol Biol Phys.2006; 65: 624-630.
162. Viswanathan, A. N., Cormack, R., Holloway, C. L., Tanaka, C., O'Farrell, D., Devlin, P. M., and Tempany, C. "Magnetic resonance-guided interstitial therapy for vaginal recurrence of endometrial cancer," Int J Radiat Oncol Biol Phys. 2006; 66: 91-99.
163. Pelloski, C. E., Palmer, M., Chronowski, G. M., Jhingran, A., Horton, J., and Eifel, P. J. Comparison between CT-based volumetric calculations and ICRU reference-point estimates of radiation doses delivered to bladder and rectum during intracavitary radiotherapy for cervical cancer. Int J Radiat Oncol Biol Phys. 2005; 62: 131-137.
164. Pötter, R., Dimopoulos, J., Georg, P., Lang, S., Waldhausl, C., Wachter-Gerstner, N., Weitmann, H., Reinthaller, A., Knocke, T. H., Wachter, S., and Kirisits, C. Clinical impact of MRI assisted dose volume adaptation and dose escalation in brachytherapy of locally advanced cervix cancer," Radiother Oncol. 2007; 83: 148-155.
165. Pötter, R., Georg, P., Dimopoulos, J. C., Grimm, M., Berger, D., Nesvacil, N., Georg, D., Schmid, M. P., Reinthaller, A., Sturdza, A., and Kirisits, C. Clinical outcome of protocol based image (MRI) guided adaptive brachytherapy combined with 3D conformal radiotherapy with or without chemotherapy in patients with locally advanced cervical cancer. Radiother Oncol. 2011; 100: 116-123.
166. Georg, P., Kirisits, C., Goldner, G., Dorr, W., Hammer, J., Potzi, R., Berger, D., Dimopoulos, J., Georg, D., and Pötter, R. Correlation of dose-volume parameters, endoscopic and clinical rectal side effects in cervix cancer patients treated with definitive radiotherapy including MRI-based brachytherapy. Radiother Oncol 2009; 91: 173-180.
167. Georg, P., Potter, R., Georg, D., Lang, S., Dimopoulos, J. C., Sturdza, A. E., Berger, D., Kirisits, C., and Dorr, W. Dose Effect Relationship for Late Side Effects of the Rectum and Urinary Bladder in Magnetic Resonance Image-Guided Adaptive Cervix Cancer Brachytherapy. Int J Radiat Oncol Biol Phys 2012; 82;653-7.
168. Bentzen, S. M. (1993). "Quantitative clinical radiobiology," Acta Oncol 32: 259-275.
169. Perez, C. A., Grigsby, P. W., Chao, K. S., Mutch, D. G., and Lockett, M. A. Tumour size, irradiation dose, and long-term outcome of carcinoma of uterine cervix," Int J Radiat Oncol Biol Phys. 1998; 41: 307-317.
170. Petereit, D. G., Sarkaria, J. N., Chappell, R., Fowler, J. F., Hartmann, T. J., Kinsella, T. J., Stitt, J. A., Thomadsen, B. R., and Buchler, D. A. The adverse effect of treatment prolongation in cervical carcinoma. Int J Radiat Oncol Biol Phys. 1995; 32: 1301-1307.

171. Pourquier, H., Dubois, J. B., and Delard, R. Cancer of the uterine cervix: dosimetric guidelines for prevention of late rectal and rectosigmoid complications as a result of radiotherapeutic treatment. Int J Radiat Oncol Biol Phys. 1982; 8: 1887-1895.
172. Pourquier, H., Delard, R., Achille, E., Daly, N. J., Horiot, J. C., Keiling, R., Pigneux, J., Rozan, R., Schraub, S., and Vrousos, C. A quantified approach to the analysis and prevention of urinary complications in radiotherapeutic treatment of cancer of the cervix. Int J Radiat Oncol Biol Phys. 1987; 13: 1025-1033.
173. Giannouli, S., Milickovic, N., Baltas, D., Lahanas, M., Uzunoglu, N., Kolotas, C., & Zamboglou, N. Autoactivation of source dwell positions for HDR brachytherapy treatment planning. Medical Physics. 2000; 27: 2517-2520.
174. Akimoto, T., Katoh, H., Kitamoto, Y., Shirai, K., Shioya, M., & Nakano, T. Anatomy- based inverse optimization in high-dose-rate brachytherapy combined with hypofractionated external beam radiotherapy for localized prostate cancer: Comparison of incidence of acute genitourinary toxicity between anatomy-based inverse optimization. Int J Radiat Oncol Biol Phys. 2006; 64: 1360-1366.
175. Yoshioka, Y., Nishimura, T., Kamata, M., Harada, H., Kanazawa, K., Fuji, H., & Murayama Shigeyuki. Evaluation of anatomy-based dwell position and inverse optimization in high- dose-rate brachytherapy of prostate cancer: A dosimetric comparison to a conventional cylindrical dwell position, geometric optimization, and dose-point optimization. Radiother and Oncol. 2005; 75: 311-317.
176. Charra-Brunaud, C., Hsu, I.-C. J., Weinberg, V., & Pouliot, J. Analysis of interaction between number of implant catheters and dose-volume histograms in prostate high-dose-rate brachytherapy using a computer model. Int J Radiat Oncol Biol Phys. 2003; 56: 586-591.
177. Citrin, D., Ning, H., Guion, P., Li, G., Susil, R. C., Miller, R. W., Lessard, E., & Pouliot J. Inverse treatment planning based on MRI for HDR prostate brachytherapy. Int J Radiat Oncol Biol Phys. 2005 ; 61: 1267-1275.
178. Hsu, I.-C. J., Lessard, E., Weinberg, V., & Pouliot, J. Comparison of inverse planning simulated annealing and geometrical optimization for prostate high-doserate brachytherapy. Brachytherapy.2004; 3:147-152.
179. Pouliot, J., Lessard, E., & Hsu, I.-C. Advanced 3D planning. In B. Thomadson, M. Rivard, & W. Butler (Eds.), Brachytherapy physics (2nd. ed., pp. 393-414). 2005; Seattle, WA: AAPM.
180. Lahanas, M., Baltas, D., & Giannouli, S. Global convergence analysis of fast multiobjective gradient based dose optimization algorithms for high dose rate brachytherapy. Physics in Medicine and Biology. 2003; 48: 599-617.
181. Van der Laarse, R., & De Boer, R. W. Computerized high dose rate brachytherapy treatment planning. In A. A. Martinez, C. G. Orton, & R. F. Mould (Eds.), Brachytherapy HDR and LDR (pp. 169-183). Columbia: Nucletron.
182. Van der Laarse, R., & Prins, T. P. Introduction to brachytherapy optimization. In R. F. Mould (Ed.), Brachytherapy from radium to optimization (pp. 331-351). Veenendaal: Nucletron. 1994.
183. Kolkman-Deurloo, I.-K. K., Visser, A. G., Niël, C. G., Driver, N., & Levendag, P. C. Optimization of interstitial volume implants. Radiother and Oncol. 1994; 31: 229-239.
184. Kestin, L. L., Jaffray, D. A., Edmundson, G. K., Martinez, A. A., Wong, J. W., Kini, V. R., Chen, P. Y., & Vicini F. A. Improving the dosimetric coverage of interstitial high-dose- rate breast implants. Int J Radiat Oncol Biol Phys.2000; 46:35-43.
185. Van der Laarse, R., & Prins, T. P. Introduction to brachytherapy optimization. In R. F. Mould (Ed.), Brachytherapy from radium to optimization (pp. 331-351). Veenendaal: Nucletron. 1994.

186. Jamema, S. V., Saju, S., Shetty, U. M., Pallad, S., Deshpande, D. D., & Shrivastava, S. K. Dosimetric comparison of inverse optimization with geometric optimization in combination with graphical optimization for HDR prostate implants. Journal of Medical Physics. 2006; 31: 89-94.
187. Tanderup, K., Hellebust, T. P., Honor e, H. B., Nielsen, S. K., Olsen, D. R., Grau, C., & Lindegaard J. C. Dose optimization in single plane interstitial brachytherapy. Radiother and Oncol. 2006; 81: 105-111.
188. Colaço, M. J., & Dulikravich, G. S. A survey of basic deterministic, heuristic and hybrid methods for single objective optimization and response surface generation. Proceedings of Thermal Measurement and Inverse Techniques 4 (METTI 4). 2009.
189. Kirkpatrick, S., Gelatt, C. D., & Vecchi, M. P. Optimization by simulated. Science. 1983; 220: 671-680.
190. Lessard, E., & Pouliot, J. Inverse planning anatomy-based dose optimization for HDR-brachytherapy of the prostate using fast simulated annealing algorithm and dedicated objective function. Medical Physics. 2001; 25: 773-779.
191. Milickovic, N., Lahanas, M., Papagiannopoulou, M., Karouzakis, K., Baltas, D., & Zamboglou, N. Application of multiobjective genetic algorithms in anatomy based dose optimization in brachytherapy and its comparison with deterministic algorithms. Conference Proceedings of the 23rd Annual International Conference of the IEEE Engineering in Medicine and Biology Society. 2001; 4, 3919-3922.
192. Milickovic, N., Lahanas, M., Baltas, D., & Zamboglou, N. Comparison of evolutionary and deterministic multiobjective algorithms for dose optimization in brachytherapy. Proceedings of the First International Conference on Evolutionary Multi-Criterion Optimization, 2001; 1993: 167-180.
193. Shwetha, B., Ravikumar, M., Katke, A., Supe, S. S., Giri, G. V., Ramanand, N., & Pasha T. Dosimetric comparison of various optimization techniques for high dose rate brachytherapy of interstitial cervix implants. Journal of Applied Clinical Medical Physics. 2010; 11: 225-230.
194. Baltas, D., Katsilieri, Z., Kefala, V., Papaioannou, S., Karabis, A., Mavroidis, P., & Zamboglou, N. Influence of modulation restriction in inverse optimization with HIPO of prostate implants on plan quality: Analysis using dosimetric and radiobiological indices. Proceedings of the 11th International Congress of the IUPESM (World Congress on Medical Physics and Biomedical Engineering). 2009; 25 : 283-286.
195. Karabis, A., Belotti, P., & Baltas, D. Optimization of catheter position and dwell time in prostate HDR brachytherapy using HIPO and linear programming. Proceedings of the 11th International Congress of the IUPESM (World Congress on Medical Physics and Biomedical Engineering). 2009; 25 : 612-615.
196. Karabis, A., Giannouli, S., & Baltas, D. HIPO: A hybrid inverse treatment planning optimization algorithm in HDR brachytherapy (Meeting Abstract). Radiother and Oncol. 2005; 76: S29.
197. Mavroidis, P., Katsilieri, Z., Kefala, V., Milickovic, N., Papanikolao, N., Karabis, A., Zamboglou N., & Baltas, D. Radiobiological evaluation of the influence of dwell time modulation restriction in HIPO optimized HDR prostate brachytherapy implants. Journal of Contemporary Brachytherapy, 2010; 2: 117-128.
198. Trnkov a, P., Baltas, D., Karabis, A., Stock, M., Dimopoulos, J., Georg, D., Pötter, R., & Kirisits C. A detailed dosimetric comparison between manual and inverse plans in HDR intracavitary/interstitial cervical cancer brachytherapy. Journal of Contemporary Brachytherapy. 2010; 2: 163-170.

199. Trnková, P., Pötter, R., Baltas, D., Karabis, A., Fidarova, E., Dimopoulos, J., Georg, D., & Kirisits C. New inverse planning technology for image-guided cervical cancer brachytherapy: Description and evaluation within a clinical frame. Radiother and Oncol. 2009; 93: 331-340.
200. Rivard MJ, Coursey BM, DeWerd LA, et al. Update of AAPM Taskgroup No. 43 report. A revised AAPM protocol for Brachytherapy dose calculations. Med Phys 2004;31:663–74.
201. Lang S, Kirisits C, Dimopoulos J, Georg D, Pötter R. Treatment planning for MRI assisted brachytherapy of gynaecologic malignancies based on total dose constraints. Int J Radiat Oncol Biol Phys 2007;69:619–27.
202. DeWitt K, Hsu IC, Speight J, et al. 3D inverse treatment planning for the tandem and ovoid applicator in cervical cancer. Int J Radiat Oncol Biol Phys 2005;63:1270–4.
203. Noyes WR, Peters NE, Thomadsen BR, et al. Impact of optimized treatment planning for tandem and ring and tandem and ovoids using high dose rate brachytherapy for cervical cancer. Int J Radiat Oncol Biol Phys 1995;31:79–86.
204. Shin KH, Kim TH, Cho JK, et al. CT-guided intracavitary radiotherapy for cervical cancer: comparison of conventional point a plan with clinical target volume-based three-dimensional plan using dose–volume parameters. Int J Radiat Oncol Biol Phys 2006;64:197–204.
205. Brooks S, Bownes P, Lowe J, et al. Cervical brachytherapy utilizing ring applicator: comparison of standard and conformal loading. Int J Radiat Oncol Biol Phys 2005;63:934–9.
206. Kuipers T, Koekstra CJM, van't Riet A, et al. HDR brachytherapy applied to cervical carcinoma with moderate lateral expansion: modified principles of treatment. Radiother Oncol 2001;58:25–30.
207. Cheng JC, Peng LC, Chen YH, et al. Unique role of proximal rectal dose in late rectal complications for patients with cervical cancer undergoing high-dose- rate intracavitary brachytherapy. Int J Radiat Oncol Biol Phys 2003;57:1010–8.
208. Al-Booz H, Boiangiu I, Appleby H, et al. Sigmoid colon an unexpected organ at risk in brachytherapy for cervix cancer. Egypt Natl Canc Inst 2006;18:156–60.
209. Lessard E, Hsu IC, Pouliot J. Inverse planning for interstitial gynecologic template brachytherapy: truly anatomy-based planning. Int J Radiat Oncol Biol Phys 2002; 54: 1243-1251.
210. Kubicky CD, Yeh BM, Lessard E et al. Inverse planning simu- lated annealing for magnetic resonance imaging-based intracavitary high-dose-rate brachytherapy for cervical cancer. Brachytherapy 2008; 7: 242-247.
211. Kim Y, Hsu IC, Lessard E et al. Class solution in inverse planned HDR prostate brachytherapy for dose escalation of DIL defined by combined MRI/MRSI. Radiother Oncol 2008; 88: 148-155.
212. Kim DH, Wang-Chesebro A, Weinberg V et al. High-dose rate brachytherapy using inverse planning simulated annealing for locoregionally advanced cervical cancer: a clinical report with 2-year follow-up. Int J Radiat Oncol Biol Phys 2009; 75: 1329-1334.
213. Vishwanathan AN, Cormack R, Holloway CL, et al. Magnetic reso- nance guided interstitial therapy for vaginal recurrence of endometrial cancer. Int J Radiat Oncol Biol Phys 2006;66:91-99.
214. Yoshida K, Yamazaki H, Takenaka T, et al. A dose volume analysis of magnetic resonance imaging-aided high-dose-rate image-based interstitial brachytherapy for uterine cervical cancer. Int J Radiat Oncol Biol Phys 2009; 77:765-772.
215. Susworo R, Supriana N, Ramli I. HDR interstitial perineal implant for locally advanced or recurrent uterine cervix cancer. Radiat Med 2004; 22:25.
216. Van't Riet A, Mak AC, Moerland MA, et al. A conformation number to quantify the degree of conformality in brachytherapy and external beam irradiation: Application to the prostate. Int J Radiat Oncol Biol Phys 1997; 37:731-736.

217. Jacob D, Raben A, Sarkar A, et al. Anatomy-based inverse planning simulated annealing optimization in high-dose-rate prostate brachy- therapy: Significant dosimetric advantage over other optimization techniques. Int J Radiat Oncol Biol Phys 2008; 72:820-827.
218. Morton GC, Sankreacha R, Halina P, et al. A comparison of anatomy- based inverse planning with simulated annealing and graphical opti- mization for high-dose-rate prostate brachytherapy. Brachytherapy 2008; 7:12-16.
219. Mahmoudieh A, Tremblay C, Beaulieu L, et al. Anatomy-based inverse planning dose optimization in HDR prostate implant: A toxicity study. Radiother Oncol 2005; 75:318-324.
220. Lachance B, Beliveau-Nadeau D, Lessard E, et al. Early clinical experience with anatomy based inverse planning dose optimization for high dose rate boost of the prostate. Int J Radiat Oncol Biol Phys 2002; 54:86-100.
221. Vikram B, Deore S, Beitler JJ, et al. The relationship between dose heterogeneity (hot spots) and complications following high dose rate brachytherapy. Int J Radiat Oncol Biol Phys 1999; 43:983-987.
222. Wazer DE, Lowther D, Boyle T, et al. Clinically evident fat necrosis in women treated with high-dose-rate brachytherapy alone for early-stage breast cancer. Int J Radiat Oncol Biol Phys 2001; 50: 107-111.
223. Thomadsen BR, Shahabi S, Buchler D, et al. Differential loadings of brachytherapy templates. Endocurietherapy/Hyperthermia Oncology 1990; 6:197-202.
224. Ahmad R, Hoogeman MS, Quint S, et al. Residual setup errors caused by rotation and non-rigid motion in prone-treated cervical cancer patients after online CBCT image-guidance. Radiother Oncol 2012; 103:322–6.
225. Laursen LV, Elstrom UV, Vestergaard A, et al. Residual rotational set-up errors after daily cone-beam CT image guided radiotherapy of locally advanced cervical cancer. Radiother Oncol 2012; 105:220–5.
226. Van Herk M, Remeijer P, Rasch C, et al. The probability of correct target dosage: dose-population histograms for deriving treatment margins in radiotherapy. Int J Radiat Oncol Biol Phys 2000; 47:1121–35.
227. Ahmad R, Hoogeman MS, Bondar M, et al. Increasing treatment accuracy for cervical cancer patients using correlations between bladder-filling change and cervix uterus displacements: proof of principle. Radiother Oncol 2011;98:340–6.
228. Beadle BM, Jhingran A, Salehpour M, et al. Cervix regression and motion during the course of external beam chemoradiation for cervical cancer. Int J Radiat Oncol Biol Phys 2009; 73:235–41.
229. Buchali A, Koswig S, Dinges S, et al. Impact of the filling status of the bladder and rectum on their integral dose distribution and the movement of the uterus n the treatment planning of gynaecological cancer. Radiother Oncol 1999;52:29–34.
230. Kerkhof EM, van der Put RW, Raaymakers BW, et al. Intrafraction motion in patients with cervical cancer: the benefit of soft tissue registration using MRI. Radiother Oncol 2009;93:115–21.
231. Lim K, Kelly V, Stewart J, et al. Pelvic radiotherapy for cancer of the cervix: is what you plan actually what you deliver? Int J Radiat Oncol Biol Phys 2009;74:304–12.
232. Tanderup K, Nesvacil N, Pötter R, Kirisits K, Uncertainties in image guided adaptive cervix cancer brachytherapy: Impact on planning and prescription. Radiother and Oncol 2013; 107: 1–5.
233. Kirisits C, Rivard MJ, Baltas D et al. Review of clinical brachytherapy uncertainties: analysis guidelines of GEC-ESTRO and the AAPM. Radiother Oncol. 2014; 110:199-212.

234. DeWerd L.A., Ibbott G.S., Meigooni A.S. A dosimetric uncertainty analysis for photon-emitting brachytherapy sources: report of AAPM Task Group No. 138 and GEC-ESTRO. Med Phys. 2011; 38:782–801.
235. Kirisits C., Siebert F.A., Baltas D. Accuracy of volume and DVH parameters determined with different brachytherapy treatment planning systems. Radiother Oncol. 2007; 84:290–297.
236. Aubry J.F., Cheung J., Morin O., Beaulieu L., Hsu I.C., Pouliot J. Investigation of geometric distortions on magnetic resonance and cone beam computed tomography images used for planning and verification of high-dose rate brachytherapy cervical cancer treatment. Brachytherapy. 2010;9:266–273.
237. Mizowaki T., Cohen G.N., Fung A.Y., Zaider M. Towards integrating functional imaging in the treatment of prostate cancer with radiation: the registration of the MR spectroscopy imaging to ultrasound/CT images and its implementation in treatment planning. Int J Radiat Oncol Biol Phys. 2002; 54:1558–1564.
238. Kolkman-Deurloo I.K., de Kruijf W.J., Levendag P.C. On-line implant reconstruction in HDR brachytherapy. Radiother Oncol. 2006;78: 53–59.
239. Petrič P, Hudej R, Rogelj P et al. Uncertainties of target volume delineation in MRI guided adaptive brachytherapy of cervix cancer: a multi-institutional study. Radiother Oncol. 2013;107:6-12.
240. Hellebust TP, Tanderup K, Lervåg C et al. Dosimetric impact of interobserver variability in MRI-based delineation for cervical cancer brachytherapy. Radiother Oncol. 2013; 107:13
241. De Leeuw AA, Moerland MA, Nomden C et al. Applicator reconstruction and applicator shifts in 3D MR-based PDR brachytherapy of cervical cancer. Radiother Oncol. 2009; 93:341-6.
242. Beaulieu L, Carlsson Tedgren A, Carrier JF et al. Report of the Task Group 186 on model-based dose calculation methods in brachytherapy beyond the TG-43 formalism: current status and recommendations for clinical implementation. Med Phys. 2012;39:6208-36.
243. Thomadsen B.R., Williamson J.F., Rivard M.J., Meigooni A.S. Anniversary paper: past and current issues, and trends in brachytherapy physics. Med Phys. 2008; 35:4708–4723.
244. Rivard M.J., Venselaar J.L., Beaulieu L. The evolution of brachytherapy treatment planning. Med Phys. 2009; 36:2136–2153.
245. G. Kertzscher, C.E. Andersen, F.A. Siebert, et al. Identifying afterloading PDR and HDR brachytherapy errors using real-time fiber-coupled Al(2)O(3):C dosimetry and a novel statistical error decision criterion Radiother Oncol.2011; 100 ; 456–462.
246. Jamema SV, Mahantshetty U, Tanderup K et al. Inter-application variation of dose and spatial location of D(2cm(3)) volumes of OARs during MR image based cervix brachytherapy. Radiother Oncol. 2013 ;107:58-62.
247. S. Lang, N. Nesvacil, C. Kirisits, et al. Uncertainty analysis for 3D image-based cervix cancer brachytherapy by repetitive MR imaging: assessment of DVH-variations between two HDR fractions within one applicator insertion and their clinical relevance Radiother Oncol, 2013 ;107: 26–31.
248. S. Mohamed, S.K. Nielsen, L.U. Fokdal, et al. Feasibility of applying a single treatment plan for both fractions in PDR image guided brachytherapy in cervix cancer. Radiother Oncol, 2013;107 :32–38
249. C. Anderson, G. Lowe, R. Wills, et al. Critical structure movement in cervix brachytherapy, Radiother Oncol, 2013; 107 : 39–45.

250. T.P. Hellebust, E. Dale, A. Skjonsberg, et al. Inter fraction variations in rectum and bladder volumes and dose distributions during high dose rate brachytherapy treatment of the uterine cervix investigated by repetitive CT-examinations. Radiother Oncol, 2001 ; 60 : 273–280.
251. S. Beriwal, H. Kim, D. Coon, et al. Single magnetic resonance imaging vs magnetic resonance imaging/computed tomography planning in cervical cancer brachytherapy. Clin Oncol (R Coll Radiol), 2009; 21 : 483–487.
252. Nesvacil N, Tanderup K, Hellebust TP, et al. A multicentre comparison of the dosimetric impact of inter- and intra-fractional anatomical variations in fractionated cervix cancer brachytherapy. Radiother Oncol. 2013;107:20-5.
253. NR Datta, S Kumar, KJM Das, et al. Variations of intracavitary applicator geometry during multiple HDR brachytherapy insertions in carcinoma cervix and its influence on reporting as per ICRU report 38, Radiotherapy and Oncology 2001 ; 60: 15-24.
254. Iftimia I, Cirino ET, Mower HW, et al. Treatment planning methodology for the Miami multichannel applicator following the American Brachytherapy Society recently published guidelines: the Lahey Clinic experience. J Appl Clin Med Phys 2013; 14: 214-227.
255. Zhou J, Prisciandaro J, Lee C, et al. Single or multi-channel vaginal cuff high-dose-rate brachytherapy: Is replanning necessary prior to each fraction? Pract Radiat Oncol 2014; 4: 20-26.
256. Peng J, Sinha R, Patel R, Lebovic G. A comparison of 3D dose planning regimens for vaginal cuff brachytherapy using a flexible inflatable multichannel gynecologic applicator. Scientific Poster PD66, ABS 2011 Annual Meeting.
257. Kuo HC, Mehta KJ, Yaparpalvi R, et al. Feasibility study and optimum loading pattern of a multi-ring inflatable intravaginal applicator. J Contemp Brachytherapy 2013; 5: 93-100.
258. Lapuz C, Dempsey C, Capp A, et al. Dosimetric comparison of optimization methods for multichannel intracavitary brachytherapy for superficial vaginal tumours. Brachytherapy 2013; 12: 637-644.
259. Symon Z, Menhel J, Alezra D, et al. Individual fraction optimization vs. first fraction optimization for multichannel applicator vaginal cuff high-dose-rate brachytherapy. Brachytherapy 2006; 5: 211-215.
260. Small W. To plan or not to plan? That is the question. Brachytherapy 2006; 5: 216–217.
261. Yaparpalvi R, Shah S, Sharma R, et al. Variance in bladder and rectal doses in the course of fractionated cylinder high-dose-rate brachytherapy. Brachytherapy 2009; 8: 145-148.
262. Siddiqui MU, Bellon MR, Fraser C, et al. The Nature and Dosimetric Effect of Daily Variations in Vaginal Cuff High-Dose-Rate Brachytherapy: A Prospective Study. Brachytherapy 2010; 9: S89.
263. Supe SS, Bijina TK, Varatharaj C, et al. Optimized dose distribution of Gammamed plus vaginal cylinders. Med Dosim 2009; 34: 20-25.
264. Bahadur YA, Hassouna AH, Constantinescu CT, et al. Three-dimension anatomy-based planning optimization for high dose rate vaginal vault brachytherapy. Saudi Med J 2012; 33: 640-647.
265. Longo JM, Chen S, Thompson R, et al. Measuring the interfraction variation in dose to the rectum and the bladder using CT-based treatment planning for postoperative high dose rate vaginal brachytherapy in women with endometrial cancer. Int J Radiat Oncol Biol Phys 2011; 81: S478.
266. Kirisits C, Lang S, Dimopoulos J, et al. Uncertainties when using only one MRI- based treatment plan for subsequent high-dose-rate tandem and ring applications in brachytherapy of cervix cancer. Radiother Oncol 2006; 81:269–75.
267. Holloway CL, Macklin EA, Cormack RA, et al. Should the organs at risk be contoured in vaginal cuff brachytherapy? Brachytherapy 2011; 10: 313-317.

268. Nixon E, Modrick JM, Jacobson GM. Retrospective evaluation of single treatment plan per course vs plan per fraction for high-dose-rate vaginal cylinders. Brachytherapy 2006; 5: 102.
269. Nunnery EW, Ali AN, Corso C, et al. Fractional Re-planning with Three-Dimensional CT for Single Channel Vaginal Cylinder High-Dose-Rate Brachytherapy: Imaging Technology Overkill? Int J Radiat Oncol Biol Phys 2011; 81: S474.
270. Bellon M, Fraser C, Sintay B, et al. Interfraction Geometric and Dosimetric Variations in Vaginal Cuff High Dose-rate Brachytherapy using CT Based Planning: A Prospective Study. Int J Radiat Oncol Biol Phys 2009; 75: S381-S382.
271. Fokdal L, Tanderup K, Nielsen SK, et al. Image and laparoscopic guided interstitial brachytherapy for locally advanced primary or recurrent gynaecological cancer using the adaptive GEC ESTRO target concept. Radiother Oncol 2011; 100:473–9.
272. Schmid MP, Kirisits C, Nesvacil N, Dimopoulos JC, Berger D, Pötter R. Local recurrences in cervical cancer patients in the setting of image-guided brachytherapy: a comparison of spatial dose distribution within a matched- pair analysis. Radiother Oncol 2011; 100:468–72.
273. Georg P, Pötter R, Georg D. Dose effect relationship for late side effects of the rectum and urinary bladder in magnetic resonance image-guided adaptive cervix cancer brachytherapy. Int J Radiat Oncol Biol Phys 2012; 82:653–7.
274. Andersen ES, Muren LP, Sørensen TS, Noe KO, Thor M, Petersen JB, Høyer M, Bentzen L, Tanderup K. Bladder dose accumulation based on a biomechanical deformable image registration algorithm in volumetric modulated arc therapy for prostate cancer. Phys Med Biol. 2012; 57:7089–100.
275. Andersen ES, Noe KØ, Sørensen TS, Nielsen SK, Fokdal L, Paludan M, Lindegaard JC, Tanderup K. Simple DVH parameter addition as compared to deformable registration for bladder dose accumulation in cervix cancer brachytherapy. Radiother Oncol. 2013; 107:52-7.
276. Xiong L, Viswanathan A, Stewart AJ, Haker S, Tempany CM, Chin LM, Cormack RA. Deformable structure registration of bladder through surface mapping. Med Phys. 2006 ;33:1848-56.
277. Sabater S, Andres I, Sevillano M, Berenguer R, Machin-Hamalainen S, Arenas M Dose accumulation during vaginal cuff brachytherapy based on rigid/deformable registration vs. single plan addition. Brachytherapy. 2013. pii: S1538-4721.
278. Lucas, B.D. Generalized Image Matching by the Method of Differences. Ph.D. dissertation, Dept. of Computer Science, Carnegie-Mellon University. 1984.
279. Rueckert, D., Sonoda, L. I., Hayes, C., Hill, Derek L. G., Leach, M. O., Hawkes, D. J., Non-rigid registration using free-form deformations: Application to breast MR images. IEEE Transactions on Medical Imaging 1999; 18:712-721.
280. Maes, F., Collignon, A., Vandermeulen, D., Marchal, G., Suetens, P. Multimodality image registration by maximization of mutual information. IEEE Transactions in Medical Imaging 1997; 16:187–198.
281. Wells III, W. M., Viola, P., Atsumi, H., Nakajima, S. & Kikinis, R. Multi-modal volume registration by maximization of mutual information. Medical Image Analysis 1996;1: 35–51.
282. Fabri D, Zambrano V, Bhatia A, et al. A quantitative comparison of the performance of three deformable registration algorithms in radiotherapy Z Med Phys. 2013; 23:279-90.
283. Andersen ES, Muren LP, Sørensen TS, Noe KO, Thor M, Petersen JB, Høyer M, Bentzen L, Tanderup K. Bladder dose accumulation based on a biomechanical deformable image registration algorithm in volumetric modulated arc therapy for prostate cancer. Phys Med Biol. 2012 ;57:7089-100.

284. Stanley N, Glide-Hurst C, Kim J, et al. Using patient specific phantoms to evaluate deformable image registration algorithms for adaptive radiation therapy. J Appl Clin Med Phys. 2013; 4; 43-63.
285. McCann C, Purdie T, Hope A et al. Lung sparing and dose escalation in a robust-inspired IMRT planning method for lung radiotherapy that accounts for intra-fraction motion. Med Phys. 2013; 40:061705.
286. Yeo UJ, Supple JR, Taylor ML et al. Performance of 12 DIR algorithms in low-contrast regions for mass and density conserving deformation. Med Phys.2013; 40:101701.
287. Thörnqvist S, Petersen JB, Høyer M et al. Propagation of target and organ at risk contours in radiotherapy of prostate cancer using deformable image registration. Acta Oncol. 2010; 49:1023-32.
288. Zhong H, Kim J, Chetty IJ. Analysis of deformable image registration accuracy using computational modeling. Med Phys. 2010; 37:970-9.
289. Brock KK. Results of a multi-institution deformable registration accuracy study (MIDRAS). Int J Radiat Oncol Biol Phys 2010; 76:583–96.
290. Gu X, Dong B, Wang J et al. A contour-guided deformable image registration algorithm for adaptive radiotherapy.Phys Med Biol. 2013; 58:1889-901.
291. Wognum S, Bondar L, Zolnay AG et al. Control over structure-specific flexibility improves anatomical accuracy for point-based deformable registration in bladder cancer radiotherapy. Med Phys. 2013; 40: 021702.
292. Nie K, Chuang C, Kirby N et al. Site-specific deformable imaging registration algorithm selection using patient-based simulated deformations. Med Phys. 2013; 40:041911.
293. Li S, Glide-Hurst C, Lu M et al. Voxel-based statistical analysis of uncertainties associated with deformable image registration. Phys Med Biol. 2013;58:6481-94.
294. Saarnak AE, Boersma M, van Bunningen BN, Wolterink R, Steggerda MJ. Interobserver variation in delineation of bladder and rectum contours for brachytherapy of cervical cancer. Radiother Oncol 2000; 56:37–42.
295. Damato AL, Townamchai K, Albert M et al. Dosimetric Consequences of Inter observer Variability in Delineating the Organs at Risk in Gynecologic Interstitial Brachytherapy. Int J Radiat Oncol Biol Phys. 2014: S0360-3016.